ABSTRACT

Title of Dissertation: SOURCES AND FATE OF ATMOSPHERIC NUTRIENTS OVER THE REMOTE OCEANS AND THEIR ROLE ON CONTROLLING MARINE DIAZOTROPHIC MICROORGANISMS

Ying Chen, Doctor of Philosophy, 2004

Dissertation Directed By: Assistant Professor Ronald L. Siefert
University of Maryland Center for Environmental Science – Chesapeake Biological Laboratory

Atmospheric deposition can be a major source of nutrients to the remote ocean where these nutrient species can play a critical role in major biogeochemical cycles (e.g. carbon). Atmospheric input of Fe controls phytoplankton growth in high nitrate low chlorophyll regions. Fe can also be a rate-limiting nutrient to diazotrophic microorganisms and control the N_2 fixation in the oligotrophic ocean. Due to low solubility of aerosol Fe in the seawater only a small fraction of atmospheric input of Fe may be bioavailable.

This dissertation developed an aqueous sequential extraction procedure to measure the labile Fe species in aerosols. The measured labile Fe species were compared to the photo-reducible Fe under the ambient sunlight and to the bioavailable forms of aerosol Fe to a diazotrophic microorganism. The diazotroph showed a large capacity of luxury uptake of aerosol Fe, and the uptake amount was less than the total labile Fe measured in aerosols. Labile and total aerosol Fe was found to be highly variable in time and space over the North Atlantic and North

Pacific oceans. The labile aerosol Fe was mostly associated with mineral dust transported from North Africa or Asia, although it can also be associated with anthropogenic sources and atmospheric processing. Major nutrients (soluble PO_4^{3-}, NO_3^- and NH_4^+) in aerosols were also found to be temporally variable over these two oceanic regions. Mineral dust transported from North Africa or Asia was a major source for soluble PO_4^{3-} only during a certain season. Soluble PO_4^{3-} in aerosols was sometimes strongly associated with anthropogenic tracers. Anthropogenic activities were major sources for both aerosol NO_3^- and NH_4^+. It was also found that marine biogenic source of NH_3 could be significant during the spring and summer over the remote oceans. Ratios between the atmospheric inputs of labile Fe, N and P also varied seasonally, which may result in a various nutrient limitation to the water column. The residence time of dissolved Fe in the upper Pacific was estimated longer than those in the Atlantic and the Indian oceans.

SOURCES AND FATE OF ATMOSPHERIC NUTRIENTS OVER THE REMOTE OCEANS AND THEIR ROLE ON CONTROLLING MARINE DIAZOTROPHIC MICROORGANISMS

By

Ying Chen

Dissertation submitted to the Faculty of the Graduate School of the
University of Maryland, College Park, in partial fulfillment
of the requirements for the degree of
Doctor of Philosophy
2004

Advisory Committee:
Assistant Professor Ronald L. Siefert, Chair
Professor Robert P. Mason
Professor Russell R. Dickerson
Professor H. Rodger Harvey
Associate Professor Raleigh R. Hood
Professor Edward A. Boyle, Massachusetts Institute of Technology

Preface

This dissertation is only a small part of my experience of 214 days navigation on the Atlantic and the Pacific oceans. I couldn't describe how much more I have gained during these fantastic trips. It is just like a dream where I was surrounded by the crystal blue waters, by the florid red sunsets, and by the numorous shining universals. There were dolphins, sharks, dophin fish, and blue fish swimming in the water, flying fish jumping out of the ocean, and all kinds of seabirds hovering around the boat. I have been working together with my friends and all other people for the same goal, sharing failure and success, unhappiness and happiness. I have been drinking and dancing with all those lovely people, and these beautiful memories will be appreciated and cherished in my whole life.

Acknowledgements

I would first like to thank my advisor, Ronald Siefert, for giving me the opportunity and the resources to conduct my doctoral research and to complete this dissertation. I appreciate your guidance, support, and friendship throughout the years. You have offered me many opportunities to be on the research cruise to interact with many different groups of researchers and scientists. You have also given me the chance to participate in various scientific meeting. You have directed my study to the greatest extent, from sampling preparation to analysis of aerosol sample, from independent thinking to scientific writing. I am also grateful to the other members of my committee, Robert Mason, Russell Dickerson, Rodger Harvey, Raleigh Hood, and Edward Boyle, for answering my questions, giving me valuable comments, and passing me reference papers during my doctoral study. Thank Robert Mason for providing me the privilege of using the ICP-MS in his lab. I would also like to acknowledge Sergio Sañudo-Wilhelmy at State University of New York for his collaboration during this dissertation work.

Thanks to Debby Heyes and Carrie Miller for instructing and helping me many times in the use of the ICP-MS. I am very grateful to Antonio Tovar-Sanchez for his friendship, vote of confidence, and big help during and after my research cruise.

Special thanks to my husband-to-be Yu Yuan, for giving me so much help and encouragement that made this work possible. Thanks to my family for all their love, understanding, and support through the good times and bad.

This dissertation is based upon work supported by the National Science Foundation: Ocean Sciences Division – Biological Oceanography under grants OCE-998 1218 and OCE-998-1252 (Biocomplexity: Phase I). Data collected on the Indian Ocean were supported by National Science Foundation as part of INDOEX program (ATM-9612893).

Table of Contents

List of Tables

List of Figures

Chapter 1: Executive Summary

1.1 Introduction

The atmosphere is an important pathway for the transport of many natural and anthropogenic materials from the continents to the oceans. Estimates of the atmospheric fluxes of metals and nutrients to the remote ocean suggest that the atmosphere can be a major source in terms of mass (Delany et al., 1967; Duce et al., 1991; Prospero et al., 1996) and plays a critical role in oceanic biogeochemical cycles (Jickells, 1995; Paerl, 1999). The influence of such atmospheric inputs of nutrients is expected to be particularly important in the case of oligotrophic oceanic areas such as the open North Atlantic and the North Pacific gyre (Fanning, 1989; Owens et al., 1992; Baker et al., 2003; Johnson et al., 2003). The tropical North Atlantic and western Pacific are downwind of the major arid and semiarid regions of the earth, Saharan Desert/Sahel and Gobi Desert, respectively. They are also under the impact of anthropogenic emissions from the most populated and urbanized regions of eastern Asia, western Europe and North America.

Atmospheric deposition is a dominant source of micronutrient iron (Fe) to the remote ocean (Duce and Tindale, 1991). Fe limitation to phytoplankton growth has been confirmed in high nitrate low chlorophyll (HNLC) oceanic regions where the dust loadings are low (Martin et al, 1994; Coale et al, 1996; Boyd et al, 2000; Tsuda et al, 2003). In certain areas of the oligotrophic ocean such as the tropical North Atlantic and the North Pacific gyre, Fe may also be a rate-limiting nutrient to nitrogen (N_2)-fixing microorganisms and control the N_2 fixation (Paerl et al., 1994; Howard

and Rees, 1996; Falkowski, 1997). Oceanic N_2 fixation has recently been identified as a significant part of the oceanic N cycling (Capone et al., 1997) and may directly affect the sequestration of atmospheric carbon dioxide (CO_2) in the ocean by providing a source of "new" N to the upper water column (Falkowski, 1997; Karl *et al.*, 1995). Consequently the atmospheric input of Fe to the ocean may affect the carbon (C) biogeochemical cycling and thereby global climate both at present and in the past (Martin, 1990; Petit et al., 1999; Watson and Lefevre, 1999). Atmospheric Fe flux alone, however, is not the only parameter required to assess aerosol impacts on biogeochemical cycling of C and N. Due to the low solubility of aerosol Fe in the seawater (1-10% of total aerosol Fe) (Jickells and Spokes, 2001) only a small fraction of atmospheric Fe input may be bioavailable. Thermal and photochemical reactions in atmospheric waters and surface seawater (Siefert et al., 1996; Voelker and Sedlak, 1995; Chen and Siefert, 2003) could enhance dissolution of aerosol Fe, resulting in the production of soluble ferrous Fe (Fe(II)) which is believed to be more readily used by phytoplankton (Sunda, 2001). Labile Fe species including the reducible Fe(III) and Fe(II) in aerosols may have a great influence on diazotroph growth in the oligotrophic ocean.

Atmospheric inputs of the major nutrients nitrogen (N) and phosphorus (P) may also play an important role in the oceanic biological cycles. Anthropogenic N deposition can significantly contribute to eutrophication problems in coastal waters (Paerl, 1997; Spokes et al., 2000). P limitation of N_2 fixation by *Trichodesmium* has been proposed in the tropical and central North Atlantic (Wu et al., 2000; Sañudo-Wilhelmy et al., 2001). N_2 fixation stimulated by any excess atmospheric Fe supply

will tend to drive the ecosystem towards P limitation (Baker et al., 2003). Ratios between the atmospheric fluxes of Fe, N and P may determine nutrient limitation to the ecosystem and affect diazotroph growth in the open oligotrophic ocean.

1.2 Rationale

Two large collaborative NSF funded studies, Oceanic N_2 Fixation and Climate (MANTRA) and Factors Effecting, and Impact of Diazotrophic Microorganisms in the Western Equatorial Atlantic Ocean (PIRANA), were developed partly on the basis of the influences of atmospheric Fe fluxes on oceanic N_2 fixation and diazotroph growth. During MANTRA and PIRANA, my research investigated the atmospheric inputs of Fe, labile Fe and other nutrient species to the subtropical North Pacific and western equatorial Atlantic, where there are large fluxes of atmospheric Fe and strong localized N_2 fixation (Capone et al., 1997). The atmospheric Fe fluxes to the North Atlantic and North Pacific basins account for 48% and 22% of total flux to the world oceans, respectively (Gao et al., 2001). *Trichodesmium*, the most prominent planktonic marine nitrogen fixer, occurs throughout the open waters of oligotrophic tropical and subtropical oceans (Capone et al., 1997). This cyanobacterium supplies up to half of new N used for primary production in the oligotrophic ocean (Karl et al., 1997).

Fe has been shown to limit the N_2 fixation and growth of natural and cultured populations of *Trichodesmium* spp. (Rueter et al., 1992; Paerl et al., 1994). Howard and Rees (1996) indicated that Fe is a critical nutrient co-factor for the nitrogenase enzyme. N_2-fixing *Trichodesmium* has a high Fe requirement (Berman-Frank et al., 2001; Kustka et al., 2003a, b), and has a high Fe : C quota (38 μmol mol^{-1}) that is 2.5

to 5-times greater than NH_4^+-assimilating phytoplankton (Kustka et al., 2003a, b). In general, Fe is very depleted in the surface water of the open ocean (Johnson et al., 1997). And there are indications that the delivery of Fe to the oceans in airborne dust may ultimately control the rate of N_2 fixation on regional and global scales (Michaels et al., 1996; Falkowski, 1997).

Most Fe in aerosols is locked into inaccessible refractory mineral lattices (e.g. aluminosilicates), and only a small amount of the aerosol Fe is released when in contact with seawater. Aqueous extraction (at pH 1.0 to 4.5) studies on Atlantic (Zhu et al., 1993; Johansen et al, 2000; Chen and Siefert, 2004a) and Indian Ocean (Siefert et al., 1999) aerosols have found that only a few percent (0.3 to 1.8%) of the total aerosol Fe is released as Fe(II), and the soluble Fe(II) is predominantly found in the fine aerosol fraction (with aerodynamic diameters less than 2.5μm). The mechanisms controlling the release of Fe from aerosols are not well understood. Seawater conditions, chemical and biological processes in the ocean (Gledhill & van den Berg, 1994; Rue & Bruland, 1995; Wu & Luther, 1995), atmospheric processing (e.g. cloud cycling, photochemical reactions) (Zhuang et al., 1992; Siefert et al., 1996; Zhu et al., 1997; Keene & Savoie, 1998; Chen & Siefert, 2003), and the terrestrial sources of aerosols (Johanson et al., 2000; Chen & Siefert, 2004a) can all affect the speciation of Fe in the atmosphere and the ocean. Processes that are likely to enhance the lability of aerosol Fe include: (1) partial dissolution of Fe(III) oxides by acidic aerosols, and (2) photochemical reduction to more soluble Fe(II) within humid aerosols, especially in the presence of organic matter.

The labile aerosol Fe as dissolved species has a great probability of being directly utilized by biota or precipitating into Fe oxy-hydroxide colloids that could also be bioavailable (Miller and Kester, 1994). Previous studies have shown that bioavailable forms of Fe include not only free or inorganic Fe species (Anderson and Morel, 1982; Campbell, 1995; Sunda and Huntsman, 1997), but Fe bound with organic ligands (Hutchins et al., 1999; Chen et al., 2003). Extracellular ligands such as siderophores are produced by many marine cyanobacteria as part of high-affinity Fe uptake systems (Wilhelm, 1995; Granger and Price, 1999; Reid, 1993). Algal Fe uptake is a two-step process: the diffusion of available Fe species from bulk solution to algal cell surface followed by the transport of the cell surface bound Fe into the cells (Hudson & Morel, 1990; 1993; Sunda & Huntsman, 1995). Two distinct pools of Fe, scavenged Fe adsorbed to cell surface and interior Fe, exist during the uptake process. The interior Fe pool corresponds to the intracellular "biological" fraction strongly correlated with the growth rate of phytoplankton (Sunda et al., 1991; Sunda & Huntsman, 1995; 1997). The diffusion rate of Fe to algal cell surface is inversely related to the molecular radius of the diffusing Fe species (Stokes-Einstein equation). Size-fractionated measurements (<0.2μm, and 0.2 to 0.4μm) of dissolved Fe in the seawater were expected to be important to assess the Fe bioavailability in the ocean (Wen et al., 1999; Wu et al., 2001).

A general lack of correlation between surface seawater Fe (total or dissolved) and *Trichodesmium* abundance, however, has been observed in the Arabian Sea (Capone et al., 1998), in the central North Atlantic (Sañudo-Wilhelmy et al., 2001), and along a Atlantic Meridional Transect (AMT) (Tyrrell et al., 2003). There was

little difference between dissolved Fe concentrations where *Trichodesmium* is abundant, and where it is scarce in the Atlantic Ocean (Tyrrell et al., 2003). The finding suggested that either *Trichodesmium* growth was not Fe-limited in these oceanic areas, or *Trichodesmium* uptake of Fe could be a dynamic process depending on the amount of Fe supplies (e.g. luxury Fe uptake). The rate of dust Fe supply was also not correlated with the Fe concentration in surface seawater (Johnson et al., 1997). So, the *Trichodesmium* abundance and N_2 fixation rate in the ocean may depend on the episodic fluxes of aerosol Fe instead of the Fe concentration in the seawater.

This dissertation hypothesizes that the fraction of total Fe in marine aerosols that is labile is a function of atmospheric processing and sources of the aerosol. This labile Fe and other nutrient species in aerosols are variable over the remote ocean, and this vaiability is controlled strongly by their source contributions and/or by atmospheric processing. It also hypothesizes that an abiotic reductive extraction method for quantifying labile Fe fractions can be developed and used to determine the amount of aerosol Fe that can be bioavailable to marine diazotrophic microorganisms.

The overall goals of the dissertation are to explore the relationship between the labile aerosol Fe and diazotrophic available forms of aerosol Fe and investigate the sources, fluxes and ecological impacts of labile Fe and other nutrient species in aerosols. The main objectives of the dissertation are as follows:

1. Develop an aqueous extraction procedure for shipboard analysis of the labile Fe species in marine aerosols.

2. Characterize the temporal and spatial distributions of the labile aerosol Fe over the tropical and subtropical North Atlantic and subtropical North Pacific oceans.

3. Quantify the diazotroph uptake of aerosol Fe in the surface seawater and explore the relationship between the diazotroph available forms of Fe and the labile Fe fractions in the aerosol.

4. Determine the seasonal variations of aerosol nitrate (NO_3^-), ammonium (NH_4^+) and phosphate (PO_4^{3-}) over the tropical North Atlantic, and assess their source contributions and ecosystem impacts when combined with the labile aerosol Fe.

5. Examine the atmospheric depositions of labile Fe, N and P species to the subtropical North Pacific and their sources and ecosystem impacts.

1.3 Strategy

Aerosol samples were collected during seven research cruises (6 January to 18 February 2001, 9 April to 30 April 2001, 27 June to 15 August 2001, 1 July to 16 July 2002, 22 September to 16 October 2002, 18 April to 22 May 2003, 5 August to 23 August 2003) over the subtropical and tropical North Atlantic (0°N to 30°N) and subtropical North Pacific (15°N to 30°N) oceans. The quantity and timing of the research cruises allowed for the investigation of the spatial and temporal variability in the concentrations of the labile Fe and other nutrient species in the atmosphere. A high volume dichotomous virtual impactor (HVDVI, Solomon et al., 1983) was used for collection of two size fractions (with aerodynamic diameters greater and less than 2.5μm) of aerosol particles. The sample collection was conducted under trace-metal clean techniques considering the relatively low concentration of Fe in the atmosphere.

A sequential aqueous extraction was developed to measure the labile Fe species onboard the ship immediately after collection of aerosol samples (Chapter 2; Chen and Siefert, 2003). Three fractions of labile Fe were determined based on potential degree of bioavailability to phytoplankton, including labile Fe(II) fraction and a reducible Fe(III) fraction which used hydroxylamine hydrochloride (HA) as a reductant. The HA-reducible aerosol Fe was compared to the Fe(II) produced photochemically during the photo-reductive aqueous extraction of aerosol Fe which was conducted onboard using the ambient sunlight (Chapter 2; Chen & Siefert, 2003). The purpose of this comparison was to show that HA-reducible Fe is similar to the maximum concentration of labile Fe when considering photochemical reactions of Fe(III) in the atmosphere.

After development of the sequential extraction method, field measurements of the labile Fe species in aerosols were made during the North Atlantic cruises (6 January to 18 February 2001, 27 June to 15 August 2001, 18 April to 22 May 2003). Total Fe concentrations in aerosol samples were determined by microwave assisted strong acid digestion of the aerosol samples followed by analysis using inductive coupled plasma mass spectrometer (ICPMS, HP 4500) after the cruises. The purpose of these field studies was to characterize the seasonal and spatial distributions and dry deposition fluxes of atmospheric labile and total Fe over the subtropical and tropical North Atlantic Ocean (Chapter 3, Chen & Siefert, 2004a).

After determination of the Fe distributions in the atmosphere, *in situ* *Trichodesmium* uptake of aerosol Fe in the surface seawater was investigated during the North Atlantic cruise (18 April to 22 May 2003). The purpose was to assess the

bioavailability of aerosol Fe to diazotrophs and explore the relationship between the bioavailable forms of Fe and the labile Fe species in aerosol particles (Chapter 4; Chen et al., 2004). Antonio Tovar-Sanchez and Sergio Sanudo-Wilhelmy (State University of New York) collaborated with these aerosol addition experiments. Intracellular and total Fe amounts in *Trichodesmium* colonies and dissolved and total Fe concentrations in seawater were analyzed in Sergio Sanudo-Wilhelmy's research lab by Antonio Tovar-Sanchez.

After completion of labile Fe measurements, elemental analysis of 14 elements (Al, Ca, Fe, K, Na, Mg, Cr, Co, Cu, Pb, Mn, Ni, V, Zn), and ion measurements of 11 anions (F^-, glycolate, acetate, formate, MSA^-, Cl^-, SO_4^{2-}, oxalate, Br^-, NO_3^-, PO_4^{3-}) and 6 cations (Li^+, Na^+, NH_4^+, K^+, Mg^{2+}, Ca^{2+}) in the aerosol samples were conducted after research cruises. The purpose of these chemical analyses was to quantify the atmospheric depositions of labile Fe and other nutrient species to the subtropical and tropical North Atlantic (Chapter 5; Chen & Siefert, 2004b) and subtropical North Pacific (Chapter 6; Siefert & Chen, 2004) oceans, characterize the sources of labile Fe and other nutrients in the atmosphere, and assess the ecological impacts of the aerosol nutrient inputs.

1.4 Synopsis

1.4.1 Chapter 2

The speciation of Fe in the atmosphere is critical to understanding the fraction of Fe that will be labile in surface waters after deposition and consequently has implications for the bioavailability of this atmospherically derived Fe. In this chapter, a sequential aqueous extraction procedure using a pH 4.5 buffer solution and a

chemical reductant (HA) was developed to measure various labile Fe fractions. The extraction procedure was performed immediately after aerosol sample collection and used time series measurements of Fe(II) using long path length absorbance spectroscopy (LPAS) for analysis of Fe(II). The method measured both the quantities of labile Fe and also the dissolution and reduction kinetics of the labile Fe. Comparisons of HA-reducible Fe and photo-reducible Fe concentrations were conducted on board and showed that both reduction processes had similar reduction kinetics and final Fe(II) concentrations during the initial 90 min reduction. The average pseudo-first-order rate constants for the increase in Fe(II) were 0.020 and 0.0076 min^{-1} for the photo- and HA-reductive extractions, respectively. This HA-reducible Fe amount could potentially be used to determine the maximum amount of labile atmospheric Fe that is deposited into the ocean.

1.4.2 Chapter 3

Field measurements of Fe concentrations and Fe speciation in aerosols provide information crucial to understanding the biological role of atmospheric Fe flux to the ocean. In this chapter, 24-hour aerosol samples were collected during winter (6 January to 18 February 2001) and summer (27 June to 15 August 2001) research cruises over the subtropical and tropical North Atlantic. Three labile Fe species, which included Fe(II) and reducible Fe(III) species, were measured in aerosol samples using a sequential aqueous extraction method. Microwave assisted strong acid digestion of the aerosol samples followed by ICPMS was used to quantify total elemental concentrations. A spatial gradient of over nearly 3 orders of magnitude in the total Fe concentrations (1.6 ng m^{-3} at 28.6°N to 1688 ng m^{-3} at

10.9°N) was observed during the winter, although this gradient was not as strong in the summer. The mean total Fe concentrations were approximately a factor of 2 higher during the winter (mean value of 670 ng m^{-3} between 5°N and 26°N) than in the summer (mean value of 324 ng m^{-3} between 6°N and 26°N). The highest percent of labile Fe in total aerosol Fe was observed between 26°N and 30°N during the winter with a mean value of 32%, which corresponded to low concentrations of total Fe. At latitude 0°N to 10°N where the lowest Fe concentrations were observed in the summer, the labile Fe fraction with a mean of 5.0% was similar to that in the region of 10°N to 20°N where mineral aerosols were dominant. Air mass back trajectories showed that mineral dust transported from North Africa is a significant atmospheric Fe source in this Atlantic region. However, the highest labile Fe to total Fe ratios were observed in air masses that had circulated over the ocean for greater than 7 days and also corresponded to high ratios of non-seasalt-sulfate (NSS SO_4^{2-}) to total Fe and oxalate to total Fe. The correlations with NSS SO_4^{2-} and oxalate suggest that labile Fe contents may have been influenced by anthropogenic activities from North America or Europe.

1.4.3 Chapter 4

The episodic fluxes of aerosol Fe to the surface ocean may have a significant impact on metabolism of the N_2-fixing microorganism, *Trichodesmium* spp. Shipboard aerosol addition experiments were conducted in the western tropical North Atlantic using freshly collected aerosols, seawater, and *Trichodesmium* colonies. It was found that the *Trichodesmium* took up a significant amount of aerosol Fe that included part of the colloidal or particulate Fe besides the dissolved Fe species (<0.4

μm) in the seawater. The uptake amounts increased with increasing amounts of aerosol Fe added to the seawater. Total Fe: P molar ratios in the *Trichodesmium* were found to be lower than the dissolved Fe: P ratios in the western tropical North Atlantic, suggesting that the *Trichodesmium* were not historically Fe-limited. However, a high capacity of luxury uptake of aerosol Fe (6 to 1795 times greater than needed for moderately Fe-limited growth 0.1 d^{-1}) was demonstrated in the *Trichodesmium* collected from this oceanic region, which is considered as an adaptation to the episodic nature of the dust events. *Trichodesmium* uptake of Fe was less or comparable to the total labile Fe determined by the aqueous extraction procedure suggesting that the labile Fe pool may be a threshold of aerosol Fe that can be bioavailable by *Trichodesmium*. The organic ligands produced by *Trichodesmium* may inhibit or assist the aerosol-Fe dissolution into the seawater depending on its history of Fe limitation. This is the first field study to investigate the *Trichodesmium* uptake of aerosol Fe and its influences on the aerosol Fe transfer using concurrent measurements in aerosol, seawater and *Trichodesmium* samples.

1.4.4 Chapter 5

Deposition of atmospheric aerosols is an important source of Fe and other nutrient species to the remote ocean. Two size fractions of aerosol samples were collected over the western tropical North Atlantic (WTNA, 5°N to 15°N, 40°W to 60°W) during the three month-long cruises in winter 2001, summer 2001 and spring 2003. Labile Fe species were measured onboard and soluble PO_4^{3-}, NO_3^- and NH_4^+ determined back in the laboratory using an aqueous extraction method and ion chromatography (IC). The concentrations and sources of the aerosol PO_4^{3-}, NO_3^- and

NH_4^+ over the WTNA showed a markedly seasonal variability. Total PO_4^{3-} concentrations in the winter and spring were found to be significantly higher than concentrations in the summer. The largest concentrations of NO_3^- and NH_4^+ were observed in the spring, and the NO_3^- and NH_4^+ concentrations declined in the order of spring > winter > summer, and spring > summer ≈ winter, respectively. During the winter, PO_4^{3-} in the fine aerosol fraction was principally contributed by mineral dust from North Africa, while the mixture of mining dust from North America and incineration emissions from North America and/or Europe may be a major source for the PO_4^{3-} in the coarse aerosol fraction. Biomass burning materials from North Africa were responsible for the fine fraction PO_4^{3-} during the spring. Aerosol NO_3^- and NH_4^+ concentrations measured during the winter and spring were primarily contributed by anthropogenic and marine biogenic sources, respectively. During the summer, aerosol NO_3^- may be principally derived from continental combustion emissions, whereas aerosol NH_4^+ may be contributed by both combustion and marine biogenic sources. From an only atmospheric view, aerosol inputs of LFe, DIN and DIP into the WTNA will first drive the water column towards a short-term N limitation, and later on due to the enhanced N_2 fixation the nutrient depositions will tend to deplete P in the water column. If considered other flux sources of N and P (e.g. shelf fluxes and N_2 fixation), atmospheric deposition of labile Fe to the WTNA would be a controlling factor for diazotroph growth.

1.4.5 Chapter 6

Atmospheric deposition of nutrient species to the central North Pacific plays an important role on controlling the N_2 fixation in this oceanic region. Two size

fractions of ambient aerosols were collected over the central North Pacific (15°N to 30°N, 150°W to 175°E) during the four separate cruises (9 April to 26 April 2001, 1 July to 16 July 2002, 23 September to 15 October 2002 and 6 August to 21 August 2003). Nutrient concentrations including the total and labile Fe, the soluble NH_4^+, NO_3^- and PO_4^{3-} in aerosol samples were measured, demonstrating a clear seasonality. The highest mean concentrations of the total Fe (133 ng m^{-3}), the labile Fe(II) (1.24 ng m^{-3}) and the total labile Fe (2.43 ng m^{-3}) measured in April 2001 were approximately a factor of 130, 50 and 60 larger than the lowest mean concentrations of the Fe species (correspondingly 10, 0.25, and 0.41 ng m^{-3}) measured in July 2002, respectively. The percentages of labile Fe in total aerosol Fe were found to be approximately an order of magnitude lower in April 2001 and August 2003 than in July and September 2002. The relatively low percentages were probably a signature of mineral aerosols transported from Asian desert regions, while the large labile Fe percentages may be due to anthropogenic and/or volcanic emissions. Correlation coefficients calculated between total labile Fe and other chemical components in aerosols further confirmed that the labile Fe was primarily contributed by Asian soil dust in April 2001 and August 2003, but the dust influence was not as strong in August 2003. The labile aerosol Fe observed in July 2002 was mainly associated with anthropogenic emissions from Asia or North America, while volcanic emissions from Hawaii may be responsible for the labile aerosol Fe observed in September 2002. However, the volcanic emission is only a local source and does not affect a large region of the Pacific. The largest mean concentrations of both aerosol NH_4^+ (81 ng m^{-3}) and aerosol NO_3^-(144 ng m^{-3}) were found to be in August 2003, which were

approximately a factor of 2 and 5 larger than the lowest mean concentrations observed in September 2002 and April 2001, respectively. The relatively low concentrations of aerosol NH_4^+ and NO_3^- measured in April 2001 suggests that Asian dust plumes had only a minor contribution to the two nutrient species. Nonetheless, the mean soluble PO_4^{3-} concentration in aerosols was found to be the largest (50 ng m^{-3}) in April 2001 as a result of the most intensive dust transport from Asia during this period. From an only atmospheric view, the aerosol inputs of LFe, DIP and DIN to the central North Pacific generally tend to drive the water column towards P limitation (DIN: DIP > 16) during the summer and the fall, whereas during the spring the atmospheric nutrient depositions may result in a short-term N limitation at first, and then due to the enhanced N_2 fixation the ecosystem is ultimately limited by P. If considered other flux sources of nutrients to the euphotic zone, the primary productivity in the central North Pacific may be co-limited by P and Fe.

1.4.6 Chapter 7

The new data on atmospheric fluxes of labile Fe combined with the reported dissolved Fe concentrations in the surface ocean were used to derive estimates of the residence times of dissolved Fe in the euphotic zones of three oceanic regions. Assuming only the labile fraction of aerosol Fe dissolved into the seawater, the estimated residence times of dissolved Fe would be 0.69, 2.7 and 0.72 years for the tropical and subtropical North Atlantic, the subtropical North Pacific and the North Indian Ocean, respectively. The short residence times for dissolved Fe probably reflect its rapid biological uptake and removal in the upper North Atlantic and North Indian oceans. By contrast, the relatively longer residence time of dissolved Fe may

reflect its retention in the euphotic zone as a result of P limitation in the subtropical North Pacific gyre.

1.5 Implications

The main findings and implications of these field measurements and the overall study are as follows:

(1) Given the limited *in situ* measurements of aerosol Fe over the remote ocean, mapping the temporal and spatial distributions of aerosol Fe concentrations is essential for estimation of atmospheric Fe fluxes to the global ocean. Over 400 daily aerosol samples were collected in this study and total Fe concentrations measured over the subtropical and tropical North Atlantic and subtropical North Pacific oceans during the winter, spring, summer and fall periods. These *in situ* measurements of aerosol Fe are an important supplement to the Fe data collected from large-scale atmospheric networks, which will be used in many biogeochemical models such as modeling the C and N global cycling.

(2) Chemical forms of aerosol Fe are important in oceanic biogeochemistry, thus a labile Fe extraction procedure was developed and the labile Fe species in aerosols measured along with the total Fe concentrations in this study. Interestingly, the distribution patterns of the labile aerosol Fe didn't completely follow the total aerosol Fe, and the percent of labile Fe in total Fe was significantly affected by the sources and chemical composition of the aerosols. Mineral aerosols transported from North Africa typically contained a few percent of labile Fe species, while oceanic origin aerosols (air mass has circulated over the ocean for more than 7 days) can have the labile Fe up to 32% of the total Fe. The high labile Fe percent also corresponded

to high ratios of non-seasalt-sulfate (NSS SO_4^{2-}) to total Fe and oxalate to total Fe. These *in situ* labile Fe data will be more appropriate than the total Fe for assessing the biogeochemical roles that atmospheric Fe flux plays in the oceanic ecosystem.

(3) The bioavailability of aerosol Fe to the phytoplankton was expected to be associated with the dissolvable aerosol Fe in the seawater. Quantification of either the dissolvable or bioavailable forms of aerosol Fe are crucial for connecting atmospheric Fe fluxes and phytoplankton productivity in the remote ocean. The uptake amounts of aerosol Fe by diazotrophic microorganisms and its influences on aerosol Fe dissolution were investigated in this study through the *in situ* experiments. It was found that the labile Fe fractions may be a threshold of aerosol Fe that can be taken up by diazotrophs in the seawater. *Trichodesmium* collected from the WTNA showed a high capacity of luxury uptake of aerosol Fe as a consequence of adaptation to the episodic nature of the dust events. The organic ligands produced by *Trichodesmium* may inhibit or assist the aerosol-Fe dissolution into the seawater depending on its history of Fe limitation.

(4) Liebig's law of the minimum said that under conditions of equal temperature and light, the nutrient available in the smallest quantity relative to the requirement of the plant will limit productivity. Atmospheric deposition can be a major source of nutrient inputs to the remote ocean surface. Ratios between the atmospheric inputs of labile Fe and other nutrient species will determine the nutrient limitation to the oceanic ecosystem and N_2-fixing microorganisms. Field measurements of other nutrient species such as NH_4^+, NO_3^- and PO_4^{3-} in aerosols were conducted over the subtropical and tropical North Atlantic and subtropical

North Pacific oceans during the winter, spring, summer and fall periods. It is interesting to note that seasons played a significant role in the concentrations and the sources of nutrient species present over the two oceanic areas. From an only atmospheric view, aerosol inputs of labile Fe, DIN and DIP into the western tropical North Atlantic (WTNA) will first drive the water column towards a short-term N limitation (DIN: DIP < 16), and later on due to the enhanced N_2 fixation the nutrient depositions will tend to deplete P in the water. If considered other flux sources of N and P (e.g. shelf fluxes and N_2 fixation), atmospheric deposition of labile Fe to the WTNA would be a controlling factor for diazotroph growth. The same scenario is expected to occur in the central North Pacific.

(5) The residence time of Fe was one of the most important parameters required in modeling the biogeochemical cycling of Fe in the global ocean. The new data of atmospheric fluxes of labile Fe collected in this study together with the dissolved Fe concentrations were used to derive estimates of the residence times of dissolved Fe in the euphotic zones of the tropical and subtropical North Atlantic, the subtropical North Pacific and the North Indian Ocean. The short residence times in the studied Atlantic and Indian oceans may reflect a rapid biological uptake and removal of atmospheric-deposited Fe, while the relatively longer residence time may suggest Fe retention in the euphotic zone as a result of P limitation in the subtropical North Pacific.

Chapter 2: Determination of Various Types of Labile Atmospheric Iron over the Remote Ocean

2.1 Introduction

Fe is a critical micronutrient that limits the phytoplankton growth in high-nitrate low chlorophyll (HNLC) oceans (Martin, 1990; Martin et al., 1994; Coale et al., 1996; Boyd et al., 2000). Fe may also be one of the limiting factors for nitrogen-fixing organisms that provide a ‘‘new’’ nitrate source to phytoplankton in oligotrophic oceans (Falkowski, 1997). There have been many studies investigating the speciation and distributions of Fe in the open ocean where the dissolved Fe concentrations (defined as passing through a 0.4 μm filter) are typically lower than 1 nM (Martin and Gordon, 1988; Martin et al., 1993; Wu and Luther, 1994; Powell et al., 1995; Wu et al., 2001). Studies have also investigated the role of organic ligands on the solubility of Fe in seawater (Wu et al., 2001; Boye et al., 2001). Several analytical methods have been developed to quantify low Fe concentrations and speciation in seawater (for a recent review see Achterberg et al., 2001). The methods include catalytic cathodic stripping voltammetry (CCSV) (Yokoi and van den Berg, 1992), competitive ligand exchange-adsorptive cathodic stripping voltammetry (Croot and Johansson, 2000), chelating resin concentration with chemiluminescence detection (Obata et al., 1993, 1997), and isotope dilution inductively coupled plasma-mass spectrometery (ICPMS) (Wu and Boyle, 1998). Fe species in seawater have been separated as a function of size (Wu et al., 2001) or by the reactivity and lability of Fe to specific chelating agents (Gledhill et al., 1998). Fe(II) has also been

measured in seawater using chemiluminescence methods (Croot and Laan, 2002; O'Sullivan et al., 1995). The distributions and speciation of Fe in seawater have provided us with a better understanding of Fe seawater chemistry, but there are still questions regarding the relationship between Fe and phytoplankton productivity in the remote ocean.

Atmospheric Fe deposition and its seawater solubility are two other key aspects that need to be understood since atmospheric Fe is the primary source of total Fe to the open ocean (Duce and Tindale, 1991; Fung et al., 2000). The reported solubility of aerosol Fe in seawater spans over two orders of magnitude (<1 to 50% of total Fe) although most are on the low end of this range (Zhuang et al., 1990; Chester et al., 1993b; Zhu et al., 1992, 1993; Jickells, 1999). Fe solubility is a function of both the seawater conditions and the initial aerosol Fe speciation, that is a function of aerosol sources and atmospheric processing as the aerosol is transported through the atmosphere. The atmospheric processing includes both the reactions occurring in the dry or deliquesced aerosol particle, along with chemical and photochemical reactions that can occur after an aerosol particle is incorporated into cloud droplets. Subsequent evaporation of the cloud droplets would result in a chemically processed aerosol particle. Studies of rainwater have also shown that there may be ligands present that can stabilize Fe(II) after deposition to seawater (Kieber et al., 2001; Willey et al., 2004). The total atmospheric Fe flux to the ocean is the sum of Fe in dry and wet deposition. The dry deposition is difficult to measure directly and therefore aerosol concentrations are used along with a dry deposition velocity to calculate the flux of

Fe via dry deposition, and the wet deposition is often calculated by using the aerosol concentration and a scavenging ratio (Gao et al., 2001).

Fewer studies have investigated aerosol Fe speciation and concentrations, making it difficult to calculate the atmospheric flux of these Fe species over different oceanic regions and seasons. Zhu et al. (1993) measured the concentrations of total Fe, total soluble Fe, and total soluble Fe(II) in Barbados aerosol samples and indicated that Fe(II) did exist in aqueous aerosol solutions and occupied 1% of total Fe and 7.5% of soluble Fe. The concentration of mineral dust was variable at Barbados, ranging from 1.99 to 18.4 μg m^{-3}, and Fe constituted on average 3.4% of the mineral dust mass. There was a clear day/night pattern in the concentration of soluble Fe(II), with a day value (3.7 ng m^{-3}) approximately twice as much as the night value (1.5 ng m^{-3}) (Zhu et al., 1997). Siefert et al. (1999) reported total atmospheric aqueous labile Fe(II) concentrations between 4.75 and <0.4 ng m^{-3} during the intermonsoon, but below the detection limit during the southwest monsoon over the Arabian Sea, and that over 80% of this labile Fe(II) was associated with aerosol particles with an aerodynamic diameter less than 2.5 μm. The aqueous labile Fe(II) was also always less than 4% of the total Fe in the aerosol samples. The diel variability of Fe(II) is evidence of the influence of photochemical reactions on Fe speciation in the atmosphere, however, none of the previous studies determined the relationship between measured Fe species and photochemically active Fe in aerosols.

Colorimetric analysis with ferrozine (Stookey, 1970) was used to measure labile Fe in ambient aerosols in many of the previous studies due to its simplicity and high selectivity. However, the spatial and seasonal variations of labile Fe in aerosols

are difficult to detect by the conventional spectrometer cells even with 10 cm path length absorbance cells that have a detection limit greater than 10 nM. Long path length absorbance spectroscopy (LPAS) using liquid core waveguides (LCW) provides a long optical path length by constraining light propagation within a liquid medium that has a higher refractive index (RI) than the surrounding solid tubing (Wei et al., 1983). The LCWs also have a relatively small sample volume compared to conventional cells. Waterbury et al. (1997) used a 4.5-m Teflon AF-2400 LCW to lower the detection limit of colorimetric Fe(II) analysis to 0.2 nM.

This chapter describes the extraction method used to determine labile Fe fractions in aerosol samples collected over the remote Atlantic Ocean; subsequent chapters will focus on the observed spatial and temporal patterns of labile Fe. In this study, daily aerosol samples were collected over the tropical and subtropical North Atlantic Ocean, and these samples were used to develop the shipboard aqueous extraction procedure for labile Fe measurements. Labile Fe(II) (LFe(II)), labile Fe(III) (LFe(III)), and reducible particulate Fe (RPFe) in the aerosol samples are defined by the aqueous extraction procedure and quantified using the colorimetric reagent ferrozine and LPAS. The extraction method quantifies various labile Fe species and also provides dissolution and reduction kinetic information. Investigations of HA-reducible Fe and photo-reducible Fe concentrations in the extraction solutions were also performed to determine if the HA-reducible Fe was consistent with Fe photochemically reduced using ambient sunlight.

2.2 Experimental Methods

2.2.1 Aerosol Collection

A high-volume dichotomous virtual impactor (HVDVI) (Solomon et al., 1983) was setup above the bridge of the R/V Seward Johnson (winter cruise) or on the 02 deck of the R/V Knorr (summer cruise), to collect two size fractions of ambient aerosols (with aerodynamic diameters greater and less than 2.5μm). The HVDVI aerosol collector was constructed out of polycarbonate with nylon screws in order to minimize trace metal contamination and had a total flow rate of 335 ± 15 L min^{-1}. The fine and coarse sample fractions were collected on two 90-μm-diameter Teflon membrane filters (Gelman Zefluor, 1 μm pore size). The filters, HVDVI, and laboratory equipment were acid cleaned using ultrapure acids (Seastar Chemicals Inc.) and 18.2 MΩ-cm Nanopure water (Barnstead). The collector was also cleaned periodically in the field by wiping the surface with Kimwipes and ethanol. Subsampling of the filters for labile Fe analysis occurred immediately after aerosol collection, and the remaining portions of the filters were stored frozen in acid-cleaned polystyrene petri dishes inside two plastic bags during the cruises.

A sector-sampling system was used to control the aerosol collector. The system was configured to allow collection of ambient aerosol samples only when the relative wind direction was ±70° off the bow during both winter and summer Atlantic cruises. New filters were loaded every 24 hours, and the sampling duration depended on the relative wind directions.

2.2.2 Labile Iron Measurements

Labile Fe concentrations in both fine and coarse aerosol fractions collected on the two HVDVI filters were analyzed immediately (within 1 hour) after the filters were removed from the HVDVI, in order to minimize any changes in Fe oxidation state during sample storage. Fe(II) concentrations were determined colorimetrically by complexation with ferrozine (Carter, 1971) and subsequent LPAS measurements using an LCW flow cell (1 m path length), an S2000 spectrometer (Ocean Optics Inc.), and LabView data acquisition software (National Instruments Inc.). Labile Fe(III) species in the extraction solutions (formate-acetate buffer, pH 4.5) were measured by reducing the Fe(III) to Fe(II) using HA and subsequently measuring the Fe(II) using the ferrozine colorimetric method with the LCW. HA has been used by other investigators to investigate Fe(III) species in natural waters (Viollier et al., 2000). There was a linear absorbance response for Fe(II) concentrations between 1 and 250 nM. The detection limit of 1.0 nM for the Fe(II) concentration in the extraction solution was defined as three times the standard deviation of the measurement blank (absorbance was around 0.005). The sample size requirement for the analysis was less then 1 mL, and therefore multiple aliquots could be removed from the extraction solution that allowed for time series measurements.

LFe(II), LFe(III), and RPFe species were defined by a sequential aqueous extraction procedure in a pH 4.5 buffer solution according to the extraction time and addition of the chemical reductant, HA (Figure 2-1). A formate-acetate buffer solution was used since these species will not reduce Fe(III) to Fe(II) during the time period of the extractions. Formate and acetate can serve as electron donors to reduce

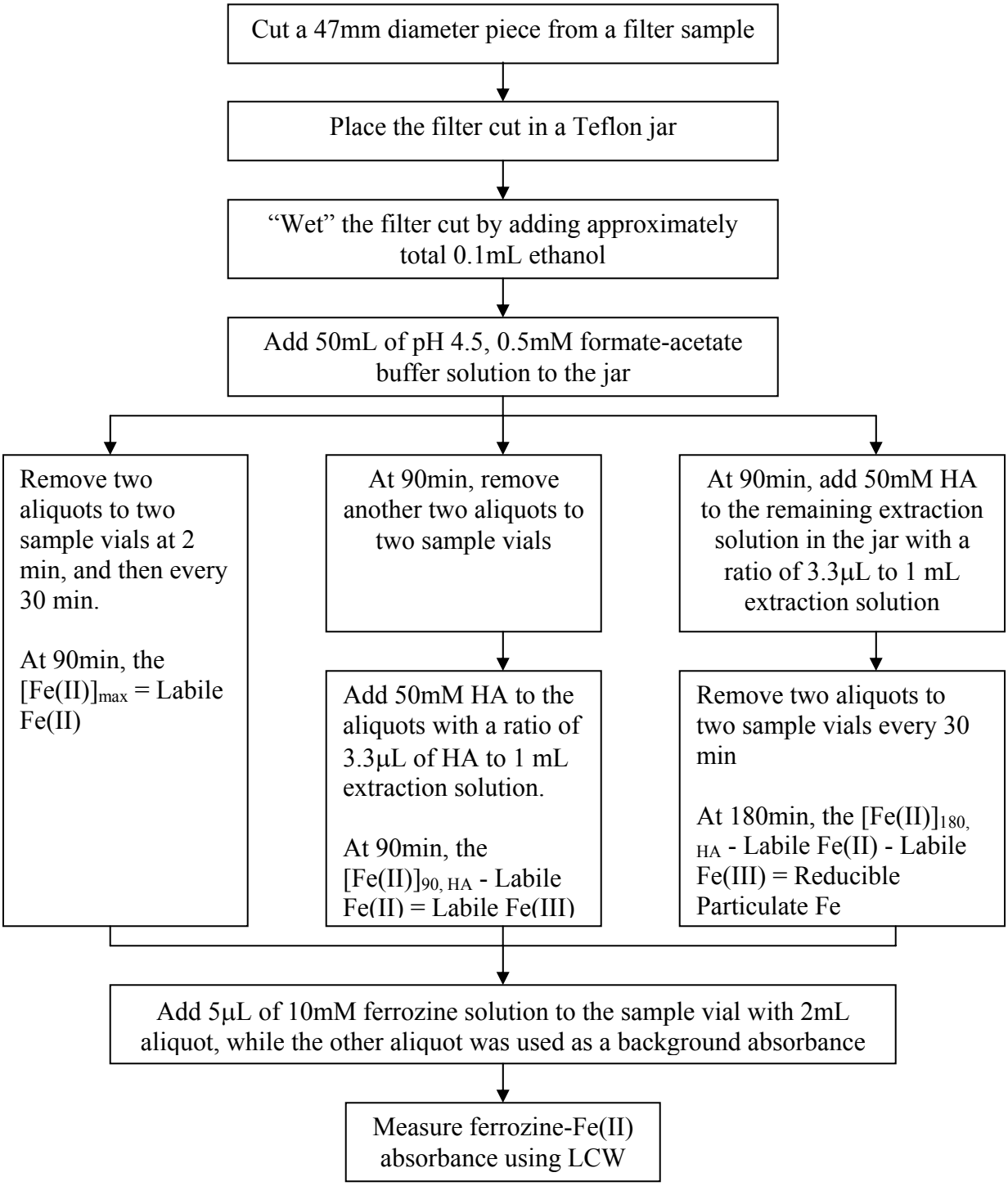

Figure 2-1. Sequential aqueous extraction procedure for measuring labile Fe species in ambient aerosol collected on Teflon membrane filters.

Fe(III) to Fe(II); however, this occurs at appreciable rates only when initiated photochemically using UV light (Pehkonen et al., 1993). A 47-mm diameter subsample from the 90-mm filter that collected the aerosol particles was cut using an acid-cleaned plastic (polycarbonate) die and a ceramic knife. The subsample was placed in a Teflon jar and ‘‘wetted’’ by adding approximately ten 0.01-mL drops of ethanol (total 0.1 mL) to increase the affinity between the aqueous extraction solution and Teflon membrane filter. Fifty milliliters of pH 4.5, 0.5 mM formate-acetate buffer solution were then added to the jar, and the jar was covered and gently swirled. After 2 min, one 2-mL aliquot and one 1-mL aliquot were removed and transferred to 5-mL sample vials. Five microliters of 10 mM ferrozine solution was added to the sample vial with 2-mL aliquot, while the 1-mL aliquot was used for a background absorbance spectrum. The ethanol and other species extracted from aerosol samples may contribute to the background absorbance. The aliquots were removed from the extraction solution every 30 min without filtration, and the ferrozine-Fe(II) absorbance was measured using LPAS. Fe(II) concentrations in the extraction solution usually reached a maximum or steady value after 60 to 90 min, and the Fe(II) concentration at the 90-min extraction time was defined as the labile Fe(II) (Figure 2-1). At 90 min, two other aliquots of the extraction solution were removed, and HA was added to the aliquots, with the ratio of 3.3 μL HA per mL of extraction solution, to reduce any dissolved or suspended labile Fe(III). The Fe(II) measured in the aliquot with HA included both the LFe(II) and the LFe(III) concentrations and was used to represent the labile (Fe(II) + Fe(III)) species. The labile Fe(III) concentration (Figure 2-1) was then calculated by subtracting the LFe(II) from the labile (Fe(II) +

Fe(III)) concentration at 90 min. HA was also added to the remaining extraction solution in the Teflon jar at 90 min, which was in contact with the filter subsample to dissolve labile Fe(III) particles that can undergo reductive dissolution. The Fe(III) particles would include Fe(III) oxyhydroxide minerals. The unfiltered aliquots were removed for Fe(II) measurements every 30 min, and the measured Fe(II) concentration at 180 min of the extraction procedure was defined as total labile Fe that includes LFe(II), LFe(III), and RPFe species. The reducible particulate Fe concentration (Figure 2-1) was then defined by subtracting the labile (Fe(II) + Fe(III)) out of the total labile Fe.

2.2.3 Iron Photo-reduction Experiments

Fe photo-reduction experiments were performed on seven aerosol filter samples using ambient sunlight. Five of these experiments were conducted using fine aerosol samples, and two of these experiments were conducted using coarse aerosol samples. Only the experiments using the fine aerosol samples are discussed since the two coarse filter samples had low labile Fe concentrations that made it difficult to follow Fe(III) reduction kinetics. Half of the 47-mm filter subsample was used for the sequential extraction procedure (Figure 2-1), and the other half was placed in a Teflon jar using a polystyrene petri dish as a window for the photo-reduction experiment. Equal volumes of the formate-acetate buffer solution were used for each extraction. The polystyrene petri dish had a transmission percent from 60% at 300 nm to 84% at 800 nm. The Teflon jar with the window was exposed to ambient sunlight that allowed labile Fe(III) to undergo photo-reduction reactions as opposed to the use of the chemical reductant, HA, that was added to the other solution after 90-min

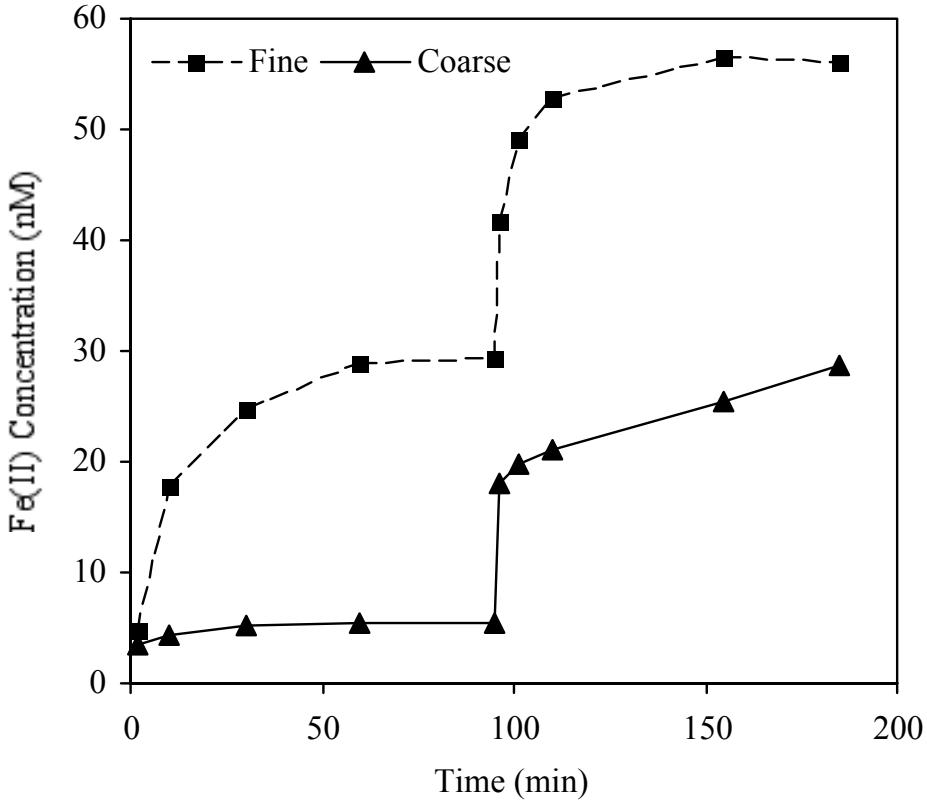

Figure 2-2. Example of the sequential extraction procedure showing Fe(II) concentrations in the extraction solution versus time; both fine and coarse fraction aerosol samples used in the extraction procedure were collected on 9 January 2001 over the sub-tropical North Atlantic Ocean. The increase in Fe(II) concentration at 90 min is where hydroxylamine (HA) was added to the extraction solution.

extraction process. Fe(II) concentrations were measured in both extraction solutions every 30 min.

2.3 Results

2.3.1 Labile Iron Measurements

The Fe(II) concentrations observed from both the fine and coarse filter samples usually increased with the extraction time and arrived at steady values after 60 to 90 min. Figure 2-2 shows the release of Fe(II) as a function of time following the procedure outlined in Figure 2-1 and using the aerosol sample collected on 9 January 2001, except that there were more time series measurements taken for the data in Figure 2-2. The sudden increase in Fe(II) concentration at 90 min (Figure 2-2) was after adding HA to the aliquots, showing that significant dissolved or suspended labile Fe(III) in the extraction solution can be quickly reduced to Fe(II) by HA. The Fe(II) concentration kept increasing after the addition of HA to the extraction solution at 90 min, and the rate of increase slowed down from 150 to 180 min (Figure 2-2) although it did not always reach a steady value. The increase of Fe(II) concentration after 90-min extraction time was probably due to the reductive dissolution of labile Fe(III) particles (e.g., Fe oxyhydroxides). Figure 2-2 also shows that the labile Fe concentrations extracted from fine fraction samples were higher than those from coarse fraction samples during the same day, which are consistent with labile Fe(II) measurements from previous studies (Johansen et al., 2000; Siefert et al., 1999).

2.3.2 Comparison between HA- and Photo-reducible Iron

A comparison of dissolution kinetics was performed between the HA extraction method and a photochemically reduced Fe extraction method using

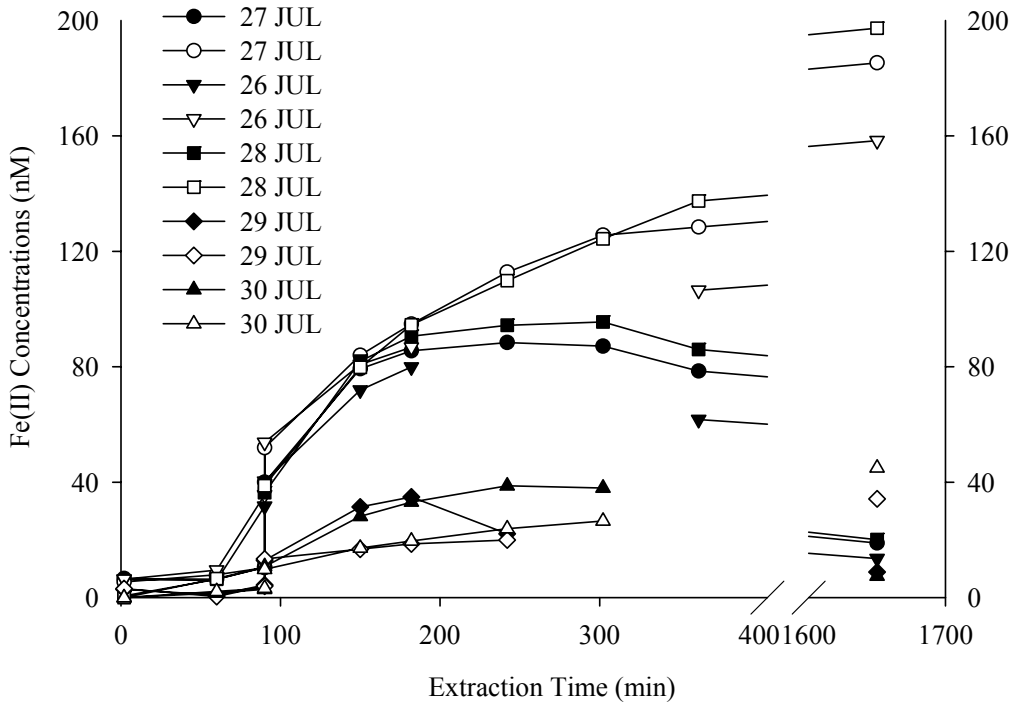

Figure 2-3. Comparison of reductive extraction processes between photoreduction (solid symbols) and HA-reduction (empty symbols). The fine aerosol fractions (with aerodynamic diameters less than 2.5μm) of five aerosol samples collected between 26 and 30 July 2001 over the tropical North Atlantic Ocean were used for the experiments.

ambient sunlight. Figure 2-3 shows all five comparison experiments that were done over a time period of 24 hours using the fine fractions of aerosol samples collected during 26 to 30 July 2001. Before the addition of HA or the exposure to ambient sunlight, labile Fe dissolution kinetics and Fe(II) concentrations in the extraction solutions were almost identical between the two methods (refer to the same-day filter samples in Figure 2-3). Then Fe(II) concentrations increased rapidly within 1 hour after the extraction solution was exposed to ambient sunlight (at approximately local noon) and reached a maximum after 90 to 150 min of exposure, where the steady state concentration of Fe(II) began to decline. This decrease in Fe(II) was probably due to a variety of reasons including the decreasing intensity of ambient sunlight, the loss of electron donating ligands, and the increase of photo-oxidants (e.g., hydrogen peroxide, hydroxyl radical, superoxide anions, and hydroperoxyl radical) that could oxidize Fe(II) in solution. The Fe(II) concentrations produced in the two extraction procedures began to diverge after 90-min extraction time due to the mechanisms described. However, it is clear that the reductive dissolution of Fe, in the case of the HA reduction, continues over a longer time period (over 1 day) compared to the photo-extraction in Figure 2-3. For both fine and coarse fractions of aerosol samples collected over the tropical and subtropical North Atlantic Oceans, the kinetics of Fe(III) reduction using HA in the extraction procedure was similar to that of Fe(III) photo-reduction in the formate-acetate buffer solution (pH 4.5) for the initial 90-min period.

2.4 Discussions

Three labile Fe species were measured and defined during the aqueous extraction procedure (Figure 2-1). The Fe(II) concentration in the extraction solution usually arrived at a maximum or steady value after 60 to 90 min (Figure 2-2), which indicated that most of the labile Fe(II) in the aerosol sample has been extracted into the solution during this time period. In some of the extractions, the Fe(II) concentrations were still increasing at 90 min; however, the rate of Fe(II) increase at 90 min was much slower than the initial rate of Fe(II) increase. The increase in Fe(II) during the first 90 min may be due to the dissolution of Fe(II) from the aerosol sample matrix and/or the reduction of Fe(III) by reductants from the aerosol sample. This labile Fe(II) species represents the most soluble and therefore the most bioavailable Fe pool from the atmospheric deposition that can be utilized by the biota in the surface seawater. Hutchins et al. (1999) observed that the uptake of organically complexed Fe was equal to or greater than inorganic Fe(III) added to phytoplankton where the inorganic Fe(III) additions were in excess of its solubility limit and suggested that these organic complexes prevented the precipitation of Fe(III) to less-available Fe(III) oxyhydroxide species. The photochemical reduction of Fe(III) complexes in seawater to form oxidized ligands and Fe(II) has also been shown to increase the bioavailability of the Fe (Barbeau et al., 2001). Miller and Kester (1994) also observed enhanced diatom growth after inoculating a solution of Fe colloids that had been exposed to light where they observed increases in Fe(II). They attributed the increase in the bioavailability of Fe to the photo-reductive dissolution of the colloidal Fe to Fe(II) and then the oxidation and precipitation of the Fe(II) to more labile Fe

oxyhydroxide colloids. The labile Fe(II) released from an aerosol particle into seawater upon deposition would be oxidized by dioxygen (with a half-life on the order of minutes) unless the Fe(II) is stabilized by a ligand (Miller et al., 1995). Once the Fe(II) is oxidized to Fe(III), the Fe(III) could become complexed with organic ligands (Millero et al., 1995) or precipitate to form Fe oxyhydroxides. Overall, the labile Fe(II) measured in the aerosol samples represents a form of Fe that is more labile than the other Fe species measured in ambient aerosol and would be initially expected to become truly dissolved in seawater. The labile Fe(II) as a dissolved species has a greater probability of being directly utilized by biota or converting to another form of dissolved Fe (e.g. organically complexed Fe(III)) that would also be bioavailable, or it could also precipitate into a bioavailable Fe oxyhydroxide colloid (Miller and Kester, 1994).

The initial increase in Fe(II) concentration at 90 min (Figure 2-2) was defined as the labile Fe(III) species. This fraction of Fe was measured by removing an unfiltered aliquot of the extraction solution at 90 min and using HA to reduce the labile Fe(III) that was either dissolved or suspended in this aliquot. The combination of labile Fe(II) and Fe(III) may represent the maximum dissolvable Fe into the seawater without considering photoredox chemistry and could include Fe-ligand complexes. However, the dissolution of aerosol Fe into the seawater is much more complicated than the extraction process due to high pH that causes the reoxidization of Fe(II) and various types of ligands that can form complexes with Fe(III) such as dissolved Fe(III)-carboxylate complexes (Voelker et al., 1997) and organic ligands (Hutchins et al., 1999). The dissolved Fe concentrations have been used as the

bioavailable Fe in the model calculation of atmospheric Fe supply to the upper ocean (Fung et al., 2000). The rate of Fe(II) increase slowed down from 150 to180 min, and the measured Fe(II) concentration at 180-min extraction time (Figure 2-2) included LFe(II), LFe(III), and RPFe species. The RPFe would significantly enlarge the bioavailable Fe pool by considering Fe reduction mechanisms that can occur both in the atmosphere and in the surface seawater. Labile Fe(II) generated photochemically in a pH 4.25 buffer solution was observed in aerosol samples collected from Whiteface Mountain, NY, and samples collected from rural and urban areas in California, and ranged from 2.8 to 100% of total aerosol Fe (Siefert et al., 1996). Voelker and Sedlak (1995) indicated that the reaction of dissolved Fe(III) with photochemically produced superoxide radical ($O_2^{\bullet -}$) is a potentially important source of Fe(II) in sunlit seawater. In the absence of organic complexation of Fe(III), approximately 60% of dissolved Fe (5 nM) was converted into Fe(II) after 20-min illumination (Voelker and Sedlak, 1995). Photoinduced ligand-to-metal charge transfer (LMCT) reaction of Fe(III)-fulvate complex was observed in the pH 3–5 experimental solutions and resulted in the reduction of Fe(III) (Voelker et al., 1997). Overall, each of these labile species of Fe can potentially be utilized by phytoplankton or diazotrophs although there may be differences in the uptake rates of the different labile forms of Fe.

The dry deposition velocity for mineral aerosol is primarily a function of particle size, ranging from 0.4 to 2 cm s^{-1} over the oceans (Prospero, 1995). Jickells and Spokes (2001) compared the dust deposition estimates and sediment trap records in the Sargasso Sea and suggested that a mean velocity of 1.0 cm s^{-1} is appropriate for

Fe. The well-mixed marine boundary layer (MBL) varies from 500 to 2000 m, so using a value of 1000 m for the MBL height and 1.0 cm s^{-1} for deposition velocity, the residence time of aerosols in the MBL can be estimated. The calculated residence time was approximately 28 hours for aerosols in the MBL, which indicated that the aerosol particles collected by the HVDVI were able to circulate in the MBL for more than 1 day before depositing to the surface seawater. And smaller particles would be expected to have a longer residence time due to the smaller deposition velocity for smaller particles. This residence time in the atmosphere exposes the aerosol particles to intense sunlight, and Fe in the aerosol may undergo photochemical reactions that process the Fe into more labile, and presumably more bioavailable, species before being deposited into the ocean. Furthermore, the residence time for aerosol particles in the atmosphere is much longer than 28 hours since they originated from terrestrial sources (e.g., North Africa) and were transported aloft for days before being entrained into the MBL. And the atmospheric processing may be different between different regions of the atmosphere (e.g., MBL, upper troposphere) because of different conditions (e.g., UV light intensity, temperature, and humidity).

The aerosol particles in the atmosphere can undergo aqueous processing when the particles become incorporated into cloud droplets or if the aerosol particles are deliquesced. Most clouds do not result in precipitation and therefore after the cloud evaporates the nonvolatile species (e.g., Fe) will remain in aerosol particles. This atmospheric processing of aerosol Fe will most likely lead to more labile forms of Fe as more refractory forms of Fe in the original source particle undergo dissolution and then precipitate out of solution as the cloud droplet evaporates. Therefore reducible

Fe was measured for both fine and coarse fractions of aerosol samples with consideration to the potential dissolution and photoredox processing of Fe in the atmosphere. The reducible Fe measurements were performed in this study using similar reaction conditions with the chemical reductant HA, and therefore the results are comparable to conditions expected in the atmosphere. In addition, many of the same Fe redox reactions occurring in the atmosphere may also be important to Fe redox chemistry in seawater (for Fe redox chemistry examples in natural waters see Emmenegger et al., 2001; Miller et al., 1995).

The production of Fe(II) in both HA and photochemical reductions can be approximated by a pseudo-first-order reaction (Siefert et al., 1996), where HA was added in excess to Fe(III) in the extraction solution. The labile Fe(III) was reduced to Fe(II) in the extraction solution with the pseudo-first-order rate constant k', and the corresponding rate law is given by

$$d[Fe(III)]/dt = -k'[Fe(III)] \qquad (1)$$

The mass balance on [Fe(II)aq] is given by

$$[Fe(II)_{aq}] = [Fe(II)_{aq}]_0 + ([Fe(III)]_0 - [Fe(III)]) \qquad (2)$$

where $[Fe(III)]_0$ is the maximum reducible Fe(III). Integrating equation (1) and combining with equation (2) yields:

$$[Fe(II)_{aq}] - [Fe(II)_{aq}]_0 = [Fe(III)]_0(1 - e^{-k/t}) \qquad (3)$$

The average rate constants for photo- and HA- reduction processes, determined by fitting the experimental data (3.5 hours of reduction processes) to equation (3), were 0.020 and 0.0076 min^{-1}, respectively (Figure 2-4). The photo-reduction of Fe(III) was about three times as fast as the HA reduction within the

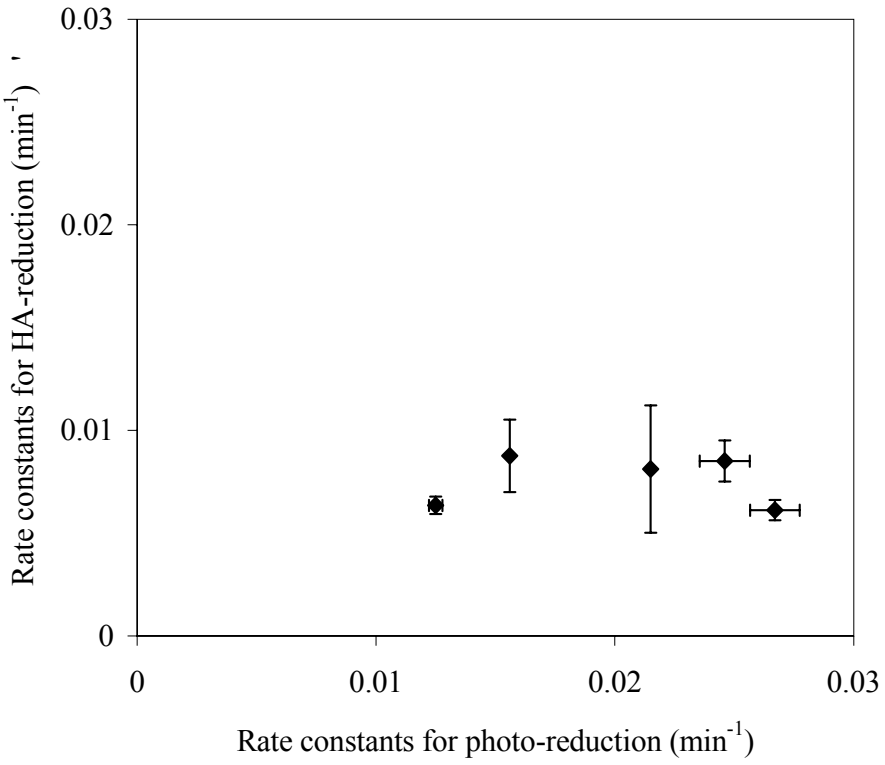

Figure 2-4. Comparison of rate constants between photo- and HA-reduction processes performed in the same buffer solution. The rate constants were determined by fitting Fe(II) production versus time to the pseudo-first-order equation. Aerosol samples used for the reduction experiments were collected during 5 continuous days (26 to 30 July 2001). The error bars are the standard error for the rate constants determined from the least squares fit of the pseudo-first-order equation.

initial 2-hour reduction period and then arrived at the maximum before the Fe(II) concentration began to decrease. The absolute rates of Fe(II) oxidation and Fe(III) reduction should be equal when the Fe(II) reaches a steady value in the photoredox experiments; however, a steady value is usually not attained for a significant period of time because of decreasing ambient light intensity or increasing photooxidants. Loss of electrondonating ligands probably has only a slight effect on photoredox kinetics of Fe in aerosol samples. For example, although it is from a polluted area, it has been reported that sufficient electron donors were present in the ambient aerosol (Pasadena, CA) for the photoreduction of Fe(III) (Siefert et al., 1996). Although the photo-reduction of Fe(III) was faster than HA-reduction, the absolute Fe(II) amounts produced by both reduction processes were similar after 60 to 90 min, considering the different reduction mechanisms. Therefore the reducible Fe concentrations, measured by using HA in the extraction procedure with a 90-min reduction time (Figure 2-1), represent the minimum photo-reducible Fe in the aerosol samples.

The clear-sky ambient sunlight photolysis rate constant for the $Fe(OH)^{2+}$ species (at 47.4°N latitude, 440 m elevation, 30 June) is 0.038 min^{-1} (Faust and Hoigne´, 1990). King et al. (1993) also found an apparent first-order rate constant of 0.08 min^{-1} (solar noon, 40°N latitude) for Fe(III) photolysis solution at pH 4.4 with 0.5 M NaCl using a solar simulator. At pH 4.5 the dominant Fe(III) hydroxyl species is $Fe(OH)^{2+}$, and this is also the dominant photo-reactive Fe(III) hydroxy species (Faust and Hoigne´, 1990). Both these rate constants are in relatively good agreement with the photochemical reduction experiments where the rate constants were between 0.012 and 0.027 min^{-1} (Figure 2-4). Overall, the rate constants observed in this study

were slightly slower than the rate constants from the laboratory studies. This may be due to several reasons including variations in actinic flux due to the configuration of the reactor vessel and window used in this study (e.g., the window had a transparency of 60% at 300 nm), the formate or acetate in the extraction solution may serve as the electron donor in the photolysis reaction (Pehkonen et al., 1993), or there may also be other organic ligands in the aerosol sample that form photoactive Fe(III)-ligand complexes.

When the irradiated solution was returned to the lab and monitored over night, the Fe(II) concentration decreased to approximately 20% of the maximum, which was still approximately twice as high as the Fe(II) concentration measured before solar irradiation. Jickells (1999) described that aerosols are exposed to low pH and high ionic strength conditions during a number of condensation evaporation cycles in clouds before finally being deposited. These conditions may enhance the Fe solubility, and this process is not totally reversible. Therefore daily solar radiation increases labile Fe concentrations in ambient aerosols. A higher percentage of labile Fe(II) in total Fe will be expected to exist in aerosol that has been transported far from the original sources and had more opportunities to undergo photochemical processing in the atmosphere.

2.5 Conclusions

Aerosol samples (24 hour) were collected using an HVDVI during research cruises in the tropical and subtropical North Atlantic Ocean. Labile Fe concentrations were measured on board by using a sequential aqueous extraction procedure that included a chemical reductant (HA) and used LPAS with a detection limit of 1 nM to

measure Fe(II). LFe(II), LFe(III), and RPFe species were defined according to the extraction time and addition of chemical reductant HA during the extraction procedure. Previous studies investigating Fe uptake by marine microorganisms suggest that the labile fractions of Fe measured in this study are related to the Fe bioavailability. The extraction procedure also followed the dissolution and reduction kinetics of the labile Fe. Reducible Fe concentrations, measured by HA in the extraction procedure, were compared to the photoreducible Fe concentrations, showing that they had not only similar kinetics (pseudo first order) for reduction processes but also approximately equal Fe(II) concentrations produced after a time period of about 90 min. This fraction of reducible Fe could potentially be used to determine the maximum amount of labile atmospheric Fe that is deposited into the ocean. These measurements provide information about the initial speciation of Fe upon deposition to surface waters. After deposition to the water, Fe can undergo a variety of dissolution, precipitation, complexation, and redox processes that can be abiotic and/or biologically controlled. Studying reducible Fe in aerosols represents an initial step toward understanding the role of atmospheric Fe solubility and bioavailability to marine microorganisms. The results from this study provide further evidence of the complexity of Fe speciation in the atmosphere and that understanding this initial speciation is critical to understanding how atmospherically derived Fe is cycled through marine systems.

Chapter 3: Seasonal and Spatial Distributions and Dry Deposition Fluxes of Atmospheric Total and Labile Iron over the Tropical and Subtropical North Atlantic Ocean

3.1 Introduction

Fe is a critical micronutrient that limits primary productivity in the high-nitrate low-chlorophyll (HNLC) regions of the ocean (Behrenfeld et al., 1996; Boyd et al., 2000). Fe is also a crucial micronutrient for diazotrophic microorganisms and therefore may influence nitrogen fixation in oligotrophic oceans (Falkowski, 1997; Gruber and Sarmiento, 1997). Atmospheric deposition is the primary source of Fe to the oligotrophic ocean, and previous studies have investigated the concentrations, deposition and solubility of atmospheric Fe. The reported solubility of atmospheric Fe in seawater spans over 2 orders of magnitude (1 to 50%) although most are at the low end of this range (Zhuang et al., 1990; Chester et al., 1993b; Zhu et al., 1992, 1993; Jickells, 1999). Measuring this soluble Fe fraction along with understanding the process that controls the Fe solubility is important since this soluble Fe may be associated with the amount of bioavailable Fe derived from the atmospheric deposition.

There are relatively few field studies investigating aerosol Fe speciation in the marine boundary layer (MBL) of oligotrophic oceans, which results in large uncertainties associated with model calculations of Fe and bioavailable Fe fluxes to world oceans. Zhu et al. (1993) measured the total soluble Fe(II), total soluble Fe and total Fe concentrations in marine aerosol samples collected at Barbados, and showed that only 1% of the total Fe and 7.5% of the soluble Fe were in the Fe(II) oxidation

state. A clear diel variability in the concentration of soluble Fe(II), with day values (mean 3.7 ng m^{-3}) about twice night values (1.5 ng m^{-3}), was also observed in marine mineral aerosols at Barbados (Zhu et al., 1997). Zhu et al. (1993) measured the soluble Fe by leaching a filter with the aerosol sample in a pH 1.0 NaCl solution for 5 min at ambient temperature, and the leached solution was filtered through a 0.2 μm Nuclepore filter for Fe(II) analysis. Siefert et al. (1999) reported that the aqueous labile Fe(II) concentrations were between 4.75 and <0.4 ng m^{-3} during the intermonsoon but below the detection limit (<0.34 ng m^{-3}) during the southwest monsoon over the Indian Ocean. Siefert et al. (1999) measured the aqueous labile Fe(II) by extracting a filter with the aerosol sample in a pH 4.2 formate buffer solution for 30 min and then filtering the extract through a 0.2 μm cellulose acetate syringe filter. Most of the labile Fe(II) was in the fine aerosol size fraction (diameter <2.5 μm) during the intermonsoon although most of the total Fe was in the coarse fraction. This fine-fraction ‘‘enrichment’’ was also observed over the tropical Atlantic ocean where the labile Fe(II) was about 0.5% of total aerosol Fe and correlated with NSS SO_4^{2-} and oxalate concentrations (Johansen et al., 2000). The correlations with NSS SO_4^{2-} and oxalate may be due to either the chemistry occurring in the aerosol or possibly a common origin for these species (e.g., anthropogenic activities, Johansen et al., 2000).

The North Atlantic and North Pacific oceans are the two oceanic basins with the highest atmospheric Fe fluxes, accounting for 48% and 22% of the total aerosol Fe flux to the world oceans, respectively (Gao et al., 2001). The Fe flux occurs as both wet and dry deposition and models predict that the fluxes due to both processes

have a similar magnitude over the coastal and open oceans (Gao et al., 2003). In wet deposition the aerosol Fe is incorporated into the rain droplets by either serving as the cloud condensation nuclei or through within-cloud or below-cloud scavenging processes. The dry deposition flux can be calculated by multiplying the atmospheric concentration by a deposition velocity that is primarily a function of particle size, wind speed and relative humidity. Several comprehensive models have been developed for particle deposition to natural water surfaces (Slinn and Slinn, 1980, 1981; Williams, 1982). Slinn and Slinn's (1981) model showed that the particles with 1 to 10 μm radius have a dry deposition velocity around 1.0 cm s^{-1} under the condition of 5 m s^{-1} wind speed and 100% relative humidity. Jickells and Spokes (2001) suggested that a mean value of 1.0 cm s^{-1} properly represented dry deposition velocity of atmospheric Fe by comparing dust deposition estimates and sediment trap records in the Sargasso Sea. The North Atlantic Ocean is under the influence of mineral dust plumes transported from North Africa (Sahel and Saharan regions) as well as anthropogenic sources from North America and Europe. Great variability in Fe concentrations and labile Fe(II) fractions have been observed in this tropical and subtropical North Atlantic region (Johansen et al., 2000). Moreover, Asian dust storms can travel all the way across North America and reach the North Atlantic Ocean as observed by Satellite based sunphotometry measurements (Thulasiraman et al., 2002) and aerosol data from the Interagency Monitoring Program for improved Visual Environments (IMPROVE) network (Jaffe et al., 2003).

This chapter presents further measurements of labile Fe concentrations using a new extraction method that analyzes for reducible labile fractions of Fe along with

aqueous labile Fe(II) species (Chen and Siefert, 2003). This more detailed investigation of labile forms of Fe in aerosols is important to understanding the processes controlling labile Fe fractions along with quantifying the flux of these species to oceanic regions where labile Fe may be an important rate limiting nutrient. Labile Fe concentrations were measured in aerosol samples collected during two research cruises (winter and summer) over the tropical and subtropical North Atlantic Ocean. Mineral dust plumes transported by trade winds from North Africa are a dominant source of Fe to this North Atlantic region. The zone of maximum dust transport off North Africa coast moves north from about 5°N in winter to 20°N in summer as evident in satellite images (Husar et al., 1997; Moulin et al., 1997). This shift is driven by the seasonal migration of the intertropical convergence zone (ITCZ). The data from the two cruises in this study were taken between 0°N and 30°N and spanned this zone of maximum dust transport. The aerosol samples were collected using a dichotomous aerosol sampler and the analysis was performed on both the fine-fraction (diameter <2.5 μm) and coarse-fraction (diameter >2.5 μm) aerosol samples. Three labile Fe species, including Fe(II) species and reducible Fe(III) species, were analyzed using an aqueous extraction procedure and LPAS (Chen and Siefert, 2003). The labile Fe fractions measured were hypothesized to have different degrees of bioavailability to marine microorganisms. The analysis of labile Fe species was performed immediately after sample collection to minimize the effects due to sample storage (e.g., redox reactions). Total Fe concentrations were determined back in the laboratory using microwave assisted strong acid digestion of the filter samples followed by analysis of the digestion solution using inductively

coupled plasma mass spectrometer (ICP-MS). The atmospheric Fe data will be presented along with the air mass back trajectories (AMBTs), giving a detailed map of distributions of Fe and labile Fe fractions in aerosols over the tropical and subtropical North Atlantic Ocean. The potential atmospheric Fe sources are discussed and mean atmospheric total and labile Fe dry deposition fluxes are calculated.

3.2 Sampling Sites and Methods

3.2.1 Aerosol Collection

Aerosol samples (approximately 24 hour sampling times) were collected during two cruises (6 January to February 2001 and 27 June to 15 August 2001) over the tropical and subtropical North Atlantic Ocean. A high-volume dichotomous virtual impactor (HVDVI) (Solomon et al., 1983) was used to collect two size fractions of ambient aerosols with an aerosol aerodynamic diameter cutoff of 2.5 μm. The fine- and coarse-fraction aerosols were collected on two 90 mm diameter Zefluor Teflon membrane filters (Gelman Zefluor, 1 μm pore size). The HVDVI aerosol collector was constructed out of polycarbonate with nylon screws in order to minimize trace metal contamination and had a total flow rate of 330 L min^{-1}. The filters, HVDVI and laboratory equipment were acid-cleaned using ultrapure acids (Seastar Chemicals, Inc.) and 18.2 MΩ cm Nanopure water (Barnstead). An orifice plate meter, gas meter and critical orifice were used to control and measure the flow rates through the collector. A sector sampling system was used to control the aerosol collector. The system was configured to allow collection of ambient aerosol samples only when the relative wind direction was ±75° relative to the ship's bow during both

the winter and summer Atlantic cruises. New filters were loaded every 24 hours, and the sampling duration depended the time that the system was in sector.

3.2.2 Labile Iron Analysis

LFe(II), LFe(III) and RPFe, were the three labile Fe species investigated using an aqueous extraction procedure and measured using LPAS immediately after sample collection. This method is briefly outlined below, and a more detailed discussion of the method is given in Chapter 2 (also see Chen and Siefert, 2003). Labile Fe species were operationally defined by the extraction time and reagents. The extraction time was determined by following the release of Fe over time and noting the characteristic time where Fe had reached a maximum for each step in the aqueous extraction procedure. A 47 mm diameter subsample from the 90 mm aerosol filter sample was cut for labile Fe measurements. The remaining portion of the aerosol filter sample was stored in a freezer and later subsampled and analyzed for total metals and soluble ions. The 47 mm subsample was placed in a Teflon jar and ‘‘wetted’’ by adding approximately ten 0.01 mL drops of spectrophotometric grade ethanol to increase the affinity between the aqueous extraction solution and the hydrophobic Teflon membrane filter. The extraction solution (50 mL of pH 4.5, 0.5 mM formate-acetate buffer solution) was then added to the jar, and the jar was covered and gently swirled. After 2 min, a 2 mL aliquot and a 1 mL aliquot were removed and transferred to 5 mL sample vials; 5 μL of 10 mM ferrozine solution was added to the sample vial with 2 mL aliquot, while the 1 mL aliquot was used for a background absorbance spectrum. The ferrozine reagent forms a colored complex with Fe(II) in solution that can be used to quantify Fe(II) using absorbance spectrometry (Stookey, 1970). Aliquots were

removed from the extraction solution every 30 min without filtration and the ferrozine-Fe(II) absorbance was measured using LPAS with a 1 m path length (Waterbury et al., 1997). The measured Fe(II) concentration at the 90 min extraction time was defined as the LFe(II) since Fe(II) concentrations typically reached a maximum by 90 min in the extraction solution. At 90 min another two aliquots of the extraction solution were removed and HA (50 mM) added to the aliquots with the ratio of 3.3 μL of HA per mL of extraction solution. The Fe(II) concentration measured in the aliquot with HA minus the LFe(II) was defined as the LFe(III). HA was also added to the remaining extraction solution in the Teflon jar at 90 min, that was in contact with the filter subsample to dissolve labile Fe(III) particles that can undergo reductive dissolution. The unfiltered aliquots were removed for Fe(II) measurements every 30 min, and the measured Fe(II) concentration at 180 min of the extraction procedure was defined as total labile Fe. The RPFe species was then calculated by subtracting the LFe(II) and LFe(III) from the total labile Fe. Chen and Siefert (2003) observed that photochemical reduction of Fe(III) species using ambient sunlight had similar Fe(II) production rates as extractions using hydroxylamine as a reducing agent.

3.2.3 Total Elemental Analysis

A strong-acid microwave digestion procedure followed by ICP-MS (HP 4500) was used to measure total elemental concentrations. The digestion procedure was run in a batch of six Teflon bombs with four filter samples, one blank and one sample of Standard Reference Material (SRM) 2709 San Joaquin Soil (U.S. Department of Commerce, National Institute of Standards and Technology) for quality control. Two

grams of 10 N nitric acid (Seastar Chemical, Inc.) were added to each Teflon bomb. The microwave heating cycle was 200 W for 5 min and then 700 W for 2 min. After being cooled to the room temperature, the bombs went through a second heating cycle: 200 W for 10 min, addition of 0.1g of 28N hydrofluoric acid (Seastar Chemical, Inc.), and then 700 W for 2 min. Finally, 28 g of 18.2W milli-Q water was added to each bomb. The mass of each bomb was monitored to check for venting of acids in the digestion process, and the total loss was controlled within 0.03 g to minimize the effects of matrix variability. A multielement internal standard of Sc, In and Bi (SPEX CertiPrep, Inc.) was added to the sample before analysis of total elemental concentrations in the digestion solution using ICP-MS. The atmospheric concentrations were then calculated using the mass of the extraction solution, the concentration of the element, the volume of the air sampled and the fraction of the filter sample used in analysis.

3.2.4 Ion Analysis

A subsample of the 90 mm Teflon filter sample was analyzed for anions and cations using an aqueous extraction technique (Derrick and Moyers, 1981) and ion chromatography using a Dionex DX-600 system. Anions were separated and eluted using an AS15 anion column (Dionex) using a KOH eluent in gradient mode, and cations were separated and eluted using a CS12A cation column (Dionex) using a methanesulfonic acid (MSA) eluent in gradient mode. The atmospheric concentrations were then calculated using the mass of the extraction solution, the concentration of the ion, the volume of the air sampled and the fraction of the filter sample used for the analysis. NSS SO_4^{2-} concentrations were calculated by

subtracting the sulfate contribution to the aerosol due to sea salt by using the average ratio between sulfate and sodium in the seawater along with the sodium concentrations in the aerosol (Duce et al., 1983).

3.2.5 Air Mass Back Trajectories

AMBTs were calculated from the National Oceanic and Atmospheric Administration (NOAA) FNL database using the Hybrid Single-Particle Langrangian Integrated Trajectories (HY-SPLIT) program (Draxler, 2002). The model calculation method is a hybrid between Eulerian and Lagrangian approaches. Trajectory calculations were made in the Lagrangian framework. The particle passive transport by the wind is computed from the average of the three-dimensional velocity vectors at the particle's initial-position P(t) and its first-guess position P'(t+dt). Trajectories may be integrated both forward and backward in time. The error in a trajectory calculation is primarily due to the fact that meteorological fields, which vary continuously in space and time. The other error is that a particular trajectory may have little relationship to the pollutant plume dispersion pattern. Trajectories only represent the flow path of a single particle at the time of the initial release. As a pollutant spreads out both horizontally and vertically, due to dispersion, it may take many different paths in addition to the initial trajectory. The model calculation requires surface pressure or terrain height, horizontal wind components, temperature, and moisture, but not the settling velocities of the particles. If wet deposition is to be included, the model also requires the rainfall field.

AMBTs were performed at 100 m, 500 m and 1500 m height levels over the sampling position at 2000 UTC (corresponding to 7:00 PM local time that was about

midway during the sample collection period) for each day of the cruises. Atmospheric aerosols do not always follow these trajectories due to scavenging processes and gravitational settling of the aerosol (Ellis and Merrill, 1995), and there are errors associated with these AMBTs due to the data sets and models. However, the AMBTs still provide useful information about the synoptic situation and general source of the air mass sampled.

3.3 Results and Discussions

3.3.1 Spatial and Seasonal Distributions of Atmospheric Iron

Table 3-1 lists the concentrations of LFe(II), LFe(III), RPFe, and total Fe in both the fine- and coarse-fraction aerosols along with the sampling dates and locations. The data have been placed into five categories: (1) 26°N to 30°N Atlantic region in winter (WIN26), (2) 5°N to 26°N Atlantic region in winter (WIN15), (3) 26°N to 30°N Atlantic region in summer (SUM26), (4) 6°N to 26°N Atlantic region in summer (SUM15), and (5) 0°N to 6°N Atlantic region in summer (SUM5). This categorization was done according to total Fe concentrations, locations, and dates of aerosol sample collection (see Figure 3-1). Total NSS SO_4^{2-} and oxalate concentrations are also listed in Table 3-1.

Table 3-1. Concentrations of labile and total Fe, NSS-sulfate and oxalate in both fine and coarse fraction aerosols collected during the winter (6 January 2001 to 19 February 2001) and summer (27 June 2001 to 15 August 2001) research cruises over the Atlantic Ocean

Location		Date	Labile Fe(II) ng m^{-3}		Labile Fe(III) ng m^{-3}		Reducible particulate Fe, ng m^{-3}		Total Fe ng m^{-3}		NSS-Sulfate nmol m^{-3}	Oxalate nmol m^{-3}
Latitude N	Longitude W	Julian Day	Coarse	Fine	Coarse	Fine	Coarse	Fine	Coarse	Fine	Coarse + Fine	Coarse + Fine
26°N to 30°N Atlantic region in winter (WIN26)												
-	-	6	-	-	-	-	-	-	17.8	13.5	20.4	1.49
27.8	75.5	7	-	-	-	-	-	-	25.9	15.1	19.4	1.05
28.1	70.9	8	0.37	1.98	0.13	0.12	0.14	0.25	6.05	4.58	20.3	1.21
28.4	66.9	9	0.32	0.32	0.42	0.34	0.08	0.10	2.84	<2.5	5.27	0.4
28.6	63.3	10	0.10	0.34	0.09	0.08	0.18	0.09	0.81	0.83	8.94	0.2
29.2	55.2	12	0.05	0.36	0.04	0.14	0.07	0.26	<0.3	2.44	2.69	0.13
29.5	51.3	13	-	-	-	-	-	-	0.72	2.11	1.99	0.15
29.9	48.2	14	0.04	0.13	<0.05	0.02	0.04	0.20	3.73	2.08	1.61	0.1
29.6	46.5	15	0.01	0.05	<0.04	0.02	0.03	0.05	0.1	<0.4	1.08	0.1
27.8	45	16	0.02	0.1	0.03	0.04	0	0.09	0.29	1.67	1.68	0.15
Average			0.13	0.47	0.14	0.11	0.08	0.15	6.47	5.29		
5°N to 26°N Atlantic region in winter (WIN15)												
25.3	45	17	0.07	0.44	0.13	0.17	0.11	0.24	13.9	21.3	2.19	0.23
21.5	45	18	0.04	0.73	0.25	0.31	0.20	0.36	18.9	18	3.87	0.32
16.8	45	19	0.30	1.13	0.94	2.30	0.65	<0.07	108	186	7.54	0.27
13.2	45	20	1.43	2.89	0.51	0.16	3.89	<0.06	249	397	17.8	1.24
10.2	45.2	21	0.89	3.87	0.42	15.2	1.79	0.86	161	729	15.8	0.59
10.2	46.5	22	0.49	3.31	0.47	9.38	1.75	4.99	181	230	9.92	0.59
10.5	47.8	29	0.16	1.78	0.78	1.83	0.25	1.36	32.9	87.7	2.84	0.24
9.36	47.5	34	1.25	4.15	0.28	0.99	0.58	2.04	67	116	5.97	0.59
7.41	48.2	35	3.71	10.8	0.67	7.81	3.29	8.93	320	647	14.8	1.62
6.31	47.1	36	0.98	6.88	1.79	6.27	4.06	13.5	142	454	8.72	0.85
7.22	45.1	37	2.10	10.7	1.76	14.7	3.23	1.24	139	529	9.09	0.6
7.17	43	38	3.79	10.1	0.78	5.33	2.03	5.33	137	418	6.86	0.57
8.61	41.3	39	2.48	5.44	<0.05	12.4	2.49	7.82	128	301	5.28	0.36
9.34	41.5	40	1.75	5.52	1.95	0.90	0.76	9.96	170	345	5.19	0.43

Location		Date	Labile Fe(II) ng m^{-3}		Labile Fe(III) ng m^{-3}		Reducible particulate Fe, ng m^{-3}		Total Fe ng m^{-3}		NSS-Sulfate nmol m^{-3}	Oxalate nmol m^{-3}
Latitude N	Longitude W	Julian Day	Coarse	Fine	Coarse	Fine	Coarse	Fine	Coarse	Fine	Coarse + Fine	Coarse + Fine
10.9	42.4	41	7.90	19.9	5.97	5.06	6.92	17.2	369	404	16.9	1.09
10.1	44.7	42	5.02	12.1	2.63	10.0	2.73	14.3	352	729	5.02	0.92
9.81	44.5	43	2.67	22.4	5.65	5.32	3.43	14.4	383	836	10	0.89
10.6	46.6	44	6.71	15.8	0.77	6.07	2.30	12.1	213	484	5.42	0.82
9.44	49.2	45	5.97	14.4	2.68	5.11	1.69	13.5	149	415	14.3	0.79
9.08	51.8	46	3.48	7.80	0.75	4.96	1.40	3.39	154	351	11	0.61
9.41	55.3	47	5.77	12.5	0.84	12.1	3.26	7.75	500	1084	16.6	0.87
10.9	56.1	48	3.68	9.54	2.35	12.3	4.97	7.22	521	1167	7.31	0.61
11.3	54.8	49	8.89	12.1	2.97	16.7	4.34	7.52	352	607	4.73	0.5
Average			3.02	8.46	1.61	6.75	2.44	7.34	211	459		
26°N to 30°N Atlantic region in summer (SUM26)												
29.2	27.4	178	≤0.05	0.07	0.06	0.07	0.03	0.13	2.67	3.15	3.99	0.24
29.3	29.6	179	0.02	0.08	0.04	0.09	0.06	0.07	1.79	2.74	3.72	0.31
29.4	33.5	180	≤0.03	0.06	0.02	0.10	0.05	0.08	4.88	2.07	3.3	0.28
29.5	37.4	181	0.09	0.11	0.07	0.08	0.17	0.10	66.4	2.4	3.85	0.38
29.5	39.3	182	0.04	0.25	0.20	0.39	0.07	0.07	79.1	23.2	6.91	0.29
29.6	43.2	183	0.01	0.24	0.06	0.40	0.02	0.03	7.17	8.53	6.81	0.25
29.6	45	184	0.17	0.74	0.84	2.28	1.71	1.54	154	80.5	10.2	0.48
Average			0.07	0.22	0.18	0.49	0.30	0.29	45.1	28.8		
6°N to 26°N Atlantic region in summer (SUM15)												
25.5	48.6	185	0.04	0.78	0.53	1.73	0.62	1.09	137	70.3	5.1	0.26
22.6	51.3	186	≤0.03	0.56	0.17	1.53	0.35	0.82	62.9	59.1	4.57	0.46
16.3	56.8	187	0.05	0.94	0.46	1.96	0.48	1.21	145	102	1.82	0.24
-	-	188	-	-	-	-	-	-	114	115	5.33	0.31
11.8	54.4	190	≤0.05	0.53	0.43	1.57	0.56	0.98	61.7	79.7	1.41	0.17
11.8	54.4	190	0.08	0.27	0.43	0.99	0.57	0.81	77.4	91.4	4.35	0.23
10.4	48.1	191	0.41	1.54	1.48	6.88	1.22	2.87	356	320	8.51	0.52
10.4	48.1	192	0.08	1.02	0.71	3.15	0.99	2.40	117	199	4.05	0.34
10.4	48.1	193	-	0.33	-	0.85	-	1.14	81.1	108	11.8	0.59
9.8	45.3	194	0.17	-	0.85	-	0.65	-	195	223	6.41	0.29

Location		Date	Labile Fe(II) ng m^{-3}		Labile Fe(III) ng m^{-3}		Reducible particulate Fe, ng m^{-3}		Total Fe ng m^{-3}		NSS-Sulfate nmol m^{-3}	Oxalate nmol m^{-3}
Latitude N	Longitude W	Julian Day	Coarse	Fine	Coarse	Fine	Coarse	Fine	Coarse	Fine	Coarse + Fine	Coarse + Fine
10.1	45.4	195	0.09	0.63	0.89	3.28	0.72	1.63	266	256	7.9	0.32
10.2	45.5	196	0.09	0.66	0.57	2.40	0.96	1.85	283	205	6.42	0.4
11	49.3	197	0.22	1.36	1.45	5.65	0.32	1.58	558	304	6.96	0.49
-	-	198	-	-	-	-	-	-	242	271	5.1	0.32
11.6	58.2	200	0.01	0.70	1.08	6.01	0.80	1.97	263	229	4.67	0.6
10.3	56.3	201	0.26	0.49	0.80	2.97	0.98	1.26	147	92.8	3.94	0.68
10.2	56.3	202	0.09	1.15	1.12	3.69	0.97	2.20	138	143	2.33	0.55
10.2	56.3	203	0.20	-	0.68	-	0.93	-	61.2	106	3.56	0.71
11.9	54.9	207	0.02	0.50	0.34	2.34	0.66	1.74	95.7	104	2.37	0.25
10.4	53	208	0.10	0.81	0.58	3.24	1.31	3.35	249	250	6.62	0.31
8.74	51	209	0.02	0.60	0.41	1.60	0.55	3.16	67.3	137	4.02	0.33
7.23	48.5	210	<0.03	0.20	0.17	0.48	0.17	0.27	20	22.4	4.38	0.93
8.21	52.8	219	0.10	0.82	0.50	1.99	0.64	1.41	147	120	3.66	0.4
10.5	55	221	<0.03	1.34	0.60	3.68	0.89	2.22	157	223	4.75	0.13
10.6	55.8	222	<0.04	1.44	0.46	1.54	0.84	2.32	126	125	3.24	0.3
12.5	55.1	223	0.08	1.42	0.31	7.18	1.55	2.45	290	384	7.01	0.3
12.5	54.1	224	0.26	0.94	1.19	4.11	0.97	2.54	240	194	<0.1	0.01
11.4	53.8	225	<0.05	1.61	0.28	2.51	1.02	1.48	48.2	90.3	1.54	0.28
11.8	54.6	226	0.05	0.18	0.11	0.33	0.17	0.05	23	15.7	4.42	0.95
Average			0.12	0.83	0.64	2.87	0.76	1.71	164	160		
0°N to 6°N Atlantic region in summer (SUM5)												
5.65	46.4	211	0.02	0.16	0.14	0.32	0.16	0.47	23.7	19.8	2.56	0.45
4.76	43.9	212	<0.03	0.03	0	0.05	0.03	0.06	0.75	2.18	1.12	0.08
3.83	42.8	213	0.01	0.26	0.05	0.06	0.06	0.45	6.37	12.2	<0.1	<0.1
3.27	44.2	214	0.05	0.07	0.06	0.03	0.14	0.19	8.64	3.16	2	0.24
3.93	46.1	215	<0.07	0.18	0.01	0.08	0.16	0.24	11.3	0.39	1.75	0.24
5.79	48	216	0.11	0.22	0.04	0.10	0.04	0.35	9.2	9.61	<0.2	0.27
6.17	50.2	217	0.03	0.13	0.07	0.13	0.13	0.16	10.1	5.86	2.1	0.46
Average			0.04	0.15	0.05	0.11	0.10	0.28	10	7.6		

The detection limit (DL) varied for each sample and species measured because of the DL of the analytical method and the air volume collected for each sample.

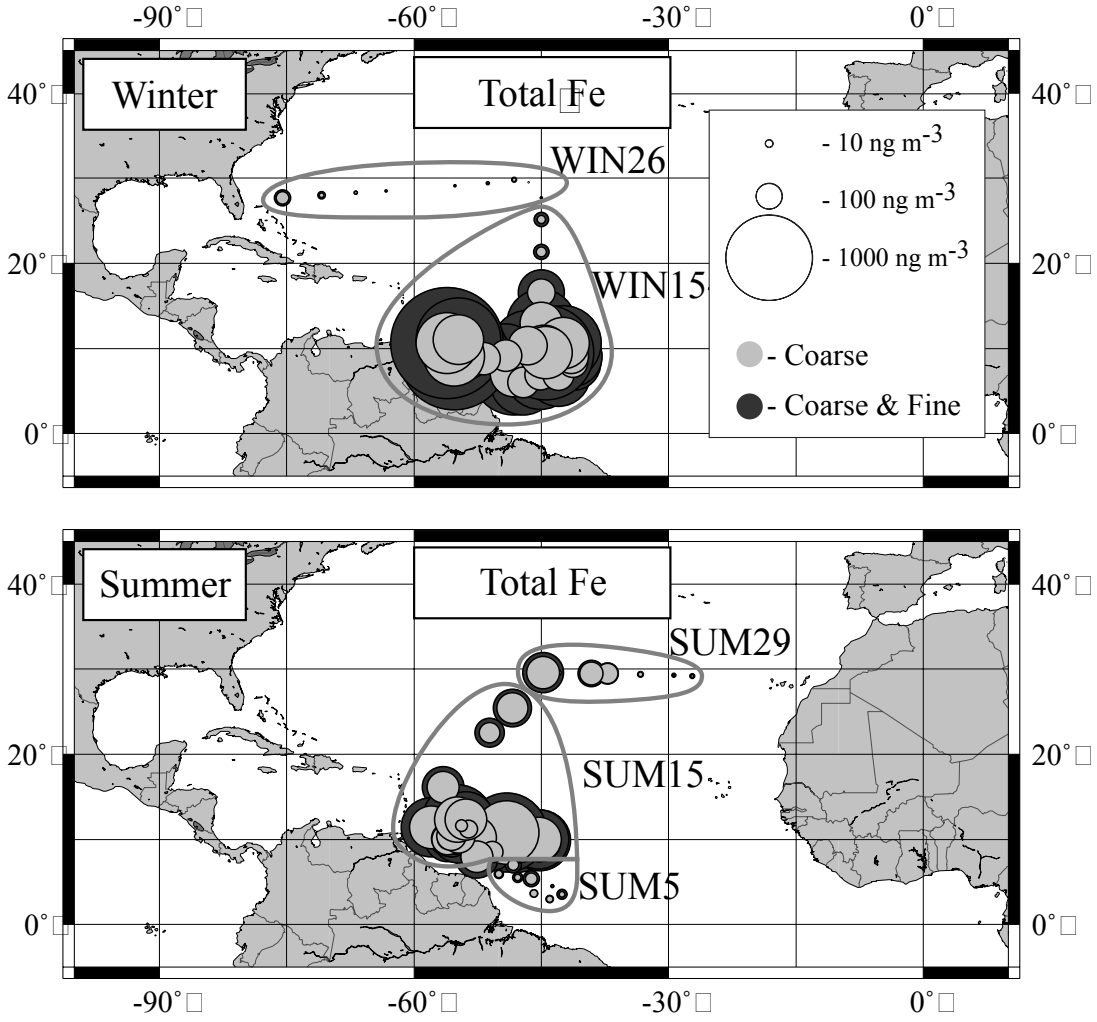

Figure 3-1. Spatial, size, and seasonal distributions of total Fe in aerosols collected during winter (6 January to 19 February 2001) and summer (27 June to 15 August 2001) research cruises over the Atlantic Ocean. The bubble areas are proportional to the concentrations of total Fe. Note that there is a bias toward showing the ‘‘coarse total Fe’’ bubbles when data are located close together on the map since all of the ‘‘coarse total Fe’’ bubbles are placed over all of the ‘‘coarse and fine total Fe’’ bubbles.

Total Fe concentrations in the fine- and coarse-fraction aerosols were extremely low near latitude 30°N during the winter (Figure 3-1). A spatial gradient of over nearly 3 orders of magnitude in the total Fe concentrations (from 1.6 ng m^{-3} at 28.6°N to 1688 ng m^{-3} at 10.9°N) was observed during the winter, while this gradient was not as strong in the summer. A similar spatial gradient, although not as large in magnitude as aerosol Fe, has also been observed for the dissolved Fe concentrations in Atlantic surface seawater (Wu and Boyle, 2002; Sanudo-Wilhelmy et al., 2001). The observed Fe concentrations were 0.2 nM at latitude 31°N, 0.8 nM at 26°N, and 0.77 nM at 10°N to 16°N, respectively. It was suggested that the gradient distribution of surface seawater Fe is mostly attributed to the latitudinal variation of atmospheric Fe deposition that is evident in the winter data (Figure 3-1). However, the latitudinal gradient of atmospheric total Fe concentrations over this oceanic region was not as significant during the summer. One reason for this decreased latitudinal gradient during the summer is that the maximum zone of African dust plume migrated to latitude 20°N with the ITCZ (Husar et al., 1997; Moulin et al., 1997), which extended the dust impacts to higher latitudes (up to 30°N). The total Fe concentration (fine + coarse) reached 235 ng m^{-3} at the position 29.6°N 45°W, while the averaged Fe concentrations in SUM15 were 324 ng m^{-3} during the summer (Figure 3-1). Low concentrations of atmospheric total Fe (mean 17.6 ng m^{-3}) were observed at lower latitudes where the influence of mineral dust plumes from North Africa was weaker due to the northward migration of the ITCZ in summer. The low Fe concentrations and weaker latitudinal gradient may also be caused by the episodic nature of dust plumes. Overall, the atmospheric total Fe concentrations in the MBL were

approximately a factor of 2 higher during the winter than in the summer when comparing the mean total Fe concentrations in the maximum dust plume zone (mean 670 ng m^{-3} (median 596 ng m^{-3}) in WIN15 and 324 ng m^{-3} (median 251 ng m^{-3}) in SUM15).

Long-term measurements of mineral dust concentrations have been done at Sal Island (16°45'N, 22°57'W) located in the zone of maximum dust transport. These measurements showed a pronounced seasonal pattern with the maximum dust concentrations during winter (Chiapello et al., 1995). However, Gao et al. (2001) indicated that the highest Fe flux including wet deposition to the tropical and subtropical Atlantic Ocean occurred in the summer using their model. At Barbados, Gao et al. (2001) predicted the average Fe flux to be about 45 mg m^{-2} $month^{-1}$ in the summer and significantly higher than the average Fe flux in the winter (about 20 mg m^{-2} $month^{-1}$). This different seasonal pattern at Barbados is probably a consequence of the long distance between North Africa and Barbados (it takes about 1 week for a dust event to travel from North Africa to the Caribbean). This travel time weakens the impact of the African mineral dust, especially in winter when a low-level dust transport replaces a high-level dust layer in summer (Guelle et al., 2000). Higher concentrations of atmospheric total Fe (mean 900 ng m^{-3}) were also observed for a few days during the summer cruise when the ship was close to Barbados, where other atmospheric Fe sources (e.g., crustal source from South America) may have an effect. The winter versus summer trends observed for the aerosol Fe during these two cruises highlights the strong gradients and episodic nature of the dust events and does not

apply in general for seasonal variations since this data are limited to certain regions during 1 year.

3.3.2 Labile Iron Features

Three labile Fe species in the aerosol samples were measured using an aqueous extraction procedure and LPAS. Most of the total labile Fe concentrations (mean 82%) were found in the fine-fraction aerosol (see Figure 3-2 and Table 3-1). However, the fine fraction only contributed half (mean 50%) of the total Fe concentrations, showing the ‘‘enrichment’’ of the labile Fe species in the fine fraction compared to the coarse aerosols. This has previously been observed in aerosol samples collected during the intermonsoon season over the Arabian Sea by Siefert et al. (1999) where more than 80% of total atmospheric aqueous-labile Fe(II) concentrations were present in the fine fraction, and over the tropical Atlantic Ocean (Johansen et al., 2000). Siefert et al. (1999) indicated that fine and coarse fractions of aerosol particles might have different origins, and over the Arabian Sea, pollution sources (e.g., combustion of fossil fuels) may have contributed to the fine aerosols with high labile Fe(II) contents. However, differences in the atmospheric processing of the fine and coarse aerosol may also explain these observations. Most atmospheric Fe in this Atlantic region is carried by the mineral dust plumes originating from North Africa, and this long-range transport will favor the suspension of fine particles over larger particles due to the greater settling velocity of larger particles. The fine particles will therefore have more opportunities to undergo condensation-evaporation cycles and be exposed to reductive processes (e.g., photochemical redox reactions) and acidic pH conditions that can transform refractory Fe species into more labile Fe

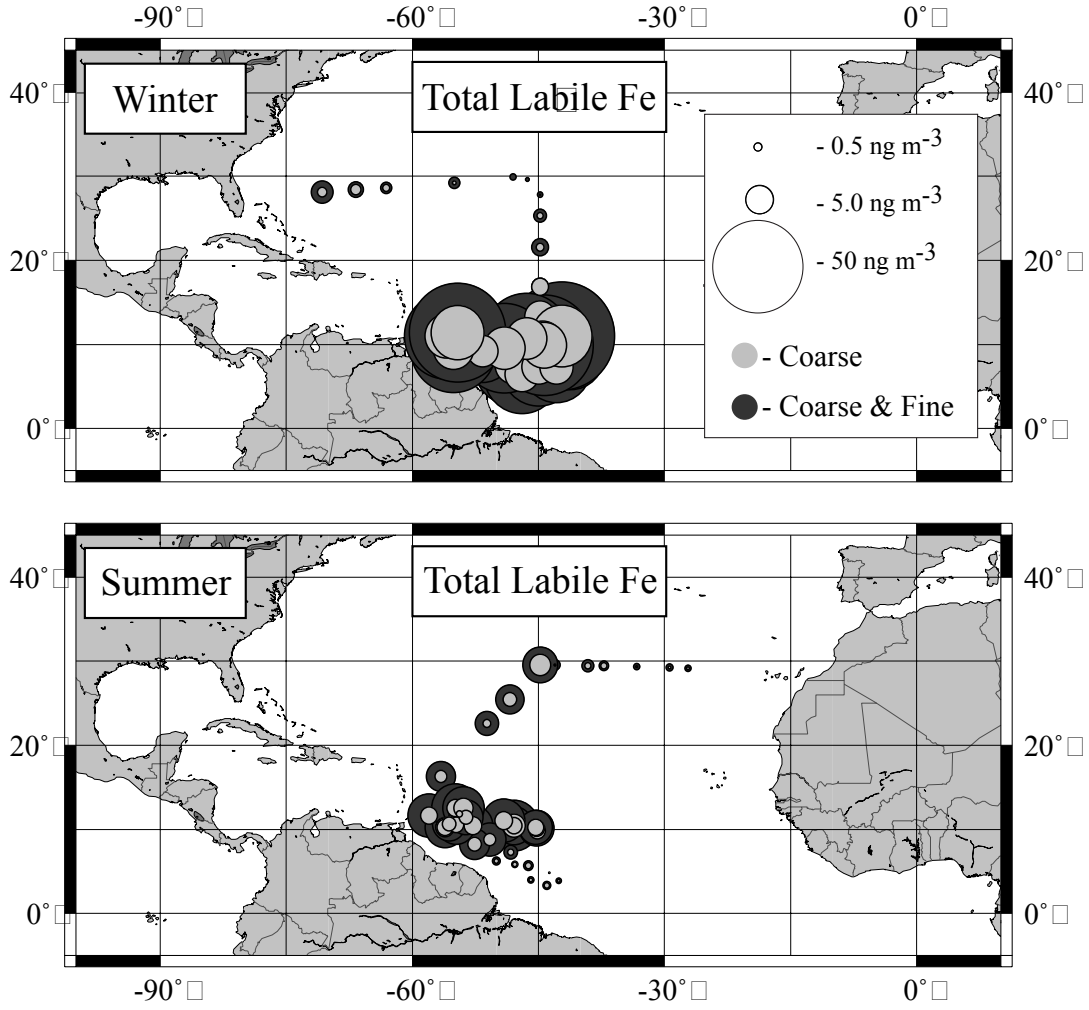

Figure 3-2. Spatial, size, and seasonal distributions of labile Fe in aerosols collected during winter (6 January to 19 February 2001) and summer (27 June to 15 August 2001) research cruises over the Atlantic Ocean. The bubble areas are proportional to the concentrations of total labile Fe. Note that there is a bias toward showing the ‘‘coarse total labile Fe’’ bubbles when data are located close together on the map since all of the ‘‘coarse total labile Fe’’ bubbles are placed over all of the ‘‘coarse and fine total labile Fe’’ bubbles.

species (Chen and Siefert, 2003). Fine particles also have a higher surface area to volume ratio than coarse particles, which may also enhance their aqueous dissolution.

Higher percentages of total labile Fe to total Fe ratios were observed in the fine-fraction aerosol than in the coarse fraction for most of the samples except during WIN26 where the percentages of total labile Fe to total Fe in both coarse and fine fractions became extremely large (mean 33% and 37%, respectively) and not significantly different (see Figure 3-3). For labile Fe(II) species (see Table 3-1), fine-fraction aerosols had even higher percentages than the coarse fraction, including the WIN26 where the labile Fe(II) percentage to total Fe in the fine fraction (mean 19%) was about twice as much as that in the coarse fraction (mean 8.6%), accounting for most of the total labile Fe (mean 58%) observed in fine-fraction aerosols. This large contribution of labile Fe(II) to labile Fe species (58% of total labile Fe) in the fine fraction in WIN26 suggest a longer atmospheric transportation time for the fine aerosols, or possibly a distinctive air mass source in this Atlantic region during this time period. These fine aerosols may be associated with high concentrations of organic matter that could stabilize the labile Fe(II) produced by photochemical reduction process.

Total Fe concentrations were strongly correlated with the concentrations of total Mn and total Al in aerosols collected during both cruises with the exception of the fine-fraction aerosols in WIN26 (Table 3-2). Aluminum is typically used as the tracer to quantify the mineral aerosol abundance in the atmosphere (Taylor and McLennan, 1985). Crustal enrichment factors (EFs) based on X/Al ratios have been widely used to identify contribution of crustal and noncrustal sources on observed

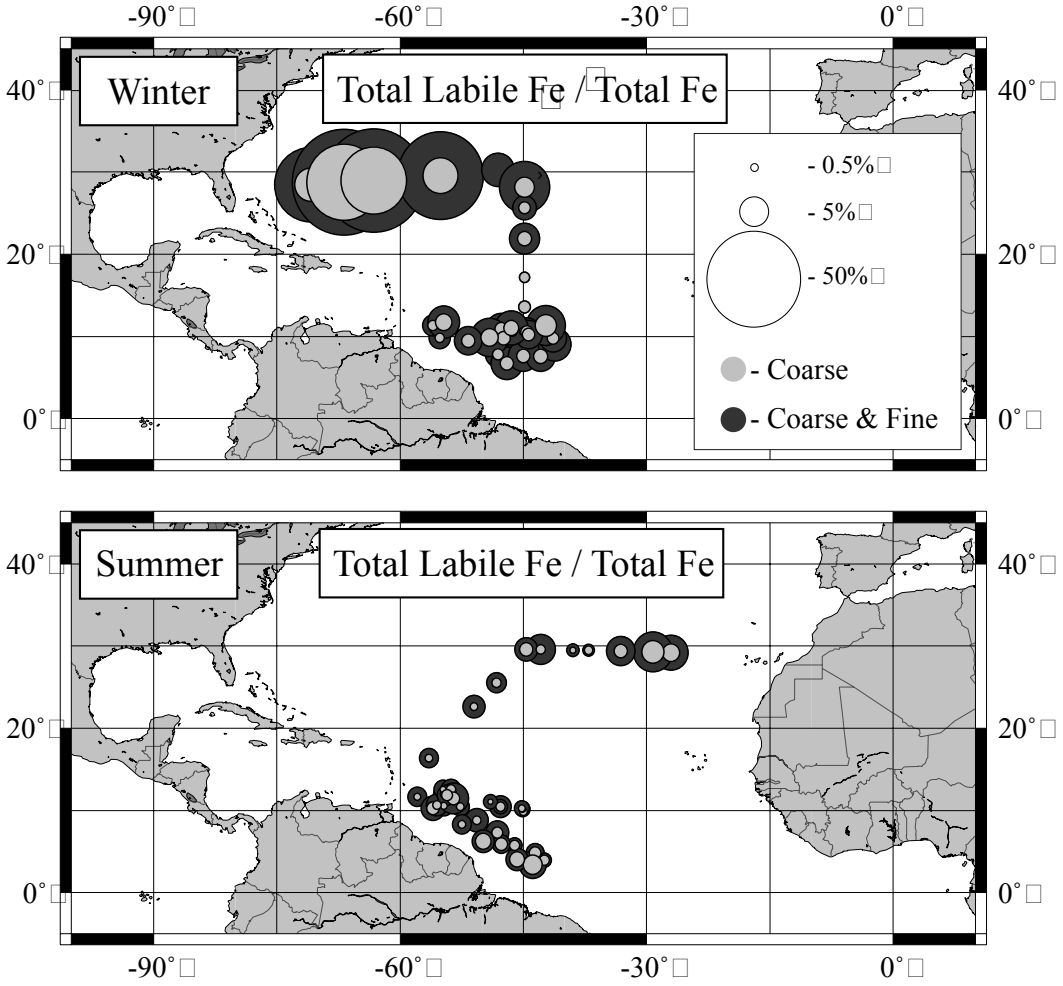

Figure 3-3. Spatial, size, and seasonal distributions of the ratio of labile Fe to total Fe concentrations for aerosols collected during winter (6 January to 19 February 2001) and summer (27 June to 15 August 2001) research cruises over the Atlantic Ocean. The ratio in all cases is to the sum of the coarse and fine total Fe concentrations. Note that there is a bias toward showing the ‘‘coarse total labile Fe to total Fe’’ bubbles when data are located close together on the map since all of the ‘‘coarse total labile Fe to total Fe’’ bubbles are placed over all of the ‘‘coarse and fine total labile Fe to total Fe’’ bubbles.

concentrations of trace elements (Kaya and Tuncel, 1997; Al-Momani et al., 1998; Chester et al., 1993a; Yatin et al., 2000; Huang et al., 2001). High correlation coefficients between the total Fe and total Al (Table 3-2) suggested that the mineral dust transported from the Sahel region was the dominant Fe source over the tropical and subtropical North Atlantic Ocean. However, total Fe measured in fine aerosols in WIN26 showed a weak correlation with Al (0.386) but large correlation coefficients with Cu (0.755), Ni (0.809), and V (0.817), which indicated that the aerosol Fe was probably influenced strongly by the noncrustal anthropogenic sources from North America or Europe. The second Aerosol Characterization Experiment (ACE-2) showed that both North American and European urban/industrial sources contributed to the aerosols over the North Atlantic region, with North American sources dominating under conditions of a strong Azores high (Benkovitz et al., 2003). The northeastern United States burns residual oil in winter, and some of the aerosol associated with this oil combustion may be transported to the subtropical North Atlantic region (Huang et al., 2001). Noncrustal V in the atmosphere is most often associated with the combustion of heavy fuel oil (Rahn and Lowenthal, 1984; Yatin et al., 2000). High loadings of Cu at Mumbai, India, were generally from nonferrous industrial emissions, and Ni may be from pollution sources such as oil and refuse burning (Venkataraman et al., 2002). The Fe observed in the fine aerosols during this specific time and region may be caused by wearing of metals used in motor vehicles (Yatin et al., 2000) or ferrous industries (e.g., metallurgic plants, steel mills, castings) in North America. Other statistical methods such as principal component analysis (PCA) were also employed for identification of source contributions to the labile

Table 3-2. Correlation Matrix Between the Concentrations of Trace Elements and Total Fe in Both Coarse- and Fine-Fraction Aerosols Collected During Winter (6 January 2001 to 19 February 2001) and Summer (27 June to 15 August 2001) Over the Tropical and Subtropical North Atlantic Ocean[a]

	Coarse-Fraction Aerosols				Fine-Fraction Aerosols			
Elements	WIN26	WIN15	SUM15	SUM5	WIN26	WIN15	SUM15	SUM5
Al	0.726[b]	0.989[b]	0.956[b]	0.882[b]	0.386	0.994[b]	0.954[b]	0.972[b]
Ca	0.179	0.892	0.942	0.226	0.503	0.884	0.908[b]	-0.096
K	0.155	0.915[b]	0.834	0.468	0.715	0.931[b]	0.728	-0.042
Na	0.372	-0.044	0.551	0.099	0.515	0.252	0.429	-0.358
Mg	0.072	0.528	0.575	0.095	0.415	0.881	0.460	-0.344
Cr	0.294	0.624	0.815	0.624	-0.080	0.917	0.776	-0.031
Co	—	0.302	0.162	0.378	—	0.706	0.416	—
Cu	0.755[b]	-0.174	0.670	-0.176	0.773	-0.055	0.637	0.044
Pb	0.037	0.493	0.687	0.514	0.712	0.711	0.335	-0.077
Mn	0.763[b]	0.961[b]	0.998[b]	0.892[b]	0.844[b]	0.986[b]	0.994[b]	0.950[b]
Ni	0.243	-0.179	0.840	0.463	0.809[b]	0.055	0.748	-0.084
V	0.597	0.530	0.971[b]	0.766[b]	0.817[b]	0.927	0.863	-0.124
Zn	0.038	0.586	0.782	0.099	0.776	0.649	0.670	-0.261
Fe	1	1	1	1	1	1	1	1

[a] Definitions are as follows: WIN26, 26°N to 30°N Atlantic region in winter; WIN15, 5°N to 26°N Atlantic region in winter; SUM26, 26°N to 30°N Atlantic region in summer; SUM5, 0°N to 6°N Atlantic region in summer.
[b] The three largest values (i.e., close to 1) are indicated.

aerosol Fe over the Atlantic Ocean, and the results from PCA are listed in appendices II. The rotated component matrix showed that mineral dust (component 1) had a major contribution to aerosol particles over this Atlantic region and the labile Fe were mostly associated with this component. However, it is difficult to identify a single source for each component which usually represented a mixed source contrbution and/or atmospheric processing of the aerosol. Therefore our source analysis for labile aerosol Fe was based on the correlation matrix which was more straightforward.

An increase in labile Fe to total Fe ratio generally corresponds to a decrease in total Fe concentration (Figure 3-4). In WIN26 the percentage of labile Fe in total Fe (mean 35%) was approximately 7 factors higher than that in WIN15 (mean 5.0%) when an opposite spatial gradient of atmospheric total Fe concentrations was observed (Figure 3-3). The percentage of labile Fe in total Fe in SUM26 was around 5.7%, only slightly higher than that in SUM15 (mean 2.6%), which corresponded to the summer pattern of total Fe concentrations in the atmosphere with a weaker spatial gradient (Figure 3-1). In addition, SUM5 had the lowest concentrations of atmospheric total Fe observed; however, the labile Fe to total Fe ratio (mean 5.0%) was still close to the northern regions. Therefore a low concentration of atmospheric total Fe would not always imply a high percentage of labile Fe fractions. Moreover, the correlation coefficients between the Fe and Al concentrations in SUM5 were high for both fine- (0.972) and coarse- (0.882) fraction aerosols (Table 3-2), indicating a crustal source origin for Fe (mineral dust). Ion concentrations in the aerosol samples showed that WIN26 had much higher ratios of oxalate and NSS SO_4^{2-} anions to total Fe (oxalate/Fe and NSS SO_4^{2-} /Fe mean ratios are 4.8 and 88, respectively) than in

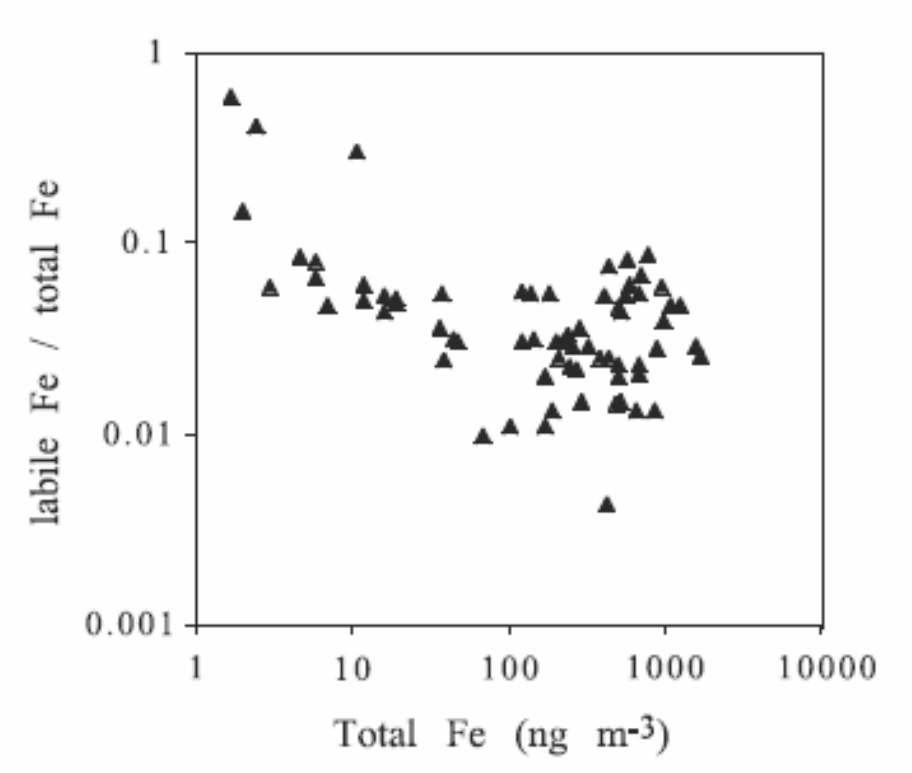

Figure 3-4. Ratio of labile Fe to total Fe versus total Fe concentrations in aerosols collected during the winter (6 January to 19 February 2001) and summer (27 June to 15 August 2001) research cruises over the tropical and subtropical North Atlantic Oceans.

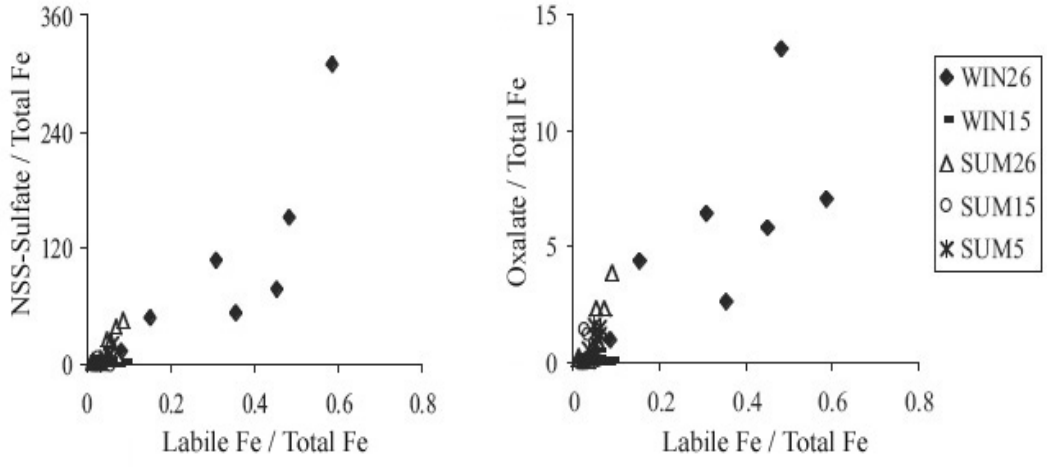

Figure 3-5. Ratios of NSS-sulfate to total Fe and oxalate to total Fe versus the ratio of labile Fe to total Fe in aerosol samples collected during the winter (6 January to 19 February 2001) and summer (27 June to 15 August 2001) research cruises over the tropical and subtropical North Atlantic Oceans.

SUM5 (oxalate/Fe and NSS SO_4^{2-}/Fe mean ratios are 1.1 and 10, respectively) (Figure 3-5). These species along with condensation-evaporation cycles in clouds and photochemical redox processes may produce the high labile Fe fractions observed in these aerosol samples. The source of the Fe may also be noncrustal as indicated by the weak correlation with Al (Table 3-2). Oxalate is the final product of photochemically induced reactions involving many organic precursors (Kawamura and Ikushima, 1993), and it is known to be an efficient electron donor for the photochemical reduction of Fe(III) in atmospheric waters (Zuo and Hoigne, 1992). Sulfate may indicate a lower aerosol pH which could increase the "stability" of Fe(II) with respect to oxidation (Johansen et al., 2000) and also increase the solubility of Fe minerals (Meskhidze et al., 2003). Thus the air mass characterized by the highest percentage of labile Fe in total Fe in WIN26 may have a different source contribution (polluted air masses from North America or Europe) from the others characterized by much lower labile Fe percents.

Previous studies have investigated the percentage of labile Fe(II) species in total Fe concentrations in aerosols using various extractions techniques. The labile Fe(II) results in this study are comparable to the previous observations. Siefert et al. (1999) reported that never more than 4% of the total Fe was released as Fe(II) after 22 hours of extraction for aerosol samples collected over Arabian Sea, and $Fe(II)_{labile}/Fe_{total}$ ratios in Barbados aerosol samples were observed between 0.47 and 0.92% (Zhu et al., 1993), which are consistent with our measurements that labile Fe(II) species that were approximately 1.8%, 1.0%, 0.33%, and 1.1% of total Fe concentrations in WIN15, SUM26, SUM15, and SUM5, respectively. However,

much higher percentages of labile Fe(II) in total Fe (10–100% and 2.2–49%) have been observed in marine aerosols over the central North Pacific Ocean and Barbados (Zhuang et al., 1992), which was explained as a result of increased cloud processing of the aerosols. In this study, a high percentage of labile Fe(II) to total Fe (around 16%) was also observed in WIN26, which may be attributed to different sources (e.g., anthropogenic sources from North America or Europe) of the aerosol particles.

3.3.3 Air Mass Back Trajectories (AMBTs)

AMBTs were calculated using the HY-SPLIT (isentropic program) for a 7-day period. Figure 3-6 shows seven representative AMBTs for this data set. The AMBTs showed the dominant northeasterly trade winds transporting mineral dust from North Africa over the 0° to 30°N Atlantic region. However, at both ends of this region the air masses were seasonally affected by other circulations as a result of latitudinal shifting of the ITCZ, which effected the variations of total Fe concentrations and labile Fe percents.

The spatial gradient of increased total Fe concentrations from 30°N to 10°N in the winter indicated a stronger impact of African dust in this region. The AMBTs for 30°N to 10°N in the winter (Figures 3-6b and 3-6c) were consistent with these higher concentrations and showed the air masses to have either passed over North Africa or to have come close to the coast. Back trajectories at 28°N 45°W (where the ship was located on 16 January 2001) showed that the air mass had circulated over the ocean for more than 7 days without contact with the land (Figure 3-6a), which was consistent with an extremely low concentration of atmospheric total Fe (see discussion in section 3.3.2).

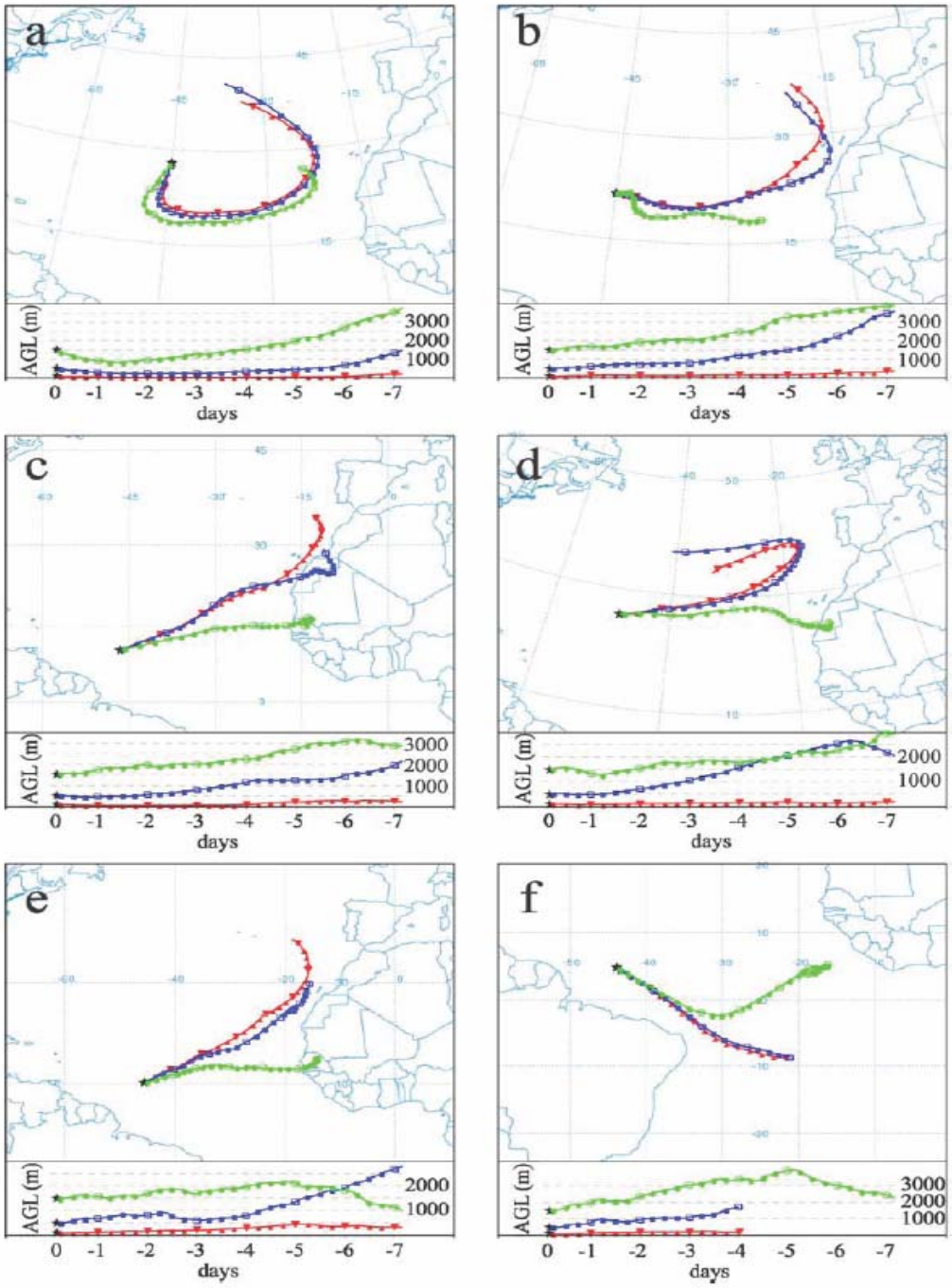

Figure 3-6. Representative 7 day air mass back trajectories for starting altitudes of 100 m, 500 m, and 1500 m above ground level (AGL) calculated from the National Oceanic and Atmospheric Administration's FNL database using the Hybrid Single-Particle Langrangian Integrated Trajectory (HY-SPLIT) model (markers are at 6 hour increments): (a) 16 January 2001 (28°N, 45°W), 2000 UTC; (b) 18 January 2001 (21°30'N, 45°W), 2000 UTC; (c) 22 January 2001 (10°N, 46°30'W), 2000 UTC; (d) 4 July 2001 (25°30'N, 48°30'W), 2000 UTC; (e) 15 July 2001 (10°N, 45°30'W), 2000 UTC; and (f) 31 July 2001 (5°N, 44°W), 2000 UTC.

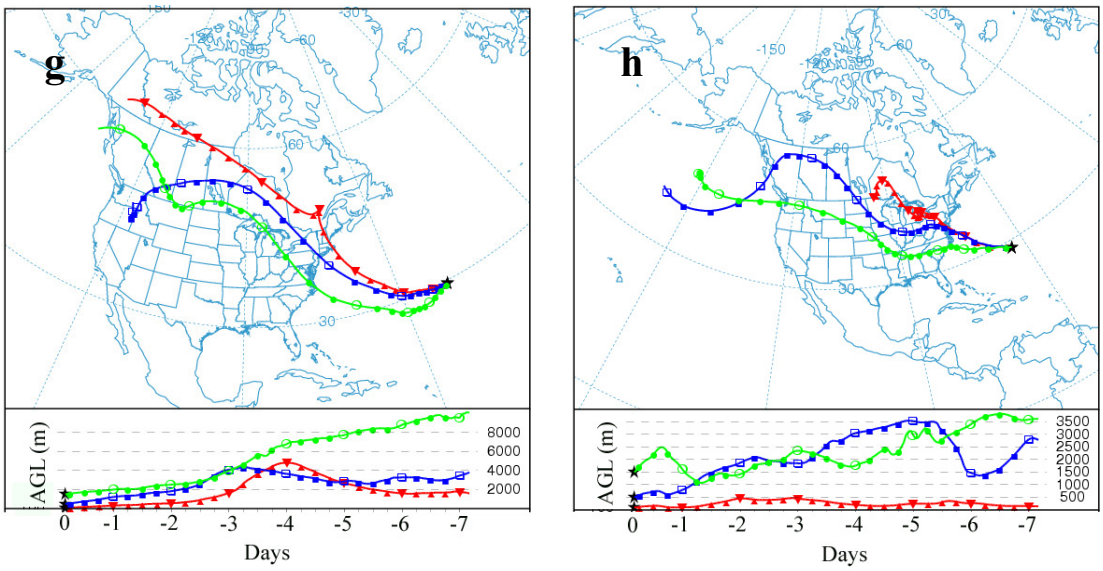

Figure 3-6 (supplement). Representative 7 day air mass back trajectories for starting altitudes of 100 m, 500 m, and 1500 m above ground level (AGL) calculated from the National Oceanic and Atmospheric Administration's FNL database using the Hybrid Single-Particle Langrangian Integrated Trajectory (HY-SPLIT) model (markers are at 6 hour increments): (g) 13 January 2001 (29°30'N, 51°W), 2000 UTC; (h) 10 January 2001 (28°30'N, 63°W)

Chiapello et al. (1997) labeled samples as ‘‘non-dusty samples’’ of oceanic origin when the AMBTs had circulated over the ocean for more than 5 days. Many of the AMBTs in this study had circulated over the ocean for more than 7 days and thereby contained very low dust concentrations (e.g. Figure 3-6a). The oceanic origin aerosols in this study (e.g., at 28°N 45°W) however, had the highest labile Fe percentages. This high labile Fe percent may be because the particles had more time to undergo photochemical processing than the fresh terrestrial dust or that the aerosol Fe had a different source. Almost equal percentages of labile Fe in total Fe were observed in both the fine- and coarse-fraction aerosols (labile Fe fraction is dominant in fine fraction of mineral dust, see discussion 3.3.2), which may indicate an impact of anthropogenic Fe sources (e.g., ferrous-industries from North America or Europe) on these oceanic origin aerosols at 28°N (Figure 3-6a). Figure 3-6g and 3-6h demonstrate that AMBTs at WIN26 region passed over North America and may transport anthropogenic emissions to this Atlantic region during the winter. The two lower back trajectories at latitude 21°30’N extended along the North African coast which corresponded to a high concentration of total Fe (Figure 3-6b). The back trajectories at10°N passed over North Africa (Figure 3-6c) and had even higher Fe concentrations. These two locations had similar African dust origins and similar labile Fe percents. The maximum concentrations of atmospheric total Fe observed in WIN15 were probably due to an additional lower layer transport (below 1.5 to 3 km in altitude) of African dust (Chiapello et al., 1995).

Dust transport off North Africa during summer occurs at high altitudes, from about 1.5 km to 5–7 km above sea level, which allows for long-range transport and

influences a larger North Atlantic region (Prospero and Carlson, 1972). The 1500 m back trajectories at latitude 25°30'N and 10°N (Figure 3-6d) passed over North Africa, while the two lower back trajectories circulated over the ocean at 25°30'N or extended along the North African coast at 10°N (Figure 3-6e). This was consistent with the weaker spatial gradient of atmospheric total Fe in the summer and the lower Fe concentrations in the MBL during the winter. Back trajectories at 5°N 44°W during the summer showed that the air mass was from the South Atlantic Ocean (Figure 3-6f), which indicated that this region was not significantly impacted by African dust, corresponding to the low concentrations of atmospheric total Fe.

3.3.4 Atmospheric Dry Deposition of Iron

The dry deposition velocity is primarily a function of dust particle size, wind speed, and relative humidity. Previous studies have found that the mass median diameters (MMD) of aerosols collected over the tropical and subtropical North Atlantic Ocean were between one to several micrometers (Prospero, 1995). This study shows that labile Fe is a function of particle size and is typically enriched in the fine aerosol compared to total Fe, and therefore it is expected that these two size fractions would have different deposition velocities and other microphysical properties. However, it is somewhat arbitrary to use different deposition velocities for the fine- and coarse-fraction aerosols investigated in this study since more information is needed about the aerosol microphysical properties (e.g., MMD). Slinn and Slinn (1981) showed that particles with 1 to 10 μm radius have a dry deposition velocity around 1.0 cm s^{-1} under the condition of 5 m s^{-1} wind speed and 100% relative humidity. The mean deposition velocity of 1.0 cm s^{-1} was also suggested by

Table 3-3. Atmospheric Dry Depositions of Total Fe and Labile Fe Species Over the Tropical and Subtropical North Atlantic Oceans During the Winter (6 January to 19 February 2001) and Summer (27 June to 15 August 2001)[a]

	WIN26	WIN15	SUM15	SUM5
Aeolian total Fe	2.5±1.44	631.1±355.5	278.4±170.9	15.2±10.93
Labile Fe(II)	0.3±0.21	11.8±7.45	0.8±0.46	0.2±0.09
Labile total Fe	0.5±0.46	20±10.7	3.9±2.42	0.3±0.17
Reducible labile Fe	0.7±0.50	29.6±15.68	6.1±3.30	0.7±0.32

[a] Distributions are given as mean±SD in mg m^{-2} d^{-1}.

comparison between dust deposition estimates and sediment trap records (Jickells, 1999). Therefore Fe dry deposition rates over the tropical and subtropical North Atlantic Oceans were calculated by multiplying Fe concentrations in the aerosols with the dry deposition velocity of 1.0 cm s^{-1}. Fe dry deposition rates were calculated for four subregions WIN26, WIN15, SUM15, and SUM5 according to the spatial and seasonal distributions of atmospheric Fe concentrations (see discussion in section 3.3.2). The dry deposition rates of the various Fe species were calculated. The three labile Fe fractions measured in this study represent Fe species with varying abilities to dissolve in aqueous solutions. The order from most labile to least labile for these fractions would be (1) labile Fe(II), (2) labile Fe(III), (3) reducible particulate Fe, and (4) the refractory Fe pool determined by strong acid digestion. The bioavailability of these Fe fractions would be expected to follow this same order. The RPFe enlarges the bioavailable Fe pool by considering Fe reduction processes in the atmosphere or seawater (Chen and Siefert, 2003). The maximum dry deposition rates of total Fe (631 mg m^{-2} d^{-1}) and labile Fe occurred in WIN15 (Table 3-3), which is comparable to the Fe dry and wet deposition rates (mean 20 mg m^{-2} $month^{-1}$ or 667 mg m^{-2} d^{-1}) at Barbados calculated by Gao et al. (2001). The dry deposition of total Fe in SUM15 was approximately 278 mg m^{-2} d^{-1}, about half of the maximum dry deposition in the winter, correspondingly, labile Fe dry deposition decreased even further (Table 3-3). Low dry deposition rates of total Fe were calculated in WIN26 and SUM5 with the former region even lower, approximately 2.5 and 15 mg m^{-2} d^{-1}, respectively. However, the dry deposition rates of labile Fe species were similar between these two regions (Table 3-3), indicating that the atmospheric dry deposition may provide

almost equal amount of bioavailable Fe to these two oceanic regions. The larger fluxes of labile aerosol Fe over WIN15 or SUM15 region may correspond to the higher diazotrophic activities over this Atlantic region. A strong spatial gradient of *Trichodesmium* biomass (7 times higher at 10°N to 16°N Atlantic than at 0° to 6°N Atlantic region) observed in April 1996 (Sanudo-Wilhelmy et al., 2001) may be related to the spatial pattern of atmospheric deposition of labile Fe, instead of the dissolved Fe concentrations in surface seawater. *Trichodesmium* blooms in offshore waters of the west Florida shelf (Lenes et al., 2001) in summer may also relate to the high atmospheric deposition of labile Fe that extended northward in summer.

3.4 Conclusions

Field measurements of Fe concentrations and speciation in aerosols were conducted during the winter and summer cruises over the tropical and subtropical North Atlantic Ocean. A spatial gradient was observed of nearly 3 orders of magnitude in the total Fe concentrations, from a low concentration of 1.6 ng m^{-3} in WIN26 to a high concentration of greater than 1688 ng m^{-3} in WIN15, while this gradient was not as significant in the summer due to the migration of the ITCZ. The atmospheric total Fe concentrations in the MBL were approximately a factor of 2 higher during the winter (mean 670 ng m^{-3} in WIN15) than in the summer (mean 324 ng m^{-3} in SUM15). The highest percentage of labile Fe in total Fe (35%) was observed in WIN26, corresponding to low concentrations of total Fe and relatively high concentrations of oxalate and NSS SO_4^{2-}. However, in SUM5, where the lowest Fe concentrations were measured, the labile Fe percent (5.0%) was similar to SUM15. AMBTs showed that mineral dust transport off North Africa was a dominant

Fe source in this region. However, labile Fe appeared to be influenced by anthropogenic activity in some of the winter samples (around 30°N) where anthropogenic metals (V, Cu, Ni) were relatively high along with other species (i.e., oxalate, NSS SO_4^{2-}) consistent with anthropogenic sources. The highest calculated dry deposition fluxes of total Fe and labile Fe occurred in WIN15, whereas the lowest fluxes were shown in both WIN26 and SUM5. The highest dry deposition fluxes of labile Fe occurred in the region of high N_2-fixing diazotrophic activity in the tropical North Atlantic region (5°N to 25°N, oligotrophic ocean where diazotrophs are favored).

Chapter 4: *Trichodesmium* Uptake of Iron from Aerosol and Its Influence on Aerosol Iron Dissolution in the Tropical North Atlantic Ocean

4.1 Introduction

Deposition of atmospheric aerosol is the dominant source of iron to the remote ocean (Duce and Tindale, 1991). Fe limitation to phytoplankton growth has been confirmed in high nitrate low chlorophyll (HNLC) areas where there is low atmospheric dust deposition (Martin et al, 1994; Coale et al, 1996; Boyd et al, 2000; Tsuda et al, 2003). During the last glacial maximum, atmospheric dust fluxes to the ocean were about a factor of 2 higher, which may have greatly enhanced phytoplankton growth and contributed to the decrease of atmospheric CO_2 level (Mahowald et al., 1999; Bopp et al., 2003).

The tropical North Atlantic Ocean is under the impact of heavy dust loadings transported from North Africa. However, due to the low solubility of aerosol Fe in seawater (1-10% of total aerosol Fe) (Jickells and Spokes, 2001) only a small fraction of aerosol Fe inputs may be bioavailable. The labile Fe(II) concentrations extracted with a low pH (1.0 to 4.5) buffer solution are typically a few percent (0.3 to 1.8%) of total Fe in marine mineral aerosols (Zhu et al., 1993; Siefert et al., 1999; Johansen et al., 2000; Chen and Siefert, 2004). Understanding the processes controlling the bioavailability of aerosol Fe that deposited to seawater is critical to assessing the role of this trace element as a rate limiting nutrient in a given oceanic region. Previous studies have shown that bioavailable forms of Fe include not only free or inorganic Fe species (Anderson and Morel, 1982; Campbell, 1995; Sunda and Huntsman, 1997),

but also Fe bound to organic ligands (Kuma et al., 2000; Wu et al., 2001; Chen et al., 2003). Recent size-fractionated measurement showed that >90% of Fe in the traditionally defined dissolved phase (<0.2μm) was in fact in the colloidal phase (>1 kDa) (Wen et al., 1999; Wells et al., 2000; Wu et al., 2001). It has been found that colloidal Fe derived from Fe(III)-hydroxide precipitation could be used by *Trichodesmium* spp. in the EDTA-buffered media (Kustka et al., 2003b).

Trichodesmium, the most prominent planktonic marine nitrogen fixer, occurs throughout the open waters of oligotrophic tropical and subtropical oceans (Capone et al., 1997). This cyanobacterium supplies up to half of new nitrogen used for primary production in oligotrophic waters (Karl et al., 1997), and thereby plays a critical role in the biogeochemical cycling of C and N (Carpenter and Romans, 1991). N_2-fixing *Trichodesmium* has a high Fe requirement (Berman-Frank et al., 2001; Kustka et al., 2003a, b), and has a high Fe : C quota (38 μmol mol^{-1}) that is 2.5 to 5-times greater than NH_4^+-assimilating phytoplankton (Kustka et al., 2003a, b). Luxury uptake of greater than 13-fold amounts of Fe than needed for moderately Fe-limited growth (0.1 d^{-1}), was also observed in N_2 supported cultures of *Trichodesmium* (Kustka et al., 2003a, b). Nonetheless, a general lack of correlation between surface seawater Fe (total or dissolved) and *Trichodesmium* abundance has been observed in the Arabian Sea (Capone et al., 1998), in the central North Atlantic (Sañudo-Wilhelmy et al., 2001), and along a Atlantic Meridional Transect (AMT) (Tyrrell et al., 2003). There was little difference between dissolved Fe concentrations where *Trichodesmium* is abundant, and where it is scarce in the Atlantic Ocean (Tyrrell et al., 2003). The finding suggested that either *Trichodesmium* growth was not Fe-limited in these

oceanic regions, or *Trichodesmium* uptake of Fe could be a dynamic process depending on the amount of Fe supplies (e.g. luxury Fe uptake). The rate of dust Fe supply was also not correlated with the Fe concentration in surface seawater (Johnson et al., 1997), which may be explained by the short residence time of Fe in surface seawater due to its rapid precipitation and biological uptake (Hutchins et al., 1993). Therefore, the *Trichodesmium* abundance and nitrogen fixation rate in the North Atlantic Ocean may depend on the episodic fluxes of aerosol Fe instead of the Fe concentration in surface seawater. Furthermore, *in situ* investigations on *Trichodesmium* uptake of aerosol Fe are important for understanding the role that dust supply plays in the global carbon cycling and climate change.

In this chapter, shipboard incubation experiments were conducted in the tropical North Atlantic Ocean using freshly collected aerosols, surface seawater and *Trichodesmium* colonies. The transfer of aerosol Fe to various components in the incubation experiments was monitored by measuring the initial total Fe amounts on aerosol filters, the total and dissolved Fe concentrations in seawater (after incubation), the Fe adsorbed or taken up by *Trichodesmium*, and the particulate Fe remaining on aerosol filters. The *Trichodesmium* uptake of aerosol Fe is compared to the amount of labile Fe species (Chen and Siefert, 2003) on the aerosol filters added to the incubation solution. We also explore the relation between the uptake Fe and the total aerosol Fe released in the seawater. The influence of *Trichodesmium* on the release of Fe from the aerosol filters and the Fe adsorption/desorption between the dissolved and suspended particulate Fe in the seawater are discussed. A conceptual model is built to demonstrate that *Trichodesmium* mediate the aerosol Fe transfer

from the aerosol filters to the colonies that in turn have an impact on the aerosol Fe release and dissolution. This is the first field study to investigate the *Trichodesmium* uptake of aerosol Fe and its influences on the aerosol Fe transfer in areas of heavy dust loadings and *Trichodesmium* blooms, using concurrent measurements in aerosol, seawater and *Trichodesmium* samples.

4.2 Experimental Section

4.2.1 Aerosol, Surface Seawater and Trichodesmium Collection

Aerosol samples (approximately 24 hour sampling times) were collected during a spring cruise (18 April to 20 May 2003) over the tropical North Atlantic Ocean. A high-volume dichotomous virtual impactor (HVDVI) (Solomon *et al*., 1983) was setup above the bridge of the R/V *Seward Johnson* to collect fine (with aerodynamic diameters less than 2.5μm) and coarse (with aerodynamic diameters greater than 2.5μm) fractions of ambient aerosols. The fine- and coarse-fraction aerosols were collected on two 90 mm diameter Teflon filters (Gelman Zefluor, 1μm pore size). More details on the aerosol sample collection are described in chapter 2 (see also Chen and Siefert, 2003).

Surface seawater was collected from a fish deployed at 2 m below the surface and towed at about 5 knots during the cruise. The seawater was pumped up through acid-cleaned Teflon tubing coupled to a 0.5 m section of C-flex tubing (for the pump head), and filtered on line through an acid-cleaned polypropylene cartridge filter (0.22 μm, MSI, Calyx®). The system was purged, rinsed and conditioned by passing at a minimum of 3 L of seawater through it, and then the filtered seawater was collected in eight acid-cleaned polycarbonate 300 mL bottles.

Trichodesmium colonies were collected using an acid-cleaned all-plastic 100-µm mesh plankton net. The net was deployed 6 m away from the ship's starboard side and towed for 5 min at a depth of 4 m. Individual colonies were removed from the acid-cleaned polyethylene net collector with a plastic inoculating loop in a class-100 clean hood. Approximately 100 *Trichodesmium* colonies were added into each polycarbonate bottle filled with the 300 mL filtered seawater.

4.2.2 Aerosol Addition Experiments

Six aerosol addition experiments (E1 to E6) were performed during the R/V *Seward Johnson* research cruise in the tropical North Atlantic Ocean (Figure 4-1) using freshly collected aerosols, surface seawater, and natural *Trichodesmium* colonies. Four experiments (E1, E3, E4 and E6) were done at stations inside of the plume while E2 and E5 were performed at stations outside of the plume according to the salinity data of the seawater samples (Table 4-1). Each aerosol addition experiment had four treatments (with duplicates) that included a seawater blank (T1), seawater plus aerosol filter sub-samples (T2), seawater plus *Trichodesmium* colonies (T3), and seawater plus aerosol filter sub-samples and *Trichodesmium* colonies (T4). Fine and coarse fractions of aerosol filter sub-samples (Teflon filter cuts) were combined and added into the T2 and T4 treatments, and *Trichodesmium* colonies were transferred into the T3 and T4 bottles.

The total Fe added to the solution from the aerosol filter was in excess (a factor of greater than 100) compared to the dissolved seawater Fe and the Fe associated with the *Trichodesmium* colonies. The total labile Fe added to the

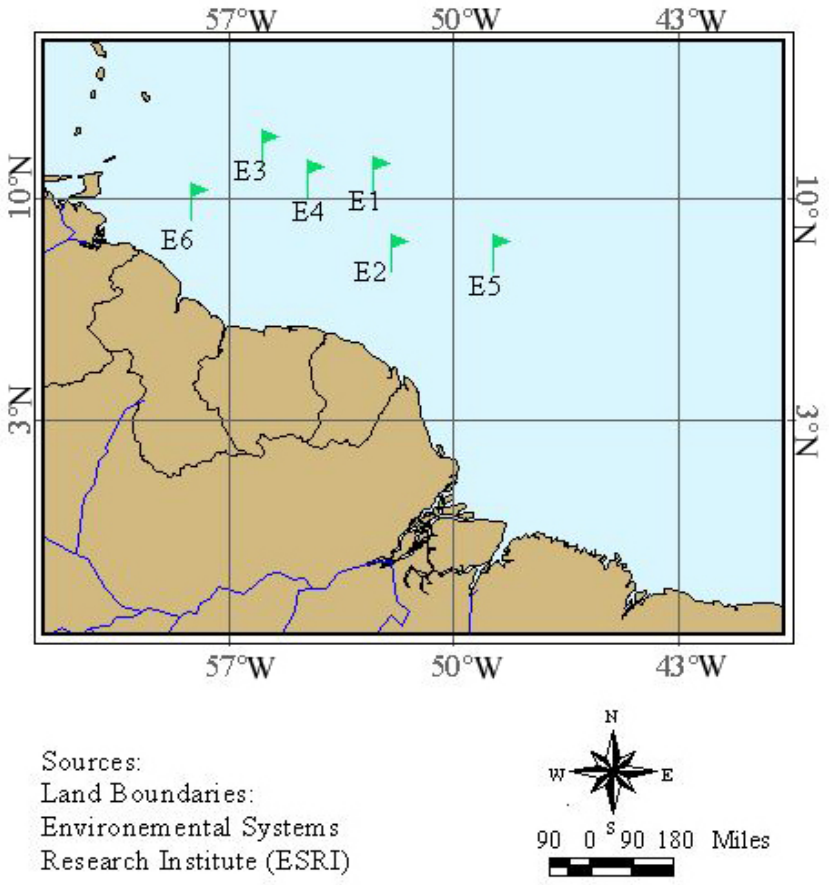

Figure 4-1. Locations of the aerosol addition experiments (E1 to E6) performed in the Tropical North Atlantic Ocean on the R/V *Seward Johnson* cruise from 18 April to 20 May 2003.

Table 4-1. Salinities, concentrations of initially dissolved Fe (DFe) and P (DP) in the seawater collected for the six aerosol addition experiments, and amounts of the aerosol Fe added (FeIA) to the incubation solutions and distributed to each component as the particulate Fe suspended in the seawater (FePS), the Fe dissolved in the seawater (FeDS), the adsorbed and/or intracellular Fe on the *Trichodesmium* (FeTT or FeIT), and the Fe remaining on the Teflon filter sub-samples (FeRF) in the two treatments T2 (seawater plus aerosols treatment) and T4 (seawater plus aerosols and *Trichodesmium* treatment) of the six aerosol addition experiments (E1 to E6). The total Fe in the seawater (FeTS) is the sum of the FePS and FeDS. Seawater blank (T1) and *Trichodesmium* blank (T3) have been deducted from the FeDS, FePS, FeTS, FeIT and FeTT values of the T2 and T4, respectively. Relative percent differences (RPD) between the FeIA and summation of all other Fe components are calculated.

Exp.	Sali.	DFe	DP		FeIA	FeDS	FePS	FeTS	FeIT/ FeTT*	FeRF	RPD
		nM	nM		μg	μg	μg	μg	μg	μg	%
E1	32.4	0.64	27.5	T2	3.00	—	—	0.002	—	3.44	13.7
				T4	5.73	—	—	0.051	0.004	6.84	18.4
E2	36.0	4.84	26.6	T2	13.5	—	—	1.54	—	10.5	-11.2
				T4	13.5	—	—	1.02	0.108	12.9	4.0
E3	34.7	2.43	—	T2	21.1	0.033	7.78	7.81	—	14.6	6.3
				T4	21.1	0.011	2.94	2.95	0.649*	16.6	-3.9
E4	32.8	2.43	6.05	T2	20.2	0.157	10.2	10.4	—	10.5	3.7
				T4	20.2	0.084	8.12	8.20	—	10.9	-5.2
E5	—	2.43	312	T2	8.20	0.017	3.14	3.16	—	6.00	11.0
				T4	8.20	0.398	3.82	4.21	—	3.89	-1.2
E6	31.5	1.62	3.76	T2	18.9	0.074	10.6	10.7	—	8.76	2.9
				T4	18.9	0.017	5.99	6.00	—	10.8	-11.8

* means the FeTT.

incubation solutions was a small fraction of the total Fe (about 2%) and would result in a concentration of 15 ± 3.8 nM if all labile Fe from the aerosol filters were to dissolve. This concentration is approximately a factor of 2 to 4 higher than the Fe initially dissolved in seawater (Table 4-1) and associated with the *Trichodesmium*. Total average atmospheric labile-Fe concentration measured over this tropical Atlantic region during this research cruise was ≈ 15 ng m^{-3}. The calculated dry depositional flux of the labile Fe to the surface ocean during this study was ≈ 13 μg m^{-2} d^{-1}, using a dry deposition velocity of 1.0 cm s^{-1}. If you assume a mixing depth for the surface ocean is on the order of 10 m (this depth is an approximate length scale based on the turbulent diffusion of an inert tracer added to the surface of a time period of 1 day) and neglect any losses of Fe (e.g. biological uptake), the rate of increase in surface seawater Fe (labile) concentration (to a depth of 10 m) would be approximately 0.02 nM d^{-1}. So, over a period of one day, the increase in the total labile aerosol Fe (15± 3.8 nM) added to the incubation solutions is almost two orders higher than the volume weighted increase in total labile Fe in the upper 10 m of the surface ocean. Therefore, the labile or total aerosol Fe additions in the experiments were much higher compared to the dust deposition of Fe to the real ocean. The choice to add this quantity of labile aerosol Fe to the experiment was a compromise between keeping it low enough to be able to relate the results to the ambient conditions during the cruise, and adding enough to be able to detect an effect within the capabilities of the analytical techniques.

The Fe initially associated with the aerosol on the Teflon filter sub-sample (Fe-Initial-Aerosol or FeIA) can dissolve into the seawater (Fe-Dissolved-Seawater or

FeDS), be suspended in the seawater as particulate Fe (Fe-Particulate-Seawater or FePS), be adsorbed onto the surface of the container (Fe-Adsorbed-Container or FeAC), be adsorbed onto the surface of the *Trichodesmium* (Fe-Adsorbed-Trichodesmium or FeAT), be taken up by *Trichodesmium* as intracellular Fe (Fe-Intracellular-Trichodesmium or FeIT), or remain on the original filter sub-sample (Fe-Remaining-Filter or FeRF). The FeDS and FePS, and the FeAT and FeIT can be summed up as the total Fe released into the seawater (FeTS = FeDS + FePS) and the total Fe associated with the *Trichodesmium* (FeTT = FeIT + FeAT), respectively. About 100 *Trichodesmium* colonies were transferred into each bottle with 300 mL incubation solution, which was comparable to a *Trichodesmium* bloom situation in the real surface ocean (Carpenter et al., 2004).

All bottles were placed in a flowing seawater incubator under ambient light for 24 hours. After the incubation, the *Trichodesmium* colonies were removed from the bottles, while the remaining solution and Teflon filter sub-samples were saved for Fe analysis for the first three experiments (E1 to E3). In the E4, E5 and E6, the whole solution for each incubation bottle was filtered through an acid-cleaned polycarbonate membrane (Nuclepore 0.4μm pore size), which resulted in the membrane collecting both the *Trichodesmium* colonies and particulate Fe, the filtered solution, the polycarbonate membrane and the Teflon filter sub-samples were saved and analyzed for Fe. The *Trichodesmium* colonies removed for the first three experiments (E1, E2 and E3) were placed on an acid-cleaned polycarbonate membrane (0.22 μm pore size) for intracellular Fe and phosphorus (P) analyses (E1 and E2), or deposited in a 3 mL Teflon vial for the total fraction analysis (E3). The

membrane was soaked in 5 mL of ultra-clean oxalate reagent (Tovar-Sanchez et al., 2003) for 5 minutes and then passed by 10 mL of Nanopure water. The oxalate reagent removes the Fe and P (Tovar-Sanchez et al., 2003; Sañudo-Wilhelmy et al., in preparation) adsorbed on *Trichodesmium* surface, allowing for intracellular fraction to be determined. All the experimental operations above and the measurements below were done following trace-metal clean techniques.

4.2.3 Labile and Total Iron, Phosphorus on Membranes

Three labile Fe species on the Teflon filter were investigated using an aqueous extraction procedure and measured using long path length absorbance spectroscopy (LPAS) immediately after sample collection. The 0.5 mM of pH 4.5 formate-acetate buffer was used as the extraction solution and the 50 mM of hydroxylamine (HA) solution used for the Fe reduction. Fe(II) concentrations were determined colorimetrically by complexation with ferrozine (Carter, 1971) and subsequent LPAS measurements (Waterbury et al., 1997). LFe(II), LFe(III) and RPFe were operationally defined by the extraction time and reagents (see details at chapter 2).

A strong-acid microwave digestion procedure followed by Inductively Coupled Plasma Mass Spectrometry (ICP-MS, HP 4500) was used to measure total Fe on the Teflon filter sub-samples (or polycarbonate membranes). 10 N of nitric acid and 28N of hydrofluoric acid (Seastar Chemical Inc.) were used in sample digestion, and a multi-element internal standard of Sc, In and Bi (SPEX CertiPrep, Inc.) applied in ICP-MS measurement (see details at chapter 3). Total Fe concentration on the filter was then calculated using the volume of the extraction solution and the ICP-MS measured Fe concentration. Water-soluble phosphate concentrations were measured

using an aqueous extraction technique (Derrick and Moyers, 1981) and Ion Chromatography (Dionex DX-600) (see details at chapter 3).

4.2.4 Iron and Phosphorus Analyses in Seawater and Trichodesmium

Seawater samples were acidified with sub-boiling quartz distilled HCl (Q-HCl) to pH less than 1.5 and stored for at least 1 month prior to analysis. Fe concentrations were determined by ICP-MS (ThermoFinigan, Element 2) after pre-concentration with an ammonium1-pyrrolidinedithiocarbamate/diethylammonium diethyldithiocarbamate (APDC/DDDC) organic extraction (Bruland et al., 1985). P concentrations were determined by MAGnesium Induced Coprecipitation (MAGIC) method (Karl and Tien, 1992). Phosphate in the seawater is scavenged by $Mg(OH)_2$ precipitation and then dissolved in an acid solution. The concentrated phosphate was measured colorimetrically by adding the molybdenum (Mo) complexing solution.

Trichodesmium colonies collected on the polycarbonate membrane or in the Teflon vial were stored frozen and transported back to the laboratory for acid digestion. The digestion procedure followed that of Kustka et al. (2003b). Fe contents were determined by ICP-MS (ThermoFinigan, Element 2) and P was quantified spectrophotometrically using the methods described by Gieskes et al. (1991).

4.3 Results

4.3.1 Mass Balance of Aerosol Iron

The FeIA, FeTS, FeIT and FeRF were measured for E1 and E2; the FeIA, FeDS, FePS, FeTT and FeRF were measured for E3; and the FeIA, FeDS, FePS and FeRF were measured for E4 to E6 (Table 4-1). The FeAC was not quantified for the

experiments, however this Fe pool was a small fraction of the total Fe based on the mass balance calculations for the experiments. The last column of Table 4-1 summarizes the mass balance for each experiment in terms of relative percent difference (RPD) of Fe between the initial aerosol Fe added (FeIA) and the summation of the Fe measured in each of the components at the end of the experiment. The initial aerosol Fe added (FeIA) was in a good agreement with the sum of the Fe distributed to each component (FeDS, FePS, FeIT and FeRA) for most of the experiments. The Fe RPD during the experimental operation was typically less than ±14% of the total aerosol Fe added, which is within our estimated error for the initial mass of aerosol Fe on the filter based on the analytical techniques and the filter sub-sampling method. The only experiment with slightly higher Fe RPD was E1 where the percent difference was 18.4% for the T4. The filter sub-samples removed from the T4 treatment may have been contaminated based on the high Fe values of the FeRF, and this contamination probably occurred after the incubation. There also may not have been any contamination to this experiment and the higher RPD may have been due to inhomogeneous distribution of Fe on the aerosol filter. The E1 was still included in the following discussion even though the RPD was slightly higher.

4.3.2 Trichodesmium Uptake of Aerosol Iron

The intracellular Fe in the *Trichodesmium* (FeIT) incubated with aerosol filters was significantly higher than those incubated without aerosols, indicating a significant uptake of aerosol Fe by *Trichodesmium* in the aerosol addition experiments (E2 and E3, Figure 4-2). *Trichodesmium* colonies were carefully removed after the incubation for intracellular Fe analysis for experiments E1 and E2.

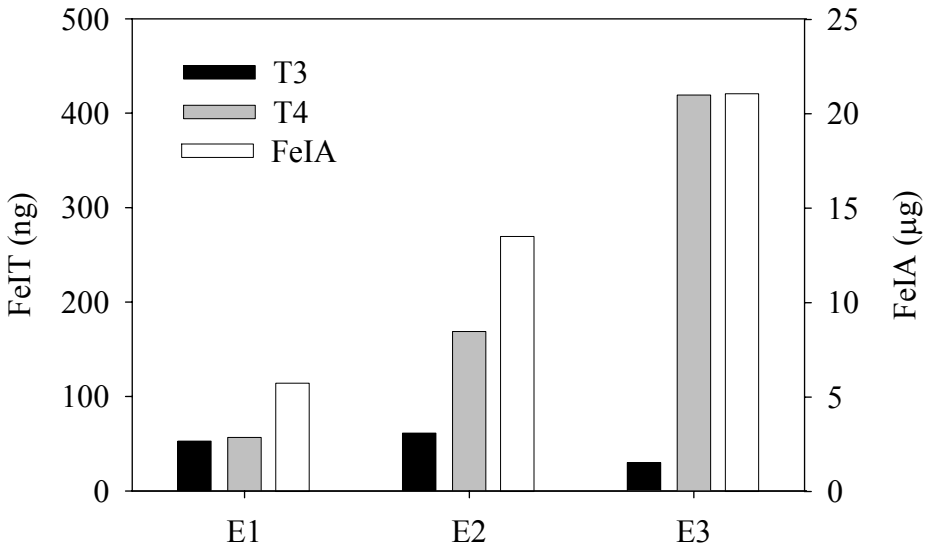

Figure 4-2. Amounts of Fe taken up by *Trichodesmium* colonies (FeIT) in the T3 (seawater plus *Trichodesmium* treatment) and T4 (seawater plus aerosols and *Trichodesmium* treatment) and amounts of the aerosol Fe added (FeIA) to the T4 of the three aerosol addition experiments (E1, E2 and E3), the intracellular Fe in the T4 of the E3 was calculated by assuming 60% of the total Fe associated with the *Trichodesmium* is interior Fe.

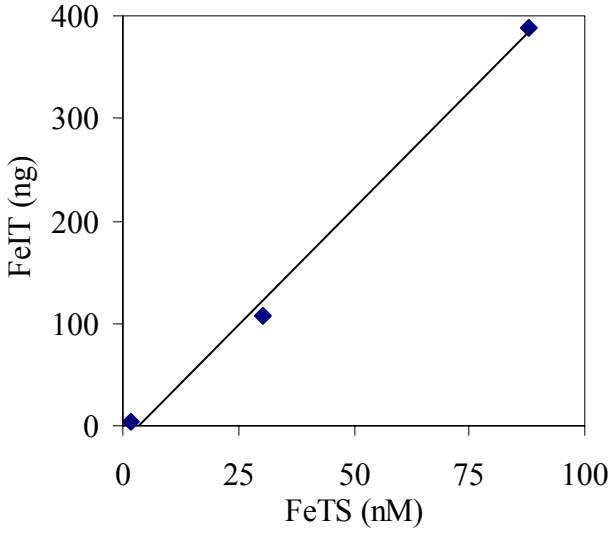

Figure 4-3. Relationship between amounts of Fe taken up by *Trichodesmium* (FeIT) and total Fe concentrations released in seawater (FeTS) in the T4 (seawater plus aerosols and *Trichodesmium* treatment) of the three aerosol addition experiments (E1, E2 and E3).

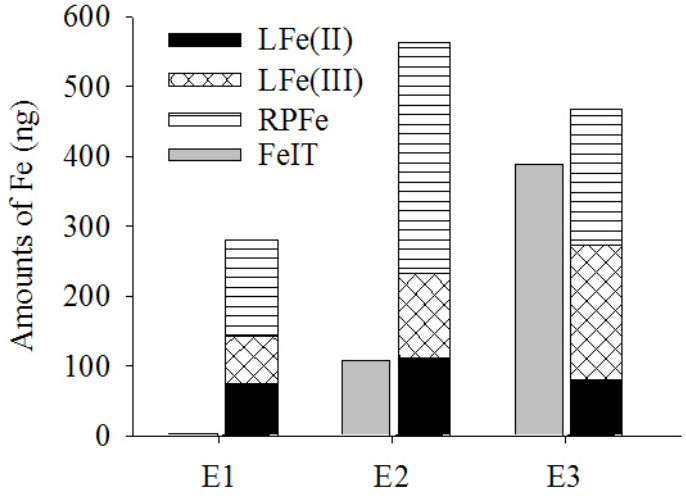

Figure 4-4. Amounts of the labile Fe(II) (LFe(II)), labile Fe(III) (LFe(III)) and reducible particulate Fe (RPFe) on the Teflon filter sub-samples added to the incubation solutions, and the Fe amounts taken up by the *Trichodesmium* (FeIT) in the three aerosol addition experiments (E1, E2 and E3).

The FeTT was measured in the E3, and the FeIT was estimated by assuming that 60% of total Fe associated with *Trichodesmium* colonies was interior Fe. This 60% value was the average percentage of the FeIT to FeTT observed for the *Trichodesmium* collected directly from the station where E3 was performed (Tovar-Sanchez, unpubl. data). The intracellular Fe was 53, 61 and 30 ng in approximately 200 *Trichodesmium* colonies (each treatment) for the E1, E2 and E3 after the 24-hour incubation in only filtered seawater (T3), respectively. However, the intracellular Fe in the *Trichodesmium* incubated with aerosol filters (T4) increased as more aerosol Fe was added to the incubation solutions from E1 to E3 (Figure 4-2). A linear relationship ($p<0.05$, $r=0.9974$) was found between the FeIT and FeTS in the T4 treatments for the three experiments (Figure 4-3).

The measured FeTT was 0.649 μg and the estimated FeIT (60% of the FeTT) was 0.389 μg in the T4 treatment for E3, which were about 20 and 12 factors higher than the total FeDS (0.033 μg) measured in the T2 of the E3, respectively (Table 4-1). Nonetheless, the FeIT amount was found to be less than the amount of the total labile Fe (LFeIA), that is the sum of the LFe(II), LFe(III) and RPFe, on the aerosol filter sub-samples added to the incubation solutions for the three experiments (E1, E2 and E3, Figure 4-4). The amounts of the total labile Fe (0.49±0.137 μg) on the Teflon filter sub-samples were at least a few factors higher than the FeDS (0.12±0.104 μg) measured in the T2 of the experiments (E3 to E6). It is difficult to determine a trend from this data but for E2 & E3 the uptake of aerosol Fe was on the order of the measured labile Fe on the filter (Figure 4-4), which is only a small fraction (about 2%) of the total Fe.

The intracellular P content in the *Trichodesmium* colonies (PIT) was also determined after the 24-hour incubation along with the FeIT for the T3 (seawater plus *Trichodesmium* only) and the T4 (seawater plus aerosols and *Trichodesmium*) of the experiment E1 and E2. The total fraction of P in the *Trichodesmium* (PTT) was measured along with the FeTT for the E3. PTT and FeTT for the first two experiments were calculated by multiplying the FeIT and PIT by factors of 2 and 4.8, respectively. Theses factors were average ratios between the Fe(P)TT and Fe(P)IT for the *Trichodesmium* colonies collected directly from the surface ocean during the cruise (Tovar-Sanchez, unpubl. data). The molar ratios of FeTT to PTT were 0.009±0.003 and 0.82±1.38 for the *Tichodesmium* control (T3) and aerosol addition treatment (T4), respectively. The initial amounts of water-soluble phosphate on the aerosol filter sub-samples (PIA) added to the incubation solutions were measured, and the LFeIA to PIA molar ratios ranged from 0.14 to 0.67.

4.3.3 Effects of Trichodesmium on Iron Dissolution in Seawater

The FeRF amounts were always higher in the T4 (contains *Trichodesmium*) than in the T2 (no *Trichodesmium*) for the aerosol addition experiments with the exception of E5 (Table 4-1). Correspondingly, the FeTS concentrations were found to be significantly lower in the T4 than in the T2 treatments for the five experiments (E1 to E4, and E6) (Figure 4-5). The mean FeDS concentration in the T4 was also found to be lower than that in the T2 (Figure 4-5), although this difference was not statistically significant. Six aerosol addition experiments were performed at different locations (Figure 4-1) and different times, and therefore the aerosols, *Trichodesmium* and seawater collected locally for each experiment may have different properties.

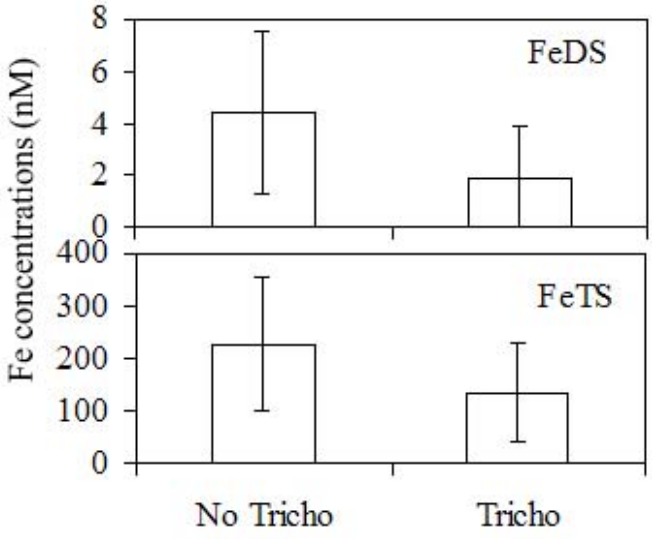

Figure 4-5. Average of the total Fe concentrations suspended in the seawater (FeTS) for the aerosol addition experiments E2, E3, E4 and E6, and the average of the dissolved Fe concentrations in the seawater (FeDS) for the experiments E3, E4 and E6 after the 24-hour incubation with (T4) and without (T2) *Trichodesmium*. The error bars represent plus/minus standard deviation.

The molar ratio of dissolved Fe (DFe) to P (DP) (Table 4-1) in the seawater collected at the station where E5 was conducted was the lowest value, about a factor of 55 lower than the highest DFe : DP ratio during the six experiments.

The FeDS (< 0.4μm) concentrations were measured after 24-hour incubation from the E3 to E6. The FeDS concentrations appear to be affected strongly by the *Trichodesmium* and not correlated with any other Fe pools in the T4 when *Trichodesmium* colonies exist. In the T2 treatments where only the aerosol-filter was added to the seawater, however, more Fe was dissolved into the seawater (FeDS) when more particulate Fe (FePS) was released off the Teflon filter sub-samples (Table 4-1).

4.4 Discussions

Filtered seawater, aerosol filters and *Trichodesmium* colonies were combined to construct a small ecosystem (T4) to investigate the uptake of Fe from ambient aerosol to *Trichodesmium*. The influence of *Trichodesmium* on the dissolution and suspension of particulate Fe from the ambient aerosol samples were also investigated. A conceptual model is built to describe the Fe transfer starting from the aerosol filters ending at the *Trichodesmium* colonies that in turn influence the Fe-transfer process in the studied ecosystem (Figure 4-6). Aerosol Fe on the Teflon filter sub-samples is released into the seawater to become the dissolved or suspended particulate Fe species, these two Fe pools can transfer Fe between each other through adsorption/desorption process, and then taken up by the *Trichodesmium*. The *Trichodesmium* in turn influences the Fe release from the Teflon filter sub-samples

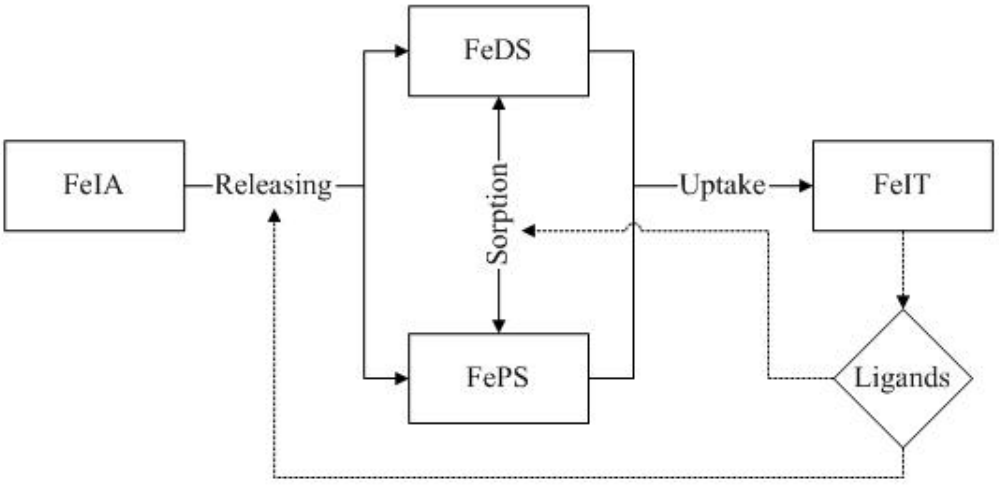

Figure 4-6. Conceptual model of the Fe transfer that starts from the Fe on the aerosol filter sub-samples (FeIA) to the dissolved and suspended particulate Fe in the seawater (FeDS and FePS), and then ends at the intracellular Fe in the *Trichodesmium* (FeIT). *Trichodesmium* in turn influences the aerosol Fe release and the adsorption/desorption between the FeDS and FePS in the seawater through the organic ligands it excretes.

and the Fe adsorption/desorption between the dissolved and particulate Fe species in the seawater through the organic ligands it excretes.

Aerosol Fe released as the dissolved or suspended particulate Fe in the seawater from the Teflon filter sub-samples were affected by the presence of *Trichodesmium* (Figure 4-6). The FeRF increased 4% to 23% by adding the *Trichodesmium* colonies into the incubation solutions (by comparing T4 and T2 in Table 4-1), and the averaged FeTS and FeDS in the T2 (no *Trichodesmium*) were about twice as much as those in the T4 (contains *Trichodesmium*) for the experiments E1 to E4 and E6 (Figure 4-5). Nonetheless, a significantly higher FeTS and FeDS were observed in the T4 treatment compared to the T2 for the E5 (Table 4-1). The E5 was done outside of the plume at the location where the lowest DFe : DP ratio was found in the ambient seawater (Table 4-1). So the discrepancy of the E5 may be explained by assuming that the *Trichodesmium* used in the experiment was historically iron-limited and thereby assisted the suspension and dissolution of the aerosol Fe. *Trichodesmium* may affect the release of aerosol Fe through the organic ligands it excretes. Extracellular ligands such as siderophores are produced by many marine cyanobacteria as part of high-affinity Fe uptake systems (Wilhelm, 1995; Granger and Price, 1999; Reid, 1993), and intracellular ligands are likely released into the water column as cells breakdown (Hutchins et al, 1999). These organic ligands may adsorb to the surface of the Teflon filters (or to the aerosol species present on the filter) which is able to lock the Fe-containing surface sites or inhibit the particle release. This inhibition may not occur for Fe dissolution in the real ocean since the Teflon filter was added artificially to the incubation solutions.

Trichodesmium had a considerable effect on the FeDS (<0.4μm) (by comparing T4 and T2 in Table 4-1), suggesting that the dissolved Fe phase had been taken up by the *Trichodesmium* (Figure 4-6). However, the FeIT (0.389μg) was about an order of magnitude higher than the FeDS (0.033μg) in the E3, and there was a significant linear relationship ($p<0.05$, $r=0.997$) between the FeTS and FeIT from the E1 to E3. This suggests that *Trichodesmium* is able to utilize part of the colloidal or particulate Fe species in addition to the dissolved Fe in the seawater (Figure 4-6). The similar behavior has been observed in the cultured *Trichodesmium* (IMS 101) (Kustka et al., 2003b) and coastal diatom *T. pseudonana* (Sunda and Huntsman, 1995). They continued to take up Fe within the region where the Fe hydroxides are precipitating. Hutchins et al. (1999) also observed the uptake of organically complexed Fe by phytoplankton when the Fe concentration had exceeded the solubility limit of inorganic Fe in seawater.

The FeIT amount was less than or comparable to the LFeIA amount (Figure 4-4) indicating that the total labile Fe determined by the aqueous extraction procedure (Chen and Siefert, 2003) may be a threshold of the Fe that was taken up by *Trichodesmium* in this study. Total labile Fe includes three labile Fe species, LFe(II), LFe(III) and RPFe. The LFe(II) has the greatest probability of being directly utilized by phytoplankton or converting to Fe colloids (e.g. organically complexed Fe(III)) that would also be bioavailable (Miller and Kester, 1994). The LFe(III) and RPFe may adsorb to the cell surface and undergo a thermal or photochemical reduction before taken up by phytoplankton, or can be reduced to bioavailable forms of Fe in the atmosphere or surface seawater (Siefert et al., 1996; Chen and Siefert, 2003;

Voelker and Sedlak, 1995). Nonetheless, due to the limited data in this study the correlation between the FeIT and LFeIA cannot be quantified.

The *Trichodesmium* colonies collected in the western tropical North Atlantic (the region where the experiments were done) had a larger Fe : P stoichiometry compared to the *Trichodesmium* in the Australian coast and central North Atlantic (Table 4-2). Sanudo-Wilhelmy et al. (2001) suggested the *Trichodesmium* colonies in the central Atlantic were not Fe-limited because the dissolved Fe : P molar ratios were 3 to 4 times higher than the ratio measured in *Trichodesmium*. In the western tropical North Atlantic the dissolved Fe : P ratios (calculated from the column 2 and 3 of Table 4-1) ranged from 7.8 to 431 mmole mol^{-1}, which were close to or orders of magnitude higher than the FeTT : PTT ratios (Table 4-2) measured in the T3 of the aerosol addition experiments. So the *Trichodesmium* colonies used in the experiments were also expected to be not historically Fe-limited. Moreover, the FeTT : PTT ratios (Table 4-2) were about 1 or 2 orders of magnitude lower than the LFeIA : PIA ratio (140 to 670 mmol mol^{-1}) added into the incubation solutions. *Trichodesmium* tended to take up aerosol Fe but not phosphorus which caused 1.2 to 215 times (compare T3 and T4 in Table 4-2) increase in the Fe : P ratio after the incubation. Therefore, the *Trichodesmium* in this Atlantic region may adapt to a luxury uptake of aerosol Fe as a consequence of the episodic nature of the dust events from North Africa. Assuming that the intracellular C : P molar ratio in *Trichodesmium* is at the Redfield ratio of 106: 1, the calculated intracellular Fe : C ratios will range from 225 to 6.82×10^{4} μmol mol^{-1} in the *Trichodesmium* after the 24-hour incubation with added aerosol filters. These Fe : C ratios are about a factor of 6

to 1795 larger than the 38 μmol mol^{-1} Fe/C ratio required for a moderately Fe-limited diazotrophic growth (0.1 d^{-1}) , which is consistent with the *Trichodesmium* luxury uptake of Fe observed by Kustka et al. (2003b). These results seem to indicate that the *Trichodesmium* collected in the western tropical North Atlantic had a large capacity for the luxury uptake of aerosol Fe.

4.5 Conclusions

The aerosol addition experiments were conducted over the tropical North Atlantic Ocean using freshly collected aerosols, seawater, and *Trichodesmium* colonies. A significant uptake of aerosol Fe by *Trichodesmium* was observed and the uptake amounts increased in incubations with increasing amounts of aerosol Fe. *Trichodesmium* was able to utilize part of the colloidal or even particulate Fe besides the dissolved Fe species in the seawater. The organic ligands produced by *Trichodesmium* may play an important role in controlling the aerosol-Fe releasing and dissolving into the seawater. *Trichodesmium* colonies collected in the western tropical North Atlantic have demonstrated a luxury uptake of aerosol Fe in the aerosol addition experiments, and the uptake amounts were at least 6 times greater than needed for moderately Fe-limited growth (0.1 d^{-1}). The *Trichodesmium* uptake of Fe was less or comparable to the total labile Fe determined by the aqueous extraction procedure suggesting that the labile Fe pool may be a threshold of the aerosol Fe that can be taken up by *Trichodesmium*.

Chapter 5: Seasonal Variations of Atmospheric Nutrient Concentrations and Sources over the Western Tropical North Atlantic

5.1 Introduction

The present study is part of a research program that focused on the factors effecting and impact of diazotrophic microorganisms in the western tropical North Atlantic (WTNA). Diazotrophs that influence other phytoplankton and trophic levels through input of fixed nitrogen (N) in this Atlantic region are under the impacts of the world's largest freshwater flow from the Amazon River and the heavy dust loadings from North Africa. Long-range transport of African dust to the WTNA, Caribbean Sea and even northeastern South America were demonstrated by numerous ground-based observations (Prospero and Carlson, 1972; Prospero et al., 1970; Prospero et al., 1981; Talbot et al., 1990; Swap et al., 1992; Chen and Siefert, 2004; Siefert et al., 1999) and satellite imagery of aerosol optical thickness (AOT) (Moulin and Chiapello, 2004). The dust mobilized by winds from arid regions (Sahara and/or Sahel regions) carries significant amounts of Fe and P to the surface ocean, and the estimated atmospheric input of Fe and P to the WTNA (5° to 15°N, 40° to 60°W) are up to 3×10^{8} and 9×10^{6} Kg y^{-1}, respectively (Prospero et al., 1996). Anthropogenic emissions from North America and Europe, and biomass burning products from Africa can also be transported over this Atlantic region during different seasons. Pollution plumes that emerge from the east coast of North America and west coast of Europe over the North Atlantic Ocean are prominent in the spring and summer as manifested by AOT distributions (Prospero et al., 1996). Anthropogenic sources in

Europe and the Mediterranean coastal region of North Africa (Med-Africa) can potentially contribute to the concentrations of NO_3^- and other constituents over the Sahara and, subsequently, at Barbados throughout the year (Savoie et al., 1989). The importance of European sources is supported by the isotopic composition of Pb in aerosols at Barbados (Hamelin et al., 1989). The transport of biomass burning products from the savannah and forest regions of North Africa to Barbados only occur during the winter and spring as evidenced by the large seasonal variation in the NO_3^- to non-sea-salt sulfate (NSS SO_4^{2-}) mass ratios (Savoie et al., 1992). During the periods impacted by biomass burning, the NO_3^-/NSS SO_4^{2-} ratios at Barbados are a factor of about 2 higher than those during the summer and during the non-impacted winter and spring periods (Savoie et al., 1992). These mineral and anthropogenic aerosols over the WTNA are a source of important nutrient species to the surface water, and may play a significant role in controlling N_2 fixation and primary production in this region.

Deposition of atmospheric aerosol is a dominant source of Fe to the remote ocean (Duce and Tindale, 1991). Recent studies have found Fe to be a rate-limiting nutrient to phytoplankton growth especially N_2-fixing organisms in certain regions of the open ocean (Martin et al, 1994; Paerl et al., 1994; Coale et al, 1996; Cooper et al., 1996; Falkowski, 1997; Sunda et al., 1997; Boyd et al, 2000). Fe in the atmosphere is dominant by ferric oxides and (oxy)hydroxides. These species can undergo thermal or photochemical reduction in atmospheric waters and surface ocean (Siefert et al., 1996; Voelker and Sedlak, 1995; Chen and Siefert, 2003) to become more soluble and therefore more bioavailable ferrous Fe (Fe(II)). Fe(II) species has been found in

aqueous aerosol solutions, and the labile Fe(II) concentrations extracted with a low pH (1.0 to 4.5) buffer solution are typically a few percent (0.3 to 1.8%) of total Fe in marine mineral aerosols (Zhu et al., 1993; Siefert et al., 1999; Johansen et al., 2000; Chen and Siefert, 2004a). Chen and Siefert (2004a) observed a seasonal and spatial variability of labile Fe(II) percent (0.3 to 16%) in aerosols over the tropical and sub-tropical North Atlantic, and indicated that aerosol source origins could influence the Fe speciation in aerosols and thereby atmospheric fluxes of bioavailable Fe to the surface ocean. A daily variability of soluble Fe(II), with the mean concentration in the day (3.7 ng m^{-3}) twice as much as the night value (1.5 ng m^{-3}), was observed in aerosols collected from this Atlantic region (Zhu et al., 1997).

Atmospheric deposition may have an impact on supplies of major nutrients N and P to the surface ocean. The N deposition can affect oceanic N cycling at locations near the coasts where atmospheric sources are large, or in the centers of the highly stratified gyres where little nitrate is supplied to the surface by vertical mixing of the ocean (Michaels et al., 1996). Anthropogenic food and energy production extensively mobilize reactive N in the watershed of the North Atlantic Ocean (Galloway et al., 1996). Anthropogenic N deposition has increased the productivity of the surface ocean (Galloway et al., 1996), and significantly contributes to eutrophication problems in coastal waters (Paerl, 1997; Spokes et al., 2000). P limitation of N_2 fixation by *Trichodesmium* has been suspected in the western and central North Atlantic Ocean (Wu et al., 2000; Sanudo-Wilhelmy et al., 2001). Baker et al. (2003) indicated that N_2 fixation stimulated by excess atmospheric Fe supply and phytoplankton utilization of atmospheric nutrient inputs (the measured aerosol N: P

was high) will tend to drive the ecosystem towards P limitation. But the N: P ratio in aerosol particles may vary seasonally and spatially due to the changes of aerosol origins.

Two size fractions of aerosol samples were collected over the WTNA (5° to 15°N, 40° to 60°W) during three separate month-long cruises in winter 2001, summer 2001 and spring 2003. Labile Fe species were measured onboard immediately after sample collection using an aqueous sequential extraction procedure (chapter 2, Chen and Siefert, 2003). Major nutrient (phosphate PO_4^{3-}, nitrate NO_3^-, and ammonium NH_4^+) concentrations were determined back in the laboratory using ion chromatography (IC). Atmospheric labile and total Fe data collected during the winter and summer 2001 cruises have been reported in chapter 3 (see also Chen and Siefert, 2004a). In this chapter we present soluble atmospheric PO_4^{3-}, NO_3^-, and NH_4^+ concentrations observed during the three seasonal cruises. Potential source contributions to atmospheric PO_4^{3-}, NO_3^-, and NH_4^+ over the WTNA are explored based on the seasonal variations of these nutrient concentrations and correlations in two size fractions of aerosol samples collected. Dry deposition fluxes of atmospheric nutrients N, P and labile Fe are calculated and their influences on the WTNA ecosystem discussed for each different season.

5.2 Sample Collection and Analysis

5.2.1 Sampling Location and Periods

Aerosol samples were collected aboard the R/V *Seward Johnson* during winter (20 January to 18 February) 2001 and spring (18 April to 20 May) 2003 and aboard the R/V *Knorr* during summer (9 July to 14 August) 2001 cruises over the

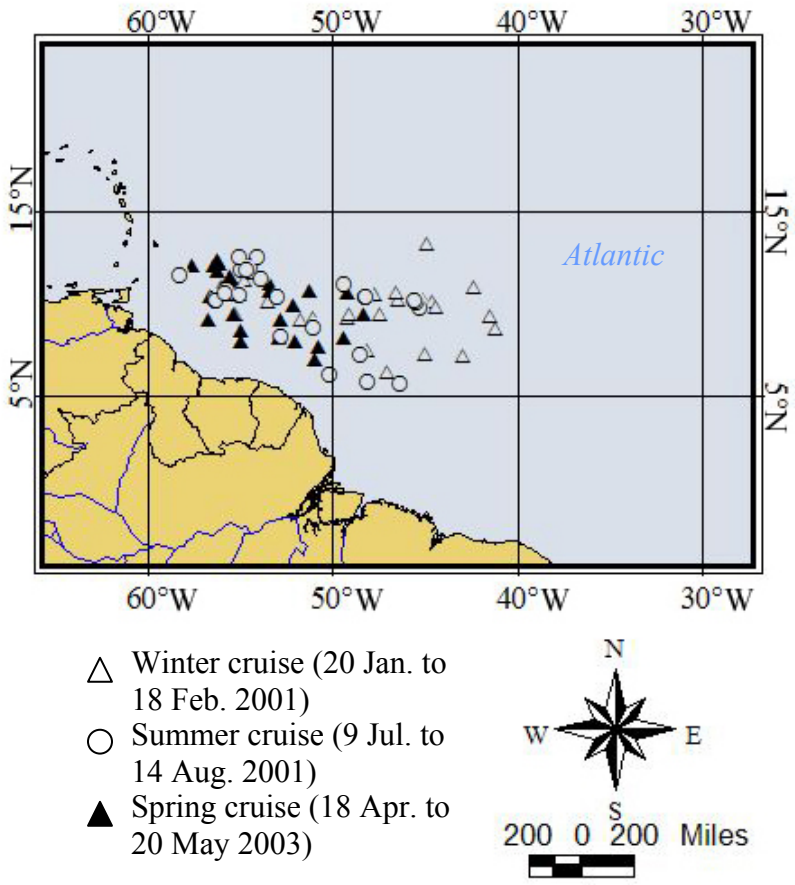

Figure 5-1. Sampling locations during three separate month-long cruises in different seasons (20 January to 18 February 2001, 9 July to 14 August 2001, 18 April to 20 May 2003) over the western tropical North Atlantic (5° to 15°N, 40° to 60°W), each marker on the map represents an approximately 24-hour aerosol sample collected.

WTNA (5° to 15°N, 40° to 60°W). The sampling locations are outlined in Figure 5-1, where each marker represents an approximately 24-hour aerosol sample collected.

Five-day isentropic air mass back trajectories (AMBTs) were calculated from the National Oceanic and Atmospheric Administration (NOAA) FNL database using the Hybrid Single-Particle Langrangian Integrated Trajectories (HY-SPLIT) program (Draxler, 2002; see Chapter 3 for model description). Although there are errors associated with these calculations due to the data sets and models, the AMBTs still provide useful information about the synoptic situation and general source of the air mass sampled. Figure 5-2 shows four typical AMBTs calculated at 20 m, 500 m and 1500 m height levels at 01 or 00 UTC (corresponding to the midway of each sampling day) over the WTNA during the sampling seasons.

5.2.2 Aerosol Collection

A high volume dichotomous virtual impactor (HVDVI) (Solomon *et al*., 1983) was setup on 02 deck of the R/V *Knorr* or above the bridge of the R/V *Seward Johnson* to collect two size fractions (with aerodynamic diameters greater than and less than 2.5μm) of ambient aerosols. The fine and coarse fraction aerosols were collected on two 90 mm diameter Teflon membrane filters (Gelman Zefluor, 1μm pore size). A sector sampling system was used to allow collection of aerosol samples only when the relative wind direction was ±75° relative to ship's bow. Aerosol sample collection and chemical analysis below were done following trace-metal clean techniques.

5.2.3 Chemical Analyses

Total labile Fe concentrations on the filter were investigated using an aqueous sequential extraction procedure and measured using long path length absorbance spectroscopy (LPAS) (Waterbury et al., 1997) immediately after sample collection. The detailed extraction procedure is given in chapter 2 (see also Chen and Siefert, 2003). Briefly, the 0.5 mM of pH 4.5 formate-acetate buffer was used as the extraction solution and the 50 mM of HA solution used for the Fe reduction. Total labile Fe was operationally defined by the extraction time and reagents. Elemental analysis of 14 elements (Al, Ca, Fe, K, Na, Mg, Cr, Co, Cu, Pb, Mn, Ni, V, Zn) on the sample filters was performed using a strong-acid microwave digestion procedure followed by an ICP-MS (HP 4500) analysis. Anion (F^-, glycolate, acetate, formate, MSA^-, Cl^-, SO_4^{2-}, oxalate, Br^-, NO_3^-, PO_4^{3-}) and cation (Li^+, Na^+, NH_4^+, K^+, Mg^{2+}, Ca^{2+}) concentrations were analyzed using an aqueous extraction technique (Derrick and Moyers, 1981) and a Dionex DX-600 IC. More details on elemental and ion analyses on the filter and calculation of atmospheric concentrations (e.g. NSS SO_4^{2-}) are described in chapter 3 (see also Chen and Siefert, 2004).

5.3 Results and Discussions

Dust transport from North Africa over the North Atlantic Ocean occurs throughout the year (Figure 5-2b), but the dust transport pathway and effected region vary due to the seasonal shift of the Inter-Tropical Convergence Zone (ITCZ) (Husar et al., 1997; Moulin et al., 1997). This seasonal north to south shift in the maximum zone of African dust from summer to winter influences other air mass circulations

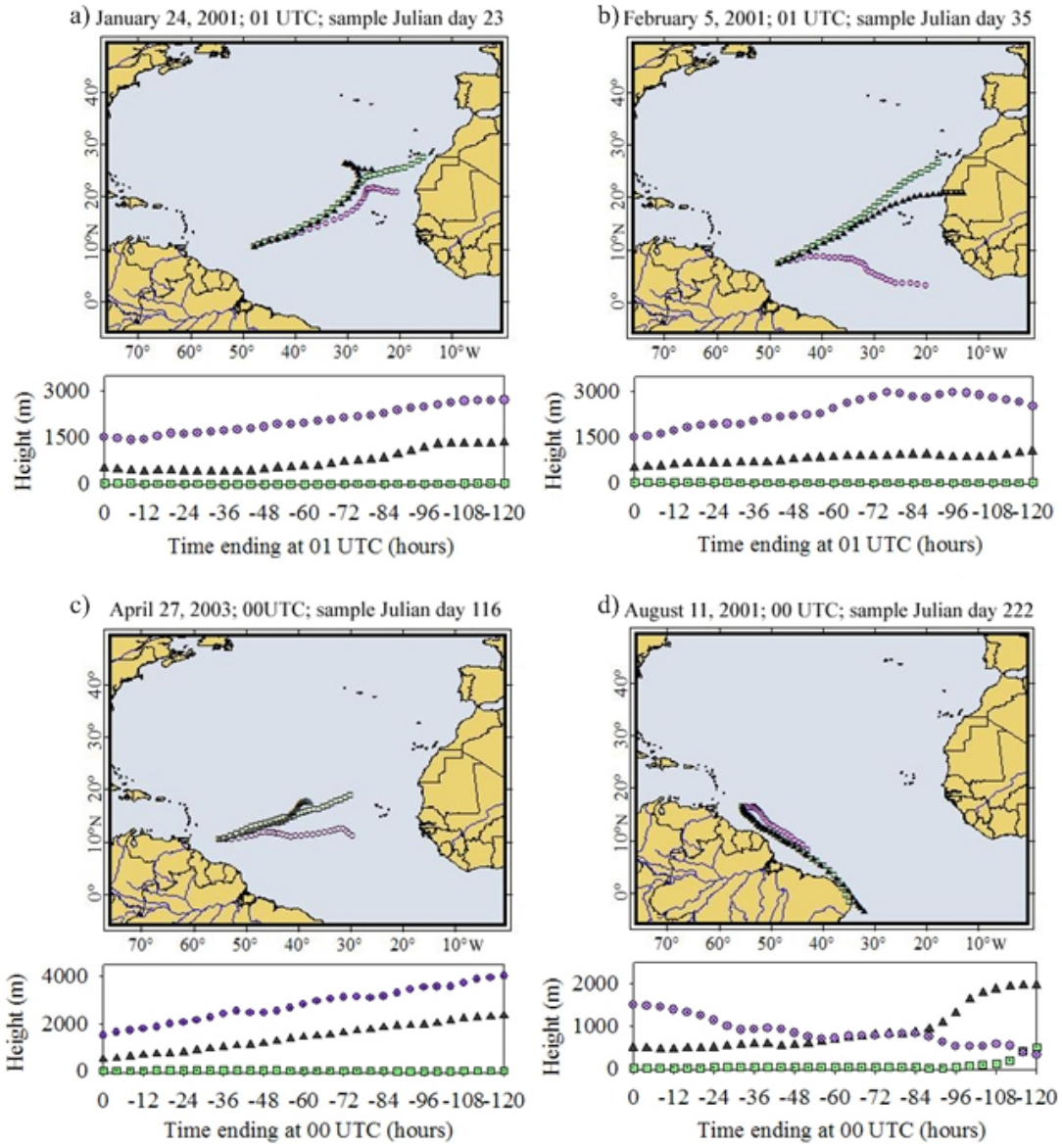

Figure 5-2. Representative 5-day air mass back trajectories over the western tropical North Atlantic during different seasons, trajectories are calculated at three different final elevations (squares, 20 m; triangles, 500 m; circles, 1500 m) above sea level for (a) January 24, 2001; (b) February 5, 2001; (c) April 27, 2003; (d) August 11, 2001.

over the studied Atlantic region. During the month of January, air masses can be transported from the central North Atlantic where they may originate from anthropogenic emissions from North America or Europe (Figure 5-2a). On the other hand, air masses swept along the eastern coast of South America can reach the sampling area during the summer (Figure 5-2d) when the maximum dust zone moves to 20°N Atlantic Ocean. Another situation is that the air masses have circulated over the WTNA for more than 5 days before being collected as shown in figure 5-2c, and the aerosols in these air masses have had more time to undergo thermal and photochemical reactions that can control the chemical composition of the aerosols. The dust transport during winter occurs at lower altitudes in the trade wind layer (Figure 5-2a & b), while the highest dust loadings at high altitudes take place during summer due to the temperature-dependent upward motion of dust-laden air (Chiapello et al., 1995, 1997). Swap et al. (1996) also indicated that dust outbreaks are most frequent and extensive during the first 6 months of the year, with an annual peak in outbreak activity observed during February through April.

5.3.1 Nutrient Concentrations in Aerosols

Aerosol samples collected during three research cruises from the WTNA were analyzed for water-soluble PO_4^{3-}, NO_3^- and NH_4^+. The percentages of observations with reported concentrations below the detection limit are 13.4%, 1.3% and 3.2% for soluble PO_4^{3-}, NO_3^- and NH_4^+, respectively. Values of half of the detection limit were used for samples that were below detection limit in the statistical analysis. The concentrations of the nutrient species in fine and coarse aerosol fractions for the different sampling seasons were graphed in Figure 5-3. Statistical analysis using one-

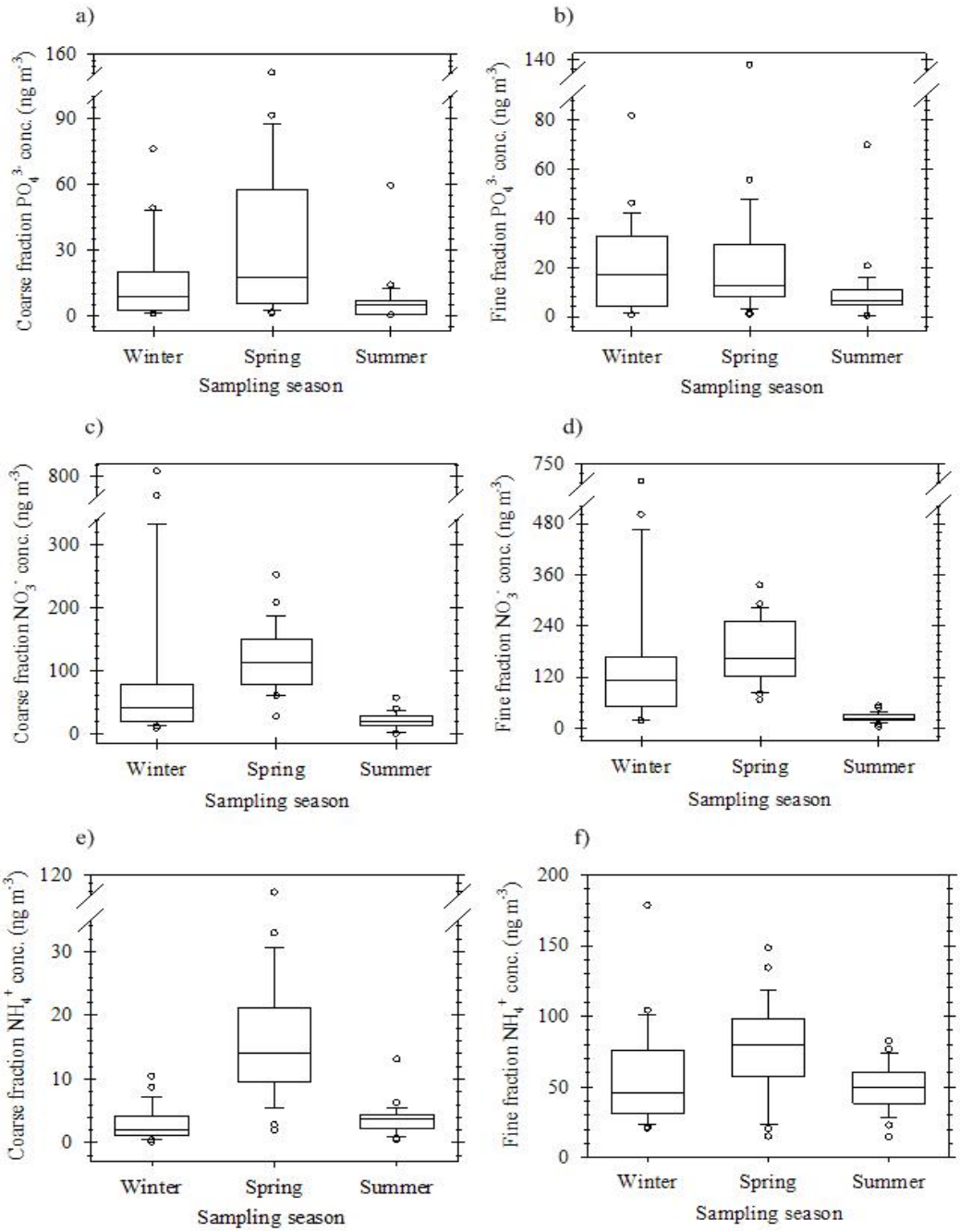

Figure 5-3. Box-and-whiskers plots comparing the concentrations of (a & b) water-soluble PO_4^{3-}, (c & d) NO_3^- and (e & f) NH_4^+ in coarse and fine fractions of aerosol particles collected during three different seasons (winter, 20 January to 18 February 2001; summer, 9 July to 14 August 2001; spring, 18 April to 20 May 2003) over the western tropical North Atlantic.

way ANOVA of the means was performed after $\log_{10}$ transformation of the data, due to non-normal distributions of the concentrations.

The highest soluble PO_4^{3-} concentrations (range from 0.63 to 82 ng m^{-3}, median 17 ng m^{-3}) were observed in the winter, and the lowest concentrations (range from 0.26 to 70 ng m^{-3}, median 6.5 ng m^{-3}) occurred in the summer (Figure 5-3a) in the fine aerosol fraction. However, soluble PO_4^{3-} concentrations in coarse fraction of aerosols were found to decrease in the order of spring > winter > summer (median 17 > 8.8 > 5.0 ng m^{-3}) (Figure 5-3b). There was no significant difference between the winter and spring in total soluble atmospheric PO_4^{3-} concentrations (fine + coarse fractions), but the concentrations in the summer were significantly lower than those in the winter ($p<0.02$) and spring ($p<0.001$). Concentrations of total soluble PO_4^{3-} (seasonal medians from 11.5 to 29 ng m^{-3}) measured in the present study are comparable to the mean concentrations of seawater leachable PO_4^{3-} in aerosols observed over the Mediterranean Sea where the air masses are influenced by both Saharan dust and European emissions (Herut et al., 1999; Migon et al., 2001). The mean concentrations of seawater leachable PO_4^{3-} were 48.6 ng m^{-3} (Herut et al., 1999) and 18.8 ng m^{-3} over the Southeast and Northwest Mediterranean, respectively. The latter one was calculated by multiplying the mean total P concentration (51 ng m^{-3}, Migon et al., 2001) with the percentage of leachable P in seawater (10 to 15%, Ridame and Guieu, 2002) and then converted to the PO_4^{3-} concentration. At Barbados, West Indies (13°15' N, 59°30' W), the reported annual (1989 to 1996) mean concentration of mineral dust was around 11 μg m^{-3} (Prospero, 1999). Given an estimation of total P concentration in Saharan aerosols is 0.09% and the maximum

solubility of P in Saharan particles is 21% (Ridame and Guieu, 2002), soluble aerosol PO_4^{3-} concentration is estimated to be around 6.4 ng m^{-3} at Barbados. This calculated concentration is slightly lower than what we measured over the WTNA, because (1) mineral dust concentrations at Barbados may be lower than those over the WTNA, and/or (2) air masses over the WTNA may be contributed by not only mineral dust from North Africa but anthropogenic emissions that contain significant amounts of P with a very high solubility. Over the WTNA, about 66% of soluble PO_4^{3-} concentration was found to be associated with the fine aerosol fraction in the winter, while during the spring the fine-fraction PO_4^{3-} was only about 41% of total soluble PO_4^{3-} concentration in aerosols.

Soluble NO_3^- and NH_4^+ concentrations in aerosols over the WTNA also demonstrated a seasonal variability. Soluble aerosol NO_3^- concentrations measured during three different seasons were significantly different from each other ($p<0.002$), and the concentrations declined in the order of spring > winter > summer for both fine (median 163 > 111 > 24 ng m^{-3}) and coarse (median 113 > 43 > 19 ng m^{-3}) fractions of aerosol samples (Figure 5-3c & d). Similarly, the highest soluble NH_4^+ concentrations were also measured during the spring for both fine (range from 15 to 148 ng m^{-3}, median 80 ng m^{-3}) and coarse (range from 2 to 112 ng m^{-3}, median 14 ng m^{-3}) fractions of aerosols, but the lowest concentrations (median 46 and 1.9 ng m^{-3} for the fine and coarse fractions, respectively) were found in the winter (Figure 5-3e & f). Differences between the total soluble aerosol NH_4^+ concentrations in the spring and those in the winter and summer were statistically significant ($p<0.001$), whereas no significant concentration difference was found between the winter and the summer.

The current measurements of total (fine + coarse) soluble NO_3^- (median 43 to 276 ng m^{-3}) and total NH_4^+ (median 48 to 94 ng m^{-3}) concentrations range similar to the previously reported data from the remote North Atlantic. Harrison and Peak (1996) reported that the average NO_3^- and NH_4^+ concentrations in aerosols collected from June 7 to 16 at Santa Maria (37°N, 25°W) were 240±120 and 80±140 ng m^{-3}, respectively. Quinn et al. (2001) divided the Atlantic into seven regions from which Northern Hemisphere marine (31 to 15.5°N, 65.8 to 43.3°W), African dust (15.5 to 8°N, 43.3 to 32.9°W) and mixture of African dust and biomass burning (8°N to 3°S, 32.9 to 26°W) regions were closest to our studying area and had mean NO_3^- and NH_4^+ concentrations ranging from 235 to 1330 ng m^{-3} and 30 to150 ng m^{-3}, respectively. 56 to 72% of total soluble NO_3^- was associated with the fine fraction of aerosol particles during the sampling seasons over the WTNA (by comparing Figure 5-3c & d). However, almost all soluble NH_4^+ (85 to 96% of total NH_4^+) concentration was found in the fine aerosol fraction (by comparing Figure 5-3e & f), which is consistent with the observations from other studies (Huebert et al., 1998; Quinn et al., 2001; Jickells et al., 2003).

5.3.2 Sources of Soluble Phosphate

Aerosols over the WTNA are influenced principally by mineral dust transported from North Africa as well as anthropogenic emission sources from the surrounding continents (Figure 5-2, AMBTs) which may become significant during certain seasonal period. African dust contains on average 0.09% particulate phosphorus (Ridame and Guieu, 2002), and copious quantities of the soil-derived dust may play an important role in controlling the atmospheric P concentration over the

WTNA. However, phosphates transported with the mineral dust are principally bound to Fe oxides or associated with Ca, Mg, Al and Fe, which are known to be weakly soluble (Bergametti et al., 1992; Ridame and Guieu, 2002). Therefore anthropogenic P emission sources (e.g. incinerators, biomass burning: Migon and Sandroni, 1999; Migon et al., 2001; fertilizers, pesticides: Herut et al., 1999) may be also responsible for an efficient contribution to soluble atmospheric PO_4^{3-} concentration over the WTNA. The aerosol P associated with the marine source is negligible (Bergametti et al., 1992).

Significantly higher concentrations of soluble aerosol PO_4^{3-} were observed during the winter and spring than in the summer (Figure 5-3a & b), which may be consistent with the most frequent and extensive dust breakouts from North Africa during February through April (Swap et al., 1996). In the winter, 66% of total concentration of soluble PO_4^{3-} was found to be in the fine fraction of aerosol particles, and the fine-fraction PO_4^{3-} was significantly ($p<0.05$) correlated with the crustal tracers Al and Fe (Table 5-1). This enrichment in the fine fraction may be a result of additional low-altitude transport (below 1.5 to 3 km) of African dust during the winter (Chiapello et al., 1995, Figure 5-2a & b) where coarse particles are removed quickly from the dust plumes and fine particles are favored in the long-range transport to the WTNA. Significant correlations between PO_4^{3-} and Al/Fe (Table 5-1) further suggested that the mineral dust from North Africa was a dominant source for soluble PO_4^{3-} in the fine fraction of aerosols during the winter. Soluble aerosol PO_4^{3-} concentrations measured during the spring showed no relationship with Al/Fe. By contrast, they were significantly coupled with the Cu ($p<0.01$), NO_3^- and NSS SO_4^{2-}

Table 5-1. Correlation coefficients between the soluble PO_4^{3-} and other chemical species in fine and coarse fractions of aerosol samples collected during the winter (20 January to 18 February 2001), spring (18 April to 20 May 2003) and summer (9 July to 14 August 2001) periods over the western tropical North Atlantic

	Winter		Spring		Summer	
	Coarse	Fine	Coarse	Fine	Coarse	Fine
Al	0.069	0.428[a]	0.054	-0.041	-0.027	0.097
Ca	0.109	0.273	0.250	0.016	-0.049	0.051
Fe	0.094	0.418[a]	0.059	0.207	-0.053	0.069
K	0.293	0.345[a]	0.152	0.038	-0.028	0.067
Cu	0.469[b]	-0.338[a]	-0.190	0.584[b]	0.278	0.084
Pb	0.203	0.366[a]	0.071	0.013	-0.034	-0.138
Zn	0.441[a]	0.381[a]	-0.155	0.176	0.115	0.126
Na^+	0.407[a]	0.669[b]	0.240	0.117	0.722[b]	0.534[b]
Cl^-	0.481[b]	0.702[b]	0.270	0.133	0.801[b]	0.462[b]
F^-	0.757[b]	0.078	0.025	0.198	-0.242	0.159
NO_3^-	0.777[b]	0.213	0.199	0.380[a]	0.259	0.036
NH_4^+	0.431[a]	0.167	0.034	0.241	-0.053	0.159
NSS SO_4^{2-}	0.454[a]	0.198	0.114	0.401[a]	0.878[b]	-0.074
MSA^-	0.232	0.050	-0.145	0.238	-0.153	-0.188
PO_4^{3-}	1	1	1	1	1	1

[a] and [b] represent <0.05 and <0.01 significance levels, respectively.

($p<0.05$) concentrations in the fine fraction of aerosol particles (Table 5-1). Yamasoe et al. (2000) indicated that savanna and tropical forest biomass burning could be responsible for a considerable emission of Cu. NO_3^- to NSS SO_4^{2-} mass ratio was used as an indicator of biomass burning materials from North Africa, and the ratios at Barbados were a factor of 4 higher during the winter and spring that are impacted by biomass burning than those in the summer and fall (Savoie et al., 1989). Likewise, over the WTNA the total atmospheric NO_3^-/NSS SO_4^{2-} mass ratios observed during the spring (median 0.52) were approximately a factor of 3 and 5 higher than those observed during the winter (median 0.16) and summer (median 0.10), respectively (Figure 5-4). Therefore, biomass burning materials instead of mineral dust transported from North Africa may be a major source for soluble PO_4^{3-} in the fine fraction of aerosols during the spring.

In the winter coarse fraction of aerosols, soluble PO_4^{3-} was correlated with the Cu, F^-, NO_3^- ($p<0.01$), and Zn, NH_4^+, NSS SO_4^{2-} ($p<0.05$), six species (Table 5-1) that are most likely to be emitted through anthropogenic activities. Due to relatively low NO_3^- /NSS SO_4^{2-} ratios (median 0.17) during the winter, these species may be a signature of the air masses influenced by anthropogenic emissions from North America and/or Europe rather than African biomass burning. F^- associated with large particulate matter and SO_2 are usually emitted during phosphate rock mining (Environmental Protection Agency). Florida and North Carolina, the southeastern coast of the US, accounted for 85% of the domestic phosphate rock produced during1993 (Llewellyn, 1993). It is speculated that the mining dust (coarse fraction aerosol) emitted at the southeastern US could be transported to the WTNA during the

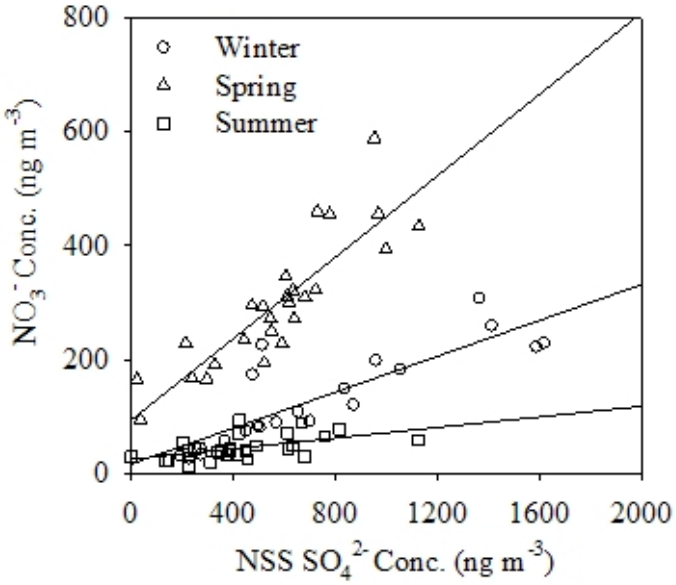

Figure 5-4. Concentrations of total soluble NO_3^- versus NSS SO_4^{2-} in fine and coarse fraction of aerosol samples collected during the winter (20 January to 18 February 2001), spring (18 April to 20 May 2003) and summer (9 July to 14 August 2001) periods over the western tropical North Atlantic

winter when the ITCZ moves to the equator. Cu, Zn (Hu et al., 2003; Feng et al., 2000), NO_3^-, NH_4^+ and NSS SO_4^{2-} may represent another PO_4^{3-} emission source, waste incineration (Migon and Sandroni, 1999; Migon et al., 2001), from North America and/or Europe. The incineration emissions may be mixed with the mining dust on its transport pathway to the WTNA, and this aerosol mixture may be a dominant contributor to soluble PO_4^{3-} in the coarse aerosol fraction during the winter. Soluble PO_4^{3-} concentrations in the coarse aerosol fraction during the summer were strongly correlated with the NSS SO_4^{2-} ($p<0.01$) concentrations (Table 5-1), which may be also a signature of anthropogenic emission sources for soluble atmospheric PO_4^{3-} over the WTNA.

5.3.3 Sources of Nitrate and Ammonium

Aerosol NO_3^- is produced by the oxidation of NO_x and aerosol NH_4^+ is produced by the gas to particle conversion of gas-phase NH_3. The predominant sources of NO_x and NH_3 are anthropogenic activities such as fuel combustion, fertilizer application, and the cultivation of certain crops (Prospero et al., 1996). In the remote marine atmosphere, a substantial natural marine source of NH_3 was also verified by air-sea exchange measurements (Quinn et al, 1988; Gibb et al., 1999), Lagrangian (Zhuang and Huebert, 1996) and isotopic (Jickells et al., 2003) analyses of marine aerosols. To explore the source contributions to the measured NO_3^- and NH_4^+ concentrations during the different seasons over the WTNA, correlation coefficients were calculated for each pair of the Cu, Zn, NO_3^-, NH_4^+, NSS SO_4^{2-} and MSA^- species in aerosols (Table 5-2).

Soluble NO_3^- concentration in aerosols was significantly correlated with Cu, Zn, NH_4^+ ($p<0.05$) and NSS SO_4^{2-} ($p<0.01$) concentrations during the winter (Table 5-2). Concurrent existence of Cu, Zn and NSS SO_4^{2-} in aerosols may be a signature of high-temperature combustion (e.g. fossil fuel combustion: Pavageau et al., 2004; incineration: Hu et al., 2003; Feng et al., 2000). No correlation was found between NSS SO_4^{2-} and MSA^- (Table 5-2), suggesting that marine biogenic NSS SO_4^{2-} produced from emissions of DMS (dimethylsulphide) (Liss and Galloway, 1993, Johansen et al., 2000) was insignificant during the winter. MSA^- is one of the oxidation products of DMS that is used as a surrogate for the biogenically derived NSS SO_4^{2-} (Johansen et al., 2000). Similarly, aerosol NH_4^+ was strongly correlated with NSS SO_4^{2-} ($p<0.01$) but not associated with MSA^- (Table 5-2), which suggests that marine biogenic emission of NH_3 was negligible. Thereafter, atmospheric NO_3^- and NH_4^+ measured during the winter over the WTNA were primarily associated with anthropogenic emission sources from North America and/or Europe.

Both soluble NO_3^- and NH_4^+ concentrations in aerosols were found to be the highest during the spring (Figure 5-3). Enhanced NO_3^- concentrations in the spring may be a signature for air masses having anthropogenic emissions, for example, biomass burning which is at its seasonal peak during the spring and winter (Savoie et al., 1992), and fertilizer application which increases greatly in the spring corresponding to crop cycles. Increased marine biological activities during this growing season may also add considerable amount of NH_3 into the atmosphere. It has been proposed that the air-sea cycling of DMS and NH_3 may be closely coupled and represent an important component of a natural biogenic climate-regulating

Table 5-2. Correlation coefficients between total concentrations (fine + coarse fractions) of chemical species in aerosols measured during the (a) winter (20 January to 18 February 2001), (b) spring (18 April to 20 May 2003) and (c) summer (9 July to 14 August 2001) periods over the western tropical North Atlantic

	Zn	NO_3^-	NH_4^+	NSS SO_4^{2-}	MSA^-
(a) Winter aerosols, n = 25					
Cu	-0.188	0.395[a]	0.066	0.232	-0.357[a]
Zn		0.436[a]	0.443[a]	0.574[b]	0.043
NO_3^-			0.346[a]	0.575[b]	-0.530[b]
NH_4^+				0.627[b]	0.315
NSS SO_4^{2-}					0.003
(b) Spring aerosols, n = 26					
Cu	0.223	0.198	0.159	0.191	0.018
Zn		0.119	0.115	0.011	0.117
NO_3^-			0.790[b]	0.867[b]	0.708[b]
NH_4^+				0.840[b]	0.623[b]
NSS SO_4^{2-}					0.697[b]
(c) Summer aerosols, n = 27					
Cu	0.785[b]	0.416[a]	0.205	0.676[b]	-0.061
Zn		0.390[a]	0.263	0.586[b]	-0.115
NO_3^-			0.455[b]	0.535[b]	-0.390[a]
NH_4^+				0.420[a]	0.342[a]
NSS SO_4^{2-}					-0.113

[a] and [b] represent <0.05 and <0.01 significance levels, respectively.

feedback system via aerosol formation (Quinn et al., 1988, 1990; Liss and Galloway, 1993; Savoie et al., 1993). During the spring, NO_3^-, NH_4^+, NSS SO_4^{2-} and MSA^- species in aerosols were found to be strongly correlated with each other ($p<0.01$) but not correlated with Cu and Zn (Table 5-2). Strong correlation between NSS SO_4^{2-} and MSA^- follows their identical major source (DMS oxidation) (Allen et al., 1997), with any continental NSS SO_4^{2-} sources having little impact on this relationship. Close relationships between NO_3^-, NH_4^+ and MSA^- (Table 5-2) suggest that marine biogenic emissions of NH_3 was a major source for aerosol NO_3^- and NH_4^+ concentrations during the spring.

During the summer, aerosol NO_3^- and NH_4^+ concentrations over the WTNA were found to be significantly anti-correlated and correlated with MSA^-, respectively (Table 5-2). Moreover, Cu and Zn in aerosols were significant coupled with NO_3^- but not with NH_4^+ (Table 5-2), implying that aerosol NO_3^- and NH_4^+ probably had differently primary source contributions during the summer. Aerosol NO_3^- concentrations over the WTNA may principally derived from emissions of high-temperature combustion from the surrounding continents (South America may also be included according to the AMBT in Figure 5-2d) due to its significant correlations with Cu, Zn and NSS SO_4^{2-} (Pavageau et al., 2004; Hu et al., 2003; Feng et al., 2000). There was also a strong correlation between NH_4^+ and NO_3^- ($p<0.01$), suggesting that both continental combustion and marine biogenic sources may contribute substantially to aerosol NH_4^+ concentrations during the summer.

5.3.4 Impact of Nutrient Deposition on Ecosystems

Dry deposition fluxes (F_d) of dissolved inorganic P (DIP), N (DIN) and labile Fe (LFe) were estimated from measured species concentrations (C_a) in air and model-derived or estimated dry deposition velocity (V_d) (Jickells et al., 1987; Duce et al., 1991) as follows:

$$F_d = C_a \times V_d$$

The term V_d varies with particles size from gravitational settling of large particles to impaction and diffusion of small particles (submicrometer) and is dependent on climatological and physical conditions in the troposphere. Our flux estimates used the V_d of 0.1 and 2 cm s^{-1} for fine and coarse aerosol particles, respectively due to these factors (Duce et al., 1991), and may have an inherent uncertainty by a factor of 3. Total labile Fe concentrations in the fine and coarse fraction of aerosols measured over the WTNA during the winter and summer 2001 have been reported in chapter 3(see also Chen and Siefert, 2004). Total labile Fe concentrations measured during the spring 2003 ranged from 1.9 to 31 (median 11) ng m^{-3} and from 0.33 to 15 (median 2.3) ng m^{-3} for the fine and coarse fraction of aerosol particles, respectively.

Table 5-3 showed the calculated medians of LFe, DIN and DIP dry fluxes, and DIN vs DIP ratios over the WTNA during the winter, spring and summer periods. The aerosol input DIN: DIP was found to be only a litter lower than the Redfield ratio (N: P = 16: 1) during all three seasons (Table 5-3). If the primary production was solely supported by the aerosol inputs of nutrients in this region, low DIN: DIP ratio would suggest that aerosol DIP input could support higher amounts of primary production (up to 60% during the winter) than does the input of DIN. Atmospheric

Table 5-3. Calculated dry fluxes (medians) of labile Fe (LFe), dissolved inorganic N (DIN: NO_3^-+NH_4^+) and P (DIP) in units of μmol m^{-2} d^{-1}, and DIN vs DIP ratios over the western tropical North Atlantic (WTNA) during the winter (20 January to 18 February 2001), spring (18 April to 20 May 2003) and summer (9 July to 14 August 2001) periods

Periods	LFe	DIN	DIP	DIN:DIP
Winter	0.24	1.8	0.18	10 : 1
Spring	0.087	5.1	0.32	15.9 : 1
Summer	0.058	1.2	0.097	12.4 : 1

fluxes would tend to drive the WTNA towards N limitation and favor diozotrophs growth (Tyrrell, 1999) which were found to be abundant in this oceanic region (Carpenter et al., in preparation). Aerosol deposition input significant amounts of total labile Fe (0.058 to 0.24 μmol m^{-2} d^{-1}, Table 5-3) that was expected to be bioavailble by N_2-fixing *Trichodesmium* (Chen et al., 2004) into the WTNA. Berman-Frank et al. (2001) indicated that Fe availability had little effect on the bulk C: N: P elemental composition of *Trichodesmium* IMS101 over the three orders of magnitude change in dissolved Fe. By using the *Trichodesmium* C: N: P ratios under Fe-replete conditions (156: 10: 1, Berman-Frank et al., 2001), we find that the aerosol input of DIN estimated here supports slightly higher C production than the DIP input (Table 5-3). Assuming that aerosol nutrient (DIN and DIP) inputs were only used for *Trichodesmium* growth, the new C production driven by aerosol deposition would be 28, 80 and 19 μmol m^{-2} d^{-1} in terms of the DIN inputs for the winter, spring and summer, respectively. These production rates would require at most 0.003 to 0.005 μmol m^{-2} d^{-1} of bioavailable Fe for *Trichodesmium* growth under Fe-replete conditions (Fe: C ratios range from 13 to 168 μmol mol^{-1}, Berman-Frank et al., 2001; Kustka et al., 2003). Therefore, aerosol input of LFe (Table 5-3) was in a large excess compared to that (0.003 to 0.005 μmol m^{-2} d^{-1}) required for the *Trichodesmium* growth driven by other aerosol nutrient (DIN & DIP) depositions.

The discussion above was from an only atmospheric view. However, the aerosol inputs of DIN and DIP may not be important compared to the horizontal fluxes of NO_3^- and PO_4^{3-} and the N_2 fixation in the WTNA. The WTNA accepts a large Amazon River discharge along with large quantities of continental materials

(Mueller-Karger et al. 1989). The estimated fluxes of NO_3^- and PO_4^{3-} from the continental shelves to the surface Atlantic Ocean (0° to 10°N) were 0.11×10^{12} and 0.014×10^{12} moles y^{-1}, respectively (Michaels et al., 1996). Assuming the shelf inputs of nutrients were dispersed northward to 15°N and eastward to 60°W by the Amazon flow (Kidd and Sander 1979), the calculated fluxes of NO_3^- and PO_4^{3-} to the WTNA would be 97 and 12 μmol m^{-2} d^{-1}, respectively. The average rate of N_2 fixation reported for the WTNA was 73 μmol N m^{-2} d^{-1} (Capone et al., 1997). However the vertical fluxes of nutrients to the euphotic zone were expected to be small in this region due to the large freshwater discharge to the ocean surface. The NO_3^- (170 μmol m^{-2} d^{-1}) and PO_4^{3-} (12 μmol m^{-2} d^{-1}) supplies from the horizontal fluxes and the N_2 fixation were found to be 1-2 orders of magnitude larger than the aerosol inputs of DIN and DIP (Table 5-3), and the ratio between the total fluxes of N and P was 14.2: 1. This N vs P ratio will tend to drive the WTNA towards N limitation and favor diozotroph growth. Similarly, the required fluxes of labile Fe (0.024 to 0.31 μmol m^{-2} d^{-1}) for the diazotroph growth driven by the P supply were estimated according to the Fe: C: P ratios in *Trichodesmium*. The required fluxes 0.024 to 0.31 μmol m^{-2} d^{-1} are just comparable to the aerosol input of labile Fe (0.058 to 0.24) to the WTNA, suggesting that the atmospheric deposition of Fe may be a rate-limiting nutrient to diazotroph growth in this oceanic region.

5.4 Conclusions

Soluble PO_4^{3-}, NO_3^- and NH_4^+ concentrations in aerosols measured over the WTNA showed a markedly seasonal variability. Total soluble PO_4^{3-} concentrations (fine + coarse fractions) in the winter and spring were found to be significantly higher

than those in the summer. The largest concentrations of soluble NO_3^- and NH_4^+ were observed in the spring, and the NO_3^- and NH_4^+ concentrations declined in the order of spring > winter > summer and spring > summer ≈ winter, respectively. Mineral dust transported from North Africa and anthropogenic emission sources from the surrounding continents all have an impact on aerosol nutrient species over the WTNA. During the winter, soluble PO_4^{3-} in the fine fraction of aerosols was principally contributed by mineral dust from North Africa, while the mixture of mining dust from North America and incineration emissions from North America and/or Europe may be a major source for soluble PO_4^{3-} in the coarse fraction of aerosols. Biomass burning materials from North Africa were responsible for soluble PO_4^{3-} concentrations in the fine fraction of aerosols during the spring. Aerosol NO_3^- and NH_4^+ concentrations measured during the winter and spring were primarily contributed by anthropogenic and marine biogenic sources, respectively. During the summer, aerosol NO_3^- may be principally derived from continental combustion emissions, whereas aerosol NH_4^+ may be contributed by both combustion and marine biogenic sources. From an only atmospheric view, aerosol inputs of LFe, DIN and DIP into the WTNA will first drive the water column towards a short-term N limitation, and later on due to the enhanced N_2 fixation the nutrient depositions will tend to deplete P in the water column. If considered other flux sources of N and P (e.g. shelf fluxes and N_2 fixation) atmospheric deposition of labile Fe to the WTNA would be a controlling factor for diazotroph growth.

Chapter 6: Atmospheric Iron and Other Nutrient Species over the Central North Pacific: Distributions, Sources, and Ecological Impacts

6.1 Introduction

In the contemporary ocean, photosynthetic carbon (C) fixation by marine phytoplankton leads to formation of about 45 gigatons of organic carbon per annum, of which 16 gigatons are exported to the ocean interior (Falkowski et al., 1998). Changes in the magnitude of total and export production can strongly influence atmospheric CO_2 levels and thereby influence climate on geological time scales. This oceanic primary production is predominantly controlled by the availability of essential nutrients such as nitrogen, phosphorus and iron and by sunlight levels. When sunlight is sufficient, there is generally a positive correlation between macronutrient concentrations and phytoplankton biomass in the water column (Levitus et al., 1993). In high-nitrate low-chlorophyll (HNLC) areas of the ocean, where the macronutrients delivered exceed that assimilated, Fe has been hypothesized to be a limiting factor for phytoplankton productivity (Martin and Fitzwater, 1988; Martin and Gordon, 1988; Martin et al., 1989, 1991). This Fe limitation hypothesis has been supported by *in situ* Fe enrichment experiments in the equatorial Pacific (IRONEX II, Coale et al., 1996), Southern Ocean (SOIREE, Boyd et al., 2000) and in the western subarctic Pacific (SEEDS, Tsuda et al., 2003). Fe was also found to be a crucial micronutrient for diazotrophic microorganisms and therefore may influence N_2 fixation in the oligotrophic ocean (Falkowski, 1997; Gruber and Sarmiento, 1997).

External nutrient supplies to the euphotic zone have three major sources, which include atmospheric deposition, vertical mixing, and riverine and continental-self sediments transport. In the open ocean such as the central Pacific gyre and the Sargasso Sea, atmospheric deposition of dust to the sea surface supplies the majority of the new (not acquired via nutrient cycling) Fe required for photosynthetic production (Duce, 1986; Duce and Tindale, 1991; Jickells and Spokes, 2001). It has been also found that episodic atmospheric N inputs can contribute to an important portion of "new production" in some oligotrophic oceans (Duce, 1986; Owens et al., 1992; Michaels et al., 1993). The aerosol inputs of Fe and P species over the central North Pacific were highly seasonal with the maximum fluxes in spring (Duce and Tindale, 1991; Perry et al., 1999). This marked seasonality was due to the springtime transport of mineral aerosols from northwestern China, the Gobi Desert and the Loess Plateau (Merrill et al., 1989; Gao et al., 1992).

Fe in aerosols is dominated by refractory minerals (e.g. aluminosilicates) and the more labile ferric oxides and (oxy)hydroxides that must dissolve in seawater before being utilized by phytoplankton. These ferric species can be photochemically reduced to soluble ferrous iron (Fe(II)) in atmospheric waters or surface seawater (Siefert et al., 1996; Voelker and Sedlak, 1995; Chen and Siefert, 2003). Studies have found that labile Fe(II) did exist in aqueous aerosol solutions, but the Fe(II) concentrations extracted with the low pH (1.0 to 4.5) buffers are only a few percent (0.3 to 1.8%) of total Fe in marine mineral aerosols (Zhu et al., 1993; Siefert et al., 1999; Johansen et al., 2000; Chen and Siefert, 2004a). P transported with the mineral aerosols is also known to be weakly soluble (Bergametti et al., 1992; Ridame and

Guieu, 2002). The concentrations of the aerosol Fe(II) and soluble aerosol P over the North Atlantic Ocean are influenced significantly by different aerosol origins during the different seasons (Chen and Siefert, 2004a; Chen and Siefert, 2004b). Asian dust, anthropogenic emissions from both Asia and North America (Perry et al., 1999), volcanic eruption on Hawaii islands and sea salts (Porter et al., 2002; Sansone et al., 2002; Carrico et al., 2003) may all have significant contributions to aerosol particles over the central North Pacific and thus affect atmospheric inputs of labile Fe and other nutrient species to this oceanic ecosystem.

Four research cruises were performed over the central North Pacific (15°N to 30°N, 150°W to 175°E) during the spring, summer and fall periods. Fine and coarse fractions of aerosol samples were collected daily on the cruises. Labile Fe species were measured onboard immediately after sample collection using an aqueous sequential extraction procedure (Chen and Siefert, 2003). Major nutrient (PO_4^{3-}, NO_3^- and NH_4^+) concentrations were determined back in the laboratory using aqueous extraction and ion chromatography (IC). Temporal distributions of labile Fe, PO_4^{3-}, NO_3^-, and NH_4^+ concentrations in aerosols over the central North Pacific are presented in this chapter. Potential source contributions to atmospheric labile Fe over the central North Pacific are explored based on the correlations between the labile Fe and other species concentrations in the two size fractions of aerosols. Dry deposition fluxes of atmospheric N, P and labile Fe are calculated and their influences on the central North Pacific ecosystem discussed for each different season.

6.2 Sample Collection and Analysis

6.2.1 Sampling Location and Periods

Aerosol samples were collected aboard the R/V *Wecoma*, R/V *Kaimikai-o-Kanalao*, R/V *Kilo Moana* and R/V *Roger Revelle* during the spring (9 April to 26 April) 2001, summer (1 July to 16 July) 2002, fall (23 September to 15 October) 2002 and summer (6 August to 21 August) 2003 periods over the central North Pacific (15°N to 30°N, 150°W to 175°E), respectively. The sampling locations are outlined in Figure 6-1, where each marker represents an approximately 24-hour aerosol sample collected.

Five-day isentropic air mass back trajectories (AMBTs) were calculated from the National Oceanic and Atmospheric Administration (NOAA) FNL database using the Hybrid Single-Particle Langrangian Integrated Trajectories (HY-SPLIT) program (Draxler, 2002). The detailed model description was presented in Chapter 3. Figure 6-2 shows four typical AMBTs calculated at 20 m, 500 m and 1500 m height levels at 04 UTC (corresponding to the midway of each sampling day) over the central North Pacific during the sampling periods.

6.2.2 Aerosol Collection

A high volume dichotomous virtual impactor (HVDVI) (Solomon *et al*., 1983) was used to collect two size fractions (with aerodynamic diameters greater than and less than 2.5μm) of aerosol samples. The fine and coarse fraction aerosols were collected on two 90 mm diameter Teflon membrane filters (Gelman Zefluor, 1μm pore size). A sector sampling system was used to allow collection of aerosol samples only when the relative wind direction was ±75° relative to ship's bow. Aerosol

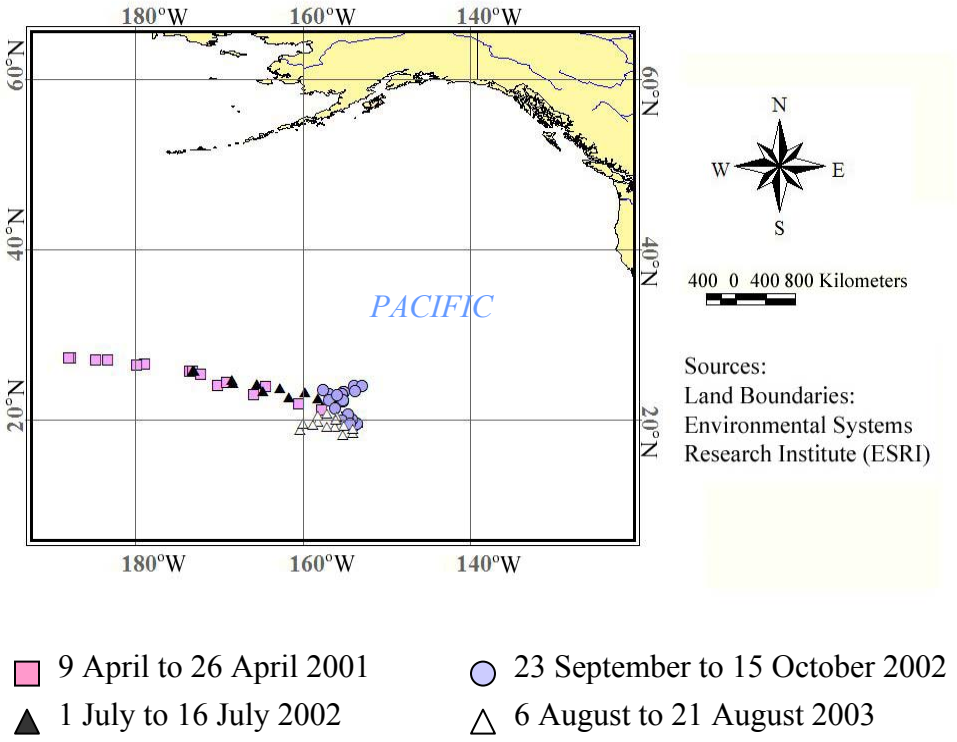

Figure 6-1. Sampling locations during four separate research cruises in different seasons (spring, 9 April to 26 April 2001; summer, 1 July to 16 July 2002; fall, 23 September to 15 October 2002; summer, 6 August to 21 August 2003) over the central North Pacific (15°N to 30°N, 150°W to 175°E), each marker on the map represents an approximately 24-hour aerosol sample collected.

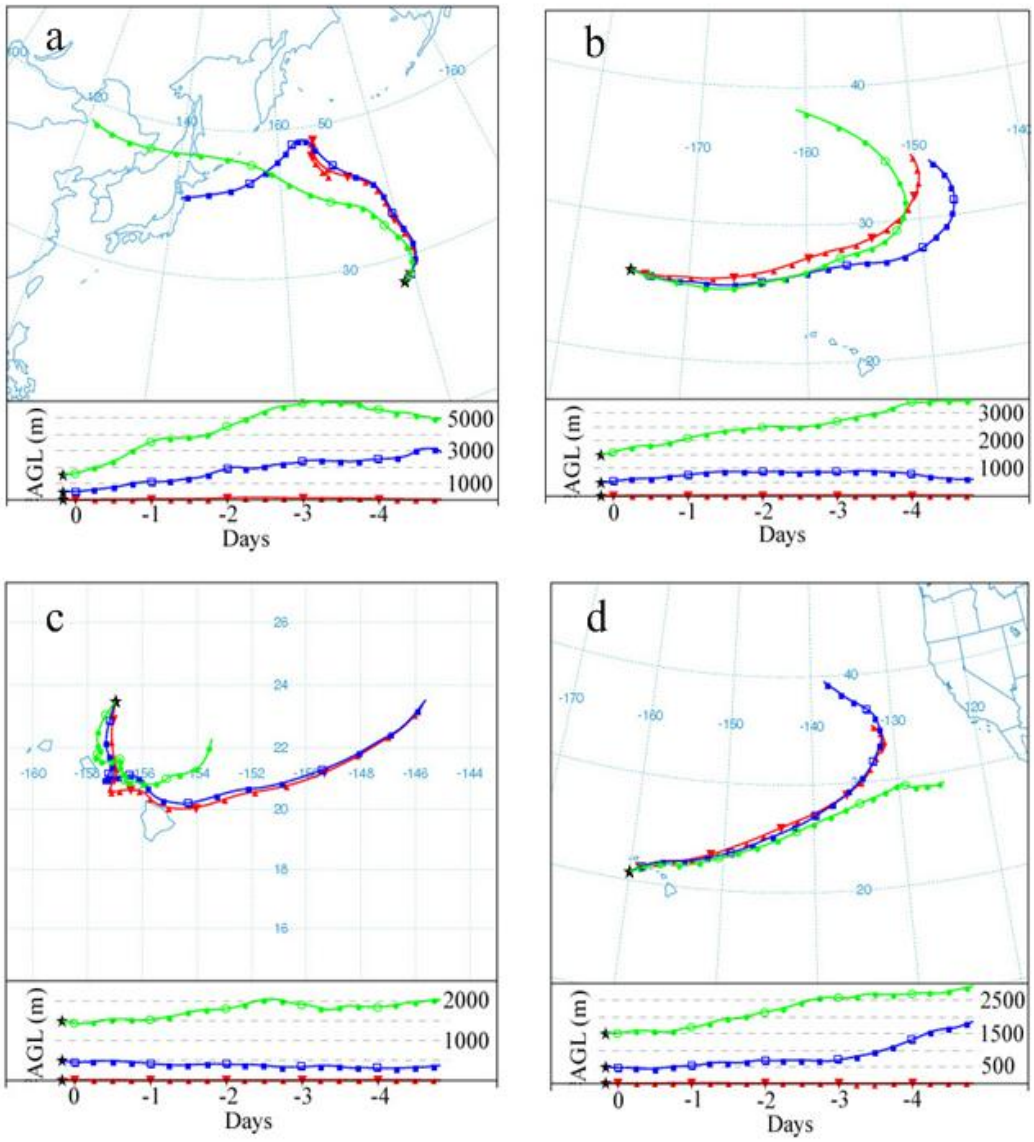

Figure 6-2. Representative 5-day air mass back trajectories over the central North Pacific during different seasons, trajectories are calculated at three different final elevations (triangles 20 m; squares, 500 m; circles, 1500 m) above sea level for (a) 19 April 2001; (b) 9 July 2002; (c) 25 September 2002; (d) 14 August 2003.

sample collection and chemical analysis below were done following trace-metal clean techniques.

6.2.3 Chemical Analyses

Total labile Fe concentrations on the filter were investigated using an aqueous sequential extraction procedure and measured using long path length absorbance spectroscopy (LPAS) (Waterbury et al., 1997) immediately after sample collection. The detailed extraction procedure is given in chapter 2 (see also Chen and Siefert, 2003). Elemental analysis of 14 elements (Al, Ca, Fe, K, Na, Mg, Cr, Co, Cu, Pb, Mn, Ni, V, Zn) on the sample filters was performed using a strong-acid microwave digestion procedure followed by an ICP-MS (HP 4500) analysis. Anion (F^-, glycolate, acetate, formate, MSA^-, Cl^-, SO_4^{2-}, oxalate, Br^-, NO_3^-, PO_4^{3-}) and cation (Li^+, Na^+, NH_4^+, K^+, Mg^{2+}, Ca^{2+}) concentrations were analyzed using an aqueous extraction technique (Derrick and Moyers, 1981) and a Dionex DX-600 IC. More details on elemental and ion analyses on the filter and calculation of atmospheric concentrations (e.g. non-sea-salt sulfate, NSS SO_4^{2-}) are described in chapter 3 (see also Chen and Siefert, 2004a).

6.3 Results and Discussions

6.3.1 Transport Pathways of Air Masses

AMBTs calculated from NOAA FNL database showed that low-level northeasterly winds at 20 m, 500 m and 1500 m levels frequently passed over the central North Pacific (15°N to 30°N, 150°W to 175°E) from July to October (Figure 6-2b, c, d). The back trajectories had circulated over the Pacific Ocean for more than five days without contacting the continent and sometimes swept through the Hawaii

islands (Figure 6-2c) before arriving at reception sites. Extremely low aerosol mass concentrations have been observed throughout most of the year at Mauna Loa Observatory (MLO) which is located on the island of Hawaii (Parrington and Zoller, 1984; Zieman et al., 1995; Holmes et al., 1997). The signature of volcanic plumes was occasionally found in the marine aerosols collected over the Pacific Ocean close to Hawaii (Carrico et al., 2003). The aerosol plume produced by lava-seawater interactions along the shoreline of Kilauea volcano at Hawaii could contribute significant amount of both toxic and nutrient elements to the atmosphere surrounding the Hawaii (Sansone et al., 2002).

In April 2001 back trajectories over the central North Pacific often lead to Asia (Figure 6-2a). Asian dust storms originating from the desert regions in China and Mongolia were lifted up to the altitudes of 5-10 km and then carried by westerlies to the Pacific Ocean mostly during the spring (Merrill et al., 1989; Zhang et al., 1998). Over the central Pacific trajectories turned southeastward, descend into the marine boundary layer and eventually reach the R/V *Wecoma* after 4-5 days (Figure 6-2a). The long-range transport of large quantities of Asian dust to the Midway Island (28°13'N, 177°22'W, Merrill et al., 1989) and the MLO at Hawaii has been observed every spring (Shaw, 1980; Bodhaine et al., 1981; Darzi and Winchester, 1982; Braaten and Cahill, 1986; Prospero, 1996; Holmes and Zoller, 1996; Holmes et al., 1997). During transport, Asian dust plume could be mixed with anthropogenic gases and aerosols over the industrialized regions of China and bring significant amount of pollutants to the Pacific Ocean (Miller, 1981; Harris and Kahl, 1990). The Asian dust transport episodes at MLO have been accompanied by increases in aerosol

optical absorption, sulfur, nitric acid, methane, and carbon monoxide (Darzi and Winchester, 1982; Levy II and Moxin, 1989; Harris et al., 1992; Bodhaine, 1995; Zieman et al., 1995; Cahill and Perry, 1996; Jaffe et al., 1997; Perry et al., 1999). These anthropogenic pollutants may have great impacts on the speciation and deposition fluxes of nutrient elements (Fe, N, P) in aerosols over the central North Pacific.

6.3.2 Temporal Distributions of Total and Labile Fe

Total Fe concentrations were measured in both fine and coarse fractions of aerosol samples collected during the four separate cruises over the central North Pacific. The highest concentrations of the total Fe were observed during the April (Figure 6-3a) for both fine and coarse aerosol fractions. The mean values of 74 ng m^{-3} for the fine fraction and 59 ng m^{-3} for the coarse fraction in April 2001 were about an order of magnitude larger than those measured in July 2002, when the lowest Fe concentrations were found with the mean values of 4.1 and 5.9 ng m^{-3} for the fine and coarse aerosol fractions, respectively (Figure 6-3b). This observation of significantly high concentrations of aerosol Fe in April 2001 was consistent with the Asian dust transport to the central Pacific during the spring (Bodhaine et al., 1981; Holmes et al., 1997; Perry et al., 1999). Perry et al. (1999) averaged the monthly elemental concentrations in fine aerosols at the MLO from 1993 to 1996 and reported that the mean Fe concentration in April was 60 ng m^{-3}, which is similar to our observations of the aerosol Fe in April 2001 (mean 74 ng m^{-3} for fine aerosol fraction). The Asian Pacific Regional Aerosol Characterization Experiment (ACE-Asia) was also performed over the Asian-Pacific region from 31 March to 4 May 2001. Field

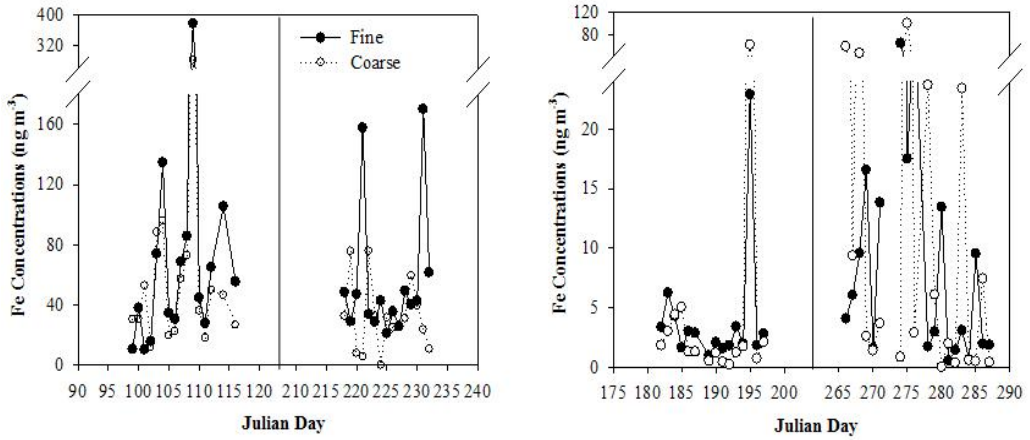

Figure 6-3. Total Fe concentrations in the fine and coarse fractions of aerosol samples collected during the a) 2001 spring (9 to 26 April) and 2003 summer (6 to 21 August), and b) 2002 summer (1 to 16 July) and 2002 fall (23 September to 15 October) cruises over the central North Pacific

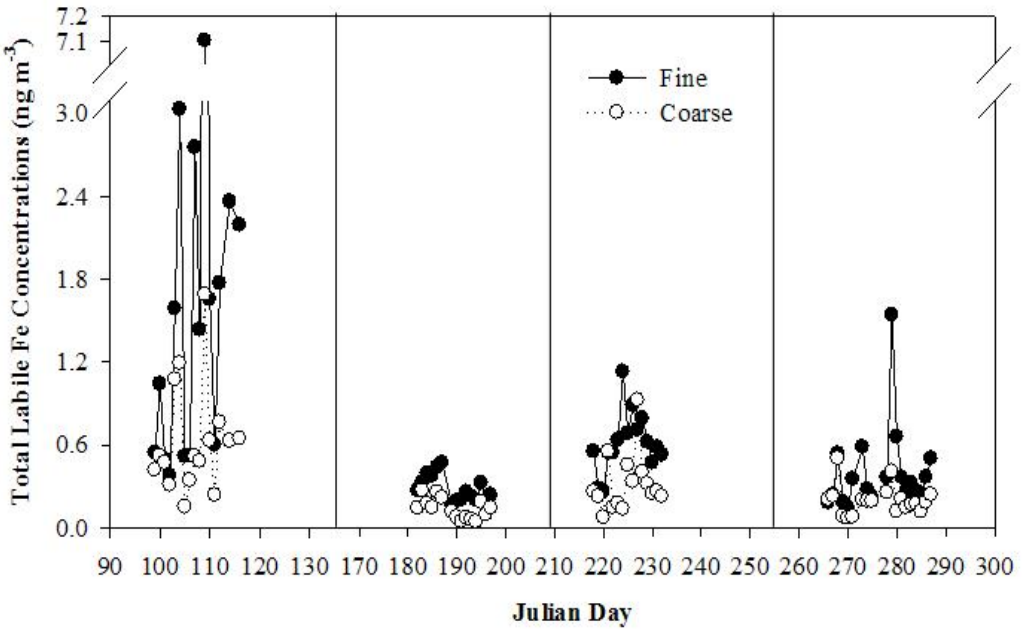

Figure 6-4. Total labile Fe concentrations in the fine and coarse fractions of aerosol samples collected during the 2001 spring (9 to 26 April), 2002 summer (1 to 16 July), 2003 summer (6 to 21 August), and 2002 fall (23 September to 15 October) cruises over the central North Pacific

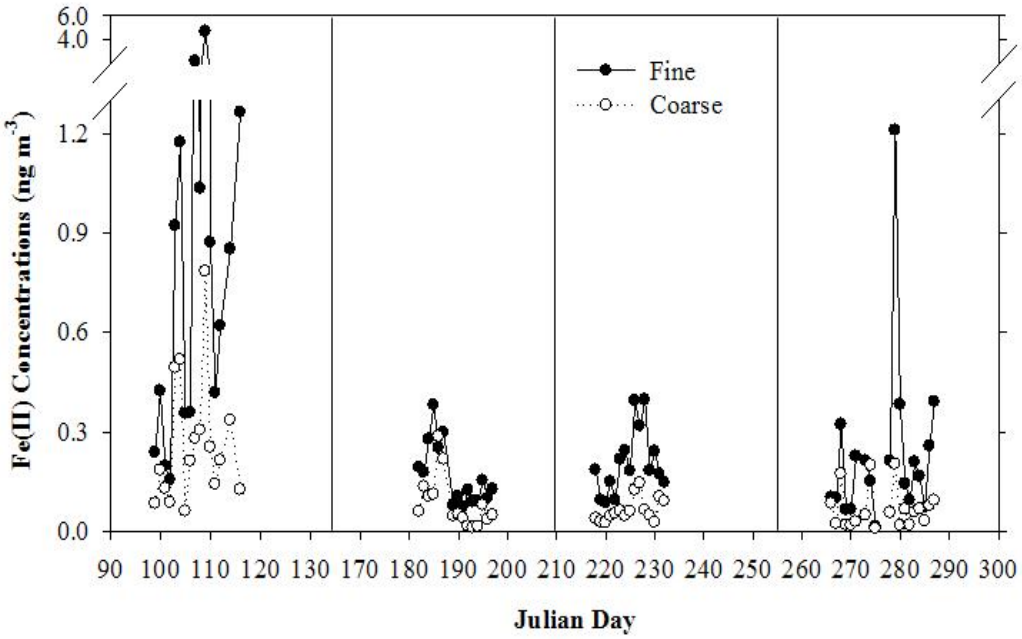

Figure 6-5. Labile Fe(II) concentrations in the fine and coarse fractions of aerosol samples collected during the 2001 spring (9 to 26 April), 2002 summer (1 to 16 July), 2003 summer (6 to 21 August), and 2002 fall (23 September to 15 October) cruises over the central North Pacific

aerosol investigations over the China Dust Storm Research (ChinaDSR) observational network stations showed that the most intense and persistent dust events occurred from 5 to 20 April 2001 (Zhang et al., 2003). The trans-Pacific transport of Asian dust plumes, particularly in the April, was demonstrated by both aerosol model simulation and satellite image during the ACE-Asia (Chin et al., 2003; Zhao et al., 2003). The Georgia Tech/Goddard Global Ozone Chemistry Aerosol Radiation and Transport (GOCART) model of aerosol optical thickness showed that the trans-Pacific dust plume extended to the 20°N of the central Pacific on 14 April 2001 (Chin et al., 2003). This southward influence of Asian dust on the Pacific atmosphere was reflected in our measurements of aerosol Fe, where the total Fe concentration in aerosols reached its second peak value (135 and 96 ng m^{-3} for the fine and coarse fractions, respectively) on 14 April 2001 (Figure 6-3a). The concentrations of total aerosol Fe measured in August 2003 (fine: mean 56 ng m^{-3}, coarse: mean 32 ng m^{-3}) were also significantly higher compared to those measured in July and September 2002 (Figure 6-3a & b). Around 64% of the mean total Fe was found to be in the fine aerosol fraction in August 2003, which was similar to the mean total Fe distribution between the fine (56%) and coarse aerosol fractions in April 2001 (Figure 6-3a). For aerosols collected in July and September 2002 the mean Fe concentrations in the fine fraction were, however, approximately 41% of the total aerosol Fe (Figure 6-3b). It was speculated that the aerosol Fe over the central North Pacific might also be affected by the dust transported from Asia in August 2003, although the effect during this time (mean total aerosol Fe: 87 ng m^{-3}) was much weaker than that in April 2001 (mean total aerosol Fe: 132 ng m^{-3}). Similarly, the marine aerosols collected in July

(mean total aerosol Fe: 10 ng m^{-3}) and September 2002 (mean total aerosol Fe: 26 ng m^{-3}) may have the same source origins and were almost free of the Asian dust impacts.

Concentrations of labile Fe(II) and total labile Fe that includes reducible Fe(III) species in both fine and coarse aerosol fractions were measured during the four separate cruises over the central North Pacific. For the two size fractions of aerosols, the highest (fine: mean 1.8 ng m^{-3}, coarse: mean 0.63 ng m^{-3}) and the lowest (fine: mean 0.28 ng m^{-3}, coarse: mean 0.13 ng m^{-3}) concentrations of the total labile Fe were observed in April 2001 and in July 2002, respectively (Figure 6-4). The mean concentrations of the total labile Fe in both fine and coarse aerosol fractions decreased in the order of April 2001 > August 2003 > September 2002 > July 2002 (Figure 6-4), which followed exactly the temporal distribution of the total Fe in aerosols.

Labile Fe(II) concentrations were found to be extremely high in April 2001 for both fine (mean 0.98 ng m^{-3}) and coarse (mean 0.26 ng m^{-3}) aerosol fractions, which were at least 4 and 3 times higher than those observed from July to October for fine and coarse aerosol fractions, respectively (Figure 6-5). The extremely high concentrations of the labile Fe(II) in April 2001 were consistent with the highest total Fe concentrations observed during this period. Nonetheless, the labile Fe(II) concentrations measured during the other three cruises (from July to October) demonstrated a different pattern from the temporal distribution of the total Fe in aerosols. Instead of approximately 8 times higher mean total Fe in August 2003 than that in July 2002, mean labile Fe(II) concentrations during the three periods were very

close to each other in both fine (0.21, 0.17, 0.23 ng m for August, July and September, respectively) and coarse (0.064, 0.083, 0.067 ng m for August, July and September, respectively) aerosol fractions (Figure 6-5). This distribution discrepancy between the labile Fe(II) and the total Fe in aerosols was probably due to the different source contributions or different atmospheric processing to the air mass over the central North Pacific during the three periods.

The percentage of labile Fe(II) in total Fe in aerosols was found to be the lowest in August 2003 (Figure 6-6). The mean values of 0.53% and 0.31% for the fine and coarse aerosol fractions, respectively, were of the same order of magnitude as the mean labile Fe(II) percent in April 2001 (Figure 6-6), which were also comparable to the typically labile Fe(II) percent (0.3% to 1.8%) in marine mineral aerosols observed elsewhere (Zhu et al., 1993; Siefert et al., 1999; Johansen et al., 2000; Chen and Siefert, 2004a). Unlike mineral aerosols, the aerosols collected during both July and September 2002 contained a significantly large fraction of the labile Fe(II) which were averaged 6.6% and 9.5% of the total Fe in the fine aerosol fraction, and 5.9% and 4.7% of the total Fe in the coarse aerosol fraction, respectively (Figure 6-6). The percentages of total labile Fe in total Fe were also found to be larger in July and September 2002 than those in April 2001 and August 2003 (Figure 6-6). The largest mean values of 16% (fine) and 12% (coarse) observed during September 2002 were comparable to the upper bound of the Fe solubility in seawater (1-10%, Jickells and Spokes, 2001). The larger percentages of labile Fe observed in July and September 2002 may correspond to the larger NSS SO_4^{2-} concentrations in

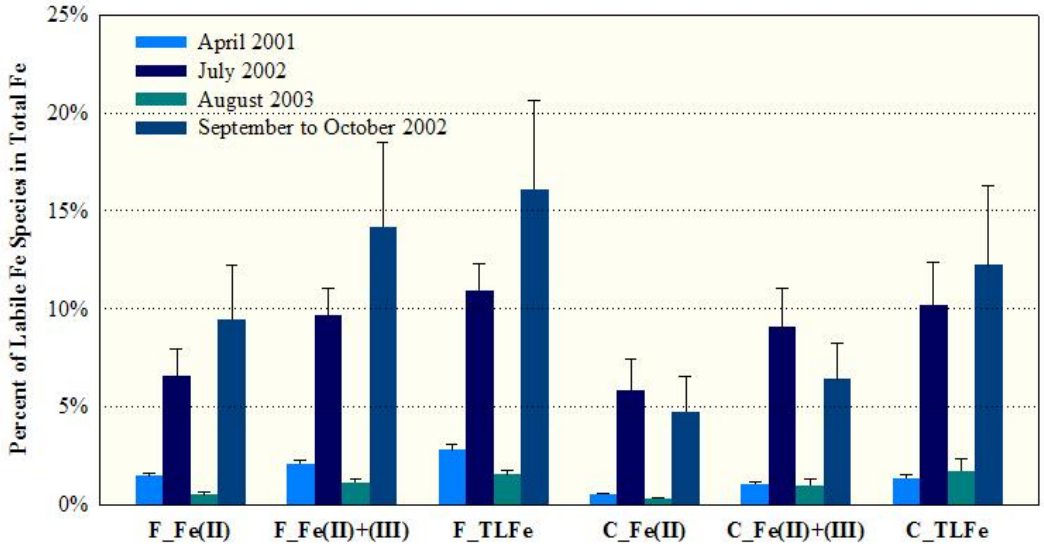

Figure 6-6. Percentages of the labile Fe species in total Fe in the fine and coarse aerosol fractions collected during the 2001 spring (9 to 26 April), 2002 summer (1 to 16 July), 2003 summer (6 to 21 August), and 2002 fall (23 September to 15 October) cruises over the central North Pacific; "F_Fe(II)", "F_Fe(II)+(III)" and "F_TLFe" mean the labile Fe(II), labile Fe(II) & (III), and total labile Fe in the fine aerosol fraction, respectively. Likewise, "C_ " means the labile Fe species in the coarse aerosol fraction.

the aerosol (mean concentrations were about a factor of 2 higher than those in April and August). It was suggested that SO_2 incorporation into the advecting dust plumes can lead to mobilization of Fe in mineral dust (Meskhidze et al., 2003).

6.3.3 Sources for Labile Aerosol Fe

Aerosol Fe concentrations over the central North Pacific are mainly influenced by Asian dust plumes during the spring, but the anthropogenic emissions transported from Asia and North America and the volcanic eruptions may have a significant contribution to aerosol Fe during the other seasons. To identify the source contributions to the labile aerosol Fe over the central North Pacific, the correlation coefficients between the total labile Fe and other chemical species in both fine and coarse aerosol fractions were calculated for April 2001, July 2002, September 2002 and August 2003 periods, respectively. The total labile Fe concentrations were found to be strongly correlated with the labile Fe(II) concentrations all the time (Table 6-1), suggesting that the total labile Fe may be used for a representative of all the labile Fe species to identify the source contributions. Other statistical methods such as principal component analysis PCA) were also employed for identification of source contributions to the labile aerosol Fe over the Atlantic Ocean, and the results from PCA are listed in appendices II. The rotated component matrix showed that mineral dust (component 1) had a major contribution to aerosol particles during the April and August and the labile Fe was mostly associated with this component. However, it is difficult to assign a single source for each component which usually represented a mixed source contrbution and/or atmospheric processing of the aerosol (especially in

Table 6-1. Correlation coefficients between the total labile Fe (TLFe) and other chemical species in fine (F) and coarse (C) fractions of aerosol samples collected during the 2001 spring (9 to 26 April), 2002 summer (1 to 16 July), 2003 summer (6 to 21 August), and 2002 fall (23 September to 15 October) cruises over the central North Pacific

Species	April 2001		July 2002		Sept.-Oct. 2002		August 2003	
	F	C	F	C	F	C	F	C
TLFe	1	1	1	1	1	1	1	1
Fe^{2+}	0.963[b]	0.927[b]	0.875[b]	0.840[b]	0.987[b]	0.739[b]	0.690[b]	0.592[a]
Fe	0.962[b]	0.883[b]	0.216	0.219	-0.138	0.314	-0.103	-0.117
Al	0.943[b]	0.891[b]	-0.356	0.215	0.106	0.353	-0.281	0.584[a]
Ca	0.332	-0.084	-0.239	0.157	0.009	-0.128	-0.443	0.180
K	0.344	-0.195	-0.341	0.182	0.246	-0.171	-0.353	0.263
Mg	0.179	-0.368	-0.271	0.136	0.044	-0.120	-0.355	0.244
Cr	0.905[b]	0.832[b]	0.111	0.182	-0.127	0.222	-0.084	-0.226
Co	0.866[b]	0.886[b]	0.794[b]	0.351	-0.125	0.182	-0.126	-0.250
Cu	0.242	-0.305	-0.201	0.254	0.896[b]	0.340	-0.395	0.098
Pb	0.700[b]	0.681[b]	-0.254	0.625[a]	0.728[b]	0.054	0.096	0.399
Mn	0.964[b]	0.883[b]	0.099	0.210	-0.152	0.385	-0.106	-0.228
Ni	0.863[b]	0.715[b]	0.127	0.169	-0.127	0.219	-0.083	-0.225
V	0.926[b]	0.851[b]	-0.200	0.637[a]	0.091	0.058	-0.049	0.258
Zn	0.716[b]	0.321	-0.104	0.462	0.372	0.198	-0.397	0.427
NSSS	-0.006	0.384	-0.253	0.277	0.848[b]	0.461	-0.027	0.097
Oxalate	0.036	0.683[b]	0.327	0.467	0.420	0.173	0.329	0.488

NSSS means the non-sea-salt-sulfate.

[a] and [b] represent <0.05 and <0.01 significance levels, respectively.

July and September). Therefore our source analysis for labile aerosol Fe was based on the correlation matrix which was more straightforward.

The total labile Fe concentrations measured in April 2001 were significantly coupled with the concentrations of Fe, Al, Cr, Co, Pb, Mn, Ni, V ($p<0.01$) in both fine and coarse aerosol fractions (Table 6-1). Al and Fe were typically crustal tracers and used to identify contribution of crustal and noncrustal sources on observed concentrations of trace elements (Kaya and Tuncel, 1997; Al-Momani et al., 1998; Chester et al., 1993a; Yatin et al., 2000; Huang et al., 2001). The strong correlation with total Fe and total Al concentrations suggested that the labile aerosol Fe in April 2001 were primarily contributed by the mineral aerosols, which further confirmed the large influence of Asian soil dust on aerosol Fe concentration over the central North Pacific during the spring. The significant correlation with oxalate ($p<0.01$) in the coarse aerosol fraction in April 2001 (Table 6-1) indicated that the labile Fe concentrations may be affected by the photochemical reduction in atmospheric waters, since oxalate is an efficient electron donor for the photochemical reduction of Fe(III) (Zuo and Hoigne, 1992). A close relationship ($p<0.05$) between the total labile Fe and the Al concentrations was observed in the coarse aerosol fraction in August 2003 (Table 6-1), which suggests that the labile Fe concentrations were also mainly contributed by mineral aerosols during this time but the influence was not as strong as the April 2001. No relationships were found between the total labile Fe and the Al or Fe concentrations in aerosols in July and September 2002 (Table 6-1), suggesting that mineral aerosols transported from Asia was not a major source for the labile aerosol Fe during the two periods. In July 2002, the total labile Fe

concentrations were significantly correlated with Co ($p<0.01$) in the fine aerosol fraction and with Pb and V ($p<0.05$) in the coarse aerosol fraction (Table 6-1). Co, Pb and V in aerosols were probably a signature of anthropogenic emissions from Asia or North America. Noncrustal V in the atmosphere is most often associated with the combustion of heavy fuel oil (Rahn and Lowenthal, 1984; Yatin et al., 2000), while Pb reaches the atmosphere through high-temperature industries such as smelting and coal combustion (Johansen and Hoffmann, 2003). There were significant correlations between the total labile Fe and the Cu, Pb and NSS SO_4^{2-} ($p<0.01$) concentrations in the fine aerosol fraction in September 2002 (Table 6-1). NSS SO_4^{2-} aerosols are generally produced by the oxidation of gaseous SO_2 that can be emitted from both anthropogenic and volcanic sources. Sulfate aerosols may also be emitted directly from volcanic vents (Allen et al., 2002). Large flux rates (average 53 Mg d^{-1}) of H_2SO_4 aerosols were observed from the Kilauea volcano Pu'u O'o vent at Hawaii (Porter et al., 2002). Model studies suggested that the Miyake-jima volcano made a major contribution to the SO_2 in the central Pacific troposphere during March and April 2001 (Tu et al., in preparation). The close relationship with the NSS SO_4^{2-} in September 2002 implies that the volcanic eruption from Hawaii islands may contribute significant amount of labile Fe species to the atmosphere in a regional scale.

6.3.4 Temporal Distributions of N and P Species

Aerosol samples collected during the four separate cruises from the central North Pacific were analyzed for water-soluble NH_4^+, NO_3^- and PO_4^{3-} concentrations. The percentages of observations with reported concentrations below the detection

Table 6-2. Concentrations (mean ± SD) of nutrient species (NH_4^+, NO_3^- and PO_4^{3-}) in the fine (F) and coarse (C) fractions of aerosol samples collected during the 2001 spring (9 to 26 April), 2002 summer (1 to 16 July), 2003 summer (6 to 21 August), and 2002 fall (23 September to 15 October) cruises over the central North Pacific

		Nutrient Species (ng m^{-3})		
		NH_4^+	NO_3^-	PO_4^{3-}
April 2001	F	40 ± 48	21 ± 11	27 ± 51
	C	1.5 ± 2.8	8.5 ± 7.4	23 ± 46
July 2002	F	32 ± 10	55 ± 29	7.4 ± 10.1
	C	11 ± 7	36 ± 17	4.4 ± 5.0
Sept.-Oct. 2002	F	30 ± 19	31 ± 22	4.1 ± 3.3
	C	4.3 ± 2.0	30 ± 17	3.9 ± 3.6
August 2003	F	69 ± 34	81 ± 45	9.6 ± 10.8
	C	12 ± 6	63 ± 51	5.5 ± 7.1

limit are 9.7%, 3.7% and 40% for aerosol NH_4^+, NO_3^- and PO_4^{3-}, respectively. Values of half of the detection limit were used for samples that were below detection limit in the statistical analysis. The mean concentrations of the nutrient species in both fine and coarse aerosol fractions measured in April 2001, July 2002, September 2002 and August 2003 were given in table 6-2.

The mean concentrations of the aerosol NH_4^+ were found to be the highest (fine: 69 ng m^{-3}, coarse: 12 ng m^{-3}) in August 2003 and the lowest (fine: 30 ng m^{-3}, coarse: 4.3 ng m^{-3}) in September 2002 (Table 6-2). The measured mean concentrations from 34.3 to 81 ng m^{-3} (fine + coarse) over the central North Pacific are in the range of the previous measurements of NH_4^+ aerosol over the Pacific Ocean (from 9 to 270 ng m^{-3}, Parungo et al., 1986), and they are also comparable to the mean concentration (95 ng m^{-3}) of NH_4^+ aerosol over the 15°N to 29°N Pacific reported by Quinn et al. (1990). The highest mean concentrations of aerosol NO_3^- (fine: 81 ng m^{-3}, coarse: 63 ng m^{-3}) were observed in August 2003, and the lowest mean concentrations (fine: 21 ng m^{-3}, coarse: 8.5 ng m^{-3}) were found in April 2001 (Table 6-2). The observation of the low NO_3^- concentrations in April seems in conflict with the monthly mean concentrations of aerosol NO_3^- observed at Midway Island from 1981 to 2000, where the highest monthly mean of 480 ng m^{-3} was reported for the April (Prospero et al., 2003). The Midway Island is located about 2000 km northwest of the Hawaii and affected predominantly by the mineral or anthropogenic aerosols transported from Asia which is the most intensive during the April. The aerosols collected in this study around the Hawaii were less affected by the Asian dust/pollutants than the Midway air. However they could be significantly

influenced by the anthropogenic emissions from North America and volcanic eruption from the Hawaii islands. The mean concentrations of the total aerosol NO_3^- (fine + coarse) measured in July (91 ng m^{-3}) and September 2002 (61 ng m^{-3}) were comparable to the reported NO_3^- concentrations (68 ng m^{-3}) over the same North Pacific region (Duce et al., 1991; Table 6-2). Similar mean concentrations of aerosol NO_3^- with the nighttime value of 82 ng m^{-3} and the daytime value of 165 ng m^{-3} were also observed at Hawaii MLO (Norton et al., 1992).

The soluble PO_4^{3-} concentrations in aerosols over the central North Pacific were generally low. The mean concentrations of aerosol PO_4^{3-} measured in July 2002, September 2002 and August 2003 were range from 4.1 to 9.6 ng m^{-3} and from 3.9 to 5.5 ng m^{-3} for the fine and coarse aerosol fractions, respectively (Table 6-2). Nonetheless, in April 2001 the mean concentrations of the soluble PO_4^{3-} reached 27 and 23 ng m^{-3} in the fine and coarse aerosol fractions, respectively (Table 6-2). The highest concentrations of the soluble PO_4^{3-} in aerosols in April 2001 were probably a result of the most intense dust transport from Asia during this period. The mineral aerosol contains 0.1% of particulate phosphorus according to the upper continental crustal abundances (Taylor and McLennan, 1985), of which about 20% is soluble (Ridame and Guieu, 2002). The soluble aerosol PO_4^{3-} may also be contributed by the anthropogenic emissions transported from Asia (e.g. incinerators, biomass burning: Migon and Sandroni, 1999; Migon et al., 2001; fertilizers, pesticides: Herut et al., 1999). The range of the mean total PO_4^{3-} concentrations (fine + coarse: from 8 to 50 ng m^{-3}, Table 6-2) was comparable to the concentrations of the soluble aerosol PO_4^{3-}

observed over the remote North Atlantic (from 12 to 29 ng m^{-3}, Chen and Siefert, 2004b) and the Southeast Mediterranean Sea (49 ng m^{-3}, Herut et al., 1999).

6.3.5 Ecological Impacts of Atmospheric Nutrient Depositions

Dry deposition fluxes (F_d) of dissolved inorganic P (DIP: PO_4^{3-}), N (DIN: $NH_4^+ + NO_3^-$) and labile Fe (LFe) were estimated from measured species concentrations (C_a) in aerosols and model derived or estimated dry deposition velocity (V_d) (Jickells et al., 1987; Duce et al., 1991) as follows:

$$F_d = C_a \times V_d$$

The term V_d varies with particles size from gravitational settling of large particles to impaction and diffusion of small particles (submicrometer) and is dependent on climatological and physical conditions in the troposphere. The flux estimates in this chapter used the V_d of 0.1 and 2 cm s^{-1} for fine and coarse aerosol particles, respectively due to these factors, and may have an inherent uncertainty by a factor of 3 (Duce et al., 1991).

Table 6-3 shows the calculated mean dry fluxes of the LFe, DIN and DIP, and DIN vs DIP ratios over the central North Pacific in April 2001, July 2002, September 2002 and August 2003 periods. The ratios between the flux rate of DIN and DIP from aerosols were generally higher than the Redfield ratio (N: P = 16: 1) from the July to October (Table 6-3). If atmospheric dry flux was the only nutrient source that is considered, the high DIN: DIP ratio would tend to drive the central North Pacific towards P limitation. Based on the Redfield ratio (C: P = 106: 1) and the Fe: C ratio (4.5 μmol: mol^{-1}) within the phytoplankton cells in the subtropical (15°N to 35°N)

Table 6-3. Calculated mean dry fluxes of labile Fe (LFe), dissolved inorganic N (DIN: NO_3^- + NH_4^+) and P (DIP: PO_4^{3-}) in units of μmol m^{-2} d^{-1}, and DIN vs DIP ratios over the central North Pacific during the 2001 spring (9 to 26 April), 2002 summer (1 to 16 July), 2002 fall (23 September to 15 October) and 2003 summer (6 to 21 August) periods

	Dry deposition fluxes (μmol m^{-2} d^{-1})			
	LFe	DIN	DIP	DIN:DIP
April 2001	0.022	0.60	0.44	1.4 : 1
July 2002	0.0044	2.29	0.087	26 : 1
Sept.-Oct. 2002	0.0068	1.44	0.075	19 : 1
August 2003	0.011	3.35	0.11	30 : 1

North Pacific (Fung et al., 2000), the Fe flux rate required for the phytoplankton growth would be 0.041, 0.036 and 0.054 nmol m^{-2} d^{-1} for July 2002, September 2002 and August 2003 periods, respectively. The required Fe supplies (based on aerosol input of DIP) are about 2 orders of magnitude lower than the measured flux rates (Table 6-3: 4.4, 6.8 and 11 nmol m^{-2} d^{-1}) of the total labile Fe (assumed bioavailable, Chen et al., 2004) from aerosols during the three periods.

In spring 2001 the flux rate of DIN vs DIP from aerosols to the central North Pacific was 1.4: 1 (Table 6-3), which was approximately an order of magnitude lower than the Redfield ratio (16: 1). With this low ratio of aerosol inputs of DIN and DIP in April 2001 tend to drive the ecosystem towards N limitation, and therefore favor the diazotroph growth (Tyrrell, 1999). The shift from N to P limitation caused by N_2 fixation has been revealed by 7 years of time-series observations in the subtropical North Pacific Ocean gyre (Karl et al., 1997). Berman-Frank et al. (2001) indicated that Fe availability had little effect on the bulk C: N: P elemental composition of *Trichodesmium* IMS101 over the three orders of magnitude change in dissolved Fe. By using the *Trichodesmium* C: N: P ratios under Fe-replete conditions (156: 10: 1, Berman-Frank et al., 2001), we find that the aerosol input of DIP estimated here can support 69 μmol m^{-2} d^{-1} of the new C production. This new production would require at most 0.90 to 12 nmol m^{-2} d^{-1} of bioavailable Fe for *Trichodesmium* growth under Fe-repletion conditions (Fe: C ratios range from 13 to 168 μmol mol^{-1}, Berman-Frank et al., 2001; Kustka et al., 2003). Thereafter, aerosol input of LFe (22 nmol m^{-2} d^{-1}) was in a large excess compared to that (from 0.90 to 12 nmol m^{-2} d^{-1}) required for the *Trichodesmium* growth driven by the aerosol DIP supply.

The discussion above was from an only atmospheric view. However, the aerosol input of DIN (0.6 to 3.35 μmol m^{-2} d^{-1}) was approximately 2 orders of magnitude lower than the N_2 fixation rate (140 μmol m^{-2} d^{-1}) measured in the central North Pacific (Karl et al., 1997). This strong N_2 fixation will tend to drive the water column towards P limitation during all seasons. There were no direct estimates for the vertical fluxes of NO_3^- and PO_4^{3-} to the euphotic zone of the central Pacific. The vertical flux of NO_3^- (148 μmol m^{-2} d^{-1}) can be calculated by subtracting the N_2 fixation rate from the export flux of particulate N from the euphotic zone (288 μmol m^{-2} d^{-1}, Karl et al., 1997). The vertical fluxes of NO_3^- vs PO_4^{3-} are typically near the Redfield ratio of 16: 1, nonetheless more vertical flux of PO_4^{3-} (greater than 9 μmol m^{-2} d^{-1}) is expected in the central North Pacfic due to the dissolved P depletion (N: P > 16) observed in the surface water (Karl et al., 1997). In this situation, phytoplankton growth will require at least 0.0043μmol m^{-2} d^{-1} of the labile Fe according to the Fe: C: P cell ratios in the subtropical North Atlantic. The lower limit of the Fe requirement is less than the dry deposition fluxes of labile Fe in April and August, but is comparable to the fluxes in July and September 2002 (Table 6-3), which suggested that primary productivity in this Pacific region may be limited by both P and Fe.

6.4 Conclusions

Asian dust storms, anthropogenic emissions transported from Asia and North America, and volcanic eruptions from Hawaii islands all affect the air mass over the central North Pacific, and their contributions to the nutrient species in aerosols over this oceanic region demonstrated a marked seasonality. The concentrations of the

total Fe and the labile Fe species in aerosols were found to be the highest in April 2001, due to the most intensive dust storms from Asia during the spring. The mean concentrations of the total Fe (133 ng m^{-3}), the labile Fe(II) (1.24 ng m^{-3}) and the total labile Fe (2.43 ng m^{-3}) measured in April 2001 were approximately a factor of 130, 50 and 60 larger than the lowest mean concentrations of the Fe species (correspondingly 10, 0.25, and 0.41 ng m^{-3}) measured in July 2002, respectively. The percentages of labile Fe(II) in total aerosol Fe were found to be similar between April 2001 and August 2003, and between July 2002 and September 2002. The mean percents of the labile Fe(II) observed in April 2001 were 1.5% and 0.53% for the fine and coarse aerosol fractions, respectively, which were approximately an order of magnitude lower than those observed (fine: 9.5%, coarse: 4.7%) in September 2002. Likewise, the percentages of total labile Fe in total aerosol Fe were significantly lower in April 2001 and August 2003 than in July and September 2002. The relatively low percentages of labile Fe species in total aerosol Fe were probably a signature of mineral aerosols transported from Asian desert regions, while the large labile Fe percents may be due to anthropogenic and/or volcanic emissions. The correlations calculated between the total labile Fe and other chemical components in aerosols further confirmed that the labile Fe species were primarily contributed by Asian soil dust in April 2001 and August 2003, but the dust influence was not as strong in August 2003. The labile aerosol Fe observed in July 2002 was mainly associated with anthropogenic emissions from Asia or North America, while the volcanic eruptions from Hawaii islands were responsible for significant amount of labile aerosol Fe over the central North Pacific in September 2002.

Seasonal variations of the soluble NH_4^+, NO_3^- and PO_4^{3-} concentrations in aerosols were also observed over the central North Pacific. The largest mean concentrations of both aerosol NH_4^+ (81 ng m^{-3}) and aerosol NO_3^-(144 ng m^{-3}) were found to be in August 2003, which were approximately a factor of 2 and 5 larger than the lowest mean concentrations observed in September 2002 and April 2001, respectively. The relatively low concentrations of aerosol NH_4^+ and NO_3^- measured in April 2001 suggests that Asian dust plumes had only a minor contribution to the two nutrient species, instead, anthropogenic emissions from North America and volcanic eruptions from Hawaii may significantly affect the N nutrient concentrations over the central North Pacific. Nonetheless, the mean soluble PO_4^{3-} concentration in aerosols was found to be the largest (50 ng m^{-3}) in April 2001 as a result of the most intensive dust transport from Asia during this period. From an only atmospheric view, the aerosol inputs of LFe, DIP and DIN to the central North Pacific generally tend to drive the water column towards P limitation (DIN: DIP > 16) during the summer and the fall, whereas during the spring the atmospheric nutrient depositions may result in a short-term N limitation at first, and then due to the enhanced N_2 fixation the ecosystem is ultimately limited by P. If considered other flux sources of nutrients to the euphotic zone, the primary productivity in the central North Pacific may be co-limited by P and Fe.

Chapter 7: Estimation of Residence Times for Dissolved Iron in the Remote Upper Oceans

7.1 Introduction

Iron (Fe) has been known to be a rate-limiting nutrient for phytoplankton production in high-nitrate low-chlorophyll (HNLC) regions of the world's oceans (Martin et al., 1994; Coale et al., 1996; Boyd et al., 2000; Tsuda et al, 2003). Fe vertical profile in the ocean exhibits a mixture of the nutrient- and scavenged-type behaviors, and its concentrations are controlled by both internal biogeochemical cycles, physical mixing and circulation patterns and external inputs (Bruland et al., 1994). Deposition of aeolian dust is the predominant external source of Fe to the remote oceans (Duce and Tindale, 1991). The atmospheric-deposited Fe is typically removed from surface waters by biological uptake and then remineralized at depth, as well as removed from the water column by scavenging onto sinking particles. It was suggested that the variable aeolian input into each oceanic basin coupled with the biological processes of uptake/regeneration and the metallic property of scavenging could explain the profile of Fe in the ocean (Bruland et al., 1994; Boyle, 1997). Several models have been developed to examine the parameterizations of Fe cycling in the global ocean which include scavenging only, scavenging and desorption of Fe to and from particles, and complexation and so on (Lefevre and Watson, 1999; Archer and Johnson, 2000; Parekh et al., 2004). The residence time of Fe was one of the most important parameters required in these model simulations. The net scavenging model was found to be able to capture the broad features of the Fe

distribution for a deep-water residence time of approximately a hundred years (Parekh et al., 2004). This 100 years assumption was in the range of the estimated residence time (between 70 and 140 years) for Fe in the deep ocean (Bruland et al., 1994), however, over the depth range 0 to 1400 m the estimated values were around 2 to 13 years (Landing and Bruland, 1987).

This paper presents a quantitative estimation of residence times for dissolved Fe in the upper ocean based on the new data of atmospheric Fe fluxes from the North Atlantic, North Pacific and Indian oceans. The dry deposition fluxes of total and labile Fe species were calculated in terms of the concentrations of total and labile aerosol Fe measured during three research cruises over the tropical and subtropical North Atlantic (Chen & Siefert, 2004a), four cruises over the subtropical North Pacific (Siefert & Chen, 2004) and one cruise over the Indian Ocean. The various types of labile Fe in the atmosphere were measured to approximate the amount of aerosol Fe that can be dissolved in the ocean by considering the dissolution and photochemical redox of Fe in atmospheric waters and seawater. Although some colloidal Fe species were found to be bioavailable (Kustka et al., 2003; Sunda and Huntsman, 1995), the dissolved Fe has the most probability of being directly utilized by phytoplankton (Brand, 1991; Wells et al., 1995; Sunda and Huntsman, 1997) and thereby plays the most critical role in the biogeochemical cycling of Fe in the ocean. It was also found that the total labile Fe may be a threshold for aerosol Fe that can be taken up by *Trichodesmium* (Chen et al., 2004). This study applies the direct measurements of the labile Fe fractions instead of an assumption of Fe solubility (1-10%, Jickells and Spokes, 2001) in the aerosol and the dissolved Fe concentrations in

the surface ocean, to quantify the residence times for bioavailable Fe in several oceanic regions.

7.2 Atmospheric Fluxes of Labile Fe

7.2.1 Sampling and Analyses

Three labile Fe species, labile Fe(II) (LFe(II)), labile Fe(III) (LFe(III)) and reducible particulate Fe (RPFe), were analyzed for the aerosol samples collected during the three cruises (6 January to 19 February 2001, 27 June to 15 August 2001, and 18 April to 20 May 2003) over the North Atlantic (0° to 30°N) and four cruises (9 April to 26 April 2001, 1 July to 16 July 2002, 23 September to 15 October 2002, 6 August to 21 August 2003) over the North Pacific (15°N to 30°N, 150°W to 175°E). The details in aerosol sample collection, labile Fe determination, temporal and spatial distributions of labile Fe concentrations, and dry deposition fluxes of labile Fe over the two Atlantic and Pacific regions have been presented by our previous papers (Chen and Siefert, 2003; Chen and Siefert, 2004a; Chen and Siefert, 2004b; Siefert and Chen, 2004).

Only total Fe concentration was analyzed for the aerosol samples collected from the Indian Ocean (20°S to 20°N) during 22 February to 30 March 1999 INDOEX campaign (Figure 7-1). A high-volume bulk sampler (Sierra Instruments) together with Whatman 41 cellulous filters were used for the sample collection (see details in Ball et al, 2003). Total Fe concentration on the cellulous filter was measured using a strong-acid digestion procedure followed by inductively coupled plasma mass spectrometer (ICP-MS, HP 4500) analysis. The digestion procedure was run in a batch of twelve acid-cleaned beakers with ten filter sample cuts (1/96 of the

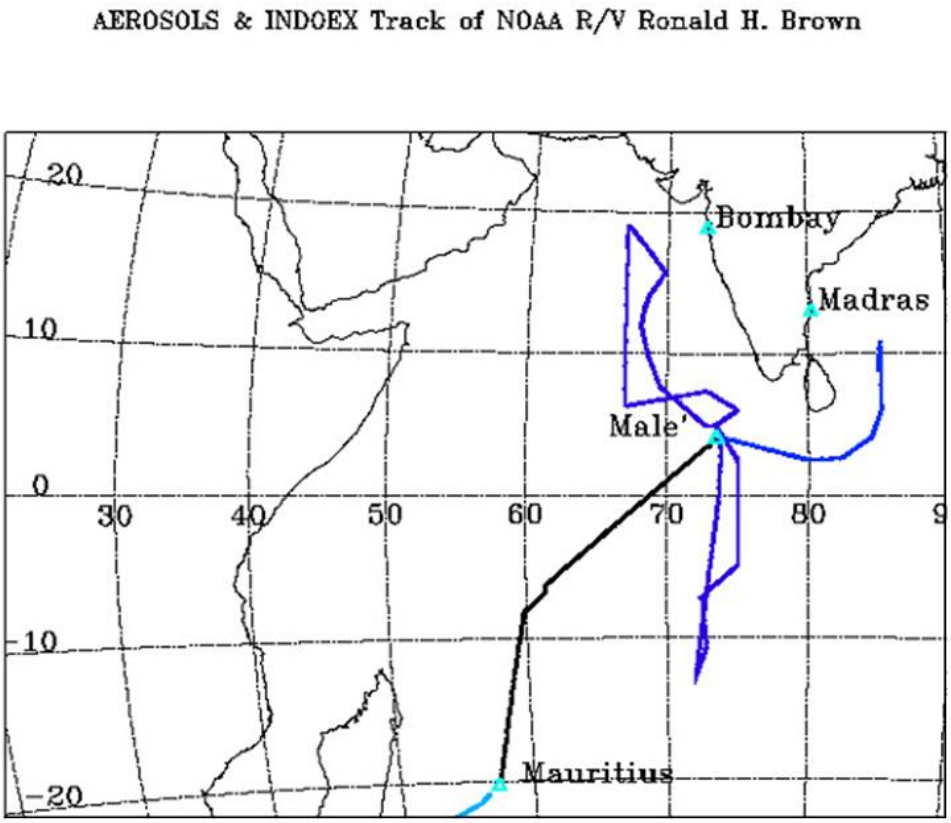

Figure 7-1. Cruise track of the R/V Ronald H. Brown during the 1999 INDOEX campaign (22 February to 30 March 1999). The ship traveled from Mauritius to Male' (from 22 February to 1 March 1999), into the Arabian Sea, south across the intertropical convergence zone (ITCZ) back north into the Bay of Bengal and back to Male' (30 March 1999).

Whatman 41 filter), one blank and one sample of Standard Reference Material 2709 San Joaquin Soil (US department of commerce, National Institute of standards and Technology) for quality control. The twelve beakers filled with the samples were placed at 550°F to undergo ashing overnight. After ashing 2 g of 10 N nitric acid (Seastar Chemical, Inc.) was added to each beaker. The beakers were then covered with watch dishes and heated at hotplate (below the boiling point) for approximately 2 hours until almost dry. After cooled to the room temperature certain amount of the nitric acid was added to compensate the lost acid during heating process. Finally, 0.1 g of 28 N hydrofluoric acid (Seastar Chemical, Inc.) and 28g of 18.2 MΩ-cm water were added to each beaker. The digestion solution was analyzed for elemental concentrations using ICP-MS (Chen and Siefert, 2004a).

7.2.2 Deposition Fluxes of Labile Fe

Dry deposition rates of labile Fe over the tropical and subtropical North Atlantic and subtropical North Pacific were calculated by multiplying mean labile Fe concentrations with the dry deposition velocity of 1.0 cm s^{-1} that was estimated from sediment trap records in the Sargasso Sea (Jickells, 1999; Jickells and Spokes, 2001) and is comparable to the particle-size-based estimates (range from 0.25 to 1.1 cm s^{-1}) of dry deposition velocities (Arimoto et al., 1997). The mean deposition fluxes of LFe(II), soluble Fe (sum of LFe(II) and LFe(III)) and total labile Fe (sum of LFe(II), LFe(III) and RPFe) over the studied Atlantic (0° to 25°N) and Pacific (15°N to 30°N, 150°W to 175°E) regions were calculated for each cruise period (Table 7-1). Due to a significantly spatial gradient of labile Fe concentrations over the North Atlantic, only the data from the aerosol samples collected between 0°N and 25°N Atlantic region

Table 7-1. Mean dry deposition fluxes of labile atmospheric Fe to the North Atlantic (0°N to 25°N), North Pacific (15°N to 30°N, 150°W to 175°E) and Indian (0°N to 20°N) oceans during the different month periods.

Oceans	Cruise Periods	Labile Fe(II)	Soluble Fe	Total labile Fe
			μmol m^{-2} yr^{-1}	
Atlantic	6 Jan. — 19 Feb. 2001	57	99	142
	27 Jun. — 15 Aug. 2001	4.3	20	31
	18 Apr. — 20 May 2003	20	50	84
Pacific	9 Apr. — 26 Apr. 2001	7.0	10	13
	1 Jul. — 16 Jul. 2002	1.4	2.0	2.3
	23 Sep. — 15 Oct. 2002	1.7	2.6	3.3
	6 Aug. — 21 Aug. 2003	1.5	3.6	5.2
Indian	22 Feb. — 1 Mar. 1999		27 — 84	

were used in the flux calculation. The calculated labile Fe(II) fluxes (Table 7-1) represent the most soluble and therefore most bioavailable Fe pool from the atmospheric deposition that may control the biogeochemical cycling of Fe in the upper ocean. The soluble Fe fluxes (Table 7-1) may represent the maximum dissolvable Fe into the seawater that can be a result of photoredox chemistry and complexation with ligands in the surface ocean. The fluxes of the total labile Fe (Table 7-1) include, moreover, the dissolvable Fe from the reduction mechanisms occurring in the atmospheric waters. This study applied the deposition fluxes of the soluble Fe for estimation of residence times because this Fe fraction was in the middle of the three labile Fe species, and was also the closest to the dust-Fe solubility (1-10%) that has been typically used in models for dissolved Fe calculation (Fung et al., 2000; Gao et al., 2003). The dry deposition fluxes of soluble Fe to the North Atlantic and North Pacific oceans showed a clear seasonality with the fluxes in a relatively "dusty" season (winter for the Atlantic, spring for the Pacific) approximately a factor of 5 larger than those in "non-dusty" seasons (Table 7-1).

Total Fe concentrations instead of the labile Fe species were measured for the aerosol samples collected over the Indian Ocean in 1999 INDOEX campaign. Relatively low concentrations of aerosol Fe were observed during the first several days of the campaign (Figure 7-2) when the ship traveled from Mauritius to Male' located south of the intertropical convergence zone (ITCZ, Figure 7-1). The mean concentration of total aerosol Fe measured at south of the ITCZ (48 ng m^{-3}) was approximately an order of magnitude lower than that measured over the North Indian Ocean (371 ng m^{-3}). Due to this large spatial variation of total aerosol Fe over the

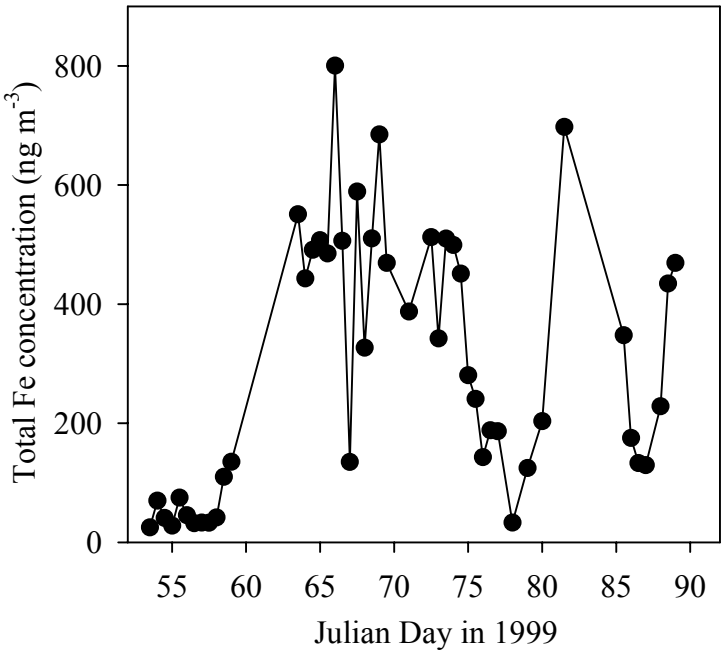

Figure 7-2. Concentrations of total aerosol Fe measured during the INDOEX campaign (22 February to 30 March 1999, Julian day 53 to 89) over the Indian Ocean; the relatively low concentrations of total aerosol Fe were observed from Julian day 53 to 58 over the South Indian Ocean, which were excluded from the calculation of the mean total Fe concentration and then the mean deposition flux of labile Fe in Table 7-1.

Indian Ocean, only the data from the North Indian Ocean was used for estimation of the labile Fe flux. Moreover, the mean concentration (371 ng m^{-3}) of aerosol Fe observed over the North Indian Ocean was close to the reported mean Fe concentration (720 ng m^{-3}) over the Arabian Sea (Johansen and Hoffmann, 2003). The dry deposition fluxes of labile Fe to the Indian Ocean were calculated by multiplying mean concentration of total aerosol Fe measured over the North Indian Ocean with the labile Fe(II) percentage (1.3 to 4%) reported for this oceanic region (Siefert et al., 1999; Johansen and Hoffmann, 2003) and then multiplied by the deposition velocity of 1.0 cm s^{-1} (Table 7-1).

Total atmospheric delivery of soluble Fe to the ocean includes the dry and wet deposition mechanisms. Both observations and model results suggested that aeolian Fe input by wet deposition accounts for an average of approximately 60% of the total deposition over open oceans (Gao et al., 2003). Thus the total deposition fluxes of soluble Fe from the atmosphere (Table 7-2) were estimated by dividing the dry deposition fluxes of 20—99, 2—10 and 27—84 μmol m^{-2} yr^{-1} by 40% for the tropical and subtropical North Atlantic, the subtropical North Pacific and the North Indian oceans, respectively. The estimated total atmospheric fluxes of soluble Fe in this study (Table 7-2) were consistent with the previous estimates of total aeolian Fe inputs (at a dust-Fe solubility of 10%) to the North Subtropics Atlantic (47 μmol m^{-2} yr^{-1}), the North Subtropics Pacific (20 μmol m^{-2} yr^{-1}) and the Indian Ocean (49 μmol m^{-2} yr^{-1}) (Fung et al., 2000).

7.3 Dissolved Fe Concentrations in the Surface Ocean

To estimate residence times of dissolved Fe in the three oceanic regions, we

Table 7-2. Estimates of residence times of dissolved Fe in the upper 100 m of the tropical and subtropical North Atlantic, the subtropical North Pacific and the North Indian Ocean.

Oceans	Periods	Atmospheric Input ($\mu mol\ m^{-2}\ yr^{-1}$)	Dissolved Fe (nM or $\mu mol\ m^{-3}$)	Upwelling Input ($\mu mol\ m^{-2}\ yr^{-1}$)	Residence time (year)
Atlantic	Jan. — Feb.	248			
	Jun. — Aug.	50		2.0	0.69
	Apr. — May	125	0.86		
Pacific	Apr.	25	0.68		
	Jul.	5		0.9	2.7
	Sep. — Oct.	7			
	Aug.	9			
Indian	Feb. — Mar.	139	1.0	3.1	0.72

applied the corresponding concentrations of the dissolved Fe in the surface oceans as listed in Table 7-2. The mean concentrations of dissolved Fe in the surface tropical (0.95 nM) and subtropical (0.77 nM) North Atlantic were measured along the two transects in April 1996 (Sanudo-Wilhelmy et al., 2001), which correspond to the atmospheric deposition flux of soluble Fe observed during the April. Similar mean concentration of dissolved Fe (0.88 nM) was also observed by Wu et al. (2001) in the eastern subtropical North Atlantic (September 1999, 22.8°N, 36.8°W), and the relatively low concentration (0.6 nM) was found to be in the North Atlantic near Bermuda (July 1998, 34.8°N, 56.8°W) (Wu et al., 2001). Bermuda is north of the Atlantic region that we calculated the atmospheric Fe fluxes for, which was less affected by African dust compared to our studied Atlantic region. Therefore an averaged concentration of dissolved Fe (0.86 nM) in the tropical and subtropical North Atlantic was used for the residence time calculation.

Johnson et al. (2003) reported the dissolved Fe concentrations in the surface seawater for a transit from California to Hawaii in March 2001 and on the return in May 2001, and the mean concentrations in the central North Pacific (155° to 160°W) were 0.22 nM and 0.68 nM for the March and the May, respectively. Boyle et al. (2004) observed a significant variability of dissolved Fe (<0.4 μm) concentrations, both inter-annually and on a seasonal and sub-seasonal basis, in the mixed layer of the central North Pacific. The dissolved Fe concentrations at Hawaii Ocean Time-series (HOT) station ALOHA ranged from 0.22 to 0.73 nM with the highest concentration (0.73 nM) seen in late April 2001 (Boyle et al., 2004). The surface Fe concentration in the central North Pacific is expected to reach the maximum in April

due to the most intense dust storms transported from Asian (Bodhaine et al., 1981; Holmes et al., 1997; Perry et al., 1999), therefore, the mean concentration of 0.68 nM along with the atmospheric deposition of soluble Fe during the April was used for estimation of Fe residence time in this Pacific region (Table 7-2).

The dissolved Fe concentrations in the surface Indian Ocean were measured during five cruises of the 1995 US JGOFS Arabian Sea Process Study (Measures and Vink, 1999). The dissolved Fe concentrations were relatively uniform between January and April ranging from 0.5 to 2.4 nM (mean 1.0 nM), which were applied for estimation of Fe residence time in the Indian Ocean (Table 7-2).

7.4 Residence Time Calculation

The atmospheric inputs were combined with values for inputs from below the euphotic zone via upwelling and diffusion and used together with surface water concentrations to yield euphotic zone residence times for dissolved Fe in the tropical and subtropical North Atlantic, the subtropical North Pacific and the North Indian oceans (Table 7-2). For this purpose, the surface zone was considered to be the upper 100 m, which is generally the depth of the mixed layer. The estimates of upwelling fluxes of dissolved Fe were rather uncertain, and were simply extracted from the previous model results for the North Subtropics Atlantic (2.0 μmol m^{-2} yr^{-1}), the North Subtropics Pacific (0.9 μmol m^{-2} yr^{-1}) and the Indian Ocean (3.1 μmol m^{-2} yr^{-1}) (Fung et al., 2000). Nonetheless, the upwelling fluxes are about 1 or 2 orders of magnitude lower than the atmospheric fluxes of dissolved Fe to the three oceanic regions and thereby are negligible (Table 7-2). High fluxes of dissolved Fe were observed from sediments on the continental shelf to the water column (Elrod et al.,

2004). The lower limit value of benthic dissolved Fe reaching the euphotic zone was estimated 2.2×10^9 mol yr^{-1}, which is of similar magnitude to global input of dissolved Fe from aerosols ($2\text{-}12\times10^9$ mol yr^{-1}, Fung et al., 2000; Jickells and Spokes, 2001). The horizontal fluxes of dissolved Fe from coastal surface water to the remote ocean depend on the extent to which the water is transported offshore. Although the influence of nearshore Fe inputs was observed at least 600 km offshore (Johnson et al., 2003), the horizontal fluxes may not significant for the remote oceans. Thus the atmospheric flux was the only source considered for the dissolved Fe to the studied upper oceans. The residence times of dissolved Fe in the upper ocean (Table 7-2) were calculated by the following equation:

$$t_r = \frac{I}{F} = \frac{C(\mu mol \cdot m^{-3}) \times 100m}{F(\mu mol \cdot m^{-2} \cdot yr^{-1})}$$

where t_r represents the residence time of dissolved Fe (yr) in the upper ocean; I means the inventory of dissolved Fe (μmol m^{-2}); C represents dissolved Fe concentrations in the surface ocean (nM or μmol m^{-3}); and F represents total fluxes of dissolved Fe to the upper ocean (μmol m^{-2} yr^{-1}). The estimated residence time of dissolved Fe (252 days, Table 7-2) in the upper 100 m of the North Atlantic is similar to the previous estimates of Fe residence times (214-291 days) in the upper Sargasso Sea (Jickells, 1999). However, Landing and Bruland (1987) suggested that the residence times for the scavenging of dissolved Fe from the upper Pacific Ocean were 2-13 years, which is comparable to the residence time of dissolved Fe (2.7 years, Table 7-2) estimated for the North Pacific in this study. The residence time of dissolved Fe in the upper North Pacific is approximately a factor of 4 longer than those estimated for the North

Atlantic and the North Indian oceans (Table 7-2). The short residence times for dissolved Fe probably reflect its rapid biological uptake and removal in the upper North Atlantic and North Indian oceans (Johnson et al., 1997; Hutchins et al., 1993). By contrast, the relatively longer residence time of dissolved Fe may reflect its retention in the euphotic zone as a result of phosphorus limitation in the subtropical North Pacific gyre (Karl, 1999).

Chapter 8: Conclusions and Future Directions

8.1 Summary of Major Findings

Atmospheric deposition of nutrient species has a great impact on biogeochemical cycling of C and N in the remote ocean. Limited field measurements of atmospheric nutrient concentrations over the remote ocean have been reported, and the fraction of aerosol Fe that can dissolve into seawater and then be bioavailable is still uncertain. This dissertation provides an expansive and unique set of atmospheric aerosol nutrient data from direct measurements performed during three research cruises over the Atlantic Ocean, four research cruises over the Pacific Ocean and one research cruise over the Indian Ocean. This data has found that atmospheric Fe is highly variable and the factors controlling the labile fraction of Fe include atmospheric processing, different source regions and anthropogenic activities. The data also shows the complicated nature of the other nutrient species in the atmosphere and that they also need to be considered. Overall, we have the following major findings:

1) Reducible particulate Fe defined is comparable to the photo-reducible Fe under ambient sunlight.

2) Trichodesmium shows a luxury uptake of aerosol Fe in the western tropical North Atlantic.

3) Total labile Fe defined may be a threshold of Fe uptake by *Trichodesmium*.

4) The labile fraction varies spatially and temporally.

5) The labile fraction is greater in the Pacific than in the Atlantic.

6) Factors such as atmospheric processes and anthropogenic activities seem to control the ratio.

7) Different terrestrial sources may also be a factor controlling the labile fraction.

8) Atmospheric contents of N and P are also affected by both natural and anthropogenic sources.

9) Dry deposition fluxes of labile Fe generally control the primary productivity in these two oceanic regions.

10) Residence time of dissolved Fe in the upper Pacific appears to be longer than those in the Atlantic and Indian oceans.

8.2 New Questions

This dissertation has provided more insight into the role of the atmosphere as a source of nutrient species to the oceans by investigating the spatial and temporal distribution of these aerosol species along with other chemical species. The measurements were also used to predict their impacts on the oceanic biological cycle. However, atmospheric deposition of nutrients and their roles on controlling biogeochemical cycling of C and N is a very complicated process, and there are many questions that have developed as a result of this dissertation.

These questions include:

1) What explains the difference observed between the Pacific and the Atlantic oceans?

2) Does anthropogenic emission of other chemical species (e.g., organics, precursor acidic specie) promote the dissolution of Fe or P during atmospheric transport?

3) What is the importance of the different source regions (e.g., Gobi Desert, Sahel) on the labile forms of Fe or P?

4) How important are direct anthropogenic sources of atmospheric labile Fe and other nutrient species (e.g., through combustion or smelting activities) on a global basis?

5) Does luxury uptake of aerosol Fe always occur?

6) What is the relationship between the labile Fe and the bioavailable forms of aerosol Fe?

8.3 Future Studies to Answer these Questions

Future studies to answer these new questions are outlined below:

1) Do further analyses and experiments based on our archived aerosol samples. We may measure other tracers of aerosol sources such as Pb isotopes and organics used for tracking biomass sources. We may do more aerosol dissolution experiments including abiotic (i.e. seawater dissolution) and biotic (using cultured organisms) dissolutions. These studies will increase our knowledge in bioavailable forms of aerosol nutrients.

2) Develop a large field program to quantify the roles of sources and atmospheric processes on controlling the labile Fe and other nutrient species in the atmosphere. We can follow an air mass (e.g. dust storm) from its over the oceans while measuring the chemical composition of the aerosol samples collected. Aircraft

sampling coordinated with land-based or ship-based platforms could be used for this large field campaign.

3) Do modeling exercises. We can hypothesize different mechanisms/processes and sources that contribute to the labile Fe and other nutrient species over the remote ocean, and then test using the field measurements.

Appendices I

Chemical compositions of aerosols measured from three cruises (6 January to 19 February 2001, 27 June to 14 August 2001, and 18 April to 20 May 2003) over the North Atlantic Ocean, four cruises (9 April to 26 April 2001, 1 July to 16 July 2002, 23 September to 15 October 2002, and 6 August to 20 August 2003) over the North Pacific Ocean, and one cruise (22 February to 30 March 1999) over the Indian Ocean

Note: The detection limit varied for each sample and species measured because of the detection limit of the analytical method and the air volumes collected for each aerosol filter samples. BDL means below detection limit.

Julian day	Latitude °N	Longitude °W	Fe(II) ng m^{-3}		Fe(II)+Fe(III) ng m^{-3}		Total Labile Fe ng m^{-3}		Fe ng m^{-3}		Al ng m^{-3}	
			Fine	coarse	Fine	coarse	Fine	coarse	Fine	coarse	Fine	coarse
1/6/01-2/19/01												
6	—	—	—	—	—	—	—	—	13.5	17.8	15.5	37.5
7	27.8	75.5	—	—	—	—	—	—	15.1	25.9	9.69	42.3
8	28.1	70.9	1.98	0.37	2.1	0.5	2.34	0.64	4.58	6.05	2.28	22.6
9	28.4	66.9	0.32	0.32	0.66	0.74	0.76	0.82	<1.3	2.83	<0.08	1.27
10	28.6	63.3	0.34	0.1	0.42	0.19	1.5	0.37	0.83	0.81	3.31	4.72
12	29.2	55.2	0.36	0.05	0.5	0.09	0.76	0.16	2.44	<5.4	2.86	1.79
13	29.5	51.3	—	—	—	—	—	—	2.11	0.72	2.21	2.08
14	29.9	48.2	0.13	0.04	0.16	0.04	0.35	0.08	2.08	3.73	0.35	<0.08
15	29.6	46.5	0.05	0.01	0.08	0.01	0.13	0.05	<0.6	0.1	<0.09	<0.09
16	27.8	45	0.1	0.02	0.14	0.04	0.23	0.04	1.67	0.29	4.21	1.07
17	25.3	45	0.44	0.07	0.61	0.19	0.85	0.31	21.3	13.9	67.2	13.7
18	21.5	45	0.73	0.04	1.03	0.29	1.39	0.49	18	18.9	19.5	27.2
19	16.8	45	1.13	0.3	3.42	1.23	2.18	1.88	186	108	250	154
20	13.2	45	2.89	1.43	3.05	1.93	2.13	5.82	397	249	769	500
21	10.2	45.2	3.87	0.89	19.1	1.3	19.9	3.09	729	161	1411	333
22	10.2	46.5	3.31	0.49	12.7	0.95	17.7	2.7	230	181	304	253
23	10.5	47.8	12.5	6.24	17.6	12.2	18	14.1	27.5	7.16	31.1	2.65
29	10.5	47.8	1.78	0.16	3.62	0.94	4.98	1.19	87.7	32.9	166	43
30	10.5	55.3	0.44	0.09	0.82	0.11	1.46	0.31	21.1	5.93	33.4	9.45
31	10.1	53.5	1.1	0.08	1.55	0.62	2.38	0.88	51.5	33	97.4	50.5
32	9.19	51.2	1.65	0.47	2.62	0.8	3.29	1.19	42.6	22.9	79	48.3
33	9.24	49.3	0.24	0.02	0.27	0.05	0.57	0.14	4.75	2.24	9.82	6.35
34	9.36	47.5	4.15	1.25	5.14	1.54	7.19	2.11	116	67	202	127
35	7.41	48.2	10.8	3.71	18.6	4.38	27.6	7.67	647	320	1211	577
36	6.31	47.1	6.88	0.98	13.2	2.77	26.7	6.83	454	142	839	280
37	7.22	45.1	10.7	2.1	25.4	3.86	26.7	7.09	529	139	964	224
38	7.17	43	10.1	3.79	15.5	4.57	20.8	6.6	418	137	748	254
39	8.61	41.3	5.44	2.48	17.8	2.1	25.7	4.59	301	128	501	228
40	9.34	41.5	5.52	1.75	6.42	3.7	16.4	4.46	345	170	613	311
41	10.9	42.4	19.9	7.9	25	13.9	42.2	20.8	404	369	756	748
42	10.1	44.7	12.1	5.02	22.2	7.65	36.5	10.4	729	352	1414	699
43	9.81	44.5	22.4	2.67	27.7	8.32	42.2	11.7	836	383	1642	824
44	10.6	46.6	15.8	6.71	21.9	7.48	34	9.78	484	213	1002	420
45	9.44	49.2	14.4	5.97	19.5	8.65	33.1	10.3	415	149	764	274
46	9.08	51.8	7.8	3.48	12.8	4.23	16.2	5.62	351	154	640	336
47	9.41	55.3	12.5	5.77	24.6	6.61	32.3	9.87	825	381	1227	602
48	10.9	56.1	9.54	3.68	21.8	6.03	29	11	1167	521	2067	988
49	11.3	54.8	12.1	8.89	28.8	11.9	36.3	16.2	698	402	1314	813
6/27/01-8/14/01												
178	29.2	27.4	0.07	<0.04	0.13	0.06	0.27	0.09	3.15	2.67	1.87	1.38
179	29.3	29.6	0.08	0.02	0.17	0.06	0.24	0.12	2.74	1.79	7.57	2.14
180	29.4	33.5	0.06	<0.03	0.16	0.02	0.24	0.07	2.07	4.88	4.96	10.2
181	29.5	37.4	0.11	0.09	0.19	0.17	0.29	0.34	2.4	66.4	4.99	206
182	29.5	39.3	0.25	0.04	0.65	0.24	0.72	0.31	23.2	79.1	48.6	244
183	29.6	43.2	0.24	0.01	0.64	0.07	0.68	0.09	8.53	7.17	18.4	15.6
184	29.6	45	0.74	0.17	3.02	1.01	4.56	2.73	80.5	154	169	424
185	25.5	48.6	0.78	0.04	2.51	0.58	3.6	1.2	70.3	137	158	375
186	22.6	51.3	0.56	<0.02	2.08	0.17	2.91	0.52	59.1	62.9	148	134
187	16.3	56.8	0.94	0.05	2.9	0.51	4.11	0.99	102	145	224	338
188	—	—	—	—	—	—	—	—	115	114	263	268
190	11.8	54.4	0.53	<0.05	2.1	0.43	3.08	0.99	79.7	61.7	241	143
190	11.8	54.4	0.27	0.08	1.26	0.51	2.07	1.08	91.4	77.4	195	214
191	10.4	48.1	1.54	0.41	8.42	1.89	11.3	3.11	320	356	797	894
192	10.4	48.1	1.02	0.08	4.17	0.79	6.57	1.78	199	117	508	285
193	10.4	48.1	0.33	—	1.19	—	2.33	—	108	81.1	315	233
194	9.8	45.3	—	0.17	—	1.02	—	1.67	223	195	575	504
195	10.1	45.4	0.63	0.09	3.91	0.98	5.54	1.7	256	266	679	701
196	10.2	45.5	0.66	0.09	3.06	0.66	4.91	1.62	205	283	538	751
197	11	49.3	1.36	0.22	7.01	1.67	8.59	1.99	304	558	788	1468
198	—	—	—	—	—	—	—	—	271	242	519	571
200	11.6	58.2	0.7	0.01	6.71	1.09	8.68	1.89	229	263	517	905
201	10.3	56.3	0.49	0.26	3.45	1.06	4.71	2.04	92.8	147	207	322
202	10.2	56.3	1.15	0.09	4.85	1.21	7.05	2.17	143	138	318	311
203	10.2	56.3	—	0.2	—	0.88	—	1.71	106	61.2	303	116
207	11.9	54.9	0.5	0.02	2.84	0.36	4.58	1.02	104	95.7	304	219
208	10.4	53	0.81	0.1	4.05	0.69	7.41	1.99	250	249	587	564
209	8.74	51	0.6	0.02	2.2	0.42	5.37	0.98	137	67.3	316	132
210	7.23	48.5	0.2	<0.03	0.69	0.17	0.95	0.34	22.4	20	42	62.8
211	5.65	46.4	0.16	0.02	0.47	0.15	0.95	0.31	19.8	23.7	61.2	29.3
212	4.76	43.9	0.03	<0.03	0.07	<0.03	0.13	0.03	2.18	0.75	1.02	<0.1
213	3.83	42.8	0.26	0.01	0.32	0.06	0.77	0.12	12.2	6.37	11.9	7.24
214	3.27	44.2	0.07	0.05	0.1	0.11	0.29	0.25	3.16	8.64	3.3	11.6
215	3.93	46.1	0.18	<0.06	0.25	0.01	0.49	0.17	0.39	11.3	0.79	18.3
216	5.79	48	0.22	0.11	0.31	0.15	0.66	0.19	9.61	9.2	10.6	11
217	6.17	50.1	0.13	0.03	0.26	0.1	0.42	0.23	5.86	10.1	6.8	14.2
219	8.21	52.8	0.82	0.1	2.81	0.6	4.22	1.24	120	147	248	301
221	10.5	55	1.34	<0.03	5.03	0.6	7.25	1.49	223	157	423	319
222	10.6	55.8	1.44	<0.04	2.98	0.46	5.3	1.3	125	126	262	256
223	12.5	55	1.42	0.08	8.6	0.39	11	1.94	384	290	722	572
224	12.5	54.1	0.94	0.26	5.05	1.45	7.59	2.42	194	240	484	494
225	11.4	53.8	1.61	<0.05	4.13	0.28	5.61	1.3	90.3	48.2	117	111
226	11.8	54.6	0.18	0.05	0.51	0.16	0.56	0.33	15.7	23	10.4	21.5

Julian day	Latitude °N	Longitude °W	Fe(II) ng m^{-3}		Fe(II)+Fe(III) ng m^{-3}		Total Labile Fe ng m^{-3}		Fe ng m^{-3}		Al ng m^{-3}	
			Fine	coarse	Fine	coarse	Fine	coarse	Fine	coarse	Fine	coarse
4/18/03-5/20/03												
108	12	57.6	—	—	—	—	—	—	35.9	59.1	29.4	101
109	11.4	55.5	0.23	0.08	0.98	0.16	2.14	0.33	16.8	46.4	6.49	5.7
110	11.1	53.4	0.49	0.16	0.97	0.27	1.92	0.52	21.1	28.6	5.11	1.3
111	9.86	52.1	1.8	0.16	3.84	0.66	9.25	1.67	114	74	97.5	56.1
112	7.93	52	3.8	0.58	7.24	1.18	16	4.64	348	156	298	177
113	6.98	51	4.24	<0.03	10.4	0.75	17.4	1.74	366	269	662	505
114	7.68	50.8	3.33	0.76	8.02	0.4	15	5.39	343	147	340	170
115	9.08	52.9	3.13	0.49	6.72	1.04	11.5	2.2	331	152	272	233
116	10.5	55.1	2.54	4.55	5.08	10.1	9.02	14.6	496	275	988	462
117	12.1	56.5	0.97	0.06	2.01	1	4.08	1.21	144	135	167	235
120	12.3	56.2	1.51	0.19	4.62	1.16	7.59	2.31	251	195	262	210
121	11	55.4	1.65	0.49	4.72	1.37	7.85	2.92	190	568	329	1061
122	9.4	55.4	2.56	0.51	7.92	1.79	11.7	3.08	325	496	561	890
123	7.98	54.9	4.49	0.65	18.3	1.48	30.9	5.45	852	708	1520	1250
124	8.53	54.9	4.73	1.05	13.6	2.02	21.3	6.95	524	401	949	739
125	10.8	55.9	4.07	<0.1	9.09	2.94	15.1	5.39	788	1223	1330	2428
126	12.1	56.1	3.87	0.75	7.29	2.2	10.6	2.99	289	482	519	627
127	11.8	56.3	1.46	0.05	3.6	0.37	5.59	1.13	172	157	283	305
130	11	55.4	1.68	0.16	2.07	1	5.68	1.68	130	106	196	185
131	10.7	53.4	1.72	0.39	4.59	0.96	7.97	2.02	290	375	471	727
132	10.6	51.3	2.69	0.5	8.92	2.16	12.2	3.2	416	473	638	869
133	10.5	49.2	3.4	0.38	7.56	0.71	11.5	1.71	390	412	724	659
134	9.4	48.4	2.4	0.65	8.7	0.73	11.8	2.33	92.2	55.5	169	115
135	8.1	49.4	6.44	2.53	18.1	3.98	21.2	7.2	730	603	1319	1103
136	8.12	53	4.01	1.06	7.36	3.77	10.5	4.65	561	410	532	816
138	9.14	56.7	3.87	0.6	8.58	1.06	12.8	2.2	286	239	416	344
139	10.3	56.6	3.98	0.18	7.52	0.79	10.5	2.11	233	201	451	361
140	10.8	55.2	2.64	0.09	6.19	0.92	9.93	2.04	280	293	559	507
4/9/01-4/26/01												
99	21.5	160	0.24	0.08	0.37	0.21	0.54	0.41	10.6	30.5	<0.2	10.1
100	22.2	162	0.42	0.18	0.7	0.39	1.04	0.52	37.8	30.6	36.5	32.4
101	23.3	168	0.2	0.13	0.33	0.27	0.49	0.47	10.3	52.8	10.3	11.1
102	24.4	172	0.15	0.09	0.27	0.19	0.37	0.31	15.6	11.7	20.7	15.8
103	26.1	175	0.92	0.49	1.13	0.95	1.59	1.07	74	88.3	135	161
104	26.8	181	1.17	0.52	2.11	1.02	3.03	1.19	135	96	352	255
105	27.3	185	0.35	0.06	0.35	0.11	0.51	0.15	34.6	19.5	61.6	40.9
106	27.6	190	0.36	0.21	0.37	0.3	0.52	0.34	30.4	22.3	39.3	30
107	27.6	190	2.19	0.28	2.37	0.57	2.76	0.51	68.7	57.3	122	105
108	27.4	187	1.03	0.3	1.17	0.58	1.43	0.48	85.6	72.7	162	145
109	26.7	182	4.68	0.78	5.57	1.42	7.1	1.69	376	282	727	557
110	26	175	0.87	0.25	1.23	0.47	1.65	0.63	44.8	36.1	60.1	50.1
111	25.6	174	0.42	0.14	0.42	0.19	0.6	0.23	27.9	17.9	35.2	21.4
112	24.8	171	0.62	0.21	1.37	0.58	1.77	0.76	65.1	50	81.5	67.7
114	24.2	166	0.85	0.33	1.75	0.51	2.36	0.63	105	46.6	136	65.7
116	22.5	158	1.26	0.12	1.75	0.48	2.19	0.64	55.4	26.7	71.7	37.5
7/1/02-7/16/02												
182	22.8	158	0.19	0.06	0.27	0.13	0.27	0.14	3.36	1.85	4.41	1.78
183	22.8	158	0.18	0.13	0.25	0.18	0.33	0.27	6.25	3.03	2.34	0.72
184	23.5	162	0.28	0.1	0.36	0.17	0.39	0.17	4.28	4.42	1.82	4.85
185	24	165	0.38	0.11	0.37	0.14	0.37	0.14	1.63	5.03	<0.2	<0.2
186	24.5	167	0.25	0.28	0.42	0.26	0.43	0.25	3.03	1.31	<0.4	<0.4
187	24.9	170	0.3	0.22	0.38	0.21	0.47	0.21	2.86	<3	<0.4	<0.4
189	26.1	175	0.08	0.05	0.14	0.1	0.16	0.11	0.98	<1	1.26	<0.1
190	26	175	0.1	0.05	0.16	0.04	0.19	0.07	2.07	1.22	11.9	<0.1
191	26	175	0.07	0.04	0.16	0.04	0.2	0.04	1.56	<0.9	0.82	<0.1
192	26	175	0.12	<0.03	0.26	0.06	0.26	0.07	1.84	0.22	1.26	<0.1
193	26	175	0.09	0.01	0.18	0.05	0.22	0.06	3.4	1.24	1.35	0.38
194	24.7	170	0.09	<0.03	0.18	0.04	0.19	0.04	1.97	1.75	<0.1	<0.1
195	23.6	167	0.15	0.08	0.25	0.15	0.32	0.18	22.9	63.9	1.07	0.7
196	22.9	164	0.1	0.04	0.13	0.07	0.18	0.09	1.86	0.71	2.52	0.71
197	22.8	160	0.13	0.05	0.16	0.12	0.24	0.14	2.81	2.11	2.46	3.54
9/23/02-10/15/02												
266	22.5	157	0.1	0.08	0.18	0.2	0.18	0.2	4.08	61.1	0.74	1.31
267	23.5	157	0.1	0.02	0.23	0.22	0.23	0.22	6.05	9.37	<0.1	0.17
268	23.5	157	0.32	0.17	0.53	0.25	0.53	0.5	9.55	49.9	2.19	6.59
269	24.2	156	0.06	0.02	0.08	0.07	0.18	0.08	16.6	2.58	1.66	1.85
270	24.2	155	0.06	0.02	0.12	0.06	0.14	0.07	1.58	1.39	2.85	2.11
271	23.7	156	0.23	0.03	0.26	0.08	0.35	0.08	13.8	3.68	6.47	3.67
273	23.3	157	0.21	0.05	0.37	0.2	0.58	0.2	—	—	—	—
274	23.3	159	0.15	0.2	0.17	0.2	0.27	0.19	66.6	<2	0.06	0.24
275	23.8	159	0.02	0.01	0.13	0.09	0.22	0.19	17.5	100	0.01	0.86
276	22.5	159	—	—	—	—	—	—	30.4	2.9	1.78	4.67
278	19.7	156	0.21	0.06	0.36	0.21	0.36	0.25	1.7	23.7	1.74	18.7
279	19.4	156	1.21	0.2	1.54	0.36	1.54	0.4	2.97	6.09	2.01	5.28
280	19.8	155	0.38	0.02	0.46	0.13	0.66	0.12	13.4	0.02	2.7	1.17
281	20.3	156	0.14	0.07	0.32	0.16	0.36	0.2	<1	1.97	1.06	1.4
282	20.1	156	0.09	0.02	0.16	0.05	0.26	0.14	1.42	<0.7	2.79	0.78
283	20.9	156	0.21	0.06	0.22	0.06	0.32	0.17	3.09	23.4	3.86	1.12
284	22.6	157	0.16	0.07	0.26	0.06	0.26	0.17	0.63	0.57	0.56	0.43
285	23.2	158	0.07	0.03	0.07	0.05	0.24	0.11	9.53	<1	1.7	2.53
286	21.6	158	0.26	0.08	0.29	0.12	0.36	0.18	1.95	7.44	2.83	6.51
287	20.2	157	0.39	0.09	0.39	0.09	0.5	0.24	1.86	<0.8	2.13	2.58
288	19.8	156	—	—	—	—	—	—	<0.7	<0.7	0.85	0.37

Julian day	Latitude °N	Longitude °W	Fe(II) ng m^{-3}		Fe(II)+Fe(III) ng m^{-3}		Total Labile Fe ng m^{-3}		Fe ng m^{-3}		Al ng m^{-3}	
			Fine	coarse	Fine	coarse	Fine	coarse	Fine	coarse	Fine	coarse
8/6/03-8/20/03												
218	19.7	157	0.18	0.04	0.38	0.16	0.55	0.26	48.4	32.6	17.9	6.81
219	18.5	157	0.09	0.03	0.17	0.13	0.28	0.22	29	75.8	0.6	<0.1
220	18.7	156	0.09	0.03	0.19	0.08	0.26	0.07	47	7.95	27.8	3.79
221	19.2	156	0.15	0.05	0.44	0.27	0.54	0.55	158	5.81	2.68	14.9
222	19.5	157	0.09	0.05	0.47	0.15	0.54	0.15	33.8	75.7	3.17	15
223	19.5	158	0.22	0.06	0.55	0.18	0.63	0.17	28.7	32.6	0.72	9.75
224	19.5	159	0.24	0.05	0.59	0.2	1.13	0.13	42.7	0.12	1.88	7.26
225	20	160	0.18	0.06	0.37	0.19	0.68	0.45	21.3	31.6	9.7	15.4
226	20.8	160	0.39	0.12	0.63	0.2	0.88	0.33	35.5	24.9	6.79	4.55
227	21	159	0.32	0.14	0.64	0.45	0.71	0.92	25.7	26.2	8.76	18.5
228	20.6	158	0.4	0.06	0.62	0.18	0.79	0.4	49.2	31	18.2	20.7
229	20.3	158	0.18	0.05	0.45	0.23	0.62	0.31	40.3	59.5	7.41	8.88
230	19.7	161	0.24	0.03	0.42	0.28	0.47	0.24	42.7	39.5	10.6	9.57
231	19.1	162	0.17	0.1	0.4	0.18	0.58	0.26	170	23.7	11.7	14.7
232	19.8	162	0.15	0.09	0.24	0.13	0.53	0.22	61.5	10.7	6.33	10.1
2/22/99-3/30/99												
53p										25.1		33.6
54a										69.7		121
54p										40.9		21
55a										28		25.8
55p										74.9		124
56a										45.4		52.9
56p										32.1		45.2
57a										32.9		48
57p										32.7		51.7
58a										41.8		40.9
58p										110		208
59a										135		254
63p										551		1395
64a										443		796
64p										491		808
65a										507		821
65p										485		826
66a										800		2501
66p										506		1097
67a										135		307
67p										589		1360
68a										327		751
68p										510		1052
69a										685		1378
69p										469		1061
71										387		730
72p										512		927
73a										342		627
73p										510		946
74a										499		919
74p										451		850
75a										281		480
75p										241		431
76a										143		238
76p										188		320
77										187		302
78										32.9		59.3
79										124		236
80										203		349
81p										697		1640
85p										348		674
86a										175		385
86p										133		248
87										129		276
88a										229		269
88p										434		467
89a										469		487

Julian day	Latitude °N	Longitude °W	Ca ng m^{-3}		K ng m^{-3}		Na ng m^{-3}		Mg ng m^{-3}		Cr ng m^{-3}	
			Fine	Coarse	Fine	Coarse	Fine	Coarse	Fine	Coarse	Fine	Coarse
1/6/01-2/19/01												
6	—	—	21.9	77.2	29.2	17.1	68.5	329	10.4	39.7	0.16	0.31
7	27.8	75.5	16.5	68.3	20.6	46.3	323	1406	33.9	160	0.07	0.24
8	28.1	70.9	14.2	47.5	28.9	46.3	551	1602	55.4	163	0.1	0.06
9	28.4	66.9	<0.9	72.8	0.08	73.2	19.9	2244	2.76	212	0.22	0.26
10	28.6	63.3	16.4	100	22.4	105	458	2123	75.1	445	<0.2	0.03
12	29.2	55.2	10.9	22	12.6	20.2	314	463	41.6	68.7	0.01	0.02
13	29.5	51.3	12.7	8.58	12.4	9.13	276	223	39.4	33.3	0.01	<0.1
14	29.9	48.2	8.63	27.7	9.59	26.5	248	658	36.8	95	<0.06	<0.06
15	29.6	46.5	9.18	18.7	7.9	17.5	405	674	32.2	61	<0.07	<0.07
16	27.8	45	11.4	24.1	10.8	21.7	362	822	30.6	74.1	<0.1	<0.1
17	25.3	45	22.9	26	44.8	19.2	879	1026	40.1	44.7	0.08	0.06
18	21.5	45	19.6	47.2	38.8	34.8	736	2211	30.5	91.2	0.1	0.05
19	16.8	45	214	266	97.7	124	1596	4409	195	403	0.66	0.41
20	13.2	45	228	285	329	198	1909	3665	259	373	1.33	0.92
21	10.2	45.2	448	173	454	108	6084	4039	490	228	2.1	0.51
22	10.2	46.5	170	256	125	173	3310	8000	203	403	1	0.63
23	10.5	47.8	55	95	63.8	98.4	2131	5062	147	315	<0.08	0.06
29	10.5	47.8	83.8	62.7	110	48.2	2196	1896	148	136	0.33	0.09
30	10.5	55.3	57.7	38.8	64.3	33.2	3149	1970	143	106	0.18	0.14
31	10.1	53.5	144	113	147	101	4763	4884	261	208	0.42	0.32
32	9.19	51.2	76.3	86.3	72.7	59.9	1238	1640	131	180	0.09	0.03
33	9.24	49.3	31.7	55.2	36.6	50.5	1258	1578	108	162	<0.07	<0.07
34	9.36	47.5	133	150	155	99.5	1842	2438	210	269	0.16	<0.07
35	7.41	48.2	639	450	457	195	1551	1661	403	305	2	0.7
36	6.31	47.1	396	214	282	98.9	1463	1056	298	154	1.41	0.48
37	7.22	45.1	374	187	318	89.1	2266	1167	361	182	1.52	0.28
38	7.17	43	328	197	255	106	1811	1500	305	206	1.08	0.37
39	8.61	41.3	202	166	181	89.5	1794	1111	324	175	0.76	0.5
40	9.34	41.5	189	176	132	97.1	777	978	169	166	0.99	0.59
41	10.9	42.4	177	323	205	205	1252	3084	303	321	0.98	1.14
42	10.1	44.7	427	312	326	156	1670	1161	309	215	1.94	0.97
43	9.81	44.5	470	366	425	211	2696	1781	529	283	2.42	1.22
44	10.6	46.6	250	187	244	108	1571	993	193	157	1.44	0.67
45	9.44	49.2	202	146	231	95.4	671	725	225	189	1.76	0.75
46	9.08	51.8	37.7	226	211	128	877	1066	226	251	0.81	<0.2
47	9.41	55.3	358	322	350	202	1397	1643	361	325	2.18	1.15
48	10.9	56.1	586	379	486	249	1001	918	465	267	3.22	1.39
49	11.3	54.8	412	376	306	223	900	1390	346	290	1.78	1.09
6/27/01-8/14/01												
178	29.2	27.4	17.5	30.3	9.33	21.5	234	377	19.7	61.6	0.07	<0.1
179	29.3	29.6	16.4	26.6	7.73	12.8	179	224	14.5	35.7	0	<0.07
180	29.4	33.5	13.7	21	8.42	18.5	96.7	221	17.7	47.4	0.01	0.05
181	29.5	37.4	7.3	72.2	8.42	73.5	105	271	17	80.4	<0.07	0.2
182	29.5	39.3	106	59.9	128	62.6	561	162	226	42	0.11	0.29
183	29.6	43.2	60.5	34.8	30.4	25.7	206	314	74.5	51.1	0.06	0.28
184	29.6	45	87.1	271	85.3	332	676	6908	289	929	0.3	1.15
185	25.5	48.6	83.5	169	125	218	2272	4400	249	620	0.62	0.68
186	22.6	51.3	119	127	111	125	2680	2262	360	270	0.47	0.37
187	16.3	56.8	105	209	113	189	1681	3026	219	356	0.53	0.65
188	—	—	80	151	90.3	125	587	1299	115	226	0.78	0.66
190	11.8	54.4	51.9	79.8	49.6	67.9	343	616	83.5	120	0.29	0.76
190	11.8	54.4	75.6	105	62.6	71.3	972	1555	117	168	0.21	0.5
191	10.4	48.1	287	418	154	220	1419	2979	223	375	1.14	1.28
192	10.4	48.1	166	136	101	76.9	1240	1336	165	139	0.9	0.55
193	10.4	48.1	156	106	84.3	83.7	1652	2164	176	205	0.26	0.4
194	9.8	45.3	247	175	151	117	2016	1504	273	185	0.9	0.78
195	10.1	45.4	216	221	169	151	3044	1904	330	236	1	0.97
196	10.2	45.5	152	336	145	326	2175	6144	251	632	0.97	1.2
197	11	49.3	209	473	165	368	1352	3334	212	470	1.19	2.04
198	—	—	160	212	120	133	590	1620	144	242	1.22	1.06
200	11.6	58.2	150	261	101	132	794	1091	156	210	1	1.02
201	10.3	56.3	83.4	138	89.7	75.8	1244	478	265	83.7	0.81	0.92
202	10.2	56.3	105	155	91.3	74.5	556	348	90.9	87	1.3	0.91
203	10.2	56.3	72.9	84.1	69	45.7	615	826	80	86.1	<0.08	0.12
207	11.9	54.9	88.8	113	60.6	70.5	862	1170	98.3	123	<0.08	0.19
208	10.4	53	190	237	127	223	1387	1929	184	229	1.03	1
209	8.74	51	91.7	72.6	61.1	44.1	443	743	70.3	79.8	0.67	0.41
210	7.23	48.5	22.2	28.3	30.9	24.7	491	672	45.4	59.2	0.08	0.07
211	5.65	46.4	32.1	56.7	40	79.6	944	1787	73.9	145	0.04	0.1
212	4.76	43.9	23.8	35.2	31	34.5	884	1355	72	113	<0.07	<0.07
213	3.83	42.8	19.5	48.1	20	72	497	1629	46.4	139	0.02	<0.1
214	3.27	44.2	47.5	69.9	52.5	65.7	1968	2631	151	196	0.01	0.06
215	3.93	46.1	39.6	96.3	40.5	95.2	1522	3856	114	285	<0.2	<0.2
216	5.79	48	38.7	93.7	42.3	94.5	1328	3727	106	287	<0.2	<0.2
217	6.17	50.1	19.5	40.6	26.4	34.4	737	1302	56.4	101	0.67	<0.06
219	8.21	52.8	80.3	138	58.4	80	325	590	74.4	112	0.58	0.54
221	10.5	55	132	132	91.9	70	348	338	105	83.9	0.83	0.7
222	10.6	55.8	77.3	118	67.5	72.6	280	502	64.1	80.8	0.8	0.54
223	12.5	55	364	323	201	173	1188	1723	223	229	1.37	0.98
224	12.5	54.1	155	288	120	177	1016	2719	151	318	0.3	0.76
225	11.4	53.8	69.5	68.1	69.8	53.6	652	1256	81	122	<0.1	<0.1
226	11.8	54.6	31	64.9	66.8	62.7	1028	2214	91	274	0.02	0.01

Julian day	Latitude °N	Longitude °W	Ca ng m^{-3}		K ng m^{-3}		Na ng m^{-3}		Mg ng m^{-3}		Cr ng m^{-3}	
			Fine	Coarse	Fine	Coarse	Fine	Coarse	Fine	Coarse	Fine	Coarse
4/18/03-5/20/03												
108	12	57.6	25.3	74.7	26.9	58.9	761	2072	74	225	6	6.72
109	11.4	55.5	22.3	39.4	17.4	33.6	784	1197	71.6	115	4.1	17.1
110	11.1	53.4	12.4	26	18.1	26.3	451	770	50.1	80.1	5.32	9.14
111	9.86	52.1	53.5	67.2	53.5	57.4	951	1175	101	132	7.5	8.71
112	7.93	52	139	173	122	122	1502	2633	192	300	44.7	7.35
113	6.98	51	252	310	208	182	1379	2715	232	386	3.17	7.37
114	7.68	50.8	129	116	132	94	1202	1926	158	182	54.4	14.1
115	9.08	52.9	129	206	129	163	1209	3782	161	397	57.5	12
116	10.5	55.1	425	147	264	130	2686	380	410	119	12.3	16.5
117	12.1	56.5	72.7	135	68.6	95.6	695	1968	109	216	23.8	8.57
120	12.3	56.2	91.4	88	116	79.9	571	697	110	117	47.8	37.7
121	11	55.4	109	328	109	300	1212	2634	163	446	10	6.5
122	9.4	55.4	162	359	169	295	1252	4125	230	508	19.2	7.73
123	7.98	54.9	479	422	334	308	1556	2856	436	440	29.5	40.7
124	8.53	54.9	267	284	228	199	1014	1767	264	285	21.4	18.1
125	10.8	55.9	377	805	374	566	1129	2774	327	663	43	25.4
126	12.1	56.1	141	299	143	224	1249	2980	197	393	8.99	61.6
127	11.8	56.3	92	166	107	146	1420	2556	175	304	7.9	1
130	11	55.4	89.9	121	77.9	83.1	1244	1590	142	186	9.86	8.56
131	10.7	53.4	176	429	148	309	1544	5409	224	638	14.1	1.78
132	10.6	51.3	205	391	155	255	1319	3000	236	430	18.7	7.86
133	10.5	49.2	226	330	185	226	1472	3908	256	508	12.2	24.7
134	9.4	48.4	74.3	102	52.9	63.5	604	1348	86.5	167	2.91	0.78
135	8.1	49.4	463	595	309	364	2382	5134	449	653	23.2	23
136	8.12	53	193	392	179	271	1259	4207	205	523	101	15.9
138	9.14	56.7	151	151	150	113	1519	1835	209	214	32.8	35.7
139	10.3	56.6	181	242	154	141	1175	2383	180	282	2.32	4.12
140	10.8	55.2	215	297	166	171	1320	2526	213	313	2.45	9.15
4/9/01-4/26/01												
99	21.5	160	66.8	243	69.4	351	2512	9365	323	1111	0.06	0.12
100	22.2	162	125	373	175	469	3297	—	342	1112	0.14	0.08
101	23.3	168	66.6	290	62.7	400	2319	10123	184	941	0.13	0.04
102	24.4	172	59.2	85.2	44.5	94.2	1254	1587	115	194	0.08	0.05
103	26.1	175	109	217	59.7	125	408	1048	92.6	181	0.33	0.26
104	26.8	181	181	178	128	104	363	544	167	164	0.35	0.23
105	27.3	185	905	858	1126	932	—	—	3147	2989	0.1	0.03
106	27.6	190	130	55.2	141	13.8	2003	420	207	61.1	0.07	0.03
107	27.6	190	93.6	145	90.3	92.5	1193	1771	146	224	0.22	0.15
108	27.4	187	1204	395	1709	351	—	—	4824	1026	0.29	0.26
109	26.7	182	797	355	1144	325	—	3479	2064	364	1.54	0.65
110	26	175	70.2	62.2	103	49.2	1800	912	240	107	0.02	0.03
111	25.6	174	88	59.4	81	51.1	3177	1477	195	136	0.03	0.07
112	24.8	171	98	107	67.8	72.5	1523	1628	129	162	0.08	0.06
114	24.2	166	538	108	1217	—	35581	—	2606	—	0.12	0.04
116	22.5	158	419	82.4	352	42.2	8561	1653	644	134	0.16	<0.2
7/1/02-7/16/02												
182	22.8	158	31.4	33.2	30.8	29.5	1010	1072	91.7	95.3	<0.09	<0.09
183	22.8	158	29.9	49.6	28.7	45	922	1613	82.8	197	<0.1	<0.1
184	23.5	162	30.3	72.4	34.7	65.9	218	2077	110	207	0.01	<0.2
185	24	165	23.2	59.4	25.7	58.1	—	1803	84.2	185	<0.2	<0.2
186	24.5	167	34.3	60.6	31.9	61.4	1076	2217	99.4	205	0.04	0.03
187	24.9	170	24.3	31.4	29.3	33.6	939	1287	88	120	<0.3	0.01
189	26.1	175	22.6	41.2	23.4	37.2	818	1389	77.8	131	<0.1	<0.1
190	26	175	33.9	43.9	71.9	39.1	1140	1509	107	142	<0.07	<0.07
191	26	175	33.6	38.5	33.4	35.8	1209	1345	104	118	0.08	0.02
192	26	175	44.2	58.2	42.4	53.2	1504	2074	131	238	0.05	0.09
193	26	175	56.4	63.5	34.3	48.4	1250	—	143	225	0.2	0.1
194	24.7	170	11.7	19.6	9.65	18.6	289	670	27.2	60.6	0.2	0.19
195	23.6	167	29.2	24.8	23.1	14.8	738	501	67.2	44.7	8.45	26.8
196	22.9	164	81.3	44.5	148	39.6	3480	1570	307	138	0.03	<0.07
197	22.8	160	164	61.3	109	105	2460	2377	296	313	<0.06	<0.06
9/23/02-10/15/02												
266	22.5	157	17.3	32	7.99	9.76	210	329	20.3	29.5	<0.1	23.2
267	23.5	157	14.4	7.49	5.69	7.96	132	274	11.6	25	<0.08	<0.08
268	23.5	157	9.08	22	8.5	15.1	258	569	24	54	3.46	17.6
269	24.2	156	18.8	29	17.6	25	646	852	59.5	87.7	6.51	0.76
270	24.2	155	19.8	35.6	16.7	30.7	563	1208	51.9	110	<0.08	0.14
271	23.7	156	27.8	41.5	24.9	35.2	766	1335	72.8	172	3.6	0.58
274	23.3	159	44.2	20.7	38.3	16.9	1460	1029	139	58.5	28	<0.2
275	23.8	159	30.4	38.3	28.2	37.3	1078	1332	103	123	7.54	42.7
276	22.5	159	24.2	49	23.3	38.3	791	1479	71.2	188	11.5	<0.09
278	19.7	156	16.9	57.6	19.1	46.4	648	1459	60.2	140	<0.09	0.19
279	19.4	156	25.3	38.2	27	33.9	733	1255	65.7	157	<0.08	<0.08
280	19.8	155	26.8	41.6	27.7	38.4	885	1426	80.4	124	4.91	<0.08
281	20.3	156	21.2	34.4	18.1	29.3	715	1124	64.9	102	<0.1	0.09
282	20.1	156	28.2	33.9	25.1	29.7	1038	1115	80.1	103	<0.1	<0.08
283	20.9	156	41.1	30.6	25.6	15.3	741	596	78.7	51.7	0.01	9.29
284	22.6	157	12.2	11	8.09	10.9	217	431	25.5	37.2	0.02	0.05
285	23.2	158	18.4	25.4	9.41	23.5	482	871	33.8	80.1	<0.1	<0.1
286	21.6	158	21.3	44	18.4	35	670	1291	60.3	119	<0.07	0.01
287	20.2	157	19.8	36.2	17.7	30.8	657	1356	60.5	120	<0.09	<0.09
288	19.8	156	10.3	27.4	9.71	24.3	373	957	34.8	84.6	<0.08	<0.08

Julian day	Latitude °N	Longitude °W	Ca ng m^{-3}		K ng m^{-3}		Na ng m^{-3}		Mg ng m^{-3}		Cr ng m^{-3}	
			Fine	Coarse	Fine	Coarse	Fine	Coarse	Fine	Coarse	Fine	Coarse
8/6/03-8/20/03												
218	19.7	157	177	72	173	43	4873	1249	563	151	9.57	7.61
219	18.5	157	39	42.9	35.8	37.8	818	946	107	133	11.6	30
220	18.7	156	4873	<0.4	893	—	—	95.7	5698		7.59	2.67
221	19.2	156	20.2	48	6.43	57.6	755	1182	73.1	151	63.5	<0.2
222	19.5	157	51.1	61.6	35.5	43.9	740	1007	91.5	141	8.66	17.5
223	19.5	158	34.6	76.1	37.8	58.3	764	1561	107	202	5.82	6.14
224	19.5	159	18	46.5	13.7	40.7	973	987	75.2	128	13.2	0.24
225	20	160	37.8	88.4	40.1	73.5	933	2194	114	266	7.01	7.98
226	20.8	160	35.6	50.9	39.4	46.1	872	1124	201	260	9.5	6.89
227	21	159	45.6	85.2	41.5	67.4	945	1666	217	387	5.29	1.91
228	20.6	158	397	475	427	232	—	—	2375	1388	13.5	5.15
229	20.3	158	53	172	84.9	155	2159	7381	247	921	11.2	22.6
230	19.7	161	55	130	41.1	73.9	1568	3182	213	421	11.7	10.9
231	19.1	162	68.5	98.5	60.3	81.8	2592	3813	315	473	64.8	5.21
232	19.8	162	35	82.7	33.5	51	1360	2403	170	296	24.1	0.34
2/22/99-3/30/99												
53p			148		18.7		6803		326		0.13	
54a			199		67.1		7624		356		0.89	
54p			92.1		3.55		4500		197		4.1	
55a			68.6		4.22		3160		128		0.79	
55p			132		31.4		5542		217		2.15	
56a			72.9		15.6		2252		106		0.86	
56p			64.3		10.1		2683		118		0.51	
57a			67.9		14.9		2120		82.3		0.42	
57p			66.1		12.8		2211		85.9		0.43	
58a			68.7		11.3		2707		104		0.67	
58p			118		23		3878		151		0.9	
59a			159		17.9		4649		174		0.9	
63p			473		434		5455		301		4.72	
64a			359		455		4590		231		3.01	
64p			417		645		4053		200		3.46	
65a			376		615		2536		169		4.16	
65p			474		684		3022		221		3.17	
66a			2022		244		17957		1010		3.94	
66p			1281		114		17937		837		2.67	
67a			510		38.4		8276		369		1.68	
67p			1187		154		11338		633		3.39	
68a			992		64.8		13069		565		2.01	
68p			1529		80.8		19441		911		1.97	
69a			2103		109		22514		1229		3.11	
69p			884		43.3		21711		813		4.91	
71			426		97.3		5677		247		1.8	
72p			906		116		9873		575		2.99	
73a			834		81.3		10197		554		2.69	
73p			864		61.3		10098		559		3.64	
74a			734		79.5		8412		468		3.45	
74p			680		190		8545		456		3.4	
75a			406		208		3675		213		2.74	
75p			395		32.7		5182		265		0.9	
76a			273		14		6002		309		0.19	
76p			362		15.6		8647		452		0.51	
77			471		13.1		9044		691		BDL	
78			202		15.7		9439		477		0.06	
79			340		19.9		10932		614		0.51	
80			317		21.2		5943		411		1.15	
81p			1097		70		18793		1342		2.88	
85p			446		356		2394		225		0.82	
86a			223		55.3		2397		136		0.25	
86p			217		12.9		3798		200		0.08	
87			267		18.5		8121		420		BDL	
88a			244		182		3020		171		0.84	
88p			405		648		1580		164		1.06	
89a			483		585		1187		187		1.75	

Julian day	Lat °N	Long °W	Co ng m^{-3}		Cu ng m^{-3}		Pb ng m^{-3}		Mn ng m^{-3}		Ni ng m^{-3}		V ng m^{-3}		Zn ng m^{-3}	
			Fine	Coarse	Fine	Coarse	Fine	Coarse	Fine	Coars	Fine	Coarse	Fine	Coarse	Fine	Coars
1/6/01-2/19/01																
6	—	—	—	—	0.77	0.59	0.98	0.23	0.58	0.59	1.87	0.41	4.7	0.94	10.8	4.19
7	27.8	75.5	—	—	0.42	1.62	0.45	0.15	0.31	0.55	0.39	0.07	1.13	0.14	24.2	8.97
8	28.1	70.9	<0.04	<0.04	0.16	0.47	0.39	0.06	0.12	0.12	0.98	0.05	2.98	0.16	11.9	2.11
9	28.4	66.9	<0.05	<0.05	<0.1	0.52	0.08	0.22	<0.2	<0.2	0.02	0.36	<0.1	0.25	0.45	2.37
10	28.6	63.3	<0.06	<0.06	0.09	0.38	0.17	0.03	0.03	0.01	0.02	<0.07	0.13	0.01	3.15	1.31
12	29.2	55.2	<0.2	<0.2	0.04	0.06	0.17	0.17	0.06	<0.03	0.1	<0.05	0.41	<0.01	3.49	0.6
13	29.5	51.3	<0.03	<0.03	0.07	0.04	0.14	0.02	0.03	<0.03	0.05	<0.05	0.21	<0.01	3.27	1.92
14	29.9	48.2	<0.02	<0.02	0.07	0.06	0.02	0.01	<0.05	<0.05	<0.1	<0.1	0.08	<0.03	5.06	2.34
15	29.6	46.5	<0.02	<0.02	<0.07	<0.07	0.02	<0.03	<0.04	<0.04	<0.07	0.02	0.09	<0.02	1.16	0.66
16	27.8	45	<0.04	<0.04	<0.1	0.02	0.01	<0.02	<0.03	<0.03	0.03	0.02	0.04	<0.02	1.36	0.81
17	25.3	45	<0.03	0.04	0.1	0.05	<0.02	<0.02	0.53	0.31	0.07	0.02	0.16	0.05	1.66	0.21
18	21.5	45	0.03	0.01	0.04	0.08	<0.03	<0.03	0.33	0.46	0.09	<0.07	0.19	0.04	2.57	1.16
19	16.8	45	0.11	0.06	0.34	0.51	<0.05	<0.05	4.18	2.52	0.51	0.23	0.76	0.29	7.21	2.49
20	13.2	45	0.28	0.17	0.5	0.66	0.28	0.08	9.24	6.5	0.61	0.63	1.39	0.78	4.73	1.84
21	10.2	45.2	0.35	0.07	0.77	0.28	0.49	0.06	14.5	3.37	0.93	0.18	2.7	0.53	3.31	0.53
22	10.2	46.5	0.11	0.11	0.19	1.16	<0.09	<0.09	4.7	3.73	0.4	0.33	0.75	0.49	1.59	1.47
23	10.5	47.8	<0.03	<0.03	<0.07	<0.07	<0.2	<0.2	0.3	0.06	<0.5	<0.5	<0.1	<0.1	4.85	2.23
29	10.5	47.8	0.05	0.01	0.27	0.15	0.1	<0.02	1.99	0.75	0.22	0.03	0.61	0.1	0.85	0.23
30	10.5	55.3	0.06	0.02	0.63	0.2	<0.03	0.11	0.51	0.15	0.15	0.06	0.19	<0.02	2.07	0.45
31	10.1	53.5	0.04	0.03	0.41	0.35	0.02	0.03	1.12	0.72	0.21	0.11	0.23	0.07	1.14	0.38
32	9.19	51.2	0.04	0.05	<0.09	<0.09	0.09	0.04	1.01	0.61	0.12	0.06	0.4	0.15	1.39	0.4
33	9.24	49.3	0.04	<0.02	<0.07	<0.07	0.04	<0.02	0.21	0.07	0.06	<0.05	0.18	<0.01	1.02	0.16
34	9.36	47.5	0.12	<0.02	<0.07	<0.07	0.22	0.06	2.55	1.65	0.19	0.04	0.63	0.19	3.05	0.71
35	7.41	48.2	0.32	0.13	0.78	<0.07	0.68	0.16	12.4	6.44	0.54	0.45	1.3	1.1	4.04	1.38
36	6.31	47.1	0.23	0.07	0.54	0.24	0.52	0.08	8.79	2.74	0.39	<0.05	0.88	<0.01	1.82	0.28
37	7.22	45.1	0.15	<0.03	0.69	0.19	0.72	<0.02	10.5	1.56	0.3	<0.05	1.07	<0.01	2	<0.03
38	7.17	43	0.06	<0.02	0.5	0.24	0.53	<0.02	7.18	2	0.14	<0.05	0.77	<0.01	1.31	0.22
39	8.61	41.3	0.14	2.08	0.54	<0.06	0.34	0.15	5.43	3.29	0.07	0.31	<0.02	0.68	3.19	1.18
40	9.34	41.5	0.18	0.11	0.4	<0.06	0.31	0.14	7.2	4.34	0.25	0.3	0.34	0.73	2.89	1.21
41	10.9	42.4	0.1	0.14	0.5	<0.1	0.01	0.23	5.24	9.49	<0.2	0.54	<0.06	1.27	1.43	1.54
42	10.1	44.7	0.38	0.18	0.77	0.42	0.58	0.14	15.9	8.22	0.71	0.23	1.46	0.31	3.49	0.82
43	9.81	44.5	0.37	0.23	<0.3	<0.3	0.7	0.23	18.7	9.71	<0.1	<0.1	2.97	1.28	5.29	1.27
44	10.6	46.6	0.17	0.09	<0.07	<0.07	0.44	0.14	11.3	5.65	<0.1	<0.1	1.66	0.69	2.93	0.77
45	9.44	49.2	0.21	0.09	<0.2	<0.2	0.58	0.18	14.1	6.07	0.77	0.32	2.21	0.75	6.58	1.74
46	9.08	51.8	1.29	<0.05	<0.1	<0.1	0.24	<0.05	7.77	3.8	0.12	10.8	1.2	0.48	5.41	4.75
47	9.41	55.3	0.37	0.22	<0.2	<0.2	0.46	0.19	13.8	6.66	<0.06	<0.06	2.21	1.01	5.3	1.31
48	10.9	56.1	0.6	0.26	<0.2	<0.2	0.7	0.27	23	10	0.6	0.01	3.89	1.64	3.27	1.09
49	11.3	54.8	0.19	0.08	<0.07	<0.07	0.22	0.06	14.7	8.53	<0.07	<0.07	2.26	1.18	3.2	1.2
6/27/01-8/14/01																
178	29.2	27.4	<0.04	<0.04	<0.1	<0.1	<0.04	<0.04	<0.05	<0.05	<0.09	<0.09	0.13	<0.02	0.05	0.04
179	29.3	29.6	<0.02	<0.02	<0.07	<0.07	0.01	<0.02	<0.03	<0.03	<0.06	<0.06	0.16	<0.02	0.1	<0.03
180	29.4	33.5	<0.03	<0.03	0.02	<0.08	0.1	0.01	0.07	0.11	0.05	0.02	0.14	<0.02	0.3	0.06
181	29.5	37.4	<0.02	0.04	<0.07	0.07	0.05	0.04	0.07	1.32	0.04	0.08	0.22	0.21	0.23	0.28
182	29.5	39.3	0.01	0.04	0.11	0.05	0.1	0.05	0.46	1.69	0.15	0.11	0.46	0.24	0.6	0.3
183	29.6	43.2	<0.02	0.03	0.02	0.11	0.12	0.04	0.21	0.2	0.11	0.15	0.35	<0.02	0.51	0.13
184	29.6	45	0.04	0.02	0.17	1.13	0.22	0.05	1.62	3.4	0.18	0.44	0.57	0.63	1.67	1.61
185	25.5	48.6	<0.03	0.01	0.36	0.57	0.12	0.03	1.75	2.82	0.27	0.28	0.57	0.47	0.54	0.64
186	22.6	51.3	<0.02	<0.02	0.36	0.33	0.07	<0.02	1.15	1.5	0.17	0.13	0.36	0.21	0.39	0.28
187	16.3	56.8	0.01	0.05	0.3	0.51	0.12	0.05	2.3	3.33	0.23	0.27	0.5	0.54	0.56	0.48
188	—	—	<0.03	0.01	0.24	0.35	0.1	0.01	2.66	2.73	0.25	0.22	0.58	0.47	0.51	0.38
190	11.8	54.4	0.07	<0.04	0.25	0.19	0.12	<0.04	1.62	1.41	0.09	0.2	0.29	0.24	0.34	0.37
190	11.8	54.4	<0.02	<0.02	0.03	0.2	0.05	0.01	1.95	1.73	0.1	0.12	0.37	0.27	0.4	0.42
191	10.4	48.1	0.14	0.16	0.41	0.59	0.36	0.18	6.9	7.7	0.56	0.51	1.46	1.18	1.22	1.22
192	10.4	48.1	<0.05	<0.05	0.29	0.21	0.16	<0.04	4.21	2.31	0.38	0.2	0.79	0.34	1.2	0.65
193	10.4	48.1	<0.03	<0.03	0.18	0.51	0.09	0.04	2.19	1.77	0.14	0.07	0.58	0.17	0.69	0.63
194	9.8	45.3	0.08	0.06	0.47	0.32	0.23	0.07	4.72	4.48	0.47	0.37	1.02	0.66	1.15	0.8
195	10.1	45.4	0.09	0.11	0.55	0.43	0.29	0.12	5.91	6.13	0.48	0.43	1.2	0.87	1.14	0.81
196	10.2	45.5	0.01	0.09	0.41	0.87	0.15	0.1	4.68	6.69	0.41	0.46	0.82	0.93	0.96	0.89
197	11	49.3	0.11	0.29	0.41	0.86	0.27	0.29	6.85	12.8	0.54	0.86	1.22	1.88	1.12	1.39
198	—	—	0.07	0.09	0.33	0.4	0.23	0.1	5.75	5.85	0.49	0.39	1.2	0.88	0.96	0.7
200	11.6	58.2	0.08	0.12	0.34	0.37	0.3	0.14	5.38	6.02	0.43	0.4	1.11	0.93	1.24	0.81
201	10.3	56.3	<0.03	0.01	0.23	0.21	0.06	0.03	2.08	3.19	0.28	0.28	0.43	0.48	1.66	0.39
202	10.2	56.3	<0.05	<0.05	0.21	0.15	0.1	<0.04	3.32	3.09	0.38	0.27	0.72	0.47	0.99	0.44
203	10.2	56.3	<0.03	<0.03	0.03	0.04	0.11	<0.02	1.93	1.01	0.09	0.03	0.5	0.16	0.65	0.03
207	11.9	54.9	<0.03	<0.03	0.09	0.1	<0.02	<0.02	1.92	1.71	0.07	0.06	0.37	0.28	0.27	0.03
208	10.4	53	0.04	0.06	0.39	0.39	0.22	0.06	5.15	4.96	0.48	0.35	1.02	0.74	1.42	1.28
209	8.74	51	0.01	<0.03	0.2	0.11	0.16	<0.02	2.86	1.36	0.26	0.14	0.66	0.21	0.75	0.17
210	7.23	48.5	0.01	<0.03	0.08	0.07	0.38	0.03	0.44	0.35	0.11	0.02	0.47	0.05	0.49	0.09
211	5.65	46.4	<0.02	<0.02	0.12	0.16	0.19	0.03	0.37	0.36	0.06	0.03	0.21	0.05	0.3	0.17
212	4.76	43.9	<0.02	<0.02	0.02	0.19	0.01	<0.02	0.04	0.01	0.08	<0.06	0.27	<0.02	0.2	0.07
213	3.83	42.8	<0.03	<0.03	0.02	0.08	0.11	<0.03	0.16	0.12	<0.07	<0.07	0.07	<0.02	69.9	<0.04
214	3.27	44.2	<0.05	<0.05	0.06	0.13	0.19	0.02	0.15	0.2	0.08	0.05	0.13	<0.03	0.92	0.42
215	3.93	46.1	<0.05	<0.05	0.05	0.15	0.21	0.03	0.09	0.29	0.06	<0.1	0.18	<0.03	0.91	0.11
216	5.79	48	<0.05	<0.05	0.09	0.15	0.22	0.02	0.21	0.18	0.04	<0.1	0.07	<0.03	0.94	0.25
217	6.17	50.1	<0.02	<0.02	0.4	0.1	0.36	0.03	0.18	0.24	0.47	<0.04	0.14	0.03	0.47	0.21
219	8.21	52.8	0.06	0.06	0.25	0.23	0.29	0.1	2.53	2.99	0.3	0.21	1.33	0.63	0.89	0.32
221	10.5	55	0.09	0.07	0.33	0.22	0.3	0.09	4.32	3.16	0.33	0.2	0.96	0.51	0.84	0.4
222	10.6	55.8	0.03	0.05	0.21	0.19	0.18	0.08	2.51	2.58	0.22	0.17	0.59	0.44	0.56	0.26
223	12.5	55	0.17	0.12	0.61	0.43	0.5	0.14	8.27	5.86	0.58	0.41	1.6	0.89	1.2	0.55
224	12.5	54.1	0.01	0.11	<0.1	0.12	<0.03	<0.03	3.72	5.16	0.06	0.28	0.83	0.86	1.33	0.82
225	11.4	53.8	<0.04	<0.04	<0.1	<0.1	<0.04	<0.04	1.78	0.91	0.02	<0.1	0.55	0.17	0.75	0.13
226	11.8	54.6	<0.03	<0.03	0.03	0.03	0.2	0.01	0.23	0.36	0.03	<0.08	0.49	0.09	0.74	0.15

Julian day		Lat °N	Long °W	Co ng m^{-3}		Cu ng m^{-3}		Pb ng m^{-3}		Mn ng m^{-3}		Ni ng m^{-3}		V ng m^{-3}		Zn ng m^{-3}	
				Fine	Coarse	Fine	Coarse	Fine	Coarse	Fine	Coars	Fine	Coarse	Fine	Coarse	Fine	Coars
4/18/03-5/20/03																	
	108	12	57.6	<0.05	<0.05	1.05	2.43	0.07	0.07	<0.06	0.51	3.02	3.97	<0.03	<0.03	7.15	5.07
	109	11.4	55.5	<0.03	0.01	0.21	0.35	0.06	<0.03	<0.04	0.79	1.72	8.59	<0.02	<0.02	3.25	0.55
	110	11.1	53.4	<0.03	<0.03	0.13	0.21	0.03	<0.02	<0.03	0.24	2.91	5	<0.02	<0.02	4.42	0.92
	111	9.86	52.1	<0.05	<0.05	0.33	0.29	0.08	0.01	1.2	0.9	4.3	4.79	<0.03	<0.03	12.7	5.28
	112	7.93	52	0.22	<0.07	1.06	0.57	0.22	0.05	6.43	2.53	21.8	4.01	<0.04	<0.04	54.4	11.3
	113	6.98	51	0.22	0.18	0.68	0.83	0.28	0.09	7.6	6.23	1.62	3.59	0.83	<0.02	10.9	2.67
	114	7.68	50.8	0.36	0.08	1.13	0.53	0.01	<0.08	8.36	3.54	27.7	7.03	<0.05	<0.05	21.3	4.47
	115	9.08	52.9	0.43	0.11	1.18	0.67	0.06	<0.05	8.05	3.63	29.8	6.17	<0.04	<0.04	17.1	4.35
	116	10.5	55.1	0.3	1.3	0.85	0.62	0.19	0.24	12.8	6.46	5.66	8.5	<0.04	<0.04	4.57	5.47
	117	12.1	56.5	0.18	0.09	0.54	0.41	0.11	0.03	3.88	3.72	12.6	4.64	<0.02	<0.02	4.33	1.14
	120	12.3	56.2	0.57	0.4	1.16	0.78	0.07	<0.04	5.67	4.51	25.9	20.6	<0.03	<0.03	5.21	0.79
	121	11	55.4	0.17	0.35	0.49	1.13	0.42	0.31	4.7	13.6	5.63	2.99	<0.03	0.69	6.55	3.78
	122	9.4	55.4	0.3	0.28	0.68	0.94	0.26	0.17	7.37	11.8	10.2	3.98	<0.04	<0.04	7.24	2.7
	123	7.98	54.9	0.64	0.69	1.22	1.46	0.44	0.22	19.8	17.7	15.3	22.2	<0.04	<0.04	10.8	2.05
	124	8.53	54.9	0.38	0.33	0.9	0.63	0.26	0.07	11.7	9.49	10.5	8.68	<0.04	<0.04	8.39	1.43
	125	10.8	55.9	0.64	0.78	1.16	1.69	0.27	0.95	17.3	28.8	21.2	12.8	<0.06	<0.06	8.42	5.18
	126	12.1	56.1	0.15	0.55	0.34	1.08	0.34	0.18	6.36	11.9	4.45	31.9	<0.02	<0.02	5.55	1.31
	127	11.8	56.3	0.09	0.05	0.18	0.1	0.18	0.07	3.89	3.59	4.06	0.46	<0.02	0.22	4.13	0.77
	130	11	55.4	0.05	0.08	0.27	0.34	0.14	0.06	2.95	2.53	4.57	4.49	<0.02	<0.02	3.88	1.15
	131	10.7	53.4	0.18	0.17	0.54	0.78	0.28	0.21	6.82	8.86	7.31	0.81	<0.02	0.81	4.02	1.48
	132	10.6	51.3	0.28	0.26	0.59	0.49	0.35	0.26	9.21	11.1	9.46	3.71	<0.02	<0.02	3.52	1.64
	133	10.5	49.2	0.21	0.31	0.45	0.66	0.37	0.19	8.64	9.54	6.7	12.6	<0.02	<0.02	4.07	1.6
	134	9.4	48.4	0.1	<0.1	0.41	<0.3	0.25	<0.09	1.8	0.83	1.71	0.42	0.04	<0.06	2.67	0.82
	135	8.1	49.4	0.44	0.4	0.92	0.82	0.88	0.33	16.5	14.2	11.8	11.8	<0.03	<0.03	7.62	2.88
	136	8.12	53	52.8	<0.06	1.92	0.72	0.4	0.23	13.2	9.15	52.5	8.16	<0.04	<0.04	6.38	3.63
	138	9.14	56.7	0.13	0.17	0.54	0.83	0.23	0.06	6	4.91	16.9	18.8	<0.04	<0.04	7.71	2.61
	139	10.3	56.6	0.08	0.1	0.37	0.49	0.44	0.13	5.03	4.96	1.2	1.76	0.84	<0.02	5.4	2.05
	140	10.8	55.2	0.16	0.19	0.63	0.69	0.52	0.18	6.36	7.32	1.29	4.54	1.05	<0.02	8.93	2.57
4/9/01-4/26/01																	
	99	21.5	160	<0.04	<0.04	0.92	0.65	0.17	0.08	0.11	0.43	0.19	0.13	0.2	0.12	0.53	0.97
	100	22.2	162	<0.06	<0.06	0.3	0.93	0.57	0.08	0.91	0.68	0.08	0.06	0.01	0.03	1.28	0.49
	101	23.3	168	<0.06	<0.06	0.14	2.12	0.13	0.03	0.23	0.41	0.11	0.04	<0.04	<0.04	0.72	1.36
	102	24.4	172	0.03	0.01	0.22	0.33	0.12	0.04	0.41	0.32	0.1	0.02	0.08	0.02	0.43	0.17
	103	26.1	175	0.03	0.05	0.13	0.18	0.3	0.15	1.99	2.47	0.14	0.14	0.22	0.26	0.68	7.84
	104	26.8	181	0.06	0.05	0.2	0.19	0.45	0.11	3.69	2.69	0.21	0.16	0.45	0.28	0.46	0.03
	105	27.3	185	0.03	<0.04	2.34	1.67	0.09	0.02	0.96	0.51	0.19	0.07	0.08	0.01	<.06	<0.06
	106	27.6	190	<0.03	<0.03	0.21	0.01	0.13	0.03	0.77	0.63	0.07	0.04	0.12	0.03	0.39	0.13
	107	27.6	190	0.03	0.02	0.31	0.22	1.79	0.22	2.14	1.59	0.22	0.15	0.42	0.17	3.45	0.6
	108	27.4	187	0.04	0.03	2.84	0.65	2.02	0.21	2.69	2.02	0.23	0.28	0.42	0.18	2.81	1.6
	109	26.7	182	0.18	0.12	1.85	0.39	2.82	0.34	11.1	8.16	0.76	0.38	1.19	0.94	4.44	0.95
	110	26	175	<0.08	<0.08	0.15	0.79	0.64	0.13	1.39	1.12	0.11	0.11	0.05	0.04	1.08	0.38
	111	25.6	174	<0.03	0.02	0.59	0.2	0.88	0.05	0.87	0.49	0.13	0.05	0.1	0.02	1.44	0.29
	112	24.8	171	0.02	<0.09	0.09	0.05	0.66	0.06	1.74	1.35	<0.2	<0.2	0.1	0.02	1.25	0.29
	114	24.2	166	<0.02	<0.1	2.73	0.7	0.37	<0.1	2.75	1.28	0.13	<0.3	0.21	<0.08	1.24	1.39
	116	22.5	158	0.05	<0.07	0.89	<0.2	2.5	0.19	1.75	0.59	<0.2	<0.2	0.27	<0.05	3.55	0.72
7/1/02-7/16/02																	
	182	22.8	158	<0.03	<0.03	0.01	<0.09	0.01	<0.03	0.07	0.04	0.01	0.02	0.09	<0.02	0.11	0.07
	183	22.8	158	<0.04	<0.04	<0.1	<0.1	<0.03	<0.03	0.1	0.05	0.01	<0.08	0.02	<0.02	0.15	<0.04
	184	23.5	162	<0.07	<0.07	<0.2	<0.2	0.03	<0.06	0.06	0.06	<0.1	<0.2	0.03	0.01	<.01	0.48
	185	24	165	<0.06	<0.06	<0.2	<0.2	<0.01	<0.06	0.01	0.01	<0.1	0.03	0.07	<0.04	0.05	0.14
	186	24.5	167	<0.1	<0.1	<0.3	<0.3	<0.01	<0.09	0.01	<0.01	<0.2	<0.2	<0.06	<0.06	0.28	1.85
	187	24.9	170	<0.09	<0.09	<0.3	<0.3	0.01	<0.08	0.04	<0.1	0.02	<0.2	0.02	<0.06	0.14	0.12
	189	26.1	175	<0.04	0.01	0.02	0.05	0.01	0.01	0.02	0.02	0.01	0.02	0.01	<0.04	0.06	0.21
	190	26	175	<0.02	<0.02	0.04	0.05	0.03	<0.02	0.05	0.02	0.03	0.01	0.05	<0.02	0.24	0.33
	191	26	175	0.01	<0.01	4.31	<0.09	0.02	<0.03	0.05	0.01	0.06	0.01	0.13	<0.02	0.2	0.03
	192	26	175	0.02	<0.03	0.1	0.28	0.05	<0.02	0.06	0.01	0.03	1.33	0.07	<0.02	0.28	0.12
	193	26	175	<0.02	<0.02	<0.06	0.02	0.02	<0.02	0.06	0.03	0.03	0.01	<0.01	<0.01	0.02	<0.02
	194	24.7	170	<0.03	<0.03	<0.07	<0.07	<0.02	<0.02	0.04	0.03	0.02	0.03	<0.02	<0.02	<.03	<0.03
	195	23.6	167	0.06	0.24	0.04	0.27	<0.02	<0.02	0.41	1.07	4.32	14.2	<0.01	<0.01	0.07	0.04
	196	22.9	164	<0.02	<0.02	0.05	<0.06	<0.02	<0.02	0.02	<0.01	0.02	<0.05	0.05	<0.01	0.36	0.04
	197	22.8	160	<0.02	<0.02	0.09	0.08	0.02	<0.02	0.05	0.05	0.02	<0.04	0.1	0.01	0.1	0.05
9/23/02-10/15/02																	
	266	22.5	157	<0.03	0.2	<0.09	0.28	0.03	0.02	<0.04	1.1	<0.07	12.7	0.04	<0.02	0.27	0.25
	267	23.5	157	<0.03	<0.03	<0.08	<0.08	0.02	<0.02	<0.03	0.02	<0.06	<0.06	0.02	<0.02	0.29	0.15
	268	23.5	157	0.01	0.12	0.08	0.3	0.07	<0.03	0.19	1.13	2.21	9.39	<0.02	<0.02	0.13	<0.04
	269	24.2	156	0.02	<0.02	0.08	0.04	0.03	<0.02	0.36	0.05	3.41	0.43	<0.02	<0.02	0.14	0.03
	270	24.2	155	<0.03	<0.03	<0.07	<0.04	0.05	<0.02	0.03	0.01	<0.06	<0.06	0.06	<0.02	0.07	<0.03
	271	23.7	156	0.01	<0.02	0.08	0.09	0.17	0.02	0.32	0.09	1.95	0.28	<0.01	<0.01	0.24	0.01
	274	23.3	159	0.17	<0.06	0.28	<0.2	0.02	0.05	1.37	<0.07	15.2	<0.1	<0.04	<0.04	<.07	<0.07
	275	23.8	159	<0.04	0.37	0.06	0.48	0.03	0.01	0.46	1.75	4.06	23	<0.02	<0.02	<.04	<0.04
	276	22.5	159	0.12	<0.03	0.25	0.07	0.09	0.03	0.58	0.07	7.08	<0.07	<0.02	0.08	1.49	0.07
	278	19.7	156	<0.03	<0.03	0.06	0.08	0.05	0.01	0.02	0.64	<0.07	<0.07	0.02	0.04	0.2	0.12
	279	19.4	156	<0.03	<0.03	0.91	0.07	0.31	0.02	0.01	0.15	<0.06	<0.06	0.1	<0.02	1.13	0.08
	280	19.8	155	<0.03	<0.03	0.29	0.05	0.08	0.01	0.22	<0.03	2.56	<0.06	<0.02	<0.02	0.21	<0.03
	281	20.3	156	<0.04	<0.04	<0.1	<0.1	0.06	0.21	<0.05	<0.05	<0.09	<0.09	<0.02	<0.02	0.12	<0.05
	282	20.1	156	<0.03	<0.03	<0.07	<0.07	0.1	<0.02	0.03	<0.03	<0.06	<0.06	0.01	<0.02	0.26	<0.03
	283	20.9	156	<0.02	0.06	0.2	0.18	0.13	0.02	0.07	0.57	<0.05	5.05	0.03	<0.01	0.31	<0.03
	284	22.6	157	<0.02	<0.02	<0.07	<0.07	0.03	0.01	<0.03	<0.03	<0.05	<0.05	<0.01	<0.01	0.34	0.01
	285	23.2	158	<0.04	<0.04	<0.1	<0.1	0.02	<0.01	<0.03	<0.04	0.01	<0.08	0.12	<0.02	1.54	<0.04
	286	21.6	158	0.01	<0.02	0.01	0.05	0.23	0.03	0.05	0.18	0.93	0.07	0.53	0.07	1.23	0.09
	287	20.2	157	<0.03	<0.03	0.01	<0.09	0.05	<0.03	<0.03	<0.04	0.01	<0.07	0.09	<0.02	0.23	<0.04
	288	19.8	156	<0.03	<0.03	<0.07	<0.08	0.01	<0.02	<0.03	<0.03	<0.06	<0.06	0.01	<0.02	0.24	0.05

Julian day	Lat °N	Long °W	Co ng m^{-3}		Cu ng m^{-3}		Pb ng m^{-3}		Mn ng m^{-3}		Ni ng m^{-3}		V ng m^{-3}		Zn ng m^{-3}	
			Fine	Coarse	Fine	Coarse	Fine	Coarse	Fine	Coars	Fine	Coarse	Fine	Coarse	Fine	Coars
8/6/03-8/20/03																
218	19.7	157	0.04	0.01	1.1	0.27	0.12	0.12	1.22	0.78	5	3.91	<0.02	<0.02	1.44	0.23
219	18.5	157	0.04	0.16	0.24	0.57	<0.03	<0.03	0.87	2.15	5.7	14.9	<0.02	<0.02	1.86	0.31
220	18.7	156	0.07	<0.02	3.19	<0.06	0.03	<0.02	0.72	0.11	4.52	1.36	<0.01	<0.01	1.05	0.49
221	19.2	156	0.31	<0.06	1.14	0.13	<0.06	<0.06	4.47	0.09	33.2	<0.1	<0.04	<0.04	1.06	0.28
222	19.5	157	0.06	0.17	0.23	0.45	0.02	<0.03	0.69	1.65	4.55	9.23	<0.02	<0.02	0.11	0.07
223	19.5	158	<0.04	0.1	0.22	1.87	0.04	0.04	0.46	0.7	3.15	3.33	<0.02	<0.02	0.5	0.98
224	19.5	159	0.02	<0.03	0.28	0.09	<0.03	<0.03	0.87	0.1	6.77	0.19	<0.02	<0.02	0.32	0.1
225	20	160	<0.04	0.01	0.2	0.4	0.01	<0.03	0.48	0.82	3.6	4.2	<0.02	<0.02	0.36	0.42
226	20.8	160	0.07	0.08	0.27	0.29	0.04	0.03	0.24	0.19	5.32	3.77	<0.01	<0.01	0.27	0.14
227	21	159	0.08	0.02	0.28	0.76	0.15	0.07	<0.03	0.05	3.42	1.08	<0.02	<0.02	0.97	0.88
228	20.6	158	0.14	0.05	1.47	0.85	0.15	0.03	1.28	0.64	7.24	2.68	<0.02	<0.02	1.46	0.51
229	20.3	158	0.06	0.17	0.33	0.85	0.03	0.02	0.93	1.67	5.66	11.9	<0.02	<0.02	0.97	0.31
230	19.7	161	0.13	0.1	0.35	0.41	0.12	<0.03	<0.05	0	6.2	5.67	<0.02	<0.02	0.47	0.15
231	19.1	162	0.61	0.08	0.94	0.33	0.06	0.01	2.36	0.15	34.4	2.73	<0.01	<0.01	0.63	0.17
232	19.8	162	0.22	<0.03	0.41	0.17	0.04	<0.02	1.18	0.24	12.5	0.19	<0.02	<0.02	0.22	0.14
2/22/99-3/30/99																
53p			BDL		1.82		0.92		0.01		0.05		BDL		0.49	
54a			BDL		2.52		2.47		0.36		0.28		BDL		1.12	
54p			BDL		4.66		0.2		0.11		4.19		BDL		1.97	
55a			BDL		4.18		BDL		BDL		0.17		BDL		0.87	
55p			BDL		9.14		0.44		0.5		1.17		BDL		8.93	
56a			BDL		2.96		0.46		0.17		0.32		BDL		0.89	
56p			BDL		1.17		0.48		0.21		0.14		BDL		1.24	
57a			BDL		2.99		0.41		0.22		0.1		BDL		0.09	
57p			BDL		2.32		0.61		0.31		0.13		BDL		0.96	
58a			BDL		4.65		0.91		0.31		0.23		BDL		1.61	
58p			BDL		2.45		4.46		5.08		0.58		1.14		13.1	
59a			BDL		9.35		4.25		5.57		0.65		1.56		13.2	
63p			0.23		4.21		10.2		16.2		2.84		4.45		34.1	
64a			0.15		5.29		10.8		15.3		2.45		4.72		31.9	
64p			0.19		3.35		10.3		12.8		1.85		3.74		33.1	
65a			0.23		4.18		10		19		1.92		3.53		30	
65p			0.27		4.9		10.4		12		2.15		4.53		27.9	
66a			0.26		4.03		2.76		29.1		2.44		5.41		6.07	
66p			0.12		4.53		1.26		17.7		2.15		3.74		3.07	
67a			BDL		3.41		0.56		7.23		1.09		1.09		1.36	
67p			0.14		7.01		1.17		22.5		1.84		2.12		2.6	
68a			BDL		2.58		1.3		11		0.99		1.22		1.92	
68p			0.11		2.81		0.45		17.1		1.26		1.95		1.79	
69a			0.17		3		1.11		22.8		2.09		4.27		3.66	
69p			0.03		5.94		6.62		17.2		1.9		3.56		20.4	
71			0.11		3.85		2.67		12.8		1		2.83		9.3	
72p			0.33		2.84		3.49		14.5		1.65		4.22		8.95	
73a			0.31		3.24		2.8		11.4		1.47		3.41		8.28	
73p			0.32		3.61		5.04		16.8		1.73		4.62		12.6	
74a			0.34		3.29		4.24		15.5		1.76		4.26		12.6	
74p			0.34		3.23		6.5		13.1		1.74		4.25		14.4	
75a			0.24		2.34		3.85		7.86		1.06		2.24		11.1	
75p			0.07		2.76		2.46		7.27		0.85		1.76		7.3	
76a			BDL		5.75		0.22		4.52		1.11		0.79		5.32	
76p			BDL		1.67		0.46		4.95		0.51		0.86		2.65	
77			BDL		1.75		BDL		5.17		0.46		0.92		2.29	
78			BDL		1.41		0.09		0.6		BDL		0.07		0.59	
79			BDL		1.7		0.32		2.94		BDL		0.55		0.97	
80			BDL		1.25		0.37		4.62		BDL		1.11		1.88	
81p			0.05		3.7		1.22		18.9		BDL		5.1		9.48	
85p			BDL		2.28		3.66		8.12		BDL		2.99		10.5	
86a			BDL		2.14		1.94		4.69		BDL		1.44		5.59	
86p			BDL		1.77		1.54		3.71		BDL		1.19		4.59	
87			BDL		2.32		1.88		3.87		BDL		1.03		5.52	
88a			0.04		2.79		3.85		6.81		1		2.51		8.68	
88p			0.23		3.05		5.6		14		1.04		2.18		13.9	
89a			0.19		3.35		25.7		14.6		1.19		1.9		13.9	

Julian day	Lat °N	Long °W	Fluoride nmol m^{-3}		Glycolate nmol m^{-3}		Acetate nmol m^{-3}		Formate nmol m^{-3}		MSA nmol m^{-3}		Chloride nmol m^{-3}	
			Fine	Coarse	Fine	Coarse	Fine	Coarse	Fine	Coarse	Fine	Coarse	Fine	Coarse
1/6/01-2/19/01														
6			0.27	0.19	0.12	0	0.07	<2E-3	0.62	<0.02	<0.01	<0.01	0.56	5.19
7	27.8	75.5	0.23	0.17	0.04	<2E-4	0.01	<2E-3	0.14	<0.02	<0.01	<0.01	7.93	52.2
8	28.1	70.9	0.32	0.19	3E-4	<2E-4	0.03	<3E-3	0.08	0.17	<0.01	<0.01	6.07	48.9
9	28.4	66.9	0.76	0.29	<7E-4	<7E-4	<0.01	<0.01	<0.08	0.33	<0.05	<0.05	23.6	9.41
10	28.6	63.3	0.1	0.07	<1E-4	<1E-4	<2E-3	<2E-3	0.02	0.05	<0.01	<0.01	26.9	38.8
12	29.2	55.2	0.05	0.06	<8E-5	<8E-5	<1E-3	<1E-3	<0.01	<0.01	<5E-3	<5E-3	10.8	17.9
13	29.5	51.3	0.05	0.07	<9E-5	<9E-5	<1E-3	<1E-3	<0.01	<0.01	<0.01	<0.01	13.3	6.69
14	29.9	48.2	0.24	0.06	<2E-4	<2E-4	<2E-3	<2E-3	<0.02	<0.02	<0.01	<0.01	13	25.3
15	29.6	46.5	0.13	0.04	<1E-4	<1E-4	<2E-3	<2E-3	<0.01	<0.01	<0.01	<0.01	11.9	12.6
16	27.8	45	<0.04	0.06	<1E-4	<1E-4	<1E-2	<1E-2	0.69	<0.01	<0.01	<0.01	16.4	16.5
17	25.3	45	0.09	<0.04	<9E-5	<9E-5	<1E-3	<1E-3	<0.01	<0.01	<0.01	<0.01	7.6	12.4
18	21.5	45	0.17	0.1	<1E-4	<1E-4	0.02	<1E-3	0.03	0.02	<0.01	<0.01	12	23.1
19	16.8	45	0.37	0.21	<2E-4	0.01	<3E-3	0.06	0.05	0.34	<0.01	<0.01	42.3	128
20	13.2	45	1.66	0.14	0.08	0.02	0.21	<3E-3	0.4	0.16	<0.01	<0.01	69.6	194
21	10.2	45.2	0.71	0.43	0.08	<1E-4	0.01	0.02	0.27	0.22	<0.01	<0.01	158	103
22	10.2	46.5	3.75	0.97	<1E-4	<4E-4	<0.01	<0.01	0.18	0.16	<0.02	<0.02	116	56.9
23	10.5	47.8	5.98	5.26	<4E-4	<8E-4	0.52	<0.01	0.51	3.47	<0.05	<0.05	108	108
29	10.5	47.8	0.21	0.08	<8E-4	<9E-5	<1E-3	<1E-3	0.02	0.01	0.07	0.01	38.8	22.3
30	10.5	55.3	0.12	0.08	<9E-5	<1E-4	<1E-3	<1E-3	<0.01	<0.01	0.06	0.02	20.7	22.1
31	10.1	53.5	0.18	0.1	<1E-4	<9E-5	0.01	<1E-3	0.04	0.06	0.05	0.01	26.3	36
32	9.19	51.2	0.19	0.11	<9E-5	<9E-5	0.02	<1E-3	0.04	0.01	0.12	0.01	64.5	28.8
33	9.24	49.3	0.14	0.11	<9E-5	<9E-5	<1E-3	<1E-3	<0.01	<0.01	0.08	0.02	42.5	36.5
34	9.36	47.5	0.21	0.12	<1E-4	<1E-4	0.04	<2E-3	0.03	0.07	0.17	0.01	95.7	72.4
35	7.41	48.2	0.25	0.25	0.09	0.02	0.08	<2E-3	0.34	0.48	0.19	0.02	116	109
36	6.31	47.1	0.2	0.12	0.03	<8E-5	0.03	0	0.24	0.16	0.17	0.02	84.2	61.7
37	7.22	45.1	0.21	0.09	<8E-5	<8E-5	0.02	<1E-3	0.11	0.19	0.14	0.01	77.6	74.4
38	7.17	43	0.17	0.07	0.02	<8E-5	0.02	0.01	0.09	0.14	0.14	0.01	71.8	110
39	8.61	41.3	0.13	0.3	<1E-4	<1E-4	<2E-3	<2E-3	0.13	0.12	0.13	<0.01	90.5	44.3
40	9.34	41.5	0.11	0.09	<9E-5	<9E-5	<1E-3	0.04	0.14	0.22	0.12	0.02	65.2	107
41	10.9	42.4	0.64	0.4	<4E-4	<4E-4	<5E-3	<5E-3	0.29	0.51	0.21	0.01	130	84.4
42	10.1	44.7	0.21	0.14	<9E-5	<9E-5	0.03	0.01	0.27	0.19	0.14	0.02	140	83.5
43	9.81	44.5	0.4	0.27	<2E-4	<2E-4	<3E-3	<3E-3	0.34	0.28	0.16	<0.01	133	109
44	10.6	46.6	0.3	0.22	<2E-4	<2E-4	0.17	<3E-3	0.82	0.23	0.13	0.01	274	75.8
45	9.44	49.2	1	0.64	<3E-4	<3E-4	<4E-3	0.07	0.35	1.02	0.13	0.01	260	181
46	9.08	51.8	0.61	0.44	<2E-4	<2E-4	<3E-3	<3E-3	0.22	0.23	0.15	<0.01	258	84
47	9.41	55.3	0.28	0.36	0.11	<9E-5	0.67	<1E-3	1.11	0.62	0.11	0.02	149	243
48	10.9	56.1	0.36	0.14	<9E-5	<9E-5	<1E-3	<1E-3	0.31	0.21	0.1	<0.01	37.3	45
49	11.3	54.8	0.5	0.24	<1E-4	0.01	0.04	0.05	0.23	0.29	0.11	0.02	84.1	83.9
6/27/01-8/14/01														
178	29.2	27.4	0.03	<0.02	<0.01	<0.01	<0.04	<0.03	<0.01	<0.01	0.2	<0.03	4.28	3.2
179	29.3	29.6	0.04	0.03	<0.01	<0.01	<0.02	<0.02	<4E-3	<4E-3	0.19	0.02	4.55	10.4
180	29.4	33.5	0.04	0.02	<0.01	<0.01	<0.02	<0.02	<5E-3	<4E-3	0.2	0.02	5.27	7.23
181	29.5	37.4	0.04	0.06	0.7	<0.01	<0.02	<0.02	<4E-3	<4E-3	0.22	0.03	2.21	14.5
182	29.5	39.3	0.05	0.07	<0.01	<0.01	<0.02	<0.02	<4E-3	<4E-3	0.32	0.02	10.1	7.07
183	29.6	43.2	0.03	0.03	<0.01	<0.01	<0.02	<0.02	<4E-3	<4E-3	0.21	0.03	2.86	12.4
184	29.6	45	0.14	0.14	<0.01	<0.01	<0.03	<0.03	<0.01	0.41	0.31	0.05	34	154
185	25.5	48.6	0.04	0.1	<0.01	<0.01	<0.02	<0.02	<5E-3	0.22	0.26	0.07	46.7	110
186	22.6	51.3	0.07	0.02	<0.01	<0.01	<0.02	<0.01	<3E-3	0.23	0.3	0.02	62.7	68.7
187	16.3	56.8	0.05	0.03	0.01	<4E-3	<0.01	<0.01	<3E-3	0.17	0.11	0.02	49.4	90.9
188	—	—	0.04	0.07	0.03	0.01	<0.02	0.08	0.02	0.36	0.09	0.02	34.3	72.1
190	11.8	54.4	0.11	0.07	<0.01	0.02	0.51	<0.03	0.36	0.06	0.06	0.02	18.6	34.7
190	11.8	54.4	0.07	0.06	0.01	0.01	<0.02	<0.02	0.01	0.17	0.1	0.02	26.4	37.1
191	10.4	48.1	0.06	0.09	<5E-3	<5E-3	<0.01	<0.01	0.04	0.13	0.14	0.02	32.4	64.8
192	10.4	48.1	0.15	0.13	<0.01	<0.01	<0.04	<0.03	0.02	0.15	0.12	<0.03	37.6	36.6
193	10.4	48.1	0.11	0.07	0.01	0.01	<0.02	<0.02	0.05	0.15	0.09	0.04	32.4	226
194	9.8	45.3	0.08	0.07	0.01	0.01	<0.02	<0.02	<4E-3	0.14	0.11	0.02	31.2	26.9
195	10.1	45.4	0.09	0.04	0.01	0.01	<0.02	<0.02	0	0.25	0.13	0.02	58.7	43.6
196	10.2	45.5	0.09	0.12	0.01	0.01	<0.03	<0.03	0.01	0.48	0.14	0.04	65.4	122
197	11	49.3	0.09	0.08	0.01	0.01	<0.02	<0.02	0.03	0.39	0.15	0.02	25.1	63.4
198	—	—	0.07	0.07	0.01	<0.01	<0.02	<0.02	0.02	0.32	0.13	0.02	25.6	26.9
200	11.6	58.2	0.05	0.04	0.04	0.02	<0.01	<0.01	0.05	0.37	0.14	0.02	11.3	20.2
201	10.3	56.3	0.06	0.06	0.01	0.01	<0.02	<0.02	0.02	0.1	0.15	0.02	12.9	15.7
202	10.2	56.3	0.17	0.14	0.02	0.01	<0.04	<0.04	0.06	0.15	0.13	0.04	56.2	6.17
203	10.2	56.3	0.05	0.08	0.01	0.01	<0.02	0.03	0.07	0.1	0.12	0.02	17.6	16.2
207	11.9	54.9	0.06	0.06	<0.01	<0.01	<0.02	<0.02	0.07	0.16	0.07	0.02	15.8	25.2
208	10.4	53	0.12	0.08	<0.01	<0.01	<0.03	<0.02	0.07	0.46	0.11	0.03	27.8	68
209	8.74	51	0.07	0.07	<0.01	<0.01	<0.02	0.05	0.01	0.23	0.08	0.03	7.91	20.6
210	7.23	48.5	0.06	0.06	0.01	<0.01	0.14	<0.01	0.19	<3E-3	0.16	0.01	9.13	15.6
211	5.65	46.4	0.09	0.09	0.04	<0.01	0.11	<0.02	0.03	<3E-3	0.07	<0.01	10.9	33.1
212	4.76	43.9	0.09	0.15	<0.01	<0.01	<0.02	<0.02	<4E-3	<4E-3	0.07	0.06	8.95	25.9
213	3.83	42.8	—	0.11	—	<0.01	—	<0.02	—	<0.01	—	0.67	—	42.9
214	3.27	44.2	0.36	0.35	<0.01	<0.01	0.08	<0.03	<0.01	<0.01	0.11	<0.03	34.4	36.5
215	3.93	46.1	0.29	0.27	<0.01	<0.01	<0.04	<0.04	<0.01	<0.01	0.09	0.05	27.7	66.9
216	5.79	48	0.13	0.16	<0.01	<0.01	<0.04	<0.04	<0.01	0.11	<0.03	0.05	8.77	59.3
217	6.17	50.1	0.15	0.05	<0.01	0.05	<0.01	<0.01	0.03	0.01	0.07	0.02	10.3	21.3
219	8.21	52.8	0.08	0.04	<3E-3	<3E-3	<0.01	<0.01	<2E-3	0.18	0.05	0.02	5.75	10.1
221	10.5	55	0.15	0.14	0.06	<0.01	0.02	5.36	0.02	<4E-3	0.07	1.19	5.9	6.84
222	10.6	55.8	0.19	0.11	0.07	<0.01	<0.02	11.7	0.1	<0.01	0.07	1.91	4.21	8.95
223	12.5	55	0.27	0.14	<0.01	<0.01	0.07	<0.03	<0.01	0.08	2.09	<0.03	22.8	27.3
224	12.5	54.1	—	0.11	—	<0.01	—	<0.02	—	0.55	—	0.04	—	23
225	11.4	53.8	0.15	0.24	0.04	0.03	7.61	<0.03	0.08	<0.01	3.24	<0.03	9.71	21.4
226	11.8	54.6	0.16	0.14	<0.01	0.17	<0.02	0.09	<0.01	<0.01	0.09	0.03	14.1	38.7

Julian day		Lat °N	Long °W	Fluoride nmol m^{-3}		Glycolate nmol m^{-3}		Acetate nmol m^{-3}		Formate nmol m^{-3}		MSA nmol m^{-3}		Chloride nmol m^{-3}	
				Fine	Coarse	Fine	Coarse	Fine	Coarse	Fine	Coarse	Fine	Coarse	Fine	Coarse
4/18/03-5/20/03															
	108	12	57.6	0.09	0.12	BDL	BDL	BDL	BDL	BDL	2.79	BDL	BDL	8.65	36.8
	109	11.4	55.5	0.04	0.01	BDL	BDL	BDL	BDL	0.33	0.05	BDL	BDL	15.3	23.7
	110	11.1	53.4	0.05	0.02	BDL	BDL	BDL	BDL	0.26	BDL	0.48	0.2	23.5	85.3
	111	9.86	52.1	0.09	0.11	BDL	BDL	BDL	BDL	0.23	0.49	0.45	0.27	20.9	41.8
	112	7.93	52	0.11	0.14	BDL	BDL	BDL	BDL	0.63	1	1.01	0.21	41.1	85.6
	113	6.98	51	0.15	0.05	BDL	BDL	BDL	BDL	0.11	1.86	1.08	0.04	39.5	63.5
	114	7.68	50.8	0.21	0.44	0.04	BDL	0.54	1.12	0.63	2.1	1.11	0.34	35.8	104
	115	9.08	52.9	0.37	0.18	0.53	BDL	0.43	0.79	0.15	1.04	1.11	0.25	30.3	104
	116	10.5	55.1	0.48	0.15	BDL	0.16	BDL	BDL	3.26	BDL	0.49	1.42	88.2	18
	117	12.1	56.5	0.08	0.1	BDL	BDL	0.79	<0.01	0.72	0.35	1.01	0.39	14.2	59.4
	121	11	55.4	0.17	0.16	0.26	0.54	BDL	0.45	0.25	2.85	0.95	0.25	19.5	79.3
	122	9.4	55.4	0.24	0.24	0.95	0.49	0.4	0.31	0.32	3.49	1.09	0.18	42.3	129
	123	7.98	54.9	0.42	0.42	1.2	BDL	0.38	BDL	1.19	2.1	1.33	BDL	50.3	80.8
	124	8.53	54.9	0.57	0.32	BDL	BDL	0.61	BDL	0.23	5.2	1.13	BDL	54.7	138
	125	10.8	55.9	0.43	0.26	1.21	0.25	3.31	BDL	2.58	5.84	0.75	0.24	46.1	107
	126	12.1	56.1	0.15	0.13	0.44	0.39	0.24	0.14	0.14	1.98	1.15	0.14	40.9	117
	127	11.8	56.3	0.15	0.18	BDL	BDL	BDL	0.17	0.03	0.64	1.02	0.14	43.2	97.2
	130	11	55.4	0.16	0.08	0.5	0.44	0.69	0.12	0.37	2.41	1.46	0.21	42.6	114
	131	10.7	53.4	0.27	0.07	0.57	0.02	BDL	BDL	0.17	0.77	1.17	BDL	51.2	76
	132	10.6	51.3	0.2	0.08	0.52	0.12	BDL	BDL	0.14	2.66	1.1	0.05	50.7	133
	133	10.5	49.2	0.22	0.2	0.6	0.24	BDL	BDL	1.71	1.21	0.67	0.14	219	141
	135	8.1	49.4	0.22	0.24	0.76	0.24	0.34	BDL	0.4	2.1	1.36	0.1	88.6	131
	136	8.12	53	0.29	0.16	0.58	BDL	BDL	BDL	0.09	1.81	1.05	0.09	71.2	102
	138	9.14	56.7	0.29	0.16	0.4	BDL	0.77	BDL	0.6	1.99	1.11	0.09	71.6	133
	139	10.3	56.6	0.1	0.04	BDL	BDL	BDL	BDL	0.67	0.87	0.66	BDL	23.9	60.6
	140	10.8	55.2	0.1	0.1	BDL	BDL	BDL	BDL	0.16	0.8	0.51	0.11	26.6	53.1
4/9/01-4/26/01															
	99	21.5	160	0.2	0.02	<1E-3	<1E-3	<4E-3	<3E-3	<0.01	0.03	0.08	<0.03	69.5	28.4
	100	22.2	162	0.27	0.01	<2E-3	<2E-3	0.08	<4E-3	<0.01	<0.01	0.1	<0.04	62.5	11
	101	23.3	168	0.26	0.19	<2E-3	<2E-3	<5E-3	<5E-3	0.05	<0.01	0.1	0.12	44.9	217
	102	24.4	172	0.2	<0.01	<7E-4	<1E-3	0.02	0.03	<3E-3	<3E-3	0.1	<0.02	12.9	1.2
	103	26.1	175	0.2	0.15	<8E-4	<1E-3	0.82	0.07	<4E-3	<4E-3	0.11	0.04	15	22.1
	104	26.8	181	0.08	0.09	<7E-4	<1E-3	11	<2E-3	<3E-3	<3E-3	0.1	0.06	8.88	15.3
	105	27.3	185	0.36	0.29	<2E-3	<2E-3	16.9	<4E-3	<0.01	<0.01	0.17	0.25	585	598
	106	27.6	190	0.21	0.11	<1E-3	<1E-3	0.02	<2E-3	<5E-3	0.06	0.15	0.05	88.1	8.03
	107	27.6	190	1.03	<0.02	<8E-4	<1E-3	<2E-3	<2E-3	0.04	0.02	0.29	<0.02	24.9	<0.5
	108	27.4	187	1.02	0.61	0.03	<1E-3	<2E-3	<2E-3	0.48	0.1	0.17	0.03	1801	<0.5
	109	26.7	182	0.19	0.96	<2E-3	<2E-3	0.07	1.54	<0.01	<0.01	0.09	0.2	47.5	90.2
	110	26	175	5.09	4.71	<3E-3	<3E-3	<0.01	<0.01	0.25	0.07	0.2	0.08	180	132
	111	25.6	174	1.98	1.77	0.03	<1E-3	0.01	<3E-3	<0.01	<0.01	0.18	0.03	27.3	39.7
	112	24.8	171	2.75	2.58	<3E-3	<3E-3	<0.01	<0.01	0.27	<0.01	0.13	<0.07	312	50.4
	114	24.2	166	4.87	3.92	<4E-3	<4E-3	0.01	<0.01	0.14	<0.02	1.07	<0.1	552	84.5
	116	22.5	158	2.57	2.14	<2E-3	<2E-3	6.7	<0.01	<0.01	<0.01	0.18	0.07	288	14.5
7/1/02-7/16/02															
	182	22.8	158	0.11	0.11	<1E-3	<1E-3	<2E-3	<3E-3	0.38	0.16	1.01	0.4	17.2	21.5
	183	22.8	158	0.12	0.12	<1E-3	<1E-3	0.04	0.27	0.31	0.53	1.28	0.51	15.2	34.6
	184	23.5	162	0.31	0.33	<2E-3	<2E-3	<0.01	<0.01	0.53	0.28	2.13	0.92	25.9	36.3
	185	24	165	0.13	0.2	<2E-3	<2E-3	0.01	<0.01	0.66	0.35	2.03	0.89	21.5	44.3
	186	24.5	167	0.38	0.27	<3E-3	<3E-3	<0.01	<0.01	0.52	0.74	2.09	1.54	23.4	47.9
	187	24.9	170	0.4	0.31	<3E-3	<3E-3	1.84	<0.01	2.64	0.23	1.7	1.08	13.9	25.4
	189	26.1	175	0.15	0.17	<1E-3	<1E-3	<3E-3	<3E-3	0.34	0.24	0.83	0.56	17.6	30.1
	190	26	175	0.08	0.1	<1E-3	<1E-3	<2E-3	<2E-3	0.18	0.12	0.86	0.33	20.5	40
	191	26	175	0.15	0.12	<1E-3	<1E-3	<3E-3	<3E-3	0.22	0.22	0.94	0.38	20.9	30.9
	192	26	175	0.09	0.08	<1E-3	<1E-3	<2E-3	<2E-3	0.15	0.14	2.15	0.31	21.9	42.4
	193	26	175	0.05	0.05	<1E-3	<1E-3	<2E-3	<2E-3	0.12	0.12	147	-14	40.6	40.3
	194	24.7	170	0.07	0.06	<1E-3	<1E-3	<2E-3	<2E-3	1.05	0.03	1.08	0.31	10.8	13.8
	195	23.6	167	0.07	0.09	<1E-3	<1E-3	<1E-3	<1E-3	0.61	0.59	1.06	0.24	12.6	25.1
	196	22.9	164	0.11	0.07	0.05	<1E-3	<2E-3	<2E-3	0.07	1.01	1.06	0.41	88.8	42.1
	197	22.8	160	0.07	0.07	<1E-3	<1E-3	<2E-3	<2E-3	0.91	0.76	1.38	0.33	69.3	43.6
9/23/02-10/15/02															
	266	22.5	157	0.07	0.11	<2E-3	<1E-3	0.15	<2E-3	0.45	0.02	0.85	0.35	3.37	4.71
	267	23.5	157	0.02	0.07	<1E-3	<1E-3	<2E-3	0.09	0.02	0.17	0.75	0.26	1.25	8.57
	268	23.5	157	0.08	0.12	<1E-3	<1E-3	<3E-3	<3E-3	0.11	0.07	1.35	0.37	3.6	8.15
	269	24.2	156	0.1	0.12	<1E-3	<1E-3	<2E-3	<2E-3	0.09	0.1	0.75	0.4	6.22	22.5
	270	24.2	155	0.06	0.09	<1E-3	<1E-3	<3E-3	<2E-3	0.07	0.06	1.22	0.37	9.11	26.4
	271	23.7	156	0.04	0.02	<1E-3	<1E-3	<2E-3	<2E-3	0.1	0.01	1.22	0.26	13.2	24.7
	273	23.3	157	0.31	0.14	<2E-3	<3E-3	<5E-3	<0.01	0.36	0.51	2.23	0.9	36.7	59.7
	274	23.3	159	0.29	0.11	<1E-3	<1E-3	0.33	<3E-3	8.71	<0.01	0.56	0.57	16.7	5.78
	275	23.8	159	0.16	0.08	<1E-3	<1E-3	<2E-3	<2E-3	1.33	<5E-3	0.69	0.31	16	16.4
	276	22.5	159	0.06	0.09	<1E-3	<1E-3	<2E-3	<3E-3	0.13	<0.01	0.77	0.4	10.9	29.2
	278	19.7	156	0.07	0.12	<1E-3	<1E-3	<2E-3	<2E-3	1.51	0.01	0.82	0.35	0.8	27.9
	279	19.4	156	0.11	0.15	<1E-3	<1E-3	<2E-3	<2E-3	0.15	0.1	0.76	0.36	2.49	22
	280	19.8	155	0.16	0.11	<2E-3	0.21	<4E-3	<3E-3	1.65	1.86	1.43	0.54	22.8	37.1
	281	20.3	156	0.1	0.09	<1E-3	<1E-3	<2E-3	<2E-3	0.07	1.33	0.57	0.47	6.85	13.1
	282	20.1	156	0.09	0.09	<1E-3	<1E-3	<2E-3	<2E-3	0.13	0.11	0.83	0.31	11.4	21.2
	283	20.9	156	0.11	0.07	<1E-3	<1E-3	<2E-3	<2E-3	1	0.57	0.89	0.35	9.9	11.9
	285	23.2	158	0.09	0.1	<1E-3	<1E-3	<3E-3	<3E-3	1.76	1.66	0.93	0.56	10.1	14.2
	286	21.6	158	0.09	0.1	<1E-3	<1E-3	0.08	<2E-3	0.46	0.08	1.21	0.32	10.1	27.6
	287	20.2	157	0.09	0.11	<1E-3	<1E-3	<3E-3	<3E-3	0.2	0.18	1.12	0.41	4.08	25.8
	288	19.8	156	0.12	0.12	<1E-3	<1E-3	<3E-3	<3E-3	0.2	0.19	0.69	0.48	5.9	19.5

Julian day		Lat °N	Long °W	Fluoride nmol m^{-3}		Glycolate nmol m^{-3}		Acetate nmol m^{-3}		Formate nmol m^{-3}		MSA nmol m^{-3}		Chloride nmol m^{-3}	
				Fine	Coarse	Fine	Coarse	Fine	Coarse	Fine	Coarse	Fine	Coarse	Fine	Coarse
8/6/03-8/20/03															
	218	19.7	157	0.05	0.07	<1E-3	<1E-3	<3E-3	0.23	0.1	1.74	0.77	0.14	78.8	56.7
	219	18.5	157	0.04	0.04	<1E-3	<1E-3	0.22	<2E-3	0.12	0	0.54	0.05	28.4	51.9
	220	18.7	156	0.09	0.03	<1E-3	<1E-3	0.36	0.07	0.86	0.13	0.3	<0.02	412	<0.5
	221	19.2	156	0.1	0.1	<2E-3	<2E-3	<5E-3	0.3	0.04	0.22	0.5	<0.05	59.6	63.1
	222	19.5	157	0.08	0.06	<1E-3	<1E-3	0.28	0.41	0.21	0.31	0.48	0.09	44.5	50.3
	223	19.5	158	0.07	0.04	<1E-3	<1E-3	0.2	<2E-3	0.16	0.04	0.62	0.09	32.1	65.3
	224	19.5	159	0.06	0.07	<1E-3	0.09	0.54	<2E-3	0.28	0.05	0.46	0.09	45.5	41.1
	225	20	160	0.25	0.13	<1E-3	<1E-3	<3E-3	<3E-3	0.13	0.12	0.33	0.13	23.4	86.5
	226	20.8	160	0.06	0.08	<1E-3	<1E-3	0.27	<2E-3	0.22	0.03	0.93	0.07	52	40.3
	227	21	159	0.06	0.2	<1E-3	0.28	<2E-3	<2E-3	0.14	0.11	1.18	0.19	25.1	63.4
	228	20.6	158	0.08	0.07	0.47	0.25	0.16	<2E-3	0.09	0.76	1.21	0.01	357	225
	229	20.3	158	0.13	0.08	<1E-3	<1E-3	<3E-3	0.34	0.09	0.11	1.07	0.06	53.6	104
	230	19.7	161	0.08	0.1	0.34	0.45	<3E-3	<3E-3	0.12	0.54	1.18	0.11	61.3	93.7
	231	19.1	162	0.07	0.06	0.26	0.31	0.2	<1E-3	0.36	0.02	1.19	0.09	36.2	111
	232	19.8	162	0.04	0.03	<0.01	<0.01	<2E-3	<2E-3	0.02	0.01	0.05	0.02	28.3	40.9
	233	—	—	0.05	0.04	0.01	<0.01	0.02	0.01	0.02	0.01	0.05	0.01	21.7	40.9

Julian day	Latitude °N	Longitude °W	Sulfate nmol m^{-3}		Oxalate nmol m^{-3}		Bromide nmol m^{-3}		Nitrate nmol m^{-3}		Phosphate nmol m^{-3}	
			Fine	Coarse	Fine	Coarse	Fine	Coarse	Fine	Coarse	Fine	Coarse
1/6/01-2/19/01												
6	—	—	20.4	1.01	1.41	0.08	<0.02	<0.02	3.71	12.1	0.08	<0.02
7	27.8	75.5	20.2	2.85	0.88	0.17	<0.02	0.03	6.3	13.3	0.3	<0.03
8	28.1	70.9	20.5	2.93	0.87	0.34	<0.03	<0.03	4.8	10.2	<0.04	<0.04
9	28.4	66.9	6.58	0.27	0.43	<0.1	<0.09	<0.09	3.69	3.13	2.89	<0.1
10	28.6	63.3	11.5	1.39	0.21	<0.02	<0.02	0.03	3.57	1.15	<0.02	<0.02
12	29.2	55.2	3.57	0.79	0.13	<0.01	<0.01	<0.01	1.42	0.88	<0.01	<0.01
13	29.5	51.3	2.71	0.42	0.12	0.03	<0.01	<0.01	1.03	0.75	<0.01	0.03
14	29.9	48.2	2.07	1.33	0.08	0.03	<0.02	0.12	0.9	0.55	0.06	0.09
15	29.6	46.5	1.52	0.71	0.07	0.03	<0.01	<0.01	0.84	0.39	0.06	<0.02
16	27.8	45	2.47	0.79	0.14	0.02	<0.01	<0.01	1.83	0.42	<0.01	<0.01
17	25.3	45	2.71	0.7	0.18	0.05	<0.01	<0.01	1.54	1.39	<0.01	<0.01
18	21.5	45	4.38	1.49	0.25	0.07	<0.01	<0.01	2.12	2.73	0.08	0.03
19	16.8	45	6.89	7.44	0.21	0.06	<0.03	0.09	3.85	2.91	0.29	0.01
20	13.2	45	15.6	11.9	1.01	0.24	<0.02	<0.02	11.4	10.6	0.19	0.46
21	10.2	45.2	18.8	6.06	0.55	0.05	0.04	0.06	7.18	1.91	0.19	0.09
22	10.2	46.5	13.8	2.5	0.58	<0.01	<0.05	<0.05	6.76	0.78	0.49	0.5
23	10.5	47.8	11.1	8.26	0.26	0.26	<0.1	<0.1	8.07	13.5	<0.1	0.8
29	10.5	47.8	5.12	1.4	0.21	0.03	<0.01	<0.01	0.53	0.19	0.03	<0.01
30	10.5	55.3	4.19	1.31	0.18	0.03	<0.01	<0.01	0.32	0.21	0.03	<0.02
31	10.1	53.5	3.5	1.96	0.17	0.04	<0.01	<0.01	0.29	0.2	<0.01	0.03
32	9.19	51.2	7.75	1.72	0.32	0.03	<0.01	<0.01	0.68	0.24	0.06	0.03
33	9.24	49.3	4.6	2.3	0.18	0.03	<0.01	<0.01	0.28	0.14	<0.01	0.04
34	9.36	47.5	10.8	3.85	0.54	0.05	<0.02	<0.02	0.98	0.45	0.08	0.03
35	7.41	48.2	18.2	7.69	1.28	0.34	<0.01	<0.01	2.81	1.36	0.18	0.09
36	6.31	47.1	12.1	3.77	0.73	0.12	<0.01	<0.01	1.8	0.59	0.34	0.03
37	7.22	45.1	11.1	5.07	0.5	0.1	<0.01	<0.01	1.25	0.69	0.15	0.05
38	7.17	43	11.4	4.64	0.48	0.09	<0.01	<0.01	1.16	0.57	0.02	0.03
39	8.61	41.3	10.1	2.32	0.28	0.08	0.04	<0.02	0.99	0.32	0.06	0.02
40	9.34	41.5	8.18	6.46	0.27	0.16	0.03	0.03	0.81	0.56	0.11	0.06
41	10.9	42.4	22.5	5.57	0.87	0.21	<0.04	0.06	2.5	1.19	<0.05	0.23
42	10.1	44.7	13	5.06	0.74	0.18	0.05	0.05	2	0.8	0.18	0.11
43	9.81	44.5	16	6.83	0.72	0.18	0.2	0.05	2.33	0.86	0.42	0.15
44	10.6	46.6	15.8	5.2	0.65	0.17	0.07	0.07	2.63	1.01	0.86	0.18
45	9.44	49.2	22.5	8.16	0.63	0.16	0.13	0.04	3	1.94	0.35	0.52
46	9.08	51.8	17.8	4.73	0.54	0.07	0.13	<0.03	2.17	0.77	0.35	0.1
47	9.41	55.3	14.3	15.3	0.63	0.25	0.08	0.18	2.21	1.36	0.34	0.23
48	10.9	56.1	8.62	3.87	0.48	0.13	0.01	0.01	1.12	0.36	0.25	0.16
49	11.3	54.8	8.1	4.87	0.38	0.12	0.02	0.07	0.86	0.35	0.24	0.19
6/27/01-8/14/01												
178	29.2	27.4	6.85	<0.05	0.24	<0.01	<0.02	<0.01	0.23	<2E-3	0.08	<0.01
179	29.3	29.6	4.01	1.13	0.22	0.09	<0.01	<0.01	0.14	0.19	0.01	0.02
180	29.4	33.5	4.25	0.51	0.23	0.05	<0.01	<0.01	0.12	0.19	0.04	0.04
181	29.5	37.4	3.87	1.48	0.28	0.1	<0.01	<0.01	0.14	0.35	0.01	<0.01
182	29.5	39.3	7.2	1.17	0.24	0.05	0.03	0.01	0.26	0.44	0.12	0.02
183	29.6	43.2	7.17	1.53	0.18	0.07	<0.01	<0.01	0.2	0.51	0.04	0
184	29.6	45	10.2	10.9	0.31	0.17	0.03	0.19	0.5	0.74	0.11	0.04
185	25.5	48.6	7.11	6.81	0.17	0.09	0.03	0.09	0.44	0.5	0.04	0.06
186	22.6	51.3	8.97	3.9	0.42	0.04	0.04	0.02	0.57	0.25	<0.01	<5E-3
187	16.3	56.8	5.41	5.09	0.2	0.04	0.02	0.04	0.52	0.35	0.01	0.02
188	—	—	4.87	5.54	0.22	0.09	<0.01	0.1	0.37	0.33	0.09	0.03
190	11.8	54.4	2.99	2.14	0.1	0.07	0.05	0.08	0.23	0.15	0.06	0.13
190	11.8	54.4	5.32	2.66	0.18	0.05	0.03	0.05	0.37	0.18	0.05	0.11
191	10.4	48.1	8.88	4.93	0.38	0.14	0.03	0.07	0.77	0.49	0.12	0.03
192	10.4	48.1	6.16	2.11	0.27	0.06	0.06	0.04	0.53	0.18	0.14	0.05
193	10.4	48.1	6.91	17.8	0.17	0.43	0.06	0.3	0.32	0.63	0.1	0.62
194	9.8	45.3	7.61	2.31	0.23	0.06	0.05	0.03	0.4	0.32	0.22	0.11
195	10.1	45.4	9.91	2.88	0.23	0.09	0.07	0.03	0.59	0.46	0.06	0.04
196	10.2	45.5	8.91	7.78	0.25	0.15	0.05	0.15	0.61	0.55	0.1	0.06
197	11	49.3	7.93	4.27	0.34	0.15	0.02	0.06	0.84	0.59	0.1	0.05
198	—	—	5.99	2.79	0.22	0.1	0.02	0.03	0.44	0.34	0.06	0.06
200	11.6	58.2	4.6	2.41	0.42	0.18	0.03	0.02	0.32	0.34	0.06	0.05
201	10.3	56.3	4.65	1.41	0.55	0.13	0.04	0.03	0.29	0.23	0.07	0.05
202	10.2	56.3	5.82	1.2	0.43	0.11	0.09	0.02	0.32	0.32	0.73	0.02
203	10.2	56.3	4.23	1.35	0.59	0.12	0.06	0.03	0.3	0.29	0.1	0.07
207	11.9	54.9	3.09	1.69	0.21	0.04	0.03	0.04	0.15	0.05	0.06	0.02
208	10.4	53	5.47	4.34	0.21	0.1	0.05	0.08	0.48	0.31	0.07	0.06
209	8.74	51	4.28	1.34	0.27	0.06	0.03	0.04	0.39	0.25	0.07	0.05
210	7.23	48.5	5.03	1.28	0.78	0.15	0.03	0.02	0.58	0.57	0.05	0.04
211	5.65	46.4	2.91	2.27	0.35	0.09	<0.01	0.08	0.34	0.35	<0.01	<0.01
212	4.76	43.9	1.64	1.9	0.06	0.02	<0.01	<0.01	0.15	0.23	<0.01	<0.01
213	3.83	42.8	—	1.66	—	<0.01	—	<0.01	—	0.16	—	<0.01
214	3.27	44.2	4.71	1.8	0.23	0.01	<0.02	<0.01	0.59	0.27	<0.01	<0.01
215	3.93	46.1	3.34	4.16	0.2	0.04	<0.02	0.15	0.46	0.46	<0.01	0.28
216	5.79	48	1.35	3.42	0.27	<0.01	<0.02	0.16	0.21	0.26	<0.01	<0.01
217	6.17	50.1	2.51	1.83	0.37	0.08	<0.01	<0.01	0.43	0.44	0.15	0.09
219	8.21	52.8	3.83	0.87	0.34	0.06	<4E-3	<4E-3	0.38	0.26	0.08	0.06
221	10.5	55	5.01	0.69	0.08	0.05	<0.01	<0.01	0.4	<1E-3	0.12	<0.01
222	10.6	55.8	3.28	0.95	0.25	0.05	<0.01	<0.01	0.32	<2E-3	0.11	<0.01
223	12.5	55	8.6	1.49	0.29	0.01	<0.01	0.12	0.22	0.26	<0.01	0.15

Julian day	Latitude °N	Longitude °W	Sulfate nmol m^{-3}		Oxalate nmol m^{-3}		Bromide nmol m^{-3}		Nitrate nmol m^{-3}		Phosphate nmol m^{-3}	
			Fine	Coarse	Fine	Coarse	Fine	Coarse	Fine	Coarse	Fine	Coarse
224	12.5	54.1	—	1.72	—	0.01	—	<0.01	—	0.17	—	<0.01
225	11.4	53.8	2.68	1.41	0.23	0.05	<0.01	0.11	0.05	0.32	<0.01	<0.01
226	11.8	54.6	5.6	2.84	0.71	0.24	0.11	0.06	0.59	0.92	<0.01	<0.01
4/18/03-5/20/03												
108	12	57.6	1.24	1.86	BDL	0.32	BDL	0.12	1.56	1.1	BDL	BDL
109	11.4	55.5	1.45	1.29	0.14	0.21	0.14	0.05	1.07	0.44	BDL	0.06
110	11.1	53.4	3.32	4.58	2.74	1.29	BDL	0.06	1.55	1.16	0.12	0.19
111	9.86	52.1	3.79	2.65	3.14	1.27	BDL	0.09	1.7	0.97	0.27	0.06
112	7.93	52	6.98	4.64	5.22	1.1	BDL	0.09	3.15	1.6	0.47	0.15
113	6.98	51	7.79	3.52	5.66	2.27	BDL	0.06	4.04	1.53	0.13	0.29
114	7.68	50.8	8.19	6.71	9.74	3.69	BDL	0.11	4.04	3.36	0.26	0.28
115	9.08	52.9	5.94	6.05	3.97	2.52	BDL	0.13	2.86	1.87	0.37	0.17
116	10.5	55.1	6.8	8.59	4.92	8.93	0.09	BDL	5.41	4.07	0.32	0.29
117	12.1	56.5	3.66	3.52	2.93	2.32	0.05	0.05	1.36	1.72	0.18	0.08
121	11	55.4	5.45	6.13	2.68	3.28	BDL	0.08	1.29	1.84	0.04	0.03
122	9.4	55.4	7.83	7.13	6.48	2.02	BDL	0.1	2.71	2.3	0.06	0.03
123	7.98	54.9	8.29	4.64	5.84	3.05	0.09	0.08	3.97	1.2	0.15	0.03
124	8.53	54.9	9.42	8.09	8.27	2.92	BDL	0.17	4.46	2.87	0.1	0.08
125	10.8	55.9	6.78	7.31	4.13	3.43	BDL	0.15	2.4	1.28	0.08	0.11
126	12.1	56.1	7.45	7.09	4.87	2.93	0.05	0.09	2.48	2.51	0.1	0.25
127	11.8	56.3	6.38	5.09	4.1	1.52	BDL	0.06	2.31	1.47	0.13	0.84
130	11	55.4	7.57	6.65	6.41	0.81	BDL	0.07	2.43	2.39	0.17	0.09
131	10.7	53.4	8.45	3.24	5.44	0.9	0.05	0.05	3.03	1	0.59	0.3
132	10.6	51.3	7.94	7.99	5.47	2.61	0.05	0.15	2.94	2.25	0.31	0.01
133	10.5	49.2	9.1	8.34	4.44	1.4	0.14	0.19	2.05	1.64	0.1	0.96
135	8.1	49.4	14.3	8.13	8.49	3.52	0.08	0.08	4.48	2.5	0.09	1.58
136	8.12	53	12.2	6.74	7.65	1.75	0.07	0.09	4.11	2.23	1.38	0.61
138	9.14	56.7	13.1	7.36	12.7	2.68	BDL	0.11	4.7	2.65	0.4	0.72
139	10.3	56.6	6.65	3.76	4.93	1.93	0.04	0.03	2.28	2.11	0.04	0.9
140	10.8	55.2	7.52	3.15	5.24	1.87	0.04	BDL	2.56	1.81	0.11	0.6
4/9/01-4/26/01												
99	21.5	160	4.18	1.41	0.05	<0.01	0.14	0.1	0.42	0.04	<0.01	<0.01
100	22.2	162	6.72	0.3	0.16	<0.01	0.16	0.11	0.61	<0.05	<0.01	<0.01
101	23.3	168	5	13.9	0.07	0.02	0.26	0.39	0.34	0.3	<0.02	<0.02
102	24.4	172	3.36	<0.2	0.09	<3E-3	<0.01	0.04	0.17	0	<0.01	<0.01
103	26.1	175	2.88	1.67	0.13	0.02	<0.02	0.07	0.46	0.05	<0.01	<0.01
104	26.8	181	3.01	1.42	0.15	0.04	0.05	0.04	0.2	0.08	0.05	<0.01
105	27.3	185	28.5	27.1	0.05	0.03	0.87	1.01	<0.05	<0.05	0.18	0.25
106	27.6	190	6.39	0.69	0.04	0.01	0.2	0.07	0.17	0.11	0.3	0.07
107	27.6	190	11.5	<0.2	0.48	<4E-3	0.11	<0.01	0.55	<0.02	0.12	<0.01
108	27.4	187	79.7	2.86	0.18	0.07	2.99	<0.01	0.6	0.27	2.14	1.62
109	26.7	182	2.95	6.56	<0.01	0.13	0.2	0.22	0.08	<0.05	0.23	1.28
110	26	175	15.8	3.3	0.35	<0.01	0.45	0.26	0.4	0.26	0.58	0.23
111	25.6	174	5.13	2.03	0.13	0.01	0.11	0.08	0.22	0.25	<0.01	<0.01
112	24.8	171	11.7	3.28	0.09	<0.01	0.28	0.2	0.37	0.33	0.34	0.36
114	24.2	166	26.5	11.9	0.02	0.04	1.1	0.24	0.43	0.22	0.61	<0.03
116	22.5	158	19.6	3.32	0.35	0	0.45	0.09	0.4	0.22	<0.02	<0.02
7/1/02-7/16/02												
182	22.8	158	2.86	1.16	1.49	0.48	0.07	0.05	1.31	0.4	0.09	<0.01
183	22.8	158	2.43	1.9	1.32	0.92	<0.02	0.09	0.84	0.67	<0.01	0.18
184	23.5	162	3.73	1.94	3.94	1.29	<0.04	<0.05	2.04	0.85	0.15	0.14
185	24	165	3.64	2.4	4.11	0.76	0.13	0.09	1.21	0.89	<0.02	<0.02
186	24.5	167	3.1	2.86	3.19	1.44	<0.07	0.15	1.34	1.19	0.34	<0.03
187	24.9	170	2.63	1.46	2.23	1.04	0.15	0.11	1.31	0.99	0.29	<0.03
189	26.1	175	1.71	1.65	0.89	0.3	<0.02	0.07	0.53	0.28	0.1	0.06
190	26	175	2.37	2.05	1.33	0.67	0.04	0.04	0.56	0.41	0.06	0.04
191	26	175	2.74	1.61	1.3	0.42	<0.02	0.06	0.57	0.38	<0.01	0.07
192	26	175	6.84	2.16	6.07	1.02	0.08	0.07	0.83	0.6	<0.01	0.05
193	26	175	8.31	2.16	4.09	0.7	<0.01	0.04	0.67	0.41	0.05	<0.01
194	24.7	170	3.6	0.87	1.93	0.93	0.05	0.03	0.46	0.43	0.05	0.06
195	23.6	167	3.23	1.35	1.24	0.55	0.03	0.04	0.39	0.31	<4E-3	<4E-3
196	22.9	164	10.9	1.62	1.56	0.75	0.18	0.07	0.45	0.37	<0.01	0.05
197	22.8	160	6.38	2.21	1.5	0.59	0.11	0.07	0.79	0.47	<0.01	<0.01
9/23/02-10/15/02												
266	22.5	157	2.92	0.45	<0.01	0.19	<0.03	<0.02	0.36	0.38	<0.01	<0.01
267	23.5	157	5.17	0.98	0.37	0.5	<0.01	<0.01	0.23	0.53	0.04	0.04
268	23.5	157	13	0.85	0.66	0.95	<0.02	<0.02	0.45	1.08	<0.01	<0.01
269	24.2	156	1.74	1.47	0.87	0.2	<0.02	0.05	0.37	0.5	<0.01	<0.01
270	24.2	155	2.61	1.52	1.03	0.19	0.05	0.04	0.73	0.81	<0.01	0.06
271	23.7	156	2.98	1.55	2.53	0.7	<0.01	<0.01	0.51	0.48	<0.01	0.03
273	23.3	157	5.51	3.19	4.57	0.51	0.1	<0.05	1.71	1.11	<0.02	0.14
274	23.3	159	1.12	1.16	0.35	0.46	<0.03	<0.03	0.29	0.25	<0.01	<0.01
275	23.8	159	1.75	0.86	0.57	0.2	<0.02	<0.02	0.32	0.21	<0.01	<0.01
276	22.5	159	3.86	1.66	0.64	0.59	<0.02	<0.02	0.61	0.54	0.07	<0.01
278	19.7	156	10	2.45	3.03	0.4	<0.02	0.06	0.2	0.36	0.06	0.09
279	19.4	156	22.2	3.29	2.11	0.11	0.07	0.04	0.18	0.54	0.04	0.07
280	19.8	155	3.68	1.92	1.22	1.13	0.07	0.06	0.8	0.49	0.1	0.07
281	20.3	156	1.25	0.7	0.35	0.03	<0.02	<0.02	0.27	0.23	0.07	0.05
282	20.1	156	2.18	1.14	0.47	0.2	<0.02	0.04	0.37	0.29	0.06	0.07
283	20.9	156	2.23	0.63	0.69	0.13	<0.02	0.03	0.42	0.23	0.08	<0.01

Julian day	Latitude °N	Longitude °W	Sulfate nmol m^{-3}		Oxalate nmol m^{-3}		Bromide nmol m^{-3}		Nitrate nmol m^{-3}		Phosphate nmol m^{-3}	
			Fine	Coarse	Fine	Coarse	Fine	Coarse	Fine	Coarse	Fine	Coarse
285	23.2	158	1.41	0.96	0.41	0.26	<0.02	0.05	0.38	0.33	0.09	0.06
286	21.6	158	4.34	1.47	1.76	0.78	0.07	0.04	1.02	0.79	0.06	0.04
287	20.2	157	8.81	1.76	1.89	0.8	0.09	0.07	0.34	0.45	0.07	<0.01
288	19.8	156	1.31	1.13	0.38	0.61	0.06	0.07	0.31	0.23	0.09	0.06
8/6/03-8/20/03												
218	19.7	157	11.4	3.79	1.8	0.64	0.08	0.07	0.89	0.76	0.07	0.06
219	18.5	157	3.16	2.75	1.05	0.36	0.05	0.06	0.5	0.3	0.07	0.2
220	18.7	156	25.9	<0.2	0.12	0.03	0.68	<0.01	0.42	0.03	0.06	0.01
221	19.2	156	6.92	3.6	1.48	0.64	0.14	0.1	0.68	0.4	0.4	0.11
222	19.5	157	9.32	3.03	2.34	0.65	0.06	0.05	0.65	0.47	0.11	0.1
223	19.5	158	10.1	3.85	3.24	1.25	0.06	0.04	0.87	0.97	0.35	<0.01
224	19.5	159	7.41	2.43	1.9	0.46	0.05	0.04	0.82	0.51	0.03	0.02
225	20	160	3.16	5.04	1.4	1.6	0.06	0.09	1	1.09	0.08	0.02
226	20.8	160	6.51	2.34	3.69	0.81	0.05	0.03	1.58	0.81	0.14	0.25
227	21	159	6.5	3.7	6.94	1.6	0.04	0.03	2.52	3.27	0.03	<0.01
228	20.6	158	25.5	21.9	2.89	1.69	0.54	0.32	2.65	0.73	0.04	0.06
229	20.3	158	8.42	5.81	2.67	1.1	0.06	0.13	1.73	0.8	0.09	0.07
230	19.7	161	11.3	7.56	4.67	0.96	0.06	0.1	2.11	2.19	0.12	<0.01
231	19.1	162	11.8	6.98	<3E-3	2.07	0.04	0.08	1.47	1.54	<5E-3	<5E-3
232	19.8	162	4.78	3.42	0.12	0.05	0.02	0.05	0.87	0.68	0.03	<0.01
233	—	—	6.85	2.65	0.22	0.05	0.03	0.03	2.09	1.74	<5E-3	<5E-3

Julian day	Latitude °N	Longitude °W	Sodium nmol m^{-3}		Ammonium nmol m^{-3}		Potassium nmol m^{-3}		Magnesium nmol m^{-3}		Calcium nmol m^{-3}	
			Fine	Coarse	Fine	Coarse	Fine	Coarse	Fine	Coarse	Fine	Coarse
1/6/01-2/19/01												
6	—	—	4.64	10.7	28	1.94	1.09	0.3	0.48	1.31	0.85	1.91
7	27.8	75.5	14.5	46	18	0.24	0.86	0.98	1.63	6.98	0.75	<0.07
8	28.1	70.9	12.9	39	16.7	0.4	0.82	0.84	1.44	4.41	0.47	0.97
9	28.4	66.9	21.6	4.84	7.67	0.52	0.83	0.33	2	0.47	0.96	0.23
10	28.6	63.3	31.6	33.6	5.42	<0.01	0.77	0.71	3.56	3.74	0.7	0.71
12	29.2	55.2	12.3	15.4	1.29	0.06	0.23	0.31	1.11	1.53	0.26	0.32
13	29.5	51.3	12.7	6.24	0.87	0.19	0.28	0.14	1.45	0.67	0.29	0.16
14	29.9	48.2	11.8	18.1	1.03	0.28	0.28	0.37	1.2	2.04	0.27	0.37
15	29.6	46.5	8.74	10.5	0.56	0.19	0.21	0.25	0.93	1.14	0.22	0.24
16	27.8	45	11.9	14.5	0.71	0.12	0.31	0.35	1.25	1.76	0.28	0.33
17	25.3	45	8.79	11.6	2.02	0.13	0.67	0.25	0.86	1.05	0.37	0.37
18	21.5	45	13.6	19.8	3.04	0.2	1.08	0.5	1.33	2.09	0.54	1
19	16.8	45	29.2	83.8	2.42	0.27	0.97	1.93	3.54	9.61	3.92	4.37
20	13.2	45	48.7	113	5.48	0.35	5.24	3.05	5.97	13.6	4.82	7.85
21	10.2	45.2	91.5	58.3	2.13	0.06	2.96	1.46	11.1	6.93	9.95	4.53
22	10.2	46.5	73.1	32.9	3.52	0.28	2.13	0.66	7.96	3.32	6.17	1.53
23	10.5	47.8	67.6	71.5	4.05	<0.07	1.91	4.82	6.85	6.43	1.98	4.18
29	10.5	47.8	41.3	20	1.2	0.02	1.16	0.53	3.82	2.48	1.59	0.78
30	10.5	55.3	22.7	21.2	1.59	0.06	0.86	0.51	2.51	2.58	0.66	0.66
31	10.1	53.5	24.9	35.1	1.51	0.09	0.93	0.73	2.6	3.54	1.21	1.35
32	9.19	51.2	67.3	26.3	1.89	0.07	2.04	0.67	5.67	3.54	2.13	1.03
33	9.24	49.3	44	31	1.37	0.11	0.91	0.82	3.79	4.25	0.96	0.79
34	9.36	47.5	89.3	55.4	4.37	<0.01	3.76	1.41	8.66	7.3	3.34	2.26
35	7.41	48.2	100	86	3.25	0.16	8.18	2.64	14.6	11.5	21.9	17.3
36	6.31	47.1	71	48.5	2.34	0.04	4.3	1.39	10.3	6.12	12.2	7.1
37	7.22	45.1	57.4	60.2	2.53	0.23	2.74	1.73	6.35	7.76	7.11	7.03
38	7.17	43	63.1	89.9	3.21	0.15	2.62	1.57	7.49	7.19	6.79	5.41
39	8.61	41.3	84.6	34.4	2.49	0.05	2.55	0.93	9.9	3.97	6.53	2.87
40	9.34	41.5	64.2	93.3	2.07	0.1	2.26	2.21	7.18	10.2	7.47	9.04
41	10.9	42.4	110	75.9	9.9	0.11	10.4	2.11	31.4	8.59	13.7	11.4
42	10.1	44.7	142	74.8	3.2	0.06	5.46	1.97	9.39	8.53	14.2	10.3
43	9.81	44.5	118	96	5.02	0.25	7.12	2.49	20.3	24.4	15.6	<0.09
44	10.6	46.6	184	75.8	4.04	0.48	5.31	2.28	9.66	9.54	9.93	8.89
45	9.44	49.2	155	118	5.78	0.58	7.66	2.57	21.8	11.1	8.19	7.58
46	9.08	51.8	144	47.1	4.96	0.23	5.19	1.34	16.4	5.9	5.83	3.72
47	9.41	55.3	97.5	120	2.35	0.29	4.77	3.26	11.9	14.9	15.1	13.6
48	10.9	56.1	52.2	34.2	1.14	0.11	3.21	1.31	7.39	5.07	20.3	10.7
49	11.3	54.8	70.8	66.6	1.49	0.13	2.44	1.48	8.17	6.62	14.1	9.33
6/27/01-8/14/01												
178	29.2	27.4	14.2	33.5	2.25	0.2	0.5	0.48	1.01	1.34	1.7	1.4
179	29.3	29.6	10.3	13.3	1.73	0.26	0.26	0.27	0.55	0.71	0.62	0.95
180	29.4	33.5	14	10.2	2.51	0.32	0.29	0.29	0.47	0.82	0.35	0.88
181	29.5	37.4	9.36	15.7	2.74	0.43	0.33	0.46	0.57	1.52	0.51	1.69
182	29.5	39.3	14.1	10.2	3.92	0.29	0.59	0.29	2.31	0.75	1.8	0.88
183	29.6	43.2	18.5	13.1	4.34	0.42	0.42	0.4	1.36	1.27	1.26	0.62
184	29.6	45	53.8	126	7.38	0.59	1.59	3.71	6	14.1	2.88	6.69
185	25.5	48.6	60.1	86.8	5.22	0.11	1.89	2.62	8.44	9.91	3.31	4.64
186	22.6	51.3	65.8	72.5	2.29	0.36	1.77	1.93	7.74	8.31	2.12	3.48
187	16.3	56.8	58.8	85.8	3.46	0.25	1.42	2.23	6.93	10.7	2.87	4.62
188	—	—	35.3	49.4	2.43	0.15	1.1	2.09	3.63	9.81	2.73	3.5
190	11.8	54.4	31	30.9	2.13	0.21	0.87	0.74	2.85	2.58	2.24	1.93
190	11.8	54.4	29.5	31.1	2.12	0.18	0.89	0.81	3.17	3.52	1.67	2
191	10.4	48.1	28.3	60.2	2.75	0.24	1.27	1.65	4.55	7.48	5.22	6.28
192	10.4	48.1	37	33.4	3	0.23	1.29	0.98	4.13	3.93	3.34	2.05
193	10.4	48.1	39.4	176	3.34	0.22	1.06	5.64	4.35	21.8	2.5	12.5
194	9.8	45.3	32.9	25.5	3.24	0.25	1.1	0.75	4.5	2.82	3	2.09
195	10.1	45.4	51.6	29.9	3.04	0.35	1.66	0.99	6.81	3.97	3.32	2.9
196	10.2	45.5	50.8	120	2.82	0.29	1.68	3.03	6.98	14.8	2.96	5.65
197	11	49.3	28.5	58.7	3.31	0.16	1.04	1.73	3.41	7.65	3.57	6.6
198	—	—	29.8	31.4	3.38	0.24	0.85	0.86	2.56	3.34	2.34	3.01
200	11.6	58.2	16.7	22.3	2.29	0.05	0.62	0.86	1.71	3.19	1.83	4.87
201	10.3	56.3	20.4	14.9	2.77	0.09	0.59	0.46	1.87	1.45	1.85	1.98
202	10.2	56.3	62.9	15.3	3.63	0.26	1.4	0.45	3.11	0.79	1.74	0.86
203	10.2	56.3	19.6	14.3	2.16	0.12	0.83	0.39	1.71	1.23	1.52	1.06
207	11.9	54.9	16.6	23.6	0.81	0.07	0.54	0.63	1.67	2.34	1.8	1.57
208	10.4	53	28.3	24.9	2.51	<0.06	0.96	0.67	2.84	2.96	2.71	1.96
209	8.74	51	10.7	16	2.44	0.12	0.42	0.42	0.87	1.34	1.19	1.19
210	7.23	48.5	17.6	14.5	4.58	0.04	0.67	0.4	1.41	1.41	0.96	0.7
211	5.65	46.4	13.2	30.5	1.84	0.18	0.5	0.75	1.4	3.29	0.78	1.12
212	4.76	43.9	15.9	24.4	1.37	0.12	0.48	0.61	1.18	2.67	0.22	0.82
213	3.83	42.8	—	38.6	—	0.25	—	1.04	—	4.68	—	1.6
214	3.27	44.2	40.6	34.5	2.21	0.19	1.11	0.83	4.37	2.92	1.72	0.62
215	3.93	46.1	32.6	63.3	2	0.26	0.87	1.52	2.99	6.64	1.27	2.18
216	5.79	48	27.6	60.2	1.26	0.3	0.88	1.39	2.99	6.37	1.9	2.01
217	6.17	50.1	14.4	22.8	1.66	0.12	0.52	0.53	0.97	2.41	0.28	0.71
219	8.21	52.8	8.84	8.52	2	0.12	0.4	0.27	0.99	0.96	1.23	1.31
221	10.5	55	9.39	6.52	3.35	0.13	0.51	0.23	1.13	0.68	2.05	1.43
222	10.6	55.8	7.55	8.98	2.53	0.28	0.39	0.28	0.72	0.85	1.34	1.42
223	12.5	55	25.3	26	4.05	0.22	1	0.57	2.91	2.35	5.83	3.13
224	12.5	54.1	—	47.2	—	0.73	—	1.33	—	5.75	—	4.67
225	11.4	53.8	21.4	21	3.69	0.22	0.82	0.55	1.55	2.01	1.84	1.08
226	11.8	54.6	24.6	42.3	4.26	0.24	1.17	0.96	1.69	4.05	0.42	1.45

Julian day		Latitude °N	Longitude °W	Sodium nmol m^{-3}		Ammonium nmol m^{-3}		Potassium nmol m^{-3}		Magnesium nmol m^{-3}		Calcium nmol m^{-3}	
				Fine	Coarse	Fine	Coarse	Fine	Coarse	Fine	Coarse	Fine	Coarse
4/18/03-5/20/03													
	108	12	57.6	16.7	37	1.42	0.54	0.41	1	0.41	1.98	0.06	0.36
	109	11.4	55.5	18.1	21.1	0.83	0.36	0.45	0.48	0.75	1.02	0.15	0.15
	110	11.1	53.4	23.2	66.8	2.25	0.48	0.55	1.66	1.55	7.15	0.26	0.94
	111	9.86	52.1	21.1	34.7	2.68	0.64	0.69	0.88	0.87	1.79	0.25	0.27
	112	7.93	52	41.4	69.9	4.78	0.49	1.39	1.74	1.89	5.16	0.73	1.36
	113	6.98	51	34.9	48.2	3.41	0.37	1.85	1.27	3.33	4.8	2.19	1.99
	114	7.68	50.8	37.2	84	6.23	1.65	2.07	2.27	1.97	7.42	1.56	2.55
	115	9.08	52.9	29.8	79.9	4.51	0.82	1.4	1.88	1.27	6.73	0.74	1.7
	116	10.5	55.1	70.1	20.6	1.12	6.2	2.43	2.04	6.17	1.02	3.74	1.5
	117	12.1	56.5	14.3	48.4	2.94	1.03	0.48	1.16	0.56	3.38	0.23	0.9
	121	11	55.4	22.3	79.9	4.85	1.27	0.82	2.33	1.13	7.72	0.69	3.05
	122	9.4	55.4	42.7	99.9	5.73	1.14	1.58	2.62	2.4	9.11	1.12	2.98
	123	7.98	54.9	43.1	62.1	4.23	0.86	2.07	1.7	3.6	4.16	3.73	2.52
	124	8.53	54.9	51.3	105	5.36	1.05	2.34	2.9	2.52	8.51	2.34	5.18
	125	10.8	55.9	44.4	87.6	3.5	1.83	1.75	2.71	2.08	6.96	2.33	6.24
	126	12.1	56.1	37.9	86	4.4	0.94	1.5	2.71	2.88	6.03	1.27	2.82
	127	11.8	56.3	38.9	75	3.3	0.75	1.19	1.85	3.1	3.87	0.83	1.76
	130	11	55.4	41.9	87.6	4.5	0.96	1.19	2.37	3.35	6.61	1.16	1.96
	131	10.7	53.4	45.5	57.2	4.17	BDL	1.77	1.37	4.67	2.62	1.67	1.88
	132	10.6	51.3	45.1	94.4	4.1	BDL	1.63	2.88	3.43	8.44	2.11	3.51
	133	10.5	49.2	192	102	4.49	0.75	3.22	2.89	5.29	9.93	3.03	1.77
	135	8.1	49.4	74.4	102	7.46	1.39	2.51	2.7	6.78	5.66	4.5	3.57
	136	8.12	53	63	79.1	5.93	0.58	2.39	2.04	5.14	6.92	2.86	2.94
	138	9.14	56.7	70.4	101	8.22	1.34	2.68	2.5	5.01	9.79	2.07	3.02
	139	10.3	56.6	31.9	47	5.92	0.73	1.62	1.21	2.82	4.9	1.42	1.99
	140	10.8	55.2	25.5	41.4	4.77	0.58	1.25	1.09	2.19	3.64	1.39	1.83
4/9/01-4/26/01													
	99	21.5	160	71.7	121	0.5	0.1	1.38	3.3	5.09	12.8	2.14	2.82
	100	22.2	162	67.7	255	1.6	0.1	1.62	6.22	6.44	28.3	2.33	6.32
	101	23.3	168	49.9	203	1.59	0.23	1.31	4.92	5.07	21.6	1.83	5.71
	102	24.4	172	16.5	4.07	1.41	<2E-3	0.42	0.11	1.66	0.49	0.72	0.13
	103	26.1	175	15.6	24.1	1.39	0.13	0.47	0.58	1.68	3.08	1.8	2.8
	104	26.8	181	10.4	13	1.67	0.1	0.34	0.37	1.43	1.67	2.09	2.59
	105	27.3	185	505	532	1.56	<4E-3	11.5	12.8	57.3	62.6	11.1	12.7
	106	27.6	190	73.5	12.6	2.15	0.02	2.39	0.25	7.53	1.23	3.41	1.07
	107	27.6	190	39.6	38.9	7.12	0.61	1.07	1.01	3.65	3.94	1.53	1.86
	108	27.4	187	1519	13.3	0.35	<2E-3	35	0.39	171	2.49	33.7	2.8
	109	26.7	182	527	47.4	9.46	<4E-3	12.7	0.84	62.4	3.28	12.8	6.16
	110	26	175	181	140	<0.01	<0.01	4.31	2.02	20.8	7.06	3.82	1.35
	111	25.6	174	37.7	40.8	1.93	<3E-3	0.74	1.04	2.47	4.59	1.49	1.34
	112	24.8	171	331	62	<0.01	<0.01	2.32	0.98	9.38	3.6	9.58	0.96
	114	24.2	166	508	101	<0.01	<0.01	13.2	0.91	61.4	2.8	9.59	10.9
	116	22.5	158	271	22.1	4.74	<0.01	6.33	0.52	30.5	1.37	5.94	2.72
7/1/02-7/16/02													
	182	22.8	158	16.1	16.7	2.01	0.23	0.67	0.56	1.45	1.52	0.4	0.33
	183	22.8	158	13.5	27.1	1.96	0.46	0.51	0.81	0.95	2.56	0.32	0.58
	184	23.5	162	23.5	25.2	2.44	0.69	0.83	0.95	1.53	1.92	0.6	0.56
	185	24	165	19.1	34.8	2.63	0.85	0.54	1.14	1.19	2.72	0.45	0.56
	186	24.5	167	19.2	37.1	2.35	1.74	0.46	1.24	0.9	2.69	0.38	0.5
	187	24.9	170	13	18.4	2.15	1.18	0.46	0.55	0.49	0.99	0.5	0.21
	189	26.1	175	14.7	22.6	1	0.55	0.44	0.6	1.02	1.83	0.19	0.4
	190	26	175	17.4	26.3	1.02	0.45	0.5	0.79	1.39	2.64	0.33	0.36
	191	26	175	18.2	20.6	1.1	0.52	0.49	0.6	1.42	1.85	0.38	0.28
	192	26	175	23.5	28.7	2.3	0.5	0.64	0.79	2.22	3.05	0.52	0.46
	193	26	175	29	31.9	1.65	0.44	0.83	0.88	3.38	3.81	0.6	0.8
	194	24.7	170	12.1	11.2	1.27	0.31	0.41	0.27	1.03	0.73	0.55	0.2
	195	23.6	167	13.4	18.9	1.33	0.31	0.35	0.52	1.26	2.05	0.38	0.38
	196	22.9	164	64	36.4	1.24	0.36	1.52	0.8	5.58	3.39	3.27	0.3
	197	22.8	160	62.2	31.8	1.9	0.42	1.48	0.81	5.66	3.57	1.24	0.59
9/23/02-10/15/02													
	266	22.5	157	4.43	4.1	1.19	0.11	0.07	0.13	0.35	0.27	0.27	0.08
	267	23.5	157	4.32	7.23	1.47	0.23	0.17	0.26	0.33	0.61	0.2	0.14
	268	23.5	157	9.43	7.49	3.12	0.2	0.4	0.27	0.75	0.6	0.59	0.22
	269	24.2	156	5.81	16.1	1.08	0.21	0.23	0.55	0.42	1.76	0.18	0.28
	270	24.2	155	8.79	18.7	1.95	0.24	0.35	0.53	0.63	1.75	0.22	0.28
	271	23.7	156	11.4	16.9	1.55	0.21	0.4	0.54	0.99	1.99	0.4	0.34
	273	23.3	157	30.7	40.3	3.24	0.55	0.93	1.11	1.87	3.65	0.66	0.63
	274	23.3	159	11.6	5.43	0.3	0.32	0.36	0.07	1.09	0.18	0.31	0.07
	275	23.8	159	12.8	10.9	0.49	0.12	0.36	0.27	0.86	0.89	0.34	0.18
	276	22.5	159	10.4	19.9	2.5	0.36	0.34	0.58	0.9	1.65	0.22	0.39
	278	19.7	156	10.6	18.3	3.05	0.28	0.33	0.6	0.66	1.93	0.34	0.41
	279	19.4	156	13	16.4	3.69	0.42	0.5	0.49	1.59	1.69	0.5	0.29
	280	19.8	155	18.7	24.8	1.73	0.25	0.67	0.62	1.57	2.52	0.39	0.4
	281	20.3	156	5.41	8.98	0.65	0.15	0.19	0.21	0.28	0.59	0.13	0.13
	282	20.1	156	8.96	11.8	0.94	0.12	0.3	0.33	0.6	0.97	0.23	0.24
	283	20.9	156	8.73	8.56	0.83	0.17	0.29	0.23	0.72	0.61	0.24	0.14
	285	23.2	158	8.85	9.52	0.73	0.2	0.21	0.27	0.33	0.64	0.14	0.22
	286	21.6	158	10.1	16.7	2.6	0.18	0.38	0.46	0.67	1.68	0.21	0.36
	287	20.2	157	9.84	13.9	1.53	0.27	0.31	0.42	0.73	1.26	0.28	0.28
	288	19.8	156	5.17	11	0.7	0.16	0.17	0.3	0.26	0.69	0.12	0.16

Julian day	Latitude °N	Longitude °W	Sodium nmol m^{-3}		Ammonium nmol m^{-3}		Potassium nmol m^{-3}		Magnesium nmol m^{-3}		Calcium nmol m^{-3}	
			Fine	Coarse	Fine	Coarse	Fine	Coarse	Fine	Coarse	Fine	Coarse
8/6/03-8/20/03												
218	19.7	157	72.4	49.4	3.98	0.46	1.65	1.47	6.28	5.13	1.17	1.01
219	18.5	157	27.2	41	1.16	0.37	0.67	0.97	1.75	3.33	0.37	0.49
220	18.7	156	300	—	0.64	—	7.5	—	28.8	—	6.16	—
221	19.2	156	54	50.4	3.38	0.63	1.21	1.19	2.65	3.14	0.23	0.49
222	19.5	157	45.8	40.3	3.73	0.4	0.71	1	2.38	3.41	0.45	0.48
223	19.5	158	33.7	51.9	3.13	0.65	1.15	1.16	3.7	4.71	0.71	1.14
224	19.5	159	45.4	35.6	2.5	0.42	0.85	0.8	2.19	2.13	0.77	0.64
225	20	160	25.4	69.9	1.78	1.05	0.56	1.57	0.74	5.63	0.55	1.12
226	20.8	160	46.8	32.4	3.7	0.55	0.99	0.76	3.04	2.33	0.83	0.51
227	21	159	29.4	52.2	4.43	0.84	0.64	1.15	1.54	4.28	0.38	0.93
228	20.6	158	258	173	5.5	0.95	6.62	3.77	26	19.8	2.82	12.5
229	20.3	158	52	81.3	4.42	0.96	1.05	1.9	2.52	7.12	0.76	1.31
230	19.7	161	59.1	73.9	7.49	1.13	0.98	2.05	2.88	8.56	1.99	2.59
231	19.1	162	41.7	86	6.07	1.06	0.99	2.1	3.15	9.9	0.83	2.11
232	19.8	162	24.2	32.8	2.87	0.71	0.65	1.05	1.43	3.4	0.19	0.81
233	—	—	24.1	29.7	6.28	0.39	0.68	0.76	2.03	2.34	0.25	0.36

Appendices II

Principal component analysis for aerosol data collected from three cruises (6 January to 19 February 2001, 26 June to 14 August 2001, and 18 April to 20 May 2003) over the North Atlantic Ocean and four cruises (9 April to 26 April 2001, 1 July to 16 July 2002, 23 September to 15 October 2002, and 6 August to 20 August 2003) over the North Pacific Ocean.

Note: 19 aerosol chemical species used for principal component analysis and their symbols in Rotated Compoenet Matrix are: labile Fe(II) (FE2), labile Fe((II)+(III)) (FE23), total labile Fe (TLFE), Fe (FE), AL (Al), CA (Ca), K, NA (Na), MG (Mg), CR (Cr), CO (Co), CU (Cu), PB (Pb), MN (Mn), NI (Ni), V, ZN (Zn), Oxalate (OXA), Non-seasalt-sulfate (NSSS). Only the components with the eigenvalues greater than 1 are listed in rotated component matrix.

1. Fine aerosol data from 01/06/01-02/19/01 Atlantic cruise

Rotated Component Matrix [a]

	Component			
	1	2	3	4
FE2	.439	.846	.104	-3.96E-02
FE23	.602	.731	5.634E-02	.124
TLFE	.555	.791	5.667E-02	9.315E-02
FE	.878	.403	9.470E-02	.186
AL	.871	.413	9.597E-02	.203
CA	.757	.392	9.233E-02	.414
K	.802	.386	.160	.383
NA	.173	-6.06E-02	-2.77E-02	.810
MG	.727	.424	7.950E-02	.457
CR	.863	.379	.150	.226
CO	.675	3.283E-02	.172	-.125
CU	9.639E-02	.204	.147	.861
PB	.695	.367	.326	.192
MN	.895	.366	.139	.145
NI	.285	-.160	.767	.409
V	.803	7.185E-02	.484	-2.56E-02
ZN	.173	-5.64E-02	.825	-.284
OXA	.280	.532	.612	.236
NSSS	4.912E-02	.389	.836	.160

Extraction Method: Principal Component Analysis.
Rotation Method: Varimax with Kaiser Normalization.
a. Rotation converged in 9 iterations.

2. Coarse aerosol data from 01/06/01-02/19/01 Atlantic cruise

Rotated Component Matrix [a]

	Component			
	1	2	3	4
FE2	.754	-.213	.130	.473
FE23	.755	-.163	8.677E-02	.524
TLFE	.840	-.104	5.649E-02	.430
FE	.967	7.527E-02	1.761E-02	-9.16E-04
AL	.965	2.881E-02	3.369E-02	-2.91E-03
CA	.893	.267	.118	3.099E-02
K	.896	.367	.123	6.970E-02
NA	-4.73E-02	.869	-1.33E-02	.165
MG	.464	.717	.238	.167
CR	.961	.145	-9.19E-02	-2.77E-02
CO	.292	-.148	5.440E-02	-.600
CU	-6.06E-02	.884	-2.34E-02	-.144
PB	.736	-.137	-3.13E-02	-.112
MN	.970	3.996E-02	5.731E-02	-3.57E-03
NI	-1.96E-02	-7.98E-02	.920	-3.71E-02
V	.931	2.571E-02	.116	-9.36E-02
ZN	9.781E-02	.162	.903	8.357E-02
OXA	.578	-1.04E-02	.104	.452
NSSS	.425	.286	.237	.361

Extraction Method: Principal Component Analysis.
Rotation Method: Varimax with Kaiser Normalization.
a. Rotation converged in 9 iterations.

3. Fine aerosol data from 06/27/01-08/14/01 Atlantic cruise

Rotated Component Matrix [a]

	Component		
	1	2	3
FE2	.850	4.991E-02	-6.00E-02
FE23	.939	.172	.114
TLFE	.948	.167	7.110E-02
FE	.945	.269	6.996E-02
AL	.901	.331	4.145E-02
CA	.840	.446	6.784E-02
K	.697	.659	7.067E-02
NA	4.001E-02	.920	-3.56E-02
MG	.264	.920	5.846E-02
CR	.837	.299	.185
CO	.835	8.315E-02	.185
CU	.721	.510	.154
PB	.520	4.915E-02	.657
MN	.936	.294	8.430E-02
NI	.806	.339	.263
V	.891	.211	.228
ZN	.515	.400	.391
OXA	-.112	9.136E-03	.885
NSSS	.386	.387	.265

Extraction Method: Principal Component Analysis.
Rotation Method: Varimax with Kaiser Normalization.

a. Rotation converged in 3 iterations.

4. Coarse aerosol data from 06/27/01-08/14/01 Atlantic cruise

Rotated Component Matrix [a]

	Component			
	1	2	3	4
FE2	.833	-.219	.139	-.311
FE23	.841	-.172	9.714E-02	-.366
TLFE	.906	-.109	6.326E-02	-.263
FE	.949	.108	4.606E-04	.162
AL	.948	6.208E-02	1.652E-02	.165
CA	.880	.301	9.594E-02	.114
K	.887	.395	.101	7.258E-02
NA	-1.28E-02	.867	-1.17E-02	-.184
MG	.488	.725	.215	-8.90E-02
CR	.936	.174	-.107	.183
CO	.188	-.112	3.487E-02	.679
CU	-9.34E-02	.887	-2.64E-02	9.421E-02
PB	.713	-9.47E-02	-4.87E-02	.255
MN	.953	7.365E-02	4.011E-02	.169
NI	-8.42E-03	-5.87E-02	.915	6.586E-02
V	.901	6.180E-02	9.591E-02	.258
ZN	9.679E-02	.131	.903	-5.63E-02
OXA	.658	1.234E-02	.101	-.318
NSSS	.484	.299	.234	-.266

Extraction Method: Principal Component Analysis.
Rotation Method: Varimax with Kaiser Normalization.

a. Rotation converged in 5 iterations.

5. Fine aerosol data from 04/18/03-05/20/03 Atlantic cruise

Rotated Component Matrix [a]

	Component			
	1	2	3	4
FE2	.708	.217	.517	.264
FE23	.820	9.540E-02	.387	.242
TLFE	.780	.105	.280	.432
FE	.922	.342	7.534E-02	8.520E-02
AL	.983	4.851E-02	7.364E-02	-4.44E-02
CA	.979	3.861E-02	9.861E-02	-4.83E-02
K	.953	.131	.109	-5.13E-03
NA	.672	-3.55E-02	.165	-4.41E-02
MG	.975	2.394E-02	.101	-3.61E-02
CR	9.689E-02	.962	2.521E-02	.220
CO	-5.97E-02	.856	.160	-.338
CU	.463	.807	8.258E-02	.219
PB	.613	-5.36E-02	.528	-.284
MN	.922	.362	5.191E-02	3.247E-02
NI	8.839E-02	.965	2.955E-02	.205
V	-3.50E-02	-.344	.570	-.127
ZN	-3.69E-02	.166	2.474E-02	.881
OXA	.270	.317	.662	.237
NSSS	.308	.371	.785	6.133E-02

Extraction Method: Principal Component Analysis.
Rotation Method: Varimax with Kaiser Normalization.

a. Rotation converged in 5 iterations.

6. Coarse aerosol data from 04/18/03-05/20/03 Atlantic cruise

Rotated Component Matrix [a]

	Component			
	1	2	3	4
FE2	-4.29E-02	.963	2.606E-02	6.672E-02
FE23	.149	.952	6.502E-03	-4.66E-02
TLFE	.192	.921	1.131E-02	-.172
FE	.956	.163	.192	-1.79E-02
AL	.964	.152	9.493E-02	-1.98E-02
CA	.961	9.016E-02	1.537E-02	.143
K	.978	.118	4.329E-03	.151
NA	.578	-.158	-.153	.602
MG	.868	-4.16E-02	-8.75E-02	.403
CR	.229	.146	.932	9.608E-03
CO	.410	.792	.290	-9.17E-02
CU	.848	.119	.338	-6.28E-02
PB	.899	.214	1.200E-02	-.148
MN	.949	.165	.210	6.437E-03
NI	.218	.140	.934	4.306E-03
V	.226	-4.88E-02	-.437	.543
ZN	.164	.235	-.342	-.622
OXA	.116	.921	.108	-.138
NSSS	3.184E-02	.942	9.600E-02	-9.41E-02

Extraction Method: Principal Component Analysis.
Rotation Method: Varimax with Kaiser Normalization.

a. Rotation converged in 9 iterations.

7. Fine aerosol data from 04/09/01-04/26/01 Pacific cruise

Rotated Component Matrix [a]

	Component		
	1	2	3
FE2	.947	.146	.250
FE23	.955	.121	.185
TLFE	.961	.106	.137
FE	.963	.216	-7.22E-02
AL	.960	.174	-8.86E-02
CA	.252	.953	-6.72E-03
K	.240	.958	-6.13E-02
NA	.369	.878	-.127
MG	8.100E-02	.987	-4.91E-02
CR	.965	.174	-8.64E-02
CO	.929	.144	-1.60E-02
CU	.130	.949	-9.43E-02
PB	.634	.340	.607
MN	.965	.230	-3.14E-02
NI	.922	.270	-7.49E-02
V	.938	.245	8.753E-02
ZN	.643	.277	.633
OXA	-9.60E-02	-.173	.948
NSSS	-6.44E-02	-.466	.795

Extraction Method: Principal Component Analysis.
Rotation Method: Varimax with Kaiser Normalization.

a. Rotation converged in 4 iterations.

8. Coarse aerosol data from 04/09/01-04/26/01 Pacific cruise

Rotated Component Matrix [a]

	Component			
	1	2	3	4
FE2	.912	-.170	.107	.232
FE23	.912	-.217	1.944E-02	.242
TLFE	.887	-.236	2.096E-02	.223
FE	.984	2.295E-02	9.327E-03	2.398E-02
AL	.988	-5.78E-03	-1.56E-02	-2.28E-03
CA	.145	.962	-4.69E-02	6.047E-03
K	-3.21E-02	.694	.693	5.283E-04
NA	-.114	.674	.550	-2.92E-02
MG	-.114	.188	.956	4.049E-02
CR	.972	3.325E-02	-.101	8.318E-02
CO	.908	-.154	.209	5.792E-02
CU	-.200	.786	.135	-3.48E-02
PB	.826	-.117	-.122	5.047E-03
MN	.989	-1.74E-02	1.371E-02	1.022E-02
NI	.902	7.569E-02	.162	5.382E-04
V	.977	9.925E-03	-6.79E-02	2.104E-02
ZN	.167	-1.78E-02	-2.43E-03	.970
OXA	.894	.253	.244	-8.22E-02
NSSS	.445	-1.69E-02	.840	-4.26E-02

Extraction Method: Principal Component Analysis.
Rotation Method: Varimax with Kaiser Normalization.

a. Rotation converged in 5 iterations.

9. Fine aerosol data from 07/01/02-07/16/02 Pacific cruise

Rotated Component Matrix[a]

	Component						
	1	2	3	4	5	6	7
FE2	-7.97E-02	.908	-8.94E-02	-5.54E-02	-3.04E-02	.368	2.434E-04
FE23	-1.75E-02	.952	-.233	-5.36E-02	8.536E-02	6.835E-02	-8.83E-02
TLFE	9.927E-02	.940	-.148	-7.46E-02	-7.10E-03	-3.57E-03	-.119
FE	.978	9.121E-02	-6.68E-02	-.103	-6.63E-02	-2.06E-02	-1.08E-02
AL	-6.54E-02	-.236	.111	-6.37E-02	5.818E-03	-.126	.922
CA	-1.54E-02	-.183	.862	7.988E-02	7.240E-03	7.800E-02	1.697E-02
K	-.118	-.170	.924	-6.14E-03	-2.44E-02	-.173	.176
NA	-.129	.372	3.884E-02	.105	3.320E-02	.788	-4.81E-02
MG	-.124	-.147	.963	3.179E-02	5.493E-02	-7.99E-02	-3.13E-02
CR	.985	2.187E-02	-6.10E-02	-5.39E-02	-6.58E-02	1.416E-02	-4.97E-02
CO	.536	.726	-.233	-.192	-.131	-.100	-.162
CU	-4.60E-02	-.203	-.157	.898	-4.57E-02	-.145	-.187
PB	-2.97E-02	-.235	4.396E-02	.226	.814	-.165	.314
MN	.985	-3.02E-02	-9.50E-02	-4.24E-02	-9.59E-03	-2.45E-02	2.971E-02
NI	.986	3.917E-02	-5.21E-02	-4.13E-02	-6.28E-02	5.164E-03	-4.08E-02
V	-.230	-3.49E-02	.360	.827	9.262E-02	.147	.189
ZN	-.164	.114	.448	.236	.112	-.656	.160
OXA	-.196	.352	-4.20E-02	-.115	.850	.151	-.233
NSSS	-4.03E-02	-.233	.519	-.280	.541	-8.48E-02	-.411

Extraction Method: Principal Component Analysis.
Rotation Method: Varimax with Kaiser Normalization.

a. Rotation converged in 7 iterations.

10. Coarse aerosol data from 07/01/02-07/16/02 Pacific cruise

Rotated Component Matrix [a]

	Component			
	1	2	3	4
FE2	.960	4.582E-02	-9.23E-03	-.177
FE23	.841	.224	.212	-.361
TLFE	.741	.263	.204	-.410
FE	-6.99E-02	.976	-.133	-9.80E-02
AL	-5.90E-02	6.531E-02	.772	-.438
CA	.210	-.222	.843	.301
K	.156	-.236	.896	5.505E-02
NA	-.231	-6.72E-02	.157	.617
MG	.128	-.278	.862	.285
CR	-9.33E-02	.974	-.168	-6.93E-02
CO	.131	.969	-.150	-9.29E-02
CU	.344	.697	5.391E-02	.222
PB	.923	-.101	4.799E-02	-8.52E-02
MN	-9.37E-02	.976	-.141	-9.96E-02
NI	-8.89E-02	.982	-.155	-2.96E-02
V	.904	-.115	-.163	3.503E-02
ZN	.784	-4.48E-02	.118	.153
OXA	.749	-8.24E-02	.224	9.151E-02
NSSS	.520	6.614E-02	.154	.453

Extraction Method: Principal Component Analysis.
Rotation Method: Varimax with Kaiser Normalization.

a. Rotation converged in 5 iterations.

11. Fine aerosol data from 09/23/02-10/15/02 Pacific cruise

Rotated Component Matrix [a]

	Component			
	1	2	3	4
FE2	-5.00E-03	.972	.143	.131
FE23	-7.14E-02	.988	7.583E-02	5.451E-02
TLFE	1.106E-03	.976	.122	8.777E-02
FE	.849	-7.37E-02	-.448	-6.18E-02
AL	-3.87E-02	8.845E-03	.832	7.307E-02
CA	.855	-2.46E-02	.253	-2.88E-02
K	.894	.207	.337	-9.89E-02
NA	.913	4.176E-03	.222	-4.70E-02
MG	.939	1.095E-02	.219	-8.83E-02
CR	.875	-6.18E-02	-.421	-.107
CO	.805	-4.45E-02	-.502	3.690E-02
CU	.266	.907	1.391E-02	3.744E-02
PB	3.481E-02	.655	.510	.463
MN	.891	-8.96E-02	-.353	-.113
NI	.875	-6.46E-02	-.419	-5.94E-02
V	-6.00E-02	1.198E-03	.128	.930
ZN	-.204	.285	1.540E-02	.836
OXA	-2.36E-02	.402	.579	9.877E-02
NSSS	-.271	.903	-3.28E-02	1.531E-02

Extraction Method: Principal Component Analysis.
Rotation Method: Varimax with Kaiser Normalization.

a. Rotation converged in 5 iterations.

12. Coarse aerosol data from 09/23/02-10/15/02 Pacific cruise

Rotated Component Matrix [a]

	Component				
	1	2	3	4	5
FE2	-3.26E-02	-.109	.894	-5.61E-02	4.142E-03
FE23	5.816E-02	-.117	.902	.241	-.101
TLFE	.265	-9.71E-02	.885	5.628E-02	.111
FE	.989	-6.36E-02	4.013E-02	.112	5.816E-03
AL	-1.77E-02	.482	.313	.651	.165
CA	7.207E-02	.870	-9.13E-02	.363	-2.16E-02
K	-5.36E-02	.978	-8.83E-02	.102	2.661E-02
NA	-.143	.956	-3.69E-02	-8.76E-02	4.275E-02
MG	-.132	.946	4.075E-02	-6.45E-02	7.677E-03
CR	.992	-8.27E-02	-3.84E-02	-5.80E-02	-1.48E-02
CO	.980	-5.22E-02	-4.85E-02	-5.02E-02	-6.22E-02
CU	.979	-8.22E-02	9.226E-02	-7.43E-02	4.895E-02
PB	-.127	5.706E-02	.120	-.157	-.713
MN	.973	-1.79E-02	9.953E-02	.147	5.668E-02
NI	.991	-8.64E-02	-4.05E-02	-5.49E-02	-1.70E-02
V	-.128	.292	3.317E-02	.708	.188
ZN	.171	-.405	.185	.758	-.151
OXA	-.116	.111	.126	-4.70E-02	.838
NSSS	-.281	.373	.724	.177	-2.38E-02

Extraction Method: Principal Component Analysis.
Rotation Method: Varimax with Kaiser Normalization.

a. Rotation converged in 5 iterations.

13. Fine aerosol data from 08/06/03-08/20/03 Pacific cruise

Rotated Component Matrix [a]

	Component				
	1	2	3	4	5
FE2	-1.68E-02	-.142	.796	.450	-4.68E-02
FE23	-.199	-6.59E-02	.904	.286	-3.30E-04
TLFE	-.223	-4.58E-02	.913	-.115	-8.11E-02
FE	2.245E-02	.992	-4.87E-02	-6.27E-03	6.230E-02
AL	.842	-5.88E-04	-.124	.329	-.175
CA	.889	-.106	-.265	-.171	-.117
K	.982	-.108	-.141	3.495E-02	-3.95E-02
NA	.935	-5.68E-02	7.502E-02	.140	6.374E-02
MG	.978	-8.57E-02	-.136	-9.36E-03	-5.56E-02
CR	-8.99E-02	.982	-5.67E-02	-6.33E-02	.103
CO	-2.01E-02	.940	-9.70E-02	.151	-.225
CU	.947	.216	-.174	2.039E-02	7.258E-02
PB	.153	-2.57E-02	.236	.918	5.560E-02
MN	4.182E-02	.843	-3.90E-02	-.173	.490
NI	-7.70E-02	.984	-4.97E-02	-5.19E-02	9.045E-02
V	-.307	.232	4.427E-02	-8.14E-02	.834
ZN	.314	-1.48E-02	-.348	.406	.608
OXA	-.289	-.430	.444	.575	8.319E-02
NSSS	.470	.252	.164	.524	-.327

Extraction Method: Principal Component Analysis.
Rotation Method: Varimax with Kaiser Normalization.

a. Rotation converged in 8 iterations.

14. Coarse aerosol data from 08/06/03-08/20/03 Pacific cruise

Rotated Component Matrix [a]

	Component				
	1	2	3	4	5
FE2	-1.45E-02	-.257	.749	7.534E-02	-.437
FE23	-5.53E-03	-7.93E-02	.870	.158	.259
TLFE	.108	-.138	.865	.177	.303
FE	5.509E-02	.961	7.327E-03	5.983E-02	-9.68E-03
AL	.567	-.220	.587	5.496E-02	.157
CA	.987	4.134E-02	5.866E-02	7.449E-02	1.834E-02
K	.940	.160	.187	5.684E-02	2.277E-02
NA	.955	-7.56E-02	-7.20E-02	7.776E-02	2.319E-02
MG	.926	.144	.198	2.139E-02	-8.28E-02
CR	-2.91E-02	.973	-.141	-4.00E-02	-8.13E-03
CO	4.032E-02	.920	-1.56E-02	-1.77E-02	-.128
CU	.255	.334	8.880E-02	.825	-.106
PB	-.140	-.154	.225	.459	.361
MN	3.732E-02	.901	-.219	7.967E-02	.109
NI	-2.48E-02	.978	-.130	-3.94E-02	-1.77E-02
V	4.984E-02	-8.39E-03	.138	-9.77E-03	.921
ZN	8.231E-02	-.109	.211	.912	-5.05E-04
OXA	.483	4.933E-02	.618	.258	-.272
NSSS	.963	-9.48E-02	-4.47E-02	1.962E-02	6.982E-03

Extraction Method: Principal Component Analysis.
Rotation Method: Varimax with Kaiser Normalization.

a. Rotation converged in 5 iterations.

Glossary

ACE-2 — Aerosol Characterization Experiment

AGL — above ground level

AMBTs — air mass back trajectories

AMT — Atlantic Meridional Transect

AOT — aerosol optical thickness

BDL — below detection limit

CCSV — catalytic cathodic stripping voltammetry

DFe — dissolved Fe in ambient seawater

DIN — dissolved inorganic nitrogen

DIP — dissolved inorganic phosphorus

DMS — dimethylsulphide

DP — dissolved phosphorus in ambient seawater

FeAC — Fe adsorbed to the incubation container

FeAT — Fe adsorbed to the surface of the incubation *Trichodesmium*

FeDS — Fe dissolved in the incubation seawater

FeIA — Fe in aerosols added to the incubation solution

FeIT — intracellular Fe in the incubation *Trichodesmium*

FePS — particulate Fe suspended in the incubation seawater

FeRF — Fe remaining on the Teflon filter sub-sample after the incubation

FeTS — total Fe in the incubation seawater

FeTT — total Fe associated with the incubation *Trichodesmium*

HA — hydroxylamine hydrochloride

HNLC — high nitrate low chlorophyll

HVDVI — high volume dichotomous virtual impactor

HY-SPLIT — Hybrid Single-Particle Langrangian Intergrated Trajectories

IC — ion chromatography

ICPMS — inductive coupled plasma mass spectrometer

ITCZ — intertropical convergence zone

LCW — liquid core waveguide

LFe — labile aerosol Fe

LFe(II) — labile Fe(II)

LFe(III) — labile Fe(III)

LFeIA — total labile Fe on filter subsamples added to the incubation solution

LMCT — ligand-to-metal charge transfer

LPAS — long path length absorbance spectroscopy

MAGIC — magnesium induced coprecipitation

MBL — marine boundary layer

Med-Africa — Mediterranean coastal region of North Africa

MLO — Mauna Loa Observatory

MMD — mass median diameters

MSA — methanesulfonic acid

NOAA — National Oceanic and Atmospheric Administration

NSS SO_4^{2-} — non-seasalt-sulfate

PIA — phosphorus in aerosols added to the incubation solution

PIT — intracellular phosphorus in the incubation *Trichodesmium*

PTT — total phosphorus associated with the incubation *Trichodesmium*

RPD — relative percent difference

RPFe — reducible particulate Fe

SRM — standard reference material

SUM26 — 26°N to 30°N Atlantic region in summer

SUM15 — 6°N to 26°N Atlantic region in summer

SUM5 — 0° to 6°N Atlantic region in summer

WIN26 — 26°N to 30°N Atlantic region in winter

WIN15 — 5°N to 26°N Atlantic region in winter

WTNA — western tropical North Atlantic

Bibliography

Achterberg, E. P., Holland, T. W., Bowie, A. R., Fauzi, R., Mantoura, C., and Worsfold, P. J., 2001. Determination of iron in seawater. *Anal. Chim. Acta* 442, 1-14.

Allen, A. G., Dick, A. L., and Davison, B. M., 1997. Sources of atmospheric methanesulphonate, non-sea-salt sulphate, nitrate and related species over the temperate south Pacific. *Atmospheric Environment* 31, 191-205.

Allen, A. G., Oppenheimer, C., Ferm, M., Baxter, P. J., Horrocks, L. A., Galle, B., McGonigle, A. J. S., and Duffell, H. J., 2002. Primary sulfate aerosol and associated emissions from Masaya volcano, Nicaragua. *Journal of Geophysical Research* 107, No. D23, 4682, doi: 10.1029/2002JD002120.

Al-Momani, I. F., Aygun, S., and Tuncel, G., 1998. Wet deposition of major ions and trace elements in the eastern Mediterranean basin. *Journal of Geophysical Research* 103, 8287-8293.

Anderson, M. A., and Morel, F. M. M., 1982. The influence of aqueous Fe chemistry on the uptake of Fe by the costal diatom *Thalassiosira weissflogii*. *Limnology & Oceanography* 27, 789-813.

Archer, D., and Johnson, K., 2000. A model of the iron cycle in the ocean. *Gobal Biogeochemical Cycles* 14, 269-279.

Arimoto, R., Ray, B. J., Lewis, N. F., Tomza, U., and Duce, R. A., 1997. Mass-particle size distributions of atmospheric dust and the dry deposition of dust to the remote ocean. *Journal of Geophysical Research* 102, 15,867-15,874.

Baker, A. R., Kelly, S. D., Biswas, K. F., Witt, M., and Jickells, T. D., 2003. Atmospheric deposition of nutrients to the Atlantic Ocean. *Geophysical Research Letters* 30, 2296, doi: 10.1029/2003GL018518.

Ball, W. P., Dickerson, R. R., Doddridge, B. G., Stehr, J. W., Miller, T. L., Savoie, D. L., and Carsey, T. P., 2003. Bulk and size-segregated aerosol composition observed during INDOEX 1999: Overview of meteorology and continental impacts. *Journal of Geophysical Research* 108, Art. No. 8001.

Barbeau, K., Rue, E. L., Bruland, K. W., and Butler, A., 2001. Photochemical cycling of iron in the surface ocean mediated by microbial iron(III)-binding ligands. *Nature* 413, 409– 413.

Behrenfeld, M.J., Bale, A. J., Kolber, Z. S., Aiken, J., and Falkowski, P. G., 1996. Confirmation of iron limitation of phytoplankton photosynthesis in the equatorial Pacific Ocean. *Nature* 383, 508-510.

Benkovitz, C. M., Schwartz, S. E., Kim, B. G., 2003. Evaluation of a chemical transport model for sulfate using ACE-2 observations and attribution of sulfate mixing ratios to source regions and formation processes. *Geophysical Research Letters* 30, 1641.

Bergametti, G., Remoudaki, E., Losno, R., Steiner, E., Chatenet, B., and Buat-Menard, P., 1992. Source, transport and deposition of atmospheric phosphorus over the northwestern Mediterranean. *Journal of Atmospheric Chemistry* 14, 501-513.

Berman-Frank, I., Cullen, J. T., Shaked, Y., Sherrell, R. M., and Falkowski, P. G., 2001. Fe availability, cellular Fe quotas, and nitrogen fixation in *Trichodesmium*. *Limnology & Oceanography* 46, 1249-1260.

Bodhaine, B. A., Mendonca, B. G., Harris, J. M., and Miller, J. M., 1981. Seasonal variations in aerosols and atmospheric transmission at Mauna Loa Observatroy. *Journal of Geophysical Research 86,* 7395-7398.

Bodhaine, B. A., 1995. Aerosol absorption measurements at Barrow, Mauna Loa, and the South Pole. *Journal of Geophysical Research 100,* 8967-8976.

Bopp, L., Kohfeld, K. E., and Que're' C. L., 2003. Dust impact on marine biota and atmospheric CO during glacial periods. *Paleoceanography* 18, No. 2, 1046.

Boyd, P. W., Watson, A. J., Law, C. S., Abraham, E. R., Trull, T., Murdoch, R., Bakker, D. C. E., Bowie, A. R., Buesseler, K. O., Chang, H., Charette, M., Croot, P., Downing, K., Frew, R., Gall, M., Hadfield, M., Hall, J., Harvey, M., Jameson, G., LaRoche, J., Liddicoat, M., Ling, R., Maldonado, M. T., McKay, R. M., Nodder, S., Pickmere, S., Pridmore, R., Rintoul, S., Safi, K., Sutton, P., Strzepek, R., Tanneberger, K., Turner, S., Waite, A., and Zeldis, J., 2000. A mesoscale phytoplankton bloom in the polar Southern Ocean stimulated by iron fertilization. *Nature* 407, 695-702.

Boye, M., van der Berg, C. M. G., de Jong, J. T. M., Leach, H., Croot, P., and de Baar, H. J. W., 2001. Organic complexation of iron in the Southern Ocean. *Deep Sea Research, Part I* 48, 1477– 1497.

Boyle, E., 1997. What controls dissolved iron concentrations in the world ocean?—A comment. *Marine Chemistry* 57, 163-167.

Boyle, E. A., Bergquist, B. A., Kayser, R. A., and Mahowald, N., 2004. Iron, manganese, and lead at Hawaii Ocean Time-series station ALOHA: Temporal

variability and and intermediate water hydrothermal plume. *Geochimica Cosmochimica Acta*, in press.

Braaten, D. A., and Cahill, T. A., 1986. Size and composition of Asian dust transported to Hawaii. *Atmospheric Environment* 20, 1105-1109.

Brand, L. E., 1991. Minimum iron requirements of marine phytoplankton and the implications for the biogeochemical control of new production. *Limnology & Oceanography* 36, 1756-1771.

Bruland, K.W., Coale, K. H., and Mart, L., 1985. Analysis of seawater for dissolved cadmium, copper, and lead: an intercomparison of voltametric and atomic adsorption methods. *Marine Chemistry* 17, 285– 300.

Bruland, K. W., Orians, K. J., and Cowen, J. P., 1994. Reactive trace metals in the stratified central North Pacific. *Geochimica Cosmochimica Acta* 58, 3171-3182.

Cahill, T. A., and Perry, K. D., 1996. Asian transport of aerosols to Mauna Loa Observatory, Spring 1994. In: D. J. Hofmann, J. T. Peterson, and R. M. Rosson (editors) *Climate Monitoring and Diagnostics Laboratory, No. 23: Summary Report 1994-1995.* pp. 114-116, U.S. Dept. of Commerce, Boulder, Colo.

Campbell, P. G. C., 1995. Interactions between trace metals and organisms: critique of the free-ion activity model, In: Tessier, A., Turner, D. R. (Eds.), *Metal Speciation and Bioavailability in Aquatic Systems*, Wiley, Chichester, pp. 45-102.

Capone, D.G., Zehr, J.P., Paerl, H.W., Bergman, B., and Carpenter, E.J., 1997. *Trichodesmium*: A globally significant marine cyanobacterium. *Science* 276, 1221-1229.

Capone, D. G., Subramaniam, A., Montoya, J. P., Voss, M., Humborg, C., Johansen, A. M., Siefert, R. L., and Carpenter, E. J., 1998. An extensive bloom of the N_2-fixing cyanobacterium *Trichodesmium erythraeum* in the central Arabian Sea. *Marine Ecological Progress Series* 172, 281-292.

Carpenter, E. J., and Romans, K., 1991. Major role of the cyanobacterium *Trichodesmium* in nutrient cycling in the North Atlantic Ocean. *Science* 254, 1356-1358.

Carpenter, E. J., Subramaniam, A., Capone, D. G., 2004. Biomass and primary productivity of the cyanobacterium *Trichodesmium* spp. in the tropical N Atlantic Ocean. *Deep-Sea Research I* 51, 173–203.

Carrico, C. M., Kus, P., Rood, M. J., Quinn, P. K., and Bates, T. S., 2003. Mixtures of pollution, dust, sea salt, and volcanic aerosol during ACE-Asia: Radiative properties

as a function of relative humidity. *Journal of Geophysical Research* 108, No. D23, 8650, doi: 10.1029/2003JD003405.

Carter, P., 1971. Spectrophotometric determination of serum iron at the submicrogram level with a new reagent (ferrozine). *Analytical Biochemistry* 40, 450-458.

Chen, M., Dei, R. C. H., Wang, W., and Guo, L., 2003. Marine diatom uptake of Fe bound with natural colloids of different origins. *Marine Chemistry* 81, 177-189.

Chen, Y., and Siefert, R. L., 2003. Determination of various types of labile atmospheric iron over remote oceans. *Journal of Geophysical Research* 108, 4774-4782.

Chen, Y., and Siefert, R. L., 2004a. Seasonal and spatial distributions and dry deposition fluxes of atmospheric total and labile iron over the tropical and sub-tropical North Atlantic Ocean. *Journal of Geophysical Research* 109, D09305, doi: 10.1029/2003JD003958.

Chen, Y., Tovar-Sanchez, A., Siefert, R. L., and Sañudo-Wilhelmy, S. A., 2004. *Trichodesmium* uptake of iron from aerosol and its influence on aerosol iron dissolution in the tropical North Atlantic Ocean. *Global Biogeochemical Cycle*, submitted, 2004GB002304.

Chen, Y., and Siefert, R. L., 2004b. Seasonal variation of atmospheric nutrient concentrations and sources over the western tropical North Atlantic. *Journal of Geophysical Research*, submitted, 2004JD005149.

Chester, R., Nimmo, M., Alarcon, M., Saydam, C., Murphy, K. J. T., Sanders, G. S., and Corcoran, P., 1993a. Defining the chemical character of aerosols from the atmosphere of the Mediterranean-sea and surrounding regions. *Oceanological Acta* 16, 231-246.

Chester, R., Murphy, K. J. T., Lin, F. J., Berry, A. S., Bradshaw, G. A., and Corcoran, P. A., 1993b. Factors controlling the solubilities of trace metals from non-remote aerosols deposited to the sea surface by the ‘‘dry’’ deposition mode. *Marine Chemistry* 42, 107– 126.

Chiapello, I., Bergametti, G., Gomes, L., Chatenet, B., Bousquet, P., Dulac, F., and Soares, E. S., 1997. Origins of African dust transported over the northeastern tropical Atlantic, *Journal of Geophysical Research* 102, 13,701-13,709.

Chiapello, I., Bergametti, G., Gomes, L., Chatenet, B., Dulac, F., Pimenta, J., and Soares, E. S., 1995. An additional low layer thansport of Shaelian and Saharan dust over the North-eastern Tropical Atlantic. *Geophysical Research Letters* 22, 3191-3194.

Chin, M., Ginoux, P., Lucchesi, R., Huebert, B., Weber, R., Anderson, T., Masonis, S., Blomquist, B., Bandy, A., and Thornton, D., 2003. A global aerosol model forecast for the ACE-Asia field experiment. *Journal of Geophysical Research* 108, No. D23, 8654, doi:10.1029/2003JD003642.

Coale, K. H., Johnson, K. S., Fitzwater, S. E., Gordon, R. M., Tanner, S., Chavez, F. P., Ferioli, L., Sakamoto, C., Rogers, P., Millero, F., Steinberg, P., Nightingale, P., Cooper, D., Cochlan, W. P., Landry, M. R., Constantinou, J., Rollwagen, G., Trasvina, A., And Kudela, R., 1996. A massive phytoplankton bloom induced by an eco-system-scale iron fertilization experiment in the equatorial Pacific Ocean. *Nature* 383, 495–501.

Cooper, D. J., Watson, A. J., and Nightingale, P. D., 1996. Large decrease in ocean-surface CO2 fugacity in response to in situ iron fertilization. *Nature 383*, 511–514.

Croot, P. L., and Johansson, M., 2000. Determination of iron speciation by cathodic stripping voltammetry in seawater using the competing ligand 2-(2-thiazolylazo-)p-cresol (TAC). *Electroanalysis* 12, 565 – 576.

Croot, P. L., and Laan, P., 2002. Continuous shipboard determination of Fe(II) in polar waters using flow injection analysis with chemiluminescence detection. *Anal. Chim. Acta* 466, 261–273.

Darzi, M., and Winchester, J. W., 1982. Aerosol characteristics at Mauna Loa Observatory, Hawaii, after east Asian dust storm episodes. *Journal of Geophysical Research* 87, 1251-1258.

Delany, A. C., Parkin, D. W., Griffin, J. J., Goldberg, E. D., and Reimann, B. E. F., 1967. Airborne dust collected at Barbados. *Geochimica Cosmochimica Acta* 31, 885.

Derrick, M., and Moyers, J., 1981. Precise and sensitive water soluble ion extraction method for aerosol samples collected on polytetrafluoroethylene filters. *Analytical Letters* 14, 1637-1652.

Draxler, R. R., 2002. HYSPLIT-4 user's guide. *NOAA Tech Memo, ERL ARL-230*, pp. 35.

Duce, R. A., Arimoto, R., Ray, B. J., Unni, C. K., and Harder, P. J., 1983. Atmospheric trace metal elements at Enewetak Atoll: 1, concentrations, sources, and temporal variability. *Journal of Geophysical Research* 88, 5321-5342.

Duce, R. A., 1986. The impact of atmospheric nitrogen, phosphorus, and iron species on marine biological productivity. In: P. Buat-Menard (editor), *The Role of Air-Sea Exchange in Geochemical Cycling*. pp. 497-529, D. Reidel, Norwell, Mass.

Duce, R. A., and Tindale, N. W., 1991. Atmospheric transport of iron and its deposition in the ocean. *Limnology & Oceanography* 36, 1715– 1726.

Duce, R. A., Liss, P. S., Merrill, J. T., Atlas, E. L., Buat-Menard, P., Hicks, B. B., Miller, J. M., Prospero, J. M., Arimoto, R., Church, T. M., Ellis, W., Galloway, J. N., Hansen, L., Jickells, T. D., Knap, A. H., Reinhardt, K. H., Schneider, B., Soudine, A., Tokos, J. J., Tsunogai, S., Wollast, R., and Zhou, M., 1991. The atmospheric input of trace species to the world ocean. *Global Biogeochemical Cycles* 5, 193-259.

Duce, R. A., and Tindale, N. W., 1991. Atmospheric transport of iron and its deposition in the ocean. *Limnology & Oceanography* 36, 1715-1726.

Ellis Jr., W. G., and Merrill, J. T., 1995. Trajectories for Saharan dust transported to Barbados using Stoke's Law to describe gravitational settling. *Journal of Applied Meteorology* 34, 1716-1726.

Elrod, V. A., Berelson, W. M., Coale, K. H., and Johnson, K. S., 2004. The flux of iron from continental shelf sediments: A missing source for global budgets. *Geophysical Research Letters* 31, L12307.

Emmenegger, L., Schonenberger, R., Sigg, L., and Sulzberger, B., 2001. Lightinduced redox cycling of iron in circumneutral lakes. *Limnology & Oceanography* 46, 49–61.

Fanning, K. A., 1989. Influence of atmospheric pollution on nutrient limitation in the ocean. *Nature* 339, 460-463.

Falkowski, P.G., 1997. Evolution of the nitrogen cycle and its influence on the biological sequestration of CO_2 in the ocean. *Nature* 387, 272-275.

Falkowski, P. G., Barber, R. T., and Smetacek, V., 1998. Biogeochemical controls and feedbacks on ocean primary production. *Science* 281, 200-206.

Faust, B. C., and Hoigne´, J., 1990. Photolysis of Fe(III)-hydroxy complexes as sources of OH radicals in clouds, fog and rain. *Atmospheric Environment, Part A* 24, 79– 89.

Feng, X. H., Melander, A. P., Klaue, B., 2000. Contribution of municipal waste incineration to trace metal deposition on the vicinity. *Water Air Soil Pollution* 119, 295-316.

Fung, I. Y., Meyn, S. K., Tegen, I., Doney, S. C., John, J. G., and Bishop, J. K. B., 2000. Iron supply and demand in the upper ocean. *Global Biogeochemical Cycles* 14, 281– 295.

Galloway, J. N., Howarth, R. W., Michaels, A. F., Nixon, S. W., Prospero, J. M., Dentener, F. J., 1996. Nitrogen and phosphorus budgets of the North Atlantic Ocean and its watershed. *Biogeochemistry* 35, 3-25.

Gao, Y., Arimoto, R., Zhou, M. Y., Merrill, J. T., and Duce, R. A., 1992. Relationships between the dust concentrations over eastern Asia and the remote North Pacific. *Journal of Geophysical Research* 97, 9867-9872.

Gao, Y., kaufman, Y. J., Tanre, D., Kolber, D., and Falkowski, P. G., 2001. Seasonal distributions of aeolian iron fluxes to the global ocean. *Geophysical Research Letter* 28, 29-32.

Gao, Y., Fan, S., and Sarmiento, J. L., 2003. Aerolian iron input to the ocean through precipitation scavenging: A modeling perspective and its implication for natural iron fertilization of the ocean. *Journal of Geophysical Research* 108, D7, Art. No. 4221.

Gibb, S. W., Mantoura, R. F., and Liss, P. S., 1999. Ocean-atmosphere exchange and atmospheric speciation of ammonia and methylamines in the region of the NW Arabian Sea. *Global Biogeochemical Cycles* 13, 161-178.

Gieskes, J. M., Gamo, T., and Brumsack, H., 1991. *Chemical Methods for Interstitial Water Analysis aboard Joides Resolution*, Ocean Drilling Program, Technical Report No. 15, pp. 46-47, Taxes A & M University, College Station.

Gledhill, M., and van den Berg, C. M. G., 1994. Determination of complexation of iron(III) with natural organic complexing ligands in seawater using cathodic stripping voltammetry. *Marine Chemistry* 47, 41-54.

Gledhill, M., van den Berg, C. M. G., Nolting, R. F., and Timmermans, K. R., 1998. Variability in the speciation of iron in the northern North Sea. *Marine Chemistry* 59, 283– 300.

Granger, J., and Price, N. M., 1999. The importance of siderophores in Fe nutrition of heterotrophic marine bacteria. *Limnology & Oceanography* 44, 541–555.

Gruber, N., and Sarmiento, J. L., 1997. Global patterns of marine nitrogen fixation and denitrification. *Global Biogeochemical Cycles* 11, 235-266.

Guelle, W, Balkanski, Y. J., Schulz, M., Marticorena, B., Bergametti, G., Moulin, C., Arimoto, R., and Perry, K. D., 2000. Modeling the atmospheric distribution of mineral aerosol: Comparison with ground measurements and satellite observations for yearly and synoptic timescales over the North Atlantic. *Journal of Geophysical Research* 105, 1997-2012.

Hamelin, B., Grousset, F. E., Biscaye, P. E., Zindler, A., and Prospero, J. M., 1989. Lead isotopes in trade wind aerosols at Barbados: The influence of European

emissions over the North Atlantic. *Journal of Geophysical Research* 94, 16,243-16,250.

Harris, J. M., and Kahl, J. D., 1990. A descriptive atmospheric transport climatology for the Mauna Loa Observatory, using clustered trajectories. *Journal of Geophysical Research* 95*,* 13651-13667.

Harris, J. M., Tans, P. P., Dlugokencky, E. J., Masarie, K. A., Lang, P. M., Whittlestone, S., and Steele, L. P., 1992. Variations in atmospheric methane at Mauna Loa Observatory related to long-range transport. *Journal of Geophysical Research* 97*,* 6003-6010.

Harrison, R. M., and Peak, J. D., 1996. Atmospheric aerosol major ion composition and cloud condensation nuclei over the northeast Atlantic. *Journal of Geophysical Research* 101, 4425-4434.

Herut, B., Krom, M. D., Pan, G., and Mortimer, R., 1999. Atmospheric input of nitrogen and phosphorus to the Southeast Mediterranean: sources, fluxes, and possible impact. *Limnology & Oceanography* 44, 1683-1692.

Holmes, J. L., and Zoller, W. H., 1996. The elemental signature of transported Asian dust at Mauna Loa Observatory. *Tellus, Series B* 48, 83-92.

Holmes, J., Samberg, T., McInnes, L., Zieman, J., and Zoller, W., 1997. Long-term aerosol and trace acidic gas collection at Mauna Loa Observatory 1979-1991. *Journal of Geophysical Research* 102, 19,007-19,019.

Howard, J.B., and Rees, D.C., 1996. Structural basis of biological nitrogen fixation. *Chem. Rev*. 96, 2965-2982.

Hu, C. W., Chao, M. R., Wu, K. Y., Chien, G. P. C., Lee, W. J., Chang, L. W., and Lee, W. S., 2003. Characterization of multiple airborne particulate metals in the surroundings of a municipal waste incinerator in Taiwan. *Atmospheric Environment* 37, 2845-2852.

Huang, S., Arimoto, R., and Rahn, K. A., 2001. Sources and source variations for aerosol at Mace Head, Ireland. *Atmospheric Environment* 35, 1421-1437.

Hudson, R. J. M., and Morel, F. M. M., 1990. Iron transport in marine-phytoplanktonkinetica of cellular and medium coordination reactions. *Limnology & Oceanography* 35, 1002-1020.

Hudson, R. J. M., and Morel, F. M. M., 1993. Trace-metal transport by marine microorganisms-implications of metal coordination kinetics. *Deep-Sea Research* 40, 129-150.

Huebert, B. J., Howell, S. G., Zhuang, L., Heath, J. A., Litchy, M. R., Wylie, D. J., Kreidler-Moss, J. L., Coppicus, S., and Pfeiffer, J. E., 1998. Filter and impactor measurements of anions and cations during the First Aerosol Characterization Experiment (ACE 1). *Journal of Geophysical Research* 103, 16,493-16,509.

Husar, R. B., Prospero, J. M., and Stowe, L. L., 1997. Characterization of tropospheric aerosols over the oceans with the NOAA advanced very high resolution radiometer optical thickness operational product. *Journal of Geophysical Research* 102, 16,889-16,909.

Hutchins, D. A., Di Tullio, G. R., Bruland, K. W., 1993. Fe and regenerated production: evidence for biological Fe recycling in two marine environments. *Limnology & Oceanography* 38, 1242-1255.

Hutchins, D. A., Witter, A. E., Butler, A., and Luther, G. W., 1999. Competition among marine phytoplankton for different chelated Fe species. *Nature* 400, 858-861.

Jaffe, D., Mahura, A., Kelley, J., Atkins, J., Novelli, P. C., and Merrill, J., 1997. Impact of Asian emissions on the remote North Pacific atmosphere: Interpretation of CO data from Shemya, Guam, Midway, and Mauna Loa. *Journal of Geophysical Research* 102*,* 28,627-28,635.

Jaffe, D., Snow, J., and Cooper, O., 2003. The April 2001 Asian dust events: Transport and substantial impact on surface particulate matter concentrations across the United States. *EOS* 48, 501-516.

Jickells, T. D., Church, T. M., and Deuser, W. G., 1987. A comparison of atmospheric inputs and deep-ocean particle fluxes for the Sargasso Sea. *Global Biogeochemical Cycles* 1, 117–130.

Jickells, T., 1995. Atmospheric inputs of metals and nutrients to the oceans: Their magnitude and effects. *Marine Chemistry* 48, 199-214.

Jickells, T. D., 1999. The inputs of dust derived elements to the Sargasso Sea: A synthesis. *Marine Chemistry* 68, 5– 14.

Jickells, T. D., and Spoke, L. J., 2001. Atmospheric iron inputs to the ocean. In: D. Turner and K. A. Hunter (Editor), *Biogeochemistry of Iron in Seawater*. John Wiley, New York, USA, pp. 85-121.

Jickells, T. D., Kelly, S. D., Baker, A. R., Biswas, K., Dennis, P. F., Spokes, L. J., Witt, M., and Yeatman, S. G., 2003. Isotopic evidence for a marine ammonia source. *Geophysical Research Letters* 30, 1374.

Johansen, A. M., Siefert, R. L., and Hoffmann, M. R., 2000. Chemical composition of aerosols collected over the tropical North Atlantic Ocean. *Journal of Geophysical Research* 105, 15,277– 15,312.

Johansen, A. M., and Hoffmann, M. R., 2003. Chemical characterization of ambient aerosol collected during the northeast monsoon season over the Arabian Sea: Labile-Fe(II) and other trace metals. *Journal of Geophysical Research* 108, No. D14, 4408, doi: 10.1029/2002JD003280.

Johnson, K. J., Gordon, R. M., and HCoale, K., 1997. What controls dissolved iron concentrations in the world ocean? *Marine Chemistry* 57, 181.

Johnson, K. S., Elrod, V. A., Fitzwater, S. E., Plant, J. N., Chavez, F. P., Tanner, S. J., Gordon, R. M., Westphal, D. L., Perry, K. D., Wu, J., and Karl, D. M., 2003. Surface ocean-lower atmosphere interactions in the Northeast Pacific Ocean Gyre: Aerosols, iron, and the ecosystem response. *Global Biogeochemical Cycles* 17, 1063, doi: 10.1029/2002GB002004.

Karl, D. M., and Tien, G., 1992. MAGIC: a sensitive and precise method for measuring dissolved phosphorus in aquatic environments. *Limnology & Oceanography* 37, 105-116.

Karl, D.M., Letelier, R., Hebel, D., Tupas, L., Dore, J., Christian, J., and Winn, C., 1995. Ecosystem changes in the north Pacific subtropical gyre attributed to the 1991-92 El Nino. *Nature* 373, 230-233.

Karl, D. M., Letelier, R., Tupas, L., Dore, J., Christian, J., and Hedel D., 1997. The role of nitrogen fixation in biogeochemical cycling in the subtropical North Pacific Ocean. *Nature* 388, 533-537.

Karl, D. M., 1999. A sea of change: Biogeochemical variability in the North Pacific subtropical gyre. *Ecosystems* 2, 181-214.

Kawamura, K., and Ikushima, K., 1993. Seasonal changes in the distribution of dicarboxylic acids in the urban atmosphere. *Environmental Science & Technology* 27, 2227-2235.

Kaya, G., and Tuncel, G., 1997. Trace element and major ion composition of wet and dry deposition in Ankara, Turkey. *Atmospheric Environment* 31, 3985-3998.

Keene, W. C., and Savoie, D. L., 1998. The pH of deliquesced sea-salt aerosol in polluted marine air. *Geophysical Research Letters* 25, 2181-2184.

Kidd, R., and Sander, F., 1979. Influence of the Amazon River discharge on the marine production system off Barbados, West Indies. *Journal of Marine Research* 37, 669-681.

Kieber, R. J., Williams, K., Willey, J. D., Skrabal, S., and Avery, G. B., 2001. Iron speciation in coastal rainwater: Concentration and deposition to seawater. *Marine Chemistry* 73, 83– 95.

King, D. W., Aldrich, R. A., and Charnecki, S. E., 1993. Photochemical redox cycling of iron in NaCl solutions. *Marine Chemistry* 44, 105–120.

Kuma, K., J. Tanaka, and Matsunaga, K., 2000. Effect of hydroxamate ferrisiderophore complex (ferrichrome) on Fe uptake and growth of a coastal marine diatom, *Chaetoceros sociale*. *Limnology & Oceanography* 45, 1235-1244.

Kustka, A. B., Sañudo-Wilhelmy, S. A., Carpenter, E. J., Capone, D. G., and Raven, J. A., 2003a. A revised estimate of the Fe use efficiency of nitrogen fixation, with special reference to the marine cyanobacterium *Trichodesmium* spp (Cyanophyta). *Journal of Phycology* 39, 12-25.

Kustka, A. B., Sañudo-Wilhelmy, S. A., Carpenter, E. J., Capone, D., Burns, J., and Sunda, W.G., 2003b. Fe requirements for dinitrogen- and ammonium-supported growth in cultures of *Trichodesmium* (IMS 101): Comparison with nitrogen fixation rates and Fe:carbon ratios of field populations. *Limnology & Oceanography* 48, 1869-1884.

Landing, W. M., and Bruland, K. W., 1987. The contrasting biogeochemistry of iron and manganese in the Pacific Ocean. *Geochimica Cosmochimica Acta* 51, 29-43.

Lefevre, N., and Watson, A. J., 1999. Modeling the geochemical cycle of iron in the oceans and its impact on atmospheric CO_2 concentrations. *Global Biogeochemical Cycles* 13, 727-736.

Lenes, J. M., Darrow, B. P., Cattrall, C., Heil, C. A., Callahan, M., Vargo, G. A., and Byrne, R. H., 2001. Iron fertilization and the *Trichodesmium* response on the West Florida shelf. *Limnology & Oceanography* 46, 1261-1277.

Levitus, S., Conkright, M. E., Reid, J. L., Najjar, R. G., and Mantyla, A., 1993. Distribution of nitrate, phosphate and silicate in the world oceans. *Progress Oceanography* 31, 245-273.

Levy, H., II, and Moxim, W. J., 1989. Influence of long-range transport of combustion emissions on the chemical variability of the background atmosphere. *Nature 338,* 326-328.

Liss, P. S., and Galloway, J. N., 1993. Air-Sea exchange of sulphur and nitrogen and their interaction in the marine atmosphere. In: R. Wollast, F. T. Mackenzie, and L. Chou (editors) *Interactions of C, N, P and S Biogeochemical Cycles and Global Change*. Springer Verlag, Berlin.

Llewellyn, T. O., 1993. Phosphate rock. In: *Minerals yearbook*. Bureau of Mines, pp. 813-832.

Mahowald, N., Hansson, K. K. M., Balkanski, Y., Harrison, S. P., Prentice, I. C., Schulz, M., and Rodhe, H., 1999. Dust sources and deposition during the last glacial maximum and current climate: A comparison of model results with paleodata from ice cores and marine sediments. *Journal of Geophysical Research* 104, 15,895-15,916.

Martin, J. H., and Gordon, R. M., 1988. Northeast Pacific iron distributions in relation to phytoplankton productivity. *Deep Sea Research, Part A* 35, 177–196.

Martin, J. H., and Fitzwater, S. E., 1988. Iron deficiency limits phytoplankton growth in the northeast Pacific subarctic. *Nature* 331, 341–343.

Martin, J. H., Gordon, R. M., Fitzwater, S., and Broenkow, W. W., 1989. VERTEX: Phytoplankton/iron studies in the Gulf of Alaska. *Deep Sea Research Part A* 36, 649-671.

Martin, J. H., 1990. Glacial-interglacial CO_2 change: The iron hypothesis. *Paleoceanography* 5, 1-13.

Martin, J. H., Gordon, R. M., and Fitzwater, S. E., 1991. The case for iron. *Limnology & Oceanography* 36, 1793-1802.

Martin, J. H., Fitzwater, S. E., Gordon, R. M., Hunter, C. N., and Tanner, S. J., 1993. Iron, primary production and carbon-nitrogen flux studies during the JGOFS North Atlantic Bloom Experiment. *Deep Sea Research, Part II* 40, 115– 134.

Martin, J. H., Coale, K. H., Johnson, K. S., Fitzwater, S. E., Gordon, R. M., Tanner, S. J., Hunter, C. N., Elrod, V. A., Nowicki, J. L., Coley, T. L., Barber, R. T., Lindley, S., Watson, A. J., Van Scoy, K., Law, C. S., Liddicoat, M. I., Ling, R., Stanton, T., Stockel, J., Collins, C., Anderson, A., Bidigare, R., Ondrusek, M., Latasa, M., Millero, F. J., Lee, K., Yao, W., Zhang, J. Z., Friederich, G., Sakamoto, C., Chavez, F., Buck, K., Kolber, Z., Greene, R., Falkowski, P., Chisholm, S. W., Hoge, F., Swift, R., Yungel, J., Turner, S., Nightingale, P., Hatton, A., Liss, P., and Tindale, N. W., 1994. Testing the iron hypothesis in ecosystems of the equatorial Pacific Ocean. *Nature* 371, 123–129.

Measures, C. I., and Vink, S., 1999. Seasonal variations in the distribution of Fe and Al in the surface waters of the Arabian Sea. *Deep Sea Research, Part II* 46, 1597-1622.

Merrill, J. T., Bleck, R., and Uematsu, M., 1989. Meteorological analysis of long range transport of mineral aerosols over the Pacific. *Journal of Geophysical Research* 94, 8584-8598.

Meskhidze, N., Chameides, W. L., Nenes, A., and Chen, G., 2003. Iron mobilization in mineral dust: Can anthropogenic SO emissions affect ocean productivity? *Geophysical Research Letters* 30, No. 21, 2085.

Michaels, A. F., Siegel, D. A., Johnson, R. J., Knap, A. H., and Galloway, J. N., 1993. Episodic inputs of atmospheric nitrogen to the Sargasso Sea: Contributions to new production and phytoplankton blooms. *Global Biogeochemical Cycles* 7, 339-351.

Michaels, A. F., Olson, D., Sarmiento, J. L., Ammerman, J. W., Fanning, K., Jahnke, R., Knap, A. H., Lipschultz, F., Prospero, J. M., 1996. Inputs, losses and transformations of nitrogen and phosphorus in the Pelagic North Atlantic Ocean. *Biogeochemistry* 35, 181-226.

Migon, C., and Sandroni, V., 1999. Phosphorus in rainwater: partitioning inputs and impact on the surface coastal ocean. *Limnology & Oceanography* 44, 1160-1165.

Migon, C., Sandroni, V., and Bethoux, J. -P., 2001. Atmospheric input of anthropogenic phorphorus to the northwest Mediterranean under oligotrophic conditions. *Marine Chemistry* 52, 413-426.

Miller, J. M., 1981. A five-year climatology of back trajectories from the Mauna Loa Observatory, Hawaii. *Atmospheric Environment* 15, 1553-1558.

Miller, W. L. and Kester, D. R., 1994. Photochemical iron reduction and iron bioavailability in seawater. *Journal of Marine Research* 52, 325-343.

Miller, W. L., King, D. W., Lin, J., and Kester, D. R., 1995. Photochemical redox cycling or iron in coastal seawater. *Marine Chemistry* 50, 63–77.

Millero, F. J., Yao, W. S., Aicher, J., 1995. The speciation of Fe(II) and Fe(III) in natural-waters. *Marine Chemistry* 50, 21-39.

Moulin, C., Lambert, C. E., Dulac, F., and Dayan, U., 1997. Control of atmospheric export of dust from North Africa by the North Atlantic Oscillation. *Nature* 387, 691-694.

Moulin, C., and Chiapello, I., 2004. Evidence of the control of summer atmospheric transport of African dust over the Atlantic by Sahel sources from TOMS satellites (1979-2000). *Geophysical Research Letters* 31, Art. No. L02107.

Muller-Karger, F. E., McCain, C. R., Fisher, T. R., Esaias, W. E., and Varela, R., 1989. Pigment distribution in the Caribbean Sea: Observations from space. *Progressive Oceanography* 23, 23-64.

Norton, R.B., Carroll, M. A., Montzka, D. D., Hbler, G., Huebert, B. J., Lee, G., Warren, W. W., Ridley, B. A., and Walega, G., 1992. Measurements of Nitric Acid and Aerosol Nitrate at the Mauna Loa Observatory During MLOPEX 1988. *Journal of Geophysical Research* 97, 10,415-10,426.

Obata, H., Karatani, H., and Nakayama, E., 1993. Automated determination of iron in seawater by chelating resin concentration and chemiluminescence detection. *Analytical Chemistry* 65, 1524– 1528.

Obata, H., Karatani, H., Matsui, M., and Nakayama, E., 1997. Fundamental studies for chemical speciation of iron in seawater with an improved analytical method. *Marine Chemistry* 56, 97– 106.

O'Sullivan, D. W., Hanson, A. K., and Kester, D. R., 1995. Stopped flow luminal chemiluminescence determination of Fe(II) and reducible iron in seawater at subnanomolar levels. *Marine Chemistry* 49, 65– 77.

Owens, N. J. P., Galloway, J. N., and Duce, R. A., 1992. Episodic atmospheric nitrogen deposition to the oligotrophic oceans. *Nature* 357, 397-399.

Paerl, H.W., Prufert-Bebout, L.E., and Gou, C., 1994. Iron-stimulated N2 fixation and growth in natural and cultured populations of the planktonic marine cyanobacteria *Trichodesmium* spp. *Applied Environmental Microbiology* 60, 1044-1047.

Paerl, H. W., 1997. Coastal eutrophication and harmful algal blooms: Importance of atmospheric deposition and groundwater as "new" nitrogen and other nutrient sources. *Limnology & Oceanography* 42, 1154-1165.

Paerl, H. W., Willey, J. D., Go, M., Peierls, B. L., Pinckney, J. L., and Fogel, M. L., 1999. Rainfall stimulation of primary production in western Atlantic Ocean waters: Roles of different nitrogen sources and co-limiting nutrients. *Marine Ecological Progress Series* 176, 205-214.

Parekh, P., Follows, M. J., and Boyle, E., 2004. Modeling the global ocean iron cycle. *Global Biogeochemical Cycles* 18, GB1002, doi: 10.1029/2003GB002061.

Parrington, J. R., and Zoller, W. H., 1984. Diurnal and longer-term temporal changes in the composition of atmospheric particles at Mauna Loa, Hawaii. *Journal of Geophysical Research* 89, 2522-2534.

Parungo, F. P., Nagamoto, C. T., Rosinski, J., and Haagenson, P. L., 1986. A study of marine aerosols over the Pacific Ocean. *Journal of Atmospheric Chemistry* 4, 199-226.

Pavageau, M. P., Morin, A., Seby, F., Guimon, C., Krupp, E., Peacheyran, C., Poulleau, J., and Donard, O. F. X., 2004. Partitioning of metal species during an

enriched fuel combustion experiment. Speciation in the gaseous and particulate phases. *Environmental Science & Technology* 38, 2252-2263.

Pehkonen, S. O., Siefert, R. L., Erel, Y., and Hoffmann, M. R., 1993. Photoreduction of iron oxyhydroxides in the presence of important atmospheric organic compounds. *Environmental Science & Technology* 27, 256–262.

Perry, K. D., Cahill, T. A., Schnell, R. C., and Harris, J. M., 1999. Long-range transport of anthropogenic aerosols to the National Oceanic and Atmospheric Administration baseline station at Mauna Loa Observatory, Hawaii. *Journal of Geophysical Research* 104, 18,521-18,533.

Petit, J. R., et al., 1999. Climate and atmospheric history of the past 420,000 years from the Vostok ice core, Antarctica. *Nature* 399, 429-436.

Porter, J. N., Horton, K. A., Mouginis-Mark, P. J., Lienert, B., Sharma, S. K., Lau, E., Sutton, A. J., Elias, T., Oppenheimer, C., 2002. Sun photometer and lidar measurements of the plume from the Hawaii Kilauea Volcano Pu'u O'o vent: Aerosol flux and SO_2 lifetime. *Geophysical Research Letters* 29, No. 16, doi: 10.1029/2002GL014744.

Powell, R. T., King, D. W., and Landing, W. M., 1995. Iron distributions in surface waters of the South Atlantic. *Marine Chemistry* 50, 3 –12.

Prospero, J. M., Bonatti, E., Schubert, C., and Carlson, T. N., 1970. Dust in the Caribbean atmosphere traced to an African dust storm. *Earth Planetary Science Letters 9*, 287–293.

Prospero, J. M., and Carlson, T. N., 1972. Vertical and areal distribution of Saharan dust over the western equatorial North Atlantic Ocean. *Journal of Geophysical Research* 77, 5255-5265.

Prospero, J. M., Glaccum, R. A., and Nees, R. T., 1981. Atmospheric transport of soil dust from Africa to South America. *Nature 289*, 570–572.

Prospero, J. M., 1995. The atmospheric transport of particles to the ocean, in: V. Ittekkot (editor) *The Particle Flux in the Ocean*. pp. 19–25, John Wiley, New York.

Prospero, J. M., Barrett, K., Church, T., Dentener, F., Duce, R. A., Galloway, J. N., Levy II, H., Moody, J., and Quinn, P., 1996. Atmospheric deposition of nutrients to the North Atlantic Basin. *Biogeochemistry* 35, 27-73.

Prospero, J. M., 1999. Long-range transport of mineral dust in the global atmosphere: Impact of African dust on the environment of the southeastern United States. *Proc. Natl. Acad. Sci. USA* 96, 3396–3403.

Prospero, J. M., Savoie, D. L., and Arimoto, R., 2003. Long-term record of nss-sulfate and nitrate in aerosols on Midway Island, 1981-2000: Evidence of increased (now decreasing?) anthropogenic emissions from Asia. *Journal of Geophysical Research* 108, No. D1, 4019, doi: 10.1029/2001JD001524.

Quinn, P. K., Charlson, R. J., and Bates, T. S., 1988. Simultaneous observations of ammonia in the atmosphere and ocean. *Nature* 335, 336-338.

Quinn, P. K., Bates, T. S., Johnson, J. E., Covert, J. E., and Charlson, R. J., 1990. Interactions between sulfur and reduced nitrogen cycles over the central Pacific Ocean. *Journal of Geophysical Research* 95, 16,405-16,416.

Quinn, P. K., Coffman, D. J., Bates, T. S., Miller, T. L., Johnson, J. E., Voss, K., Welton, E. J., and Neususs, C., 2001. Dominant aerosol chemical components and their contribution to extinction during the Aerosols99 cruise across the Atlantic. *Journal of Geophysical Research* 106, 20,783-20,809.

Rahn, K. A., and Lowenthal, D. H., 1984. Elemental tracers of distant regional pollution aerosols. *Science* 223, 132-139.

Reid, R. T., Live, D. H., Faulkner, D. J., and Butler, A., 1993. A siderophore from a marine bacterium with an exceptional ferric ion affinity constant. *Nature* 366, 455–458.

Ridame, C., and Guieu, C., 2002. Saharan input of phosphate to the oligotrophic water of the open western Mediterranean Sea. *Limnology & Oceanography* 47, 856-869.

Rue, E. L. and Bruland, K.W., 1995. Complexation of iron(III) by natural ligands in the central North Pacific as determined by a new competitive ligand equilibrium/adsorptive cathodic stripping voltammetry method. *Marine Chemistry* 50, 117-138.

Rueter, J.G., Hutchins, D.A., Smith R.W., and Unsworth, N., 1992. Iron nutrition of Trichodesmium. In: E.J. Carpenter, D. G. Capone and J. G. Rueter, *Marine Pelagic Cyanobacteria: Trichodesmium and Other Diazotrophs*. Dordrecht, Kluwer Academic Publ., pp. 289-306.

Sansone, F. J., Benitez-Nelson, C. R., Resing, J. A., DeCarlo, E. H., Vink, S. M., Heath, J. A., and Huebert, B. J., 2002. Geochemistry of atmospheric aerosols generated from lava-seawater interactions. *Geophysical Research Letters* 29, No. 9, 1335, doi: 10.1029/2001GL013882.

Sañudo-Wilhelmy, S. A., Kustka, A. B., Gobler, C. J., Hutchins, D. A., Yang, M., Lwiza, K., Burns, J., Capone, D. G., Raven, J. A., and Carpenter, E. J., 2001.

Phosphorus limitation of nitrogen fixation by Trichodesmium in the central Atlantic Ocean. *Nature* 411, 66-69.

Savoie, D. L, Prospero, J. M., and Saltzman, E. S., 1989. Non-seasalt sulfate and nitrate in tradewind aerosols at Barbados: Evidence for long-range transport. *Journal of Geophysical Research* 94, 5069-5080.

Savoie, D. L., Prospero, J. M., Oltmans, S. J., Graustein, W. C., Turekian, K. K., Merrill, J. T., Levy, H., 1992. Sources of nitrate and ozone in the marine boundary-layer of the tropical North-Atlantic. *Journal of Geophysical Research* 97, 11,575-11,589.

Savoie, D. L., Prospero, J. M., Larsen, R. J., Huang, F., Izaguirre, M. A., Huang, T., Snowdon, T. H., Custals, L., and Sanderson, C. G., 1993. Nitrogen and sulfur species in Antarctic aerosols at Mawson, Palmer Station, and Marsh (King George Island). *Journal of Atmospheric Chemistry* 17, 95-122.

Shaw, G. E., 1980. Transport of Asian desert aerosol to the Hawaiian Islands. *Journal of Applied Meteorology* 19, 1254-1259.

Siefert, R. L., Webb, S. M., and Hoffmann, M. R., 1996. Determination of photochemically available iron in ambient aerosols. *Journal of Geophysical Research* 101, 14,441-14,449.

Siefert, R. L., Johansen, A. M., and Hoffmann, M. R., 1999. Chemical characterization of ambient aerosol collected during the southwest monsoon and intermonsoon seasons over the Arabian Sea: Labile-Fe(II) and other trace metals. *Journal of Geophysical Research* 104, 3511 – 3526.

Slinn, S. A., and Slinn, W. G. N., 1980. Predictions of particle deposition on natural waters. *Atmospheric Environment* 14, 1013-1016.

Slinn, S. A., and Slinn, W. G. N., 1981. Modeling of atmospheric particulate deposition to natural waters. In: *Atmospheric Pollutants in Natural Waters*. Ann Arbor Science Publishers.

Solomon, P. A., Moyers, J. L., and Fletcher, R. A., 1983. High-volume dichotomous virtual impactor for fractionation and collection of particles according to aerodynamic size. *Aerosol Science Technology* 2, 455-464.

Spokes, L. J., Yeatman, S. G., Cornell, S. E., and Jickells, T. D., 2000. Nitrogen deposition to the eastern Atlantic Ocean: The importance of south-easterly flow. *Tellus* 52B, 37-49.

Stookey, L. L., 1970. Ferrozine—A new spectrophotometric reagent for iron. *Analytical Chemistry* 42, 119– 781.

Swap, R., Garstang, M., Greco, S., Talbot, R., and Kålleberg, P., 1992. Saharan dust in the Amazon Basin. *Tellus*, *Ser. B 44*, 133–149.

Swap, R., Ulanski, S., Cobbett, M., and Garstang, M., 1996. Temporal and spatial characteristics of Saharan dust outbreaks. *Journal of Geophysical Research* 101, 4205-4220.

Sunda, W.G., Swift, D. G., and Huntsman, S. A., 1991. Low iron requirement in oceanic phytoplankton. *Nature* 351, 55-57.

Sunda, W. G., and Huntsman, S. A., 1995. Iron uptake and growth limitation in oceanic and coastal phytoplankton. *Marine Chemistry* 50, 189-206.

Sunda, W. G., and Huntsman, S. A., 1997. Interrelated influence of Fe, light and cell size on marine phytoplankton growth. *Nature* 390, 389-392.

Sunda, W. G., 2001. Bioavailability and bioaccumulation of iron in the sea. In: K. A. Hunter and D. R. Turner (Eds) *Biogeochemistry of Iron in Sea Water*. John Wiley, New York, USA, pp. 41-84.

Talbot, R. W., Andreae, M. O., Berresheim, H., Artaxo, P., Garstang, M., Harriss, R. C., Beecher, K. M., and Li, S. M., 1990. Aerosol chemistry during the wet season in central Amazonia: The influence of long-range transport. *Journal of Geophysical Research 95*, 16,955–16,969.

Taylor, S. R., and McLennan, S. M., 1985. *The Continental Crust: Its Composition and Evolution*. Blackwells, Oxford, England.

Thulasuraman, S., O'Neill, N. T., Royer, A., Holben, B. N., Westphal, D., and McArthur, L. J. B., 2002. Sunphotometric observations of the 2001 Asian dust storm over Canada and the U.S. *Geophysical Research Letters* 29, 1255.

Tovar-Sanchez, A., Sanudo-Wilhelmy, S. A., Garcia-Vargas, M., Weaver, R. S., Popels, L. C., and Hutchins, D. A., 2003. A trace metal clean reagent to remove surface-bound Fe from marine phytoplankton. *Marine Chemistry* 82, 91-99.

Tsuda, A., Takeda, S., Saito, H., Nishioka, J., Nojiri, Y., Kudo, I., Kiyosawa, H., Shiomoto, A., Imai, K., Ono, T., Shimamoto, A., Tsumune, D., Yoshimura, T., Aono, T., Hinuma, A., Kinugasa, M., Suzuki, K., Sohrin, Y., Noiri, Y., Tani, H., Deguchi, Y., Tsurushima, N., Ogawa, H., Fukami, K., Kuma, K., and Saino, T., 2003. A mesoscale Fe enrichment in the western subarctic Pacific induces a large centric diatom bloom. *Nature* 300, 958-961.

Tu, F. H., Thornton, D. C., Bandy, A. R., Kim, M. S., Carmichael, G., and Tang, Y., 2004. Long-range transport of sulfur dioxide in the central Pacific. In preparation.

Tyrrell, T., 1999. The relative influences of nitrogen and phosphorus on oceanic primary production. *Nature* 400, 525-531.

Tyrrell, T., Marañon, E., Poulton, A. J., Bowie, A. R., Harbour, D. S., and Woodward, E. M. S., 2003. Large-scale latitudinal distribution of *Trichodesmium* spp. in the Atlantic Ocean. *Journal of Plankton Research* 25, 405-416.

Venkataraman, C., Reddy, C. K., Josson, S., and Reddy, M. S., 2002. Aerosol size and chemical characteristics at Mumbai, India. *Atmospheric Environment* 36, 1979-1991.

Vink, S., Boyle, E. A., Measures, C. I., and Yuan, J., 2000. Automatic high resolution determination of the trace elements Iron and Aluminium in the surface ocean using a towed fish coupled to flow injection analysis. *Deep Sea Research* I 47, 1141-1156.

Viollier, E., Inglett, P. W., Hunter, K., Roychoudhury, A. N., and Van Cappellen, P., 2000. The ferrozine method revisited: Fe(II)/F(III) determination in natural waters. *Applied Geochemistry* 15, 785–790.

Voelker, B. M., and Sedlak, D. L.,1995. Iron reduction by photoproduced superoxide in seawater. *Marine Chemistry* 50, 93-102.

Voelker, B. M., Morel, F. M. M., and Sulzberger, B., 1997. Iron redox cycling in surface waters: Effects of humic substances and light. *Environmental Science & Technology* 31, 1004–1011.

Waterbury, R. D., Yao, W. S., and Byrne, R. H., 1997. Long pathlength absorbance spectroscopy: Trace analysis of Fe(II) using a 4.5 m liquid core waveguide. *Anal. Chim. Acta* 357, 99– 102.

Watson, A. J., and Lefevre, N., 1999. The sensitivity of atmospheric CO concentrations to input of iron to the oceans. *Tellus* 51B, 453-460.

Wei, L., Fujiwara, K., and Fuwa, K., 1983. *Analytical Chemistry* 55, 951.

Wells, M. L., Price, N. M., and Bruland, K. W., 1995. Iron chemistry in seawater and its relationship to phytoplankton: a workshop report. *Marine Chemistry* 48, 157-182.

Wells, M. L., Smith, G. J., Bruland, K. W., 2000. The distribution of colloidal and particulate bioactive metals in Narragansett Bay, RI. *Marine Chemistry* 71, 143-163.

Wen, L. S., Santschi, P. H., Gill, G., Paternostro, C., 1999. Estuarine trace metal distributions in Galveston Bay: importance of colloidal forms in the speciation of the dissolved phase. *Marine Chemistry* 62, 2867-2878.

Wilhelm, S. W., 1995. Ecology of Fe-limited cyanobacteria: a review of physiological responses and implications for aquatic systems. *Aquatic Microbial Ecology* 9, 295–303.

Willey, J. D., Kieber, R. J., Avery Jr. G. B., 2004. Effects of rainwater iron and hydrogen peroxide on iron speciation and phytoplankton growth in seawater near Bermuda. *Journal of Atmospheric Chemistry* 47, 209-222.

Williams, R. M, 1982. A model for the dry deposition of particle to natural water surfaces. *Atmospheric Environment* 16, 1933-1938.

Wu, J., and Luther, G. W., 1994. Size fractionated iron concentrations in the water column of the northwest Atlantic Ocean. *Limnology & Oceanography* 39, 1119–1129.

Wu, J., and Luther, G. W., 1995. Complexation of Fe(III) by natural organic ligands in the northwest Atlantic ocean by competitive ligand equilibration method and kinetic approach. *Marine Chemistry* 50, 159-177.

Wu, J., and Boyle, E. A., 1997. Determination of iron in seawater by high resolution isotope dilution inductively coupled plasma mass spectrometry after $Mg(OH)_2$ coprecipitation, *Anal. Chim. Acta*., 367, 183-191.

Wu, J., and Boyle, E. A., 1998. Determination of iron in seawater by high resolution isotope dilution inductively coupled plasma mass spectrometry after Mg(OH)2 coprecipitation. *Anal. Chim. Acta* 367, 183–191.

Wu, J., Sunda, W., Boyle, E. A., and Karl, D. M., 2000. Phosphate Depletion in the Western North Atlantic Ocean. *Science* 289, 759-768.

Wu, J., Boyle, E., Sunda, W., and Wen, L. S., 2001. Soluble and colloidal Fe in the oligotrophic north Atlantic and north Pacific. *Science* 293, 847-849.

Wu, J., and Boyle, E., 2002. Iron in the Sargasso Sea: implications for the processes controlling dissolved Fe distribution in the ocean. *Global Biogeochemical Cycles* 16, 1086.

Yamasoe, M. A., Artaxo, P., Miguel, A. H., Allen, A. G., 2000. Chemical composition of aerosol particles from direct emissions of vegetation firs in the Amazon Basin: water-soluble species and trace elements. *Atmospheric Environment* 34, 1641-1653.

Yatin, M., Tuncel, S., Aras, N. K., Olmez, I., Aygun, S., and Tuncel, G., 2000. Atmospheric trace elements in Ankara, Turkey: 1. factor affecting chemical composition of fine particles. *Atmospheric Environment* 34, 1305-1318.

Yokoi, K., and van den Berg, C. M. G., 1992. The determination of iron in seawater using catalytic cathodic stripping voltammetry. *Electroanalysis* 4, 65– 69.

Zhang, X. Y., Gong, S. L., Shen, Z. X., Mei, F. M., Xi, X. X., Liu, L. C., Zhou, Z. J., Wang, D., Wang, Y. Q., and Cheng, Y., 2003. Characterization of soil dust aerosol in China and its transport and distribution during 2001 ACE-Asia: 1. Network observations. *Journal of Geophysical Research* 108, No. D9, 4261, doi: 10.1029/2002JD002632.

Zhang, X. Y., Arimoto, R., Zhu, G. H., Chen, T., and Zhang, G. Y., 1998. Concentration, size-distribution and deposition of mineral aerosol over Chinese desert regions. *Tellus, Series B* 50, 4317– 4331.

Zhao, T. L., Gong, S. L., Zhang, X. Y., and McKendry, I. G., 2003. Modeled size-segregated wet and dry deposition budgets of soil dust aerosol during ACE-Asia 2001: Implications for trans-Pacific transport. *Journal of Geophysical Research* 108, No. D23, 8665, doi:10.1029/2002JD003363.

Zhu, X. R., Prospero, J. M., Millero, F. J., Savoie, D. L., and Brass, G. W., 1992. The solubility of ferric iron in marine mineral aerosol solutions at ambient relative humidities. *Marine Chemistry* 38, 91– 107.

Zhu, X. R., Prospero, J. M., Savoie, D. L., Millero, F. J., Zika, R. G., and Saltzman, E. S., 1993. Photoreduction of Fe(III) in marine aerosol solutions. *Journal of Geophysical Research* 98, 9039–9046.

Zhu, X. R., Prospero, J. M., and Millero, F. J., 1997. Diel variability of soluble Fe(II) and soluble total Fe in North African dust in the trade winds at Barbados. *Journal Geophysical Research* 102, 21,297-21,305.

Zhuang, G. S., Duce, R. A., and Kester, D. R., 1990. The solubility of atmospheric iron in surface seawater of the open ocean. *Journal Geophysical Research* 95, 16,207–16,216.

Zhuang, G., Zhen, Y., Duce, R. A., and Brown, P. R., 1992. Link between iron and sulphur cycles suggested by detection of Fe(II) in remote marine aerosols. *Nature* 355, 537-539.

Zhuang, L., and Huebert, B. J., 1996. Lagrangian analysis of the total ammonia budget during Atlantic Stratocumulus Transition Experiment/ Marine Aerosol and Gas Exchange. *Journal of Geophysical Research* 101, 4341-4350.

Zieman, J. J., Holmes, J.L., Connor, D., Jensen, C. R., and Zoller, W. H., 1995. Atmospheric aerosol trace element chemistry at Mauna Loa Observatory, 1979-1985. *Journal of Geophysical Research* 100, 25,979-25,994.

Zuo, Y., and Hoigne, J., 1992. Formation of hydrogen peroxide and depletion of oxalic acid in atmospheric water by photolysis of iron(III)-oxalato compounds. *Environmental Science & Technology* 26, 1014-1022.